Reconstruction of auricular cartilage using natural-derived scaffolds with an in vivo application in rabbit model

Mira Hammad

Normandie Université

THÈSE

Pour obtenir le diplôme de doctorat

Spécialité ASPECTS MOLECULAIRES ET CELLULAIRES DE LA BIOLOGIE

Préparée au sein de l'Université de Caen Normandie

Reconstruction of auricular cartilage using natural-derived scaffolds with an in vivo application in rabbit model

Présentée et soutenue par
Mira HAMMAD

Thèse soutenue publiquement le 16/04/2021 devant le jury composé de		
Mme SYLVIE TESTELIN	Professeur des universités PraticienHosp, CHU Amiens-Picardie	Rapporteur du jury
Mme CATHERINE BAUGÉ	Maître de conférences HDR, Université Caen Normandie	Membre du jury
M. BERNARD DEVAUCHELLE	Professeur des universités PraticienHosp, Université Amiens Picardie Jules Verne	Membre du jury
M. ERIC MAUBERT	Maître de conférences HDR, Université Caen Normandie	Membre du jury
M. WALID RACHIDI	Professeur des universités, Université Grenoble Alpes	Membre du jury
M. KARIM BOUMEDIENE	Professeur des universités, Université Caen Normandie	Directeur de thèse
Mme PATRICIA ALBANESE	Professeur des universités, Université Paris-Est Créteil (UPEC)	Président du jury

Thèse dirigée par KARIM BOUMEDIENE, Biologie des tissus conjonctifs et cutanés

UNIVERSITÉ CAEN NORMANDIE

ED 497 NBISE
Normande de Biologie Intégrative, Santé, Environnement

EA7451 BioConnecT

Acknowledgments

First of all, I would like to express my great gratitude towards my supervisor Pr. **Karim BOUMEDIENE** for his professional guidance and also for welcoming me in his team. With his help, I have acquired critical thinking and logical scientific methods which are highly beneficial for my PhD work. Besides, his suggestions helped me explore several important factors in cell biology and cartilage tissue engineering field.

My sincere thanks also go to all jury members, Pr. **Patricia ALBANESE** and Pr. **Sylvie TESTELIN** for having accepted to evaluate my research work by being the reporters of this thesis and giving precious comments and remarks.

I would also like to thank Pr. **Bernard DEVAUCHELLE**, Pr. **Walid RACHIDI**, Dr. **Eric MAUBERT**, Dr. **Catherine BAUGE** for agreeing to participate in the jury by being the examiners of the thesis.

I also address my sincere thanks to **Vincent RICHARD, Walid RACHIDI** and **Mohamed OUZZINE** for having been part of my thesis follow-up committee during these three years.

Special thanks go to **Eric MAUBERT** for the immunohistochemistry and cryostat training sessions and his sincere advice.

My Sincere thanks go to **FHU SURFACE** and **Fondation des Gueules Cassées**, since this work is a part of FHU SURFACE projects and funded by "Fondation des Gueules Cassées".

I also wish to thank: Dr. Sylvain LECLERCQ and Dr. Vincent PATRON for their precious samples (femoral heads, bone marrow and nasal perichondrium samples), Dr. Didier GOUX for the Scanning electron microscopy images, Dr. Benoît BERNAY for Mass spectroscopy analyses and finally Dr. Palma PRO-SISTIAGA for the animal models.

I would like to thank BioconnecT team members: Catherine Baugé, Martine Boittin, Leila El Kihel, and my colleagues and friends with whom I had a great time: Mariya Khokhlova, Marion Berthelot, Juliette Aury-Landas, Alex Hesry, Alexis Veyssiere, Lyess Allas, Ophélie Grard, Sybille Brochard, Marion Lenté, Justin Dugué, Emma Vidal.

I would like also thank all my friends who I have met here in Caen during my 3-year stay, and with whom I shared so good time and lots of memories.

Special thanks go to **Alexandre E.** for his encouragement and support as well his precious help in the lay out of the thesis, thank you for always being there.

For our precious friendship: Helena A., Mohammad B., Rola H., Mirvana H., Clara A., Carine H., Abdelrahman M., Chimène A., Majd E., Ghinwa F., Jad K.

Last but not least, I would like to thank my parents **(Faten and Samir)** and my brother **Wael** for always believing in me every second and for having supported, and straightened me out in difficult moments. I thank you for your unconditional love and sacrifices you have made.

I love you …

Abbreviations

2D	Two dimensions
3D	Three dimensions
AB	Alcian Blue
ACAN	Aggrecan
ADSC	Adipose-derived stem cells
AFSC	Amniotic fluid-derived stem cells
ALP	Alkaline phosphatase
Alpha-MEM	Minimum Essential Medium *alpha*
ATP	Adenosine triphosphate
AuP	Auricular perichondrocytes
bFGF	Basic fibroblast growth factors
BMMSC	Bone marrow-derived mesenchymal stem cells
BMP	Bone morphogentic proteins
BMP-2	Bone morphogentic protein-2
BNC	Bacterial nanocellulose
CB-MSC	Cord blood stem cells
CHAPS	3[(3-cholamidopropyl) dimethylammonio]-1-propanesulfonate
COL II	Collagen type II
COL1	Collagen type I
COL2A1	Collagen type 2 alpha 1
COLX	Collagen type X
COMP	Cartilage oligomeric matrix protein
CSM	Cell-secreted matrices
CXCR4	C-X-C chemokine receptor type 4
DAPI	4,6-diamidino-2-phenylindole
DMEM	Dulbecco's Modified Eagle Medium
DNase I	Deoxyribonuclease I
DPSC	Dental pulp stem cells
ds DNA	Double-standed DNA
ECM	Extracellular matrix
EDTA	Ethylene diaminetetraaceticacid
ELN	Elastin
ESC	Embryonic stem cells
FCS	Fetal calf serum
GAG	Glycosaminoglycans
GAPDH	Glyceraldehyde 3-phosphate dehydrogenase
GF	Growth factors
GFP	Green fluorescent proteins
HA	Hyaluronic acid
hASCs	Human adipose-derived stem cells
HDAC4	Histone deacetylase 4
hDF	Human dermal fibroblasts
HDMEC	Human dermal microvascular endothelial cells
HE	Hematoxyline-Eosin
hfF	Human foreskin fibroblast
HIF2α	Hypoxia-inducible factor 2 αlpha
hiPSC	Human-induced pluripotent stem cells

HPRT1	Hypoxanthine Phosphoribosyltransferase 1
hPS-CM	Human pluripotent stem cell-derived cardiomyocytes
HSMC	C2C12 human skeletal muscle cells
hTERT	Human telomerase reverse transcriptase
HUVECS	Human umbilical vein endothelial cells
IGF	Insulin-like growth factors
IL6	Interleukin-6
ITS+1	Insulin-transferrin-sodium selenite 1
KEGG	Kyoto Encyclopedia of Genes and Genomes
LCST	Low critical solution temperature
MACT	Matrix-assisted autologous chondrocytes transplantation
MSC	Mesenchymal stem cells
MT	Masson's Trichrome
NIH3T3	Cell lines derived from mouse embryonic fibroblasts
NsP	Nasal perichondrocytes
OCT	Optimal cutting temperature compound
PBMC	Peripheral blood mononuclear cells
PCL	Polycaprolactone
PDMS	Poly (dimethylsiloxane)
PEG	Poly ethylene glycol
PEG-GelMA-HA	Polyethylene glycol, gelatin methacrylate hyaluronic acid
PGA	Poly(glycolic acid)
PIPAAm	Poly(N-isopropylacrylamide)
PKA	Protein kinease A
PLA	Poly lactic acid
PLGA	Poly lactic-co-glycolic acid
PM	Porous membrane
PP2A	Protein phosphatase 2
PTHrp	Parathyroid hormone-related protein
PVA	Poly vinyl alcohol
RGD	Arg-Gly-Asp
RPL13	Ribosomal Protein L13
RT-PCR	Reverse transcription polymerase chain reaction
Runx2	Runt-related transcription factor-2
SD	Sodium deoxycholate
SDS	Sodium dodecyl sulfate
SFV	Stromal vascular fraction
SO	Safranin O
SRY	Sex-determining region Y-box 9 (SOX 9)
TGF-β	Transforming growth factor-beta
TGFβ-1	Transforming growth factor beta-1
TGFβ-3	Transforming growth factor beta-3
TiO_2	Titanium oxide
VEFG	Vascular endothelial growth factor
VGEF	Vascular epithelial growth factors
ZnO	Zinc oxide
β2-MG	Beta 2 microglobulin

Table de contents :

Table of figures:

List of tables:

Summary

Successful reconstruction of auricular cartilage defects requires appropriate restoration of the cartilaginous deformities by potential cell sources as well as providing suitable tissue supports. This work aimed to investigate different scaffolds and biomaterials for *in vitro* auricular cartilage engineering as well as *in vivo* auricular cartilage repair in rabbit models. We first showed that auricular perichondrocytes are the best candidates for auricular cartilage regeneration and hypoxia is not necessary for their chondrogenic differentiation. These cells successfully formed cartilaginous cell sheets which were used to regenerate cartilage tissue *in vitro* and to fill and reconstruct cartilage defects *in vivo* in allogenic rabbit models. Furthermore, we tested cellulose-derived tissue by decellularizing apple tissue and its use as a scaffold. Repopulated with cells, these scaffolds surpassed alginate hydrogels by enhancing colonization and upregulating the cartilaginous expression in different mammalian cells. In the final part of the thesis, we examined cell-secreted matrices and used them as coating for different cell culture applications. Interestingly, these coatings promoted both allo- and xenogeneic cell culture, increased proliferation and boosted chondrogenesis. We also highlighted phenotype preservation during chondrocytes expansion on these cell-secreted matrices. Our study provides novel tools and approaches for multiple cell culture applications.

I-Introduction

1. The human ear

1.1 Sound production

Ear are constantly active, they pick up sound waves and change them into information that the brain can interpret, such as music or speech. Sound is a pressure wave that can vibrate either quickly or slowly. Sound enters the ear and is directed through the ear canal where it first reaches the eardrum. As the eardrum begins to vibrate, it sets the ossicular chain of motion. The ossicular chain consists of the hammer, anvil, and stirrup. Sound vibrations move along the ossicular chain and into the inner ear. Within the inner ear, the cochlea plays a central role (**Figure 1**). It is here that the mechanical energy of sound is converted into complex electrical signals, which are then passed to the brain. In simplified terms, the cochlea is a spiral-shaped tube filled with fluid. Sensory cells also called hair cells, line the entire length of the cochlea.

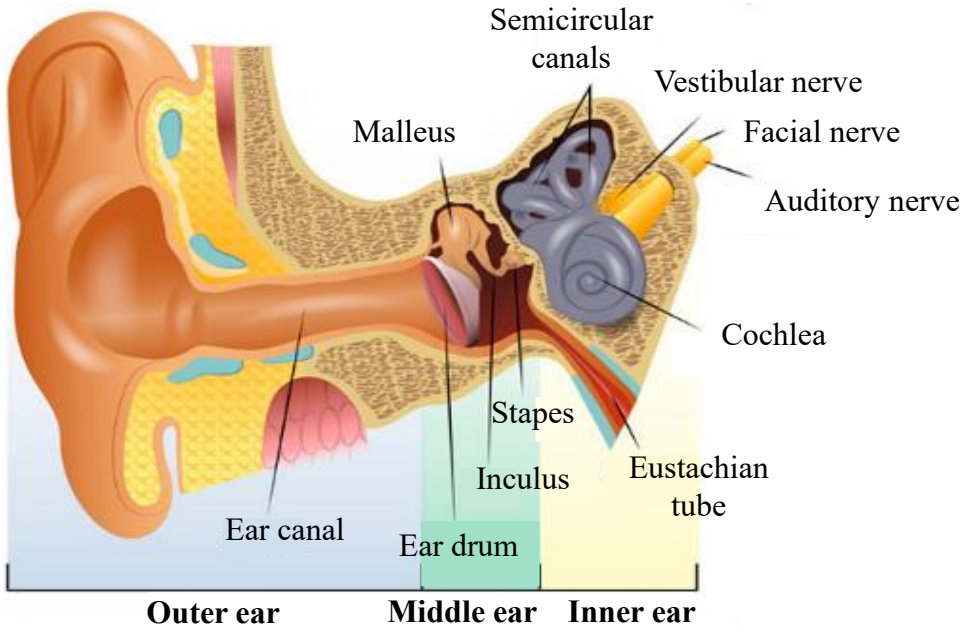

Figure 1: Diagram of the main parts of the hearing system (Hearinglink.org).

These hair cells have varying degrees of sensitivity for the detection of different tones and frequencies. This allows the ear to perceive the entire spectrum of sound. The change from mechanical vibration to electrical pulse is a complex procedure resulting from the movement of hair cells in the cochlea. Along the entire length of the cochlea, the hair cells are arranged like the keys of the piano. Hair cells located at the base or lower region of the cochlea, are responsible for high frequency, while hair cells at the apex are responsible for the low frequency. As the fluid of the cochlea is set in motion, it causes a corresponding movement of the fine structures on the surface of hair cells to take place. These movements cause tension differences, which produce electrical signals that are passed away along the hearing nerve to the brain. The auditory cortex of the brain interprets this information as sound, for e.g. as music or speech. The entire chain of events including the various steps that convert sound waves from the environment into information that the brain can interpret happens so fast that individuals can hear sound both continuously and instantaneously within this complex chain of events. There are a number of factors which can cause an individual to experience hearing loss which differs from one another depending on the part of the ear that is affected being the outer, middle or the inner ear (De Paolis *et al*., 2017).

1.2 Human external auricle (outer ear)

The external ear often referred to as the auricle or pinna, is responsible for collecting and directing sound waves through the auditory canal and tympanic membrane. This protects the fragile eardrum by blocking out unwanted noise from other directions and maintaining a sense of balance. In addition to its physiological function, the pinna boosts the self-esteem of an individual by contributing to the overall facial appearance, which is visible during social interactions (Jones *et al.,* 2020). Ears also provides many secondary functions, such as holding glasses, and headphones.

1.2.1 Anatomy

The first sign of ear development is the appearance of the otic placode on the 21st day of embryonic development. The outer ear develops around the first branchial ectodermal cleft, bordered between the first arch (mandibular) and the second arch (hyoidien). A large part derived from the mesectoderm, a subpopulation from the neural crest migrating from the neural beads of the

rhombencephalon. This cell population participates in the formation of the craniofacial skeleton, in particular the cartilaginous blastema of the lower part of the face. The pinna begins its development on the 33rd day intra-uterine growth. Mesenchymal buds appear at the dorsal banks of the 1st ectodermal branch cleft, referred to as the colliculus. On the 44th day, these buds reach their maximum size and begin their migration that leads to their fusion. The pinna of the ear has 2 faces, a medical one, a lateral one and a free edge (**Figure 2**). The auricle joins the skull to the middle part of its front third, while the other two-thirds remain free and mobile (Powles-Glover and Maconochie, 2018).

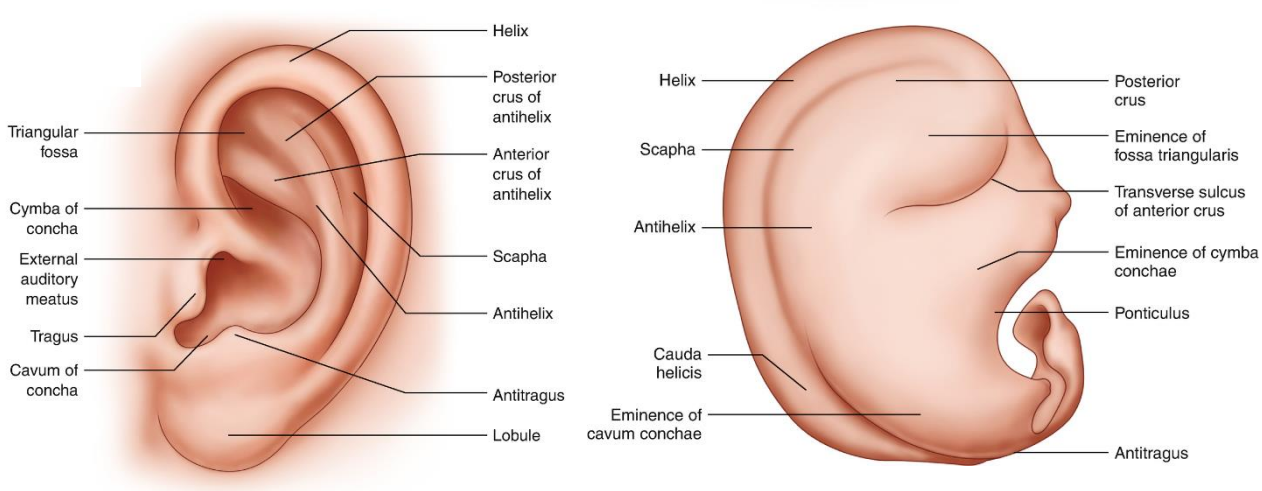

Figure 2: Auricular cartilage of right auricle, lateral and medial faces (Delas and Dehesdin, 2008).

Auricle develops from 3 pairs of auricular hillocks that arise on the lateral faces of the auricles to which they give rise. The first pharyngeal cleft gives rise to the external auditory meatus, which is connected to the tympanic membrane Auricular hillocks begin to enlarge, differentiate and fuse, producing the final shape of the ear, which is gradually translocated from the side of the neck to a more cranial and lateral site. Postnatal human ear transmits frequencies in the range of 3KHz, it could be increased by 30 to 100-fold, which corresponds to frequencies of side of the head, to allow the precise localization of the sound reaching the ear (Hackley, 2015). Pinna possesses an important sensory innervation supplied by auriculotemporal nerve. The human ear continues to develop postnatally during our entire lives and occurs in 2 different sexual forms. A study reported that 3 features stopped growing after birth, among these features were the concha, inter tragica and the

helical diameter. At birth, the auricle was known to be bigger than the head, proportionally to the rest of the body, and kept throughout childhood, until it decreases by 8 or 10 years of age. It has been noted that ear growth in males increases greater than for females (Powles-Glover and Maconochie, 2018).

1.3 Auricular cartilage

Auricular cartilage is present in all parts of the auricle except the lobule which is composed of adipose tissue. It is anchored to the human head and surrounded by a perichondrium that provides the necessary nutrients (Saka *et al*., 2019). Auricular cartilage is classified as elastic cartilage that differs from hyaline and fibrocartilage in morphology, presence of collagen and elastin fibers.

Auricular cartilage refers to the cartilage of the ear's auricle, the outermost portion of the ear. This cartilage helps maintain the shape of the ear while allowing flexibility. It is an avascular tissue that consists of cartilage cells and an extensive extracellular matrix (ECM), secreted and supported by chondrocytes (cartilage cells). This ECM is dominated by aggrecan (ACAN) and type II collagen (COLII), giving cartilage its compressive and tensile strength. The highly sulfated glycosaminoglycans (GAG) side chains of chondroitin sulfate and keratin sulfate enable the matrix to hold large amount of water, thus creating a large osmotic pressure (Chhapola and Matta, 2012). Knowing that cartilage is derived from undifferentiated mesenchymal tissue, the intermediate cell for hyaline cartilage chondrocyte is chondroblast. However, elastic chondrocyte intermediate cell is fibroblast, which will be later on differentiated finally into auricular chondrocyte. During this final step, fibril bundles surrounding cells are transformed into highly branched elastic fibers. Elastic cartilage is also found in structures that demand flexibility such as eustachian tube, epiglottis and larynx. This extensive elastic network provides flexibility as well as the yellow color and opaque appearance, which differentiate elastic cartilage from hyaline. Elastin is a polymer composed of cross-linked subunits of tropoelastin, a precursor protein. Tropoelastin consists of alternating hydrophobic and cross-linking domains. This mechanism occurs in extracellular space where ε-amino group on lysine is oxidized by lysyl oxidase and linked to a second lysine side chain to form covalent bonds between tropoelastin monomers, thus forming a mature elastin protein (Wise *et al*., 2014).

1.4 External ear anomalies

Auricular cartilage is subjected to many pathologies, mainly from congenital malformations or acquired causes, such as trauma, accidents, and sometimes cancer.

1.4.1 Microtia

Congenital auricular anomalies either occur as isolated birth defects or can be associated with other syndromes, especially those related to craniofacial region. The most severe type of malformations is microtia where it is associated with the malformation of the outer ear, ranging from 0.8 to 8.3 per 10000 live births. Microtia can affect one side (unilateral) or both sides (bilateral), where males have higher risk than females. It can also be associated with several syndromes such as Alport syndrome, spondyloeiphyseal dysplasia, resulting in hearing loss and absence of external cartilaginous structure (Hartzell and Chinnadurai, 2018). Whether a major or a minor deformity, both cases can significantly impact a child's self-esteem and self-perception while growing up, affecting his psychological health (Johns *et al.*, 2015).

Luquetti *et al*., presented in his case-studies a summary of factors that increased the risk of microtia. These included male sex, low birth weight, maternal acute illness and diabetes, multiple births, maternal use of medications, and exposure to air pollution, as well as the race where he reported the high prevalence of microtia in Chileans and Ecuadorians than previously reported worldwide. He suggested that this could be explained by a combination of gene-environment interaction, where genetic variations are combined to diet, causing high risk of microtia (Luquetti *et al.*, 2012). Nagata classified microtia depending on the specific surgical procedure used to reconstruct it. He divided them into 5 types presented in **Figure 3**.

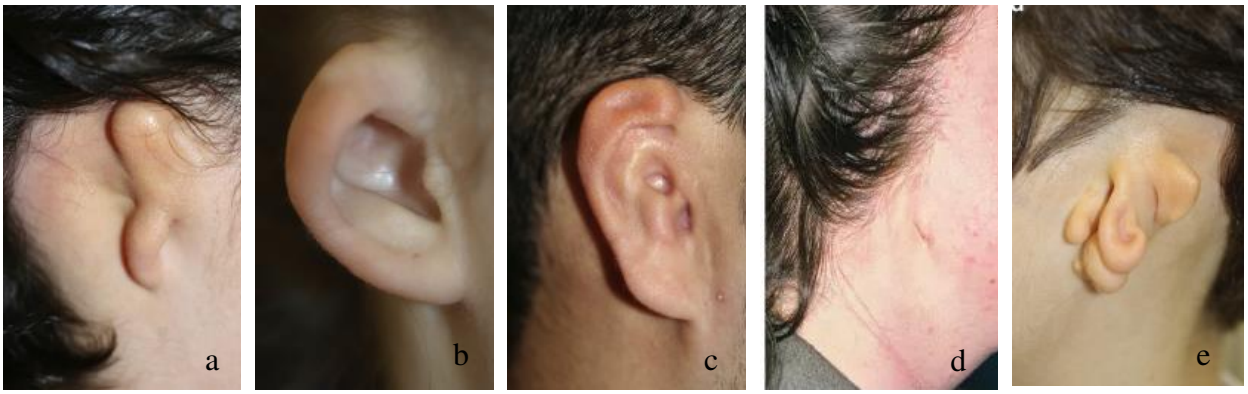

Figure 3: Different types of microtia. a. Lobule type, b. Concha type, c. Small concha type, d. Anotia, e. Atypical microtia (Firmin and Marchac, 2016).

The first photo presents that lobule type that is characterized by elongated lobes and an absence of auditory canal (a). The second present a concha type (b), that is explained by the presence of a concha and an auditory canal. Small concha type is presented in the third figure (c) where concha is replaced by smaller remnants and a wide variety of deformities, this type also lacks an auditory canal. The fourth photo displays an anotia case where the patient has no ear remnants at all (d). Finally, ear malformations can also present an atypical microtia shape that doesn't correlate with any of the above types (e).

1.4.2 External ear traumas and amputations

Since pinna is a protruding structure it is more prone to accidental damage due to traumas, amputations, burns, and cancerous lesions (**Figure 4**).

Due to their laterofacial location and their helix, the ears are largely exposed to sunshine. It is therefore logically that they are susceptible more to different carcinoma such as basal cell carcinoma, skin squamous cells carcinoma or melanoma. Also, animal bites and accidents are a common cause of trauma.

Figure 4: Ear trauma and amputations: partial ear amputation, external ear melanoma, melanoma at the ear lobe (Sawyer *et al*., 2018).

1.5 Current treatment options

1.5.1 Reconstruction using autologous cartilage

To correct a normal ear, it has always been challenging for surgeons. Tanzer was the first to describe an ear reconstruction from autologous costal cartilage that was later on considered as the gold standard method. His technique was revolutionary since it was the only solution for microtia patients. However, this latter was a heavy technique that required 6-stage surgical procedure. The first step was transposing the lobule to its normal anatomical position. He then created the framework by harvesting from ribs to reconstruct the base, the helix and the antihelix. Next, he combined the framework and after 4 months, projected the framework a little away from the head and covered the retro auricular sulcus with a thickness skin graft. After another 4 months, the ear tunnel was closed and 6 weeks later, the concha and tragus were reconstructed using cartilage grafts (Tanzer, 1959). There were other scientists that relied on Tanzer technique and optimized it.

The two surgeons who greatly contributed to the ear reconstruction were Brent and Nagata. Brent establishes a four-stage, step-by-step technique to correct microtia (Brent, 1980). He started by inserting an autologous cartilaginous framework into a skin pocket, transposing the lobule, constructing the tragus, and finally, constructing the retroauricular sulcus. Although, satisfactory results were obtained with this technique, it was criticized by Firmin, who pointed out that the contours were still imperfect and the tragus was sometimes disappointing, as well as when retroauricular flap deteriorated with time (Firmin, 1998). Nagata on the other hand presented a two-

step technique to reconstruct microtic ears. He started by constructing a complete framework of rib cartilage and carving into a semi-lunar shape. Next, he fastened the framework firmly behind the anthelix to reconstruct posterior wall of concha. This helped prevent secondary skin retraction. To finish the transplantation step, a hinged flap covered the cartilage graft was added (Nagata, 1993) as illustrated in **Figure 5**.

Figure 5: Autologous costal cartilage graft reproducing the helix, antihelix, tragus, and the antitragus (Firmin, 1998).

In France, Françoise Firmin had also performed most of her ear reconstruction in 2-stage protocol that was separated by 6-month delay (Firmin and Marchac, 2011). The main advantage of the 2-stage techniques is that they are less time consuming, however, more challenging and requiring experienced surgeons.

On the other hand, donor site morbidity was highly associated with autologous reconstruction, as well as the infection that follow it that results in skin necrosis and extrusion of the framework.

1.5.2 Reconstruction using synthetic framework

To limit the complications associated with autologous costal cartilage, and in order to eliminate donor site morbidity, the use of synthetic frameworks has been addressed by several scientists. Materials such as rubber, tantalum, polyethylene, silicone acrylic glass and polyamides were used for producing alloplastic frameworks. Several groups of scientists have developed the frameworks. The most commonly used frameworks are silicone-based or polyethylene-based (Medpor®) shown

in **Figure 6**. The first silicone framework was fabricated in 1966 that was later on ameliorated by Fox and Edgerton who used the fan-flop method to protect the implant from necrosis by covering it with muscle tissue (Fox and Edgerton, 1976). Polyethylene, the tissue friendly stable framework was then processed. This framework presented biocompatible and an easy to mold structure during surgery (Xie *et al*., 2017) . These frameworks eliminated resorption linked to cartilage frameworks, as well as the variability. On the other hand, this technique increased the risk of serious complications where it resulted in damage to overlying and adjacent tissue and sometimes induced infection and extrusion of the implant and wasn't recommended in aged patients.

Figure 6: Medpor® framework (Stephan and Reinisch, 2018).

1.5.3 Prosthetics

Prosthetic ears are other alternatives for auricular reconstruction. A prosthetic ear is an artificial ear usually fabricated from synthetic materials that mimic characterization of native tissue, such as silicone and attached to the head using magnetic clips, adhesive or by using bone-anchored titanium screws. Poly(methylmethacrylate), was one of the mostly polymer in prosthesis since the 20th century. Further innovations have produced different new polymers with different time intervals presented in **Figure 7.** More recently, renovations in prosthesis have led to the development of newly specialized materials and crosslinking methods, to optimize their suitability for 3D printing and thereby enabling a large range of mechanical and visual properties (Powell *et al*., 2020).

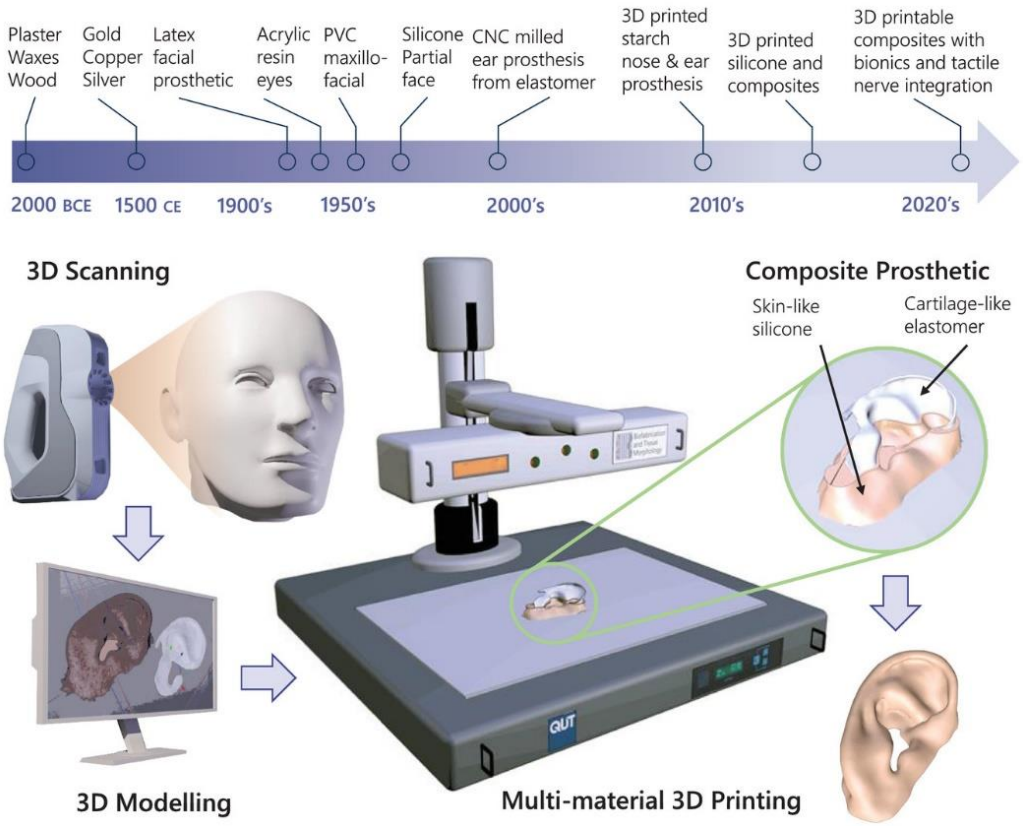

Figure 7: Timeline showing the significant improvement of prosthesis with time as well as manufacturing process to fabricate multi material prosthesis during the single printing process (Powell *et al.*, 2020).

Not only prosthetic ears enhance cosmetic reconstruction, but also it directs the sound waves into the auditory canal providing a supplying a good environment for the inner ear membranes *(Cruz et al*., 2020; Unkovskiy *et al*., 2018). Another advantage of this technique is that it also eliminates the use of costal cartilage and could be placed directly on healthy tissue remnants without the need of any surgical procedure. Moreover, it adds a great value on patient's social and psychological life. On the contrary, many limitations restricted the success of such prosthesis. The color for instance, was very difficult to match the native skin tone. The use of titanium screws caused local irritation and induced inflammation and damage to the surrounding soft tissue.

2. Tissue Engineering

2.1 Definition

Damages and degeneration of tissue and organs, due to diseases or accidents touch every organism. Correction and treatment of these problems is a major issue to be considered, especially after the shortage of donors and the low availability of the grafts needed for replacement. For that a new approach of fabricating living replacement in the laboratory was referred to as tissue engineering. Langer and Vacanti were first to define principles of tissue engineering. They defined this approach as a technology that uses the basic principles of engineering and life sciences to maintain, improve or restore tissue functions (Langer and Vacanti, 1993). The principle of tissue engineering consists of isolating and harvesting cells from different sources such as autologous cells, allogenic or even xenogeneic. These cells, later on, will be expanded and seeded on to biomaterials that provide support for cellular growth and maturation in presence of specific signals and molecules to enhance cells to migrate and replace older tissues (Bakhshandeh *et al*., 2017). All together, these three basic components form the triad of tissue engineering (**Figure 8**).

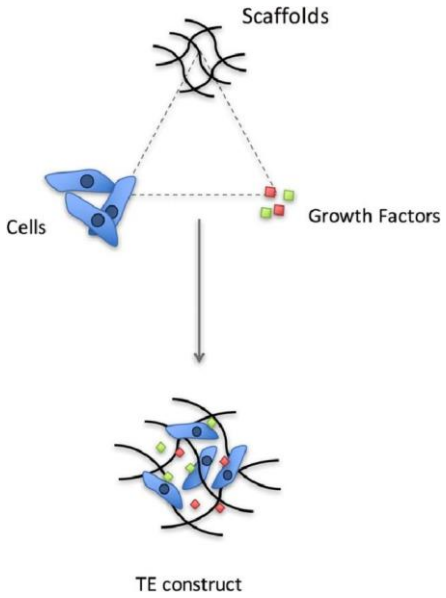

Figure 8: The triad of tissue engineering (Vieira *et al*., 2017).

The concept of tissue engineering is to regenerate neotissue, with the help of scaffolds and regulatory signals, to achieve therapeutic means to treat many demanding medical situations. Tissue engineering is the most challenging and interesting expanding area in the biomedical engineering field. In spite of the rapidly developing technology, many people die every year due to the shortage of organs and tissue donors. That's why tissue engineering is an emerging approach that can reconstruct and regenerate damaged tissues and organs *in vitro* and transplant them back *in vivo*. Although surgical reconstruction that used mechanical devices, had a good impact and saved lives of many patients, however, they didn't accomplish all functions of native tissue and presented many side effects (Berthiaume *et al.*, 2011).

As a human being, there is an urge to regenerate tissues and organs when the self-healing chances are low. The cells in tissue engineering are switched on, in presence of several regulatory signals to generate functional tissues. This is achieved by specific support known as biomaterials or matrices that guide and maintain the shape of the neotissue to be reimplanted into the patient's body (Sharma *et al.*, 2019).

The aim of tissue engineering is to engineer or reconstitute tissue by expanding patient cells *in vitro* supported by a scaffold, or by implanting an acellular biomaterial in the patient's body and allowing cells to adhere, thus repairing autologous tissue. In both cases, scaffold implanted *in vivo* should induce regeneration of injured tissue and degrade with time, leaving no toxic side effects. In addition, this technology limits the problems of grafting techniques, since a small number of cells are harvested from patient, therefore avoiding donor-site morbidity as well as tissue and organ shortage. Harvested cells are seeded in scaffolds that degrade after a certain time *in vivo*, eliminating the possibility of foreign body that might induce tissue inflammation.

Many challenges face tissue engineering, this is explained by the limited clinical trials, despite the advancement done during the last decade (C. Chen *et al*., 2020; Li *et al*., 2018).

2.2. Cell sources for tissue engineering

Tissue engineering is enormously influenced by cellular sources. 3 different cell sources are usually used in tissue engineering techniques. They include autologous cells derived from patient cells, allogenic cells obtained from the same species but other than patient's cells, and xenogeneic

sources acquired from animals. Among these sources, xenogeneic is the least preferable sources, due to the presence of porcine endogenous retrovirus in pigs. Also, xenogeneic feeder cells used for the engineering of epidermal tissue is sometimes risky due to the viral infection that could be coupled when regenerating skin tissue (Bi and Jin, 2013). The idea is using the patient's own cells (autologous cells), however for this process to occur, we need sufficient amount of cells, rendering the harvesting techniques difficult in cases of severely ill or aged patients (Samadi *et al.*, 2020).

Whether cells are directly seeded on the transplanted scaffold or amplified *in vitro*, the choice of these cells is a very critical step. Cells are the basic biological components of tissue, and thus cell sources may affect the type and the way scaffolds regenerate. Furthermore, the choice of cells should guarantee free-pathogens environment. Embryonic stem cells are pluripotent and capable of renewing and differentiating into different cell niches. They can also include adult stem cells at their different stages of maturation. After cell harvesting, they are cultured and grown *in vitro* to increase their number, maintain their profile of either differentiated or undifferentiated to be later on seeded on scaffolds to reconstruct and engineer constructs (Golchin *et al.*, 2020). Not only the profile is important, but also maintaining the mechanical properties is a requirement. To begin with, cells should adhere to the cell-adhesion site of scaffold to colonize it and start their proliferation. Next, depending on the signals or growth factors present, cells start to differentiate into their specific lineages and remodel the tissue being replaced. The cells receive their signals and molecules via proteins called integrins, anchored to the ECM.

Stem cells are defined as self-renewable, undifferentiated cells with the potential of multi differentiation abilities. They are characterized by a stable microenvironment, that stimulates and initiates different cellular and molecular signaling pathways, that control stem cell growth and pathways (Lane *et al.*, 2014; Rana *et al.*, 2017). Stem cells divide asymmetrically and give rise to a copy of the original stem cells and a progenitor daughter that can differentiate after the exposure of regulatory signals. It has been reported that in the stem cells niche, cells are exposed to many regulatory cues and signals. These include growth factors (GF), ECM proteins and molecules that mediate and support cell function and regulates cellular activities (Aamodt and Grainger, 2016; Perez *et al.*, 2014).

The interaction between stem cells and their surrounding microenvironment are pivotal to determine tissue homeostasis and stem cell renewal or differentiation and regeneration *in vivo*.

Stem cells niches have been identified and characterized in many adult tissue. **Figure 9** shows the different interactions of stem cells with their environment or niches. The critical components of stem cell niches include cellular, extracellular, biochemical, molecular and physical regulators. Thus, translational medicine aims at optimizing *in vitro* or *in vivo,* the various components and complex architecture of the niche to exploit their therapeutic potential (Vasanthan *et al.*, 2020).

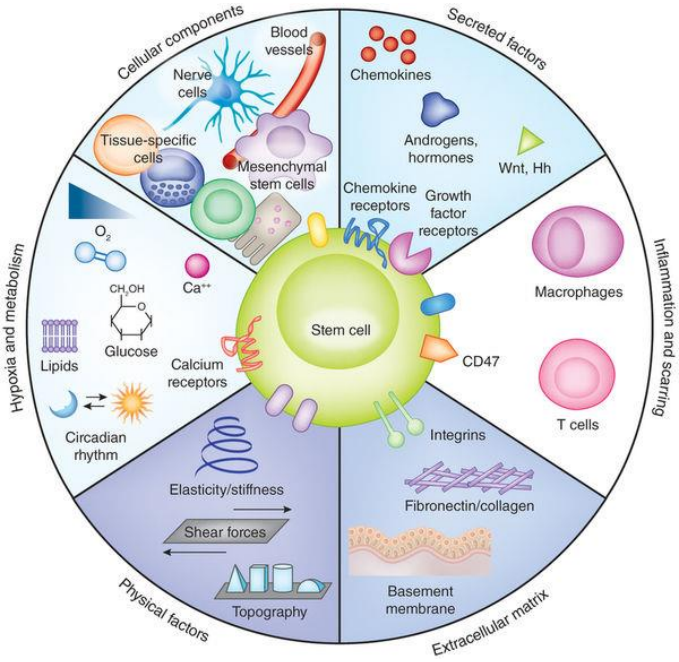

Figure 9: Stem cells and their different interactions, adapted from (Marino *et al*., 2019).

Based on their capabilities of differentiation, stem cells have been divided into four groups: unipotent, pluripotent, multipotent, and totipotent. Embryonic stem cells (ESC) are characterized as pluripotent stem cells, for their ability to differentiate into the 3 primary germ layers. These ESCs can expand to a high number of cells in culture. Also, many studies have reported that when implanted in immune-deficient animals, stem cells can divide in a noncancerous tumor that produces an advantage in using these cells in cell therapy (Javidpou *et al.*, 2020). Mesenchymal stem cells (MSC), on the other hand are multipotent stem cells obtained from different sources such as embryonic and adult sources. Bone marrow-derived mesenchymal stem cells (BMMSC) are the most common source of stem cells. These cells are simple to harvest and are characterized by good accessibility and a low risk of tumorgenicity. Nevertheless, BMMSC has some limitations,

where they can change their phenotype properties upon different factors such as donor age, sex of patients, alerting cell functions (Ohishi and Schipani, 2010). An additional source of stem cells derives from cord blood, where it consists of abundant hematopoietic stem cells. Due to their high availability, many studies have used umbilical cord blood (CB-MSC) and amniotic fluid-derived stem cells (AFSC), in regenerative medicine applications. For instance, Park *et al.*, has demonstrated that a single intravenous infusion of human CB-MSC resulted in a therapeutic potential for arthritis by upregulating regulatory T cells and downregulating T helper 17 cell expression, resulting in immune modulation and reducing the inflammatory cytokine release, thus a safe effect (Park *et al.*, 2018). In addition to the above stem cells, various cell biology techniques were used to harvest stem cells from amniotic fluid. AFSC have been employed for inducing osteogenic differentiation to form bone constructs (Eea *et al.*, 2019), tendon-like structures (Gonçalves *et al.*, 2013; Liao *et al.*, 2017) and skin graft to bioengineer autologous skin (Basler *et al.*, 2020).

Human AFSC has been reported to treat acute and chronic kidney diseases (Da Sacco *et al.*, 2018), and played a role to improve cardiac function in response to cardiac infarction (Gaggi *et al.*, 2020). Besides, adipose tissue represents an abundant source of stem cells with easy accessibility from a fresh stromal vascular fraction (SVF) cell population. Due to their low antigenicity, high proliferative and differentiation ability, adipose-derived stem cells (ADSC) are very convenient sources in many regenerative medicine approaches. ADSC was used to engineer dermo-epithelial skin substitutes where they were encapsulated in three-dimensional (3D) scaffolds and were implanted in immune-deficient rats. Neo-epidermis was efficiently reconstructed and tissue homeostasis was regenerated and sustained the epidermal coverage *in vivo* (Klar *et al.*, 2014). Since ADSC is capable of differentiating into hepatocyte-like cells, it was reported that ADSC was used as therapeutic tool to treat liver failure and restoring liver functions (Gao *et al.*, 2017; Han *et al.*, 2020). Furthermore, ADSC has great potential infertility problems and hair loss. Yoshida *et al.*, in their studies demonstrated that ADSC supports auditory hair cells, using specific proteins that enhanced the hair density and thickness (Yoshida *et al.*, 2011). It was also elucidated that ADSC could ameliorate sperm motility in male infertile patients, by secreting bioactive molecules and growth factors that positively influence the sperm motility (Cakici *et al.*, 2013). Not only can ADSC resolve male problems but also female infertility. Injection and transplantation of ADSC stimulate the ovarian follicles and thus improving the ovarian graft in rats (Fouad *et al.*, 2016).

Moreover, ADSC can be a safe treatment for damaged salivary glands. ADSC has been being transplanted into salivary glands and protected them from irradiation and mediated the regeneration of salivary gland (Lim *et al*., 2013).

Human-induced pluripotent stem cells (hiPSCs) technology, has also attracted interest in its potential therapeutic application in the field of regenerative medicine. IPSCs are more preferable than ESC since they lack ethical concerns linked with ESC. IPSC can be generated from a reprogrammed process from a wide range of cell types. Such as mesenchymal stem cells (Zhao *et al.*, 2021), cardiomyocytes, (Guo *et al.*, 2020). Nevertheless,, iPSC improved subsequent hepatic functionalization by producing liver buds with high productivity, thus facilitating therapeutic applications especially for liver diseases (Danoy *et al.*, 2021; Takebe *et al.*, 2017) and imparts hepatocyte metabolic function and resembling the hepatocyte physiology in the liver (Pettinato *et al.*, 2019).

Although adult-derived stem cells are the main source of cell-based therapy, they present many limitations. This could be related to their invasive isolation procedure and their low number of cells with limited self-renewal potential. Recently, many progenitors have been identified and they showed promising potential for auto and allogenic cell-transplantation. Among these progenitors, human nasal septum tissue has been evaluated. The nasal septum is mostly hyaline cartilage and their derived progenitors possess unique characteristics, rendering them attractive sources for cell therapy and clinical applications. Nasal-septum derived progenitors (NsP) are expandable, stable cell progenitors that can be expanded to more than 30 passages without any senescence or phenotype losing. They possess multi-lineage and self-renewal capacity (Elsaesser *et al.*, 2016). Shafiee *et al.*, have focused on NsP as potential sources for tissue engineering (Shafiee *et al.*, 2014). This was agreed by Pleumeekers *et al.*, that reported that combining nasal progenitors with MSC, reduced the required number of chondrocytes and improved chondrogenesis by reducing hypertrophy of cartilage (Pleumeekers *et al.*, 2015). Their multi-linages characteristics were proved by studies that showed differentiation into osteogenic and chondrogenic lineages where they possessed stable and chondrogenic surface markers on one hand and a superior higher chondrogenic potential and ECM production on the other hand (Shafiee *et al.*, 2016).

Dental pulp stem cells (DPSC) are highly accessible, undifferentiated mesenchymal stem cells present in the dental pulp tissue and characterized by their unlimited self-renewal as well as

multipotent differentiation potential illustrated by **Figure 10**. Dental stem cells have been used in many tissue engineering applications. Some studies showed the capacity of DPSC to express chondrogenic markers (Paino *et al.*, 2014; Westin *et al.*, 2017), other highlighted their capacity of generating capillary-like structure in presence of vascular endothelial growth factor (VEGF) (Marchionni *et al.*, 2009). Gandia *et al.*, investigated the differentiation capacity of DPSC into cardiomyocytes formation to reduce myocardial infarction (Gandia *et al.*, 2008). Several groups have reported that DPSC when seeded on multiple scaffolds such as chitosan, poly(lactide-co-glycolide) (PLGA) and collagen porous biomaterials, regenerated bone defects *in vitro* and *in vivo* in animal models (Graziano *et al.*, 2008; Yang *et al.*, 2012).

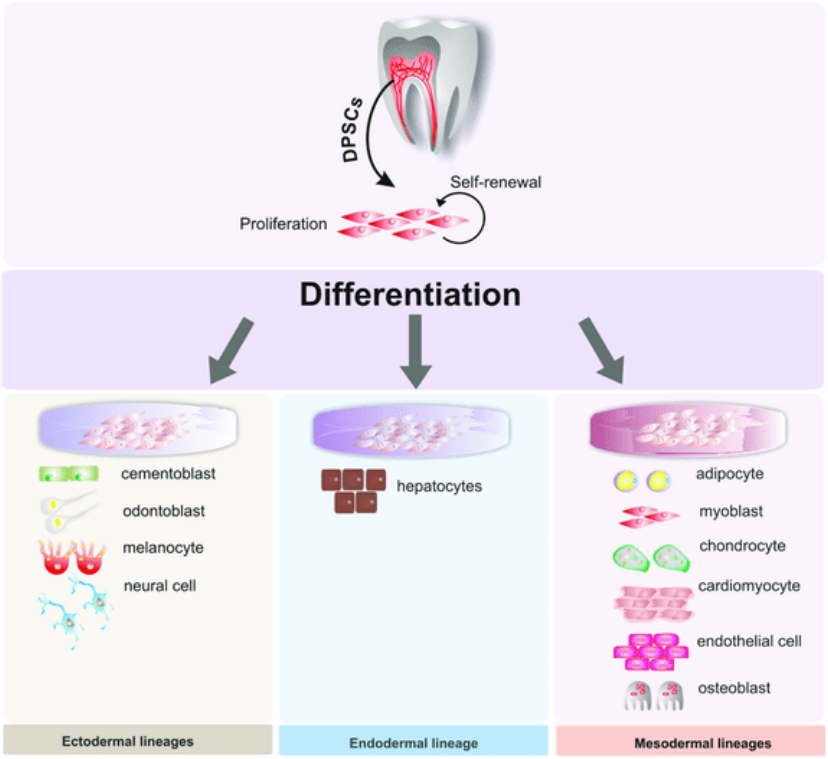

Figure 10: Multilineage potential of human dental pulp stem cells (Rodas-Junco *et al.*, 2017).

A recent study has also demonstrated that DPSC when seeded on collagen scaffolds, and cultured with fibroblast growth factor-2 (FGF-2), strongly enhanced craniofacial bone regeneration in immunodeficient mice (Novais *et al.*, 2019).

2.3 Biomaterials for tissue engineering

The scaffold is the center component that is used to support, house, and direct growth of cells either seeded within scaffold or migrated from surrounding environment. An ideal scaffold should fulfill these specifications. First of all, it should be biocompatible, thus capable to perform its function without inducing any inflammatory response. This biomaterial should also be biodegradable, to easily be eliminated from body and should integrate with no harm to the native tissue. Porosity is an important requirement for optimal interaction and penetration of cells into scaffolds. It should provide an open and interconnected pore network that facilitates the exchange of metabolites and nutrients and promotes their transport. Moreover, scaffold chosen should be easy to process and flexible to manipulate, depending on tissue needs. In addition to that, it should conserve its biomechanical function after its implantation *in vivo*, to reconstruct a fully function integrated tissue with its surrounding environment (Nasonova *et al.*, 2015).

Understanding and defining the native tissue to be reconstructed, is a critical step in tissue engineering. Before choosing cell sources and the appropriate scaffold to harbor cells, one should understand the biological and biomechanical functions of the tissue of interest. Mechanical characteristics should be studied more and the comparison between scaffold and construct should be evaluated better. Consequently, there has been a recent emphasis on increasing the biocomplexity of scaffolds to better mimic the dynamic natural of ECM.

2.3.1 Extracellular Matrix (ECM)

The ECM is an active surrounding that interacts with cells first to induce their proliferation and differentiation. The ECM itself can offer to widen proteins revealing binding sites on its structure that can affect the distribution of proteins and molecules to interact with each cell type differently.

It consists of structural proteins, proteoglycans, fibronectins that provide flexibility, collagens, elastin and 3D shape due to their high water binding ability. Glycoproteins such as integrins are also present to regulate cell adhesion and ECM-cell signaling (**Figure 11**). ECM proteins are outside the plasma membrane are connected with cytoskeleton fibers and transmembrane proteins (Xue and Jackson, 2015). The composition of ECM facilitates the diffusion of nutrients, maintains

matrix stiffness and sustains cell adhesion and migration. Proliferation and adhesion of cells depends on the matrix environment in which cells are cultured.

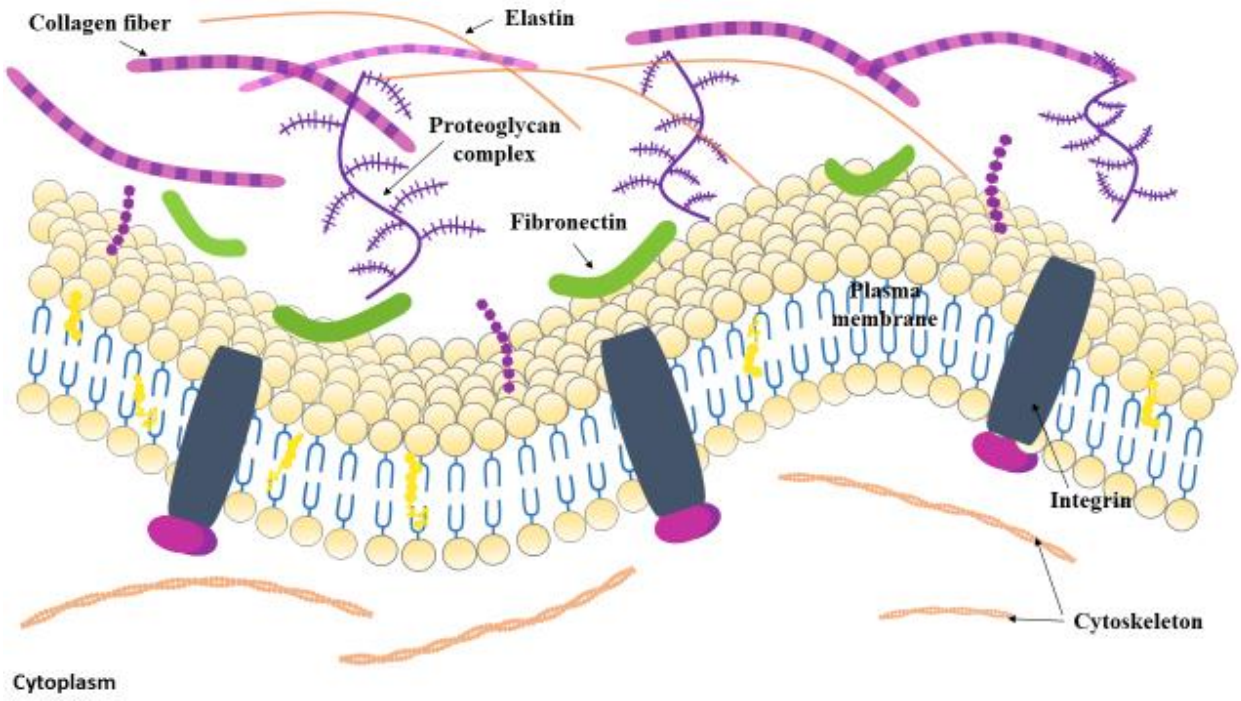

Figure 11: Major extracellular matrix components and their interactions with each other and cell membrane adapted from (Xue and Jackson, 2015).

Not only are cells responsive to ECM adhesion, but more to the stiffness and density of corresponding matrices. Furthermore, an inverse correlation is sometimes found between matrix density and cell migration. Fibroblasts, for example, migrated slowly when collagen fibers in ECM increased (Tracy *et al.*, 2016). Cells also respond to elasticity where they differentiate into different lineages, depending on stiffness and softness of biomaterial involved.

2.3.1.1 Permeability of ECM

Not only rigidity and stiffness are critical for an ideal ECM, but also permeability and diffusion of nutrients and wastes are necessary for such biomaterials. For optimal growth, an ECM that allows metabolic activity, such as nutrients and waste exchange can highly influence cellular physiology and function. Dense ECM can affect the passage of nutrients and metabolites to the interior of tissues and organs. High density can prevent the removal of wastes and unwanted compounds,

rendering the tissue necrotic (Bracaglia and Fisher, 2015). Size and organization of pores are critical for optimal function of the tissue. Porosity is important in both natural and synthetic scaffolds.

2.3.1.2 Cell-cell interactions

Cells respond differently to their surrounding environment by releasing proteases due to the composition of ECM and its degree of sensitivity to the surrounding matrix. Degradation of the matrix would influence the number of cell-matrix adhesions, thus inducing cells to initiate the remodeling of their environment to restore functional activity (Bonnans *et al.*, 2014).

Cell-cell interactions are crucial for the development and function of tissue and organs, due to the communication made between themselves that recapitulates the native environment and provides the cues for a functional tissue. These interactions and signals can mediate cellular development and differentiation; play a crucial role in tissue maintenance, and immune responses (**Figure 12**).

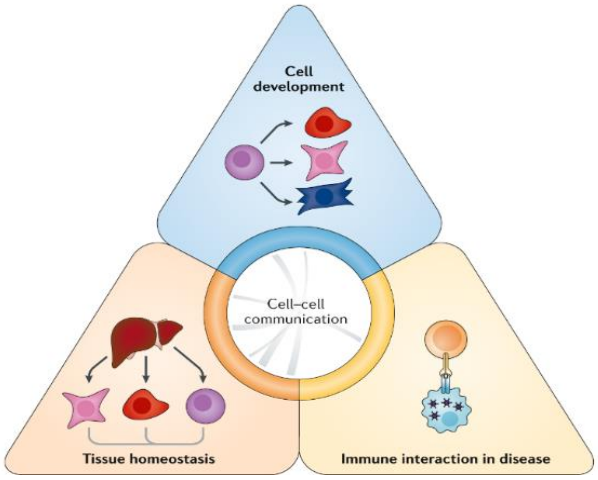

Figure 12: Main applications of cell-cell interactions (Armingol *et al*., 2021).

Researchers showed that co-culturing of both epithelial cells and myoepithelial cells formed penetrating tubes via adherens and gap junctions. This led to the development of basal and apical membranes for a proper secretory function. Integrins are the first class of receptors that manage cell-matrices adhesion. They are made up of two transmembrane units, where alpha subunit is large and beta is the smaller one. Integrin family can form a different combination of each of their subunits and can reach 24 different heterodimers (Moreno-Layseca *et al.*, 2019). They are ECM

anchors and transmit mechano-chemical signals to the cells via different mechanisms, especially intracellular transduction.

Tissue engineering has used a variety of biomaterials both natural and synthetic to repair and replace lost or diseased tissue. These biomaterials serve as 3D scaffolds, providing the appropriate environment and satisfies bulk and surface properties to avoid failure of constructs after implantation. Bulk properties are related to the type of bonding and atomic forces between scaffold components, whereas surface properties are more of physical characteristics such as energy, roughness and surface composition. In addition, interaction between materials and scaffolds should not cause any toxic or deleterious effects on the surrounding host tissue.

2.3.2 Natural scaffolds

2.3.2.1 Collagen

A Nature polymer that has been used for different applications in tissue engineering. It is the major protein component in ECM that interacts with cells in connective tissue and combines with other proteins to transmit signals for the migration, proliferation and differentiation of cells. Possessing a 3D structure, collagen encourage cellular growth and modifies morphology where it can be cross-linked in much different tissue such as bone, tendon, cartilage skin and cornea (Meyer, 2019). Compared to other proteins, collagen has a good biocompatibility and biodegradability, with high mechanical strength. Cell seeding on 3D scaffolds of bovine collagen I biomaterial created a commercialized product as a skin substitutes.

2.3.2.2 Silk fibroin

A tough natural biomaterial, derived from silkworm Bombyx mori, has a strong and elastic character and exhibits mechanical properties comparable to the best synthetic fibers produced by modern technology. It's biocompatibility and high porosity *in vitro* , that make it an excellent candidate for tissue engineering, where it has slow degradability and could be modified by several chemical treatments to be explored and used in various application such as wound healing, liver, bone and cartilage tissue engineering. It has also been shown to play a role in supporting Schwan cells and thus an interesting factor for nerve tissue engineering (Pham and Tiyaboonchai, 2020).

2.3.2.3 Chitosan

It is a polysaccharide derived from chitin, with a pH-sensitive character since it's the chain is rich in amino acid groups. It is a biological biocompatible, biodegradable and affordable polymer however, it induces rapid bone regeneration at site of implantation. Scaffold prepared from chitosan has been used in regeneration of bone and cartilage, tendon tissue and sometime chitosan is modulated with biochemical or physical properties for better performance (Rodríguez-Vázquez *et al.*, 2015).

2.3.2.4 Hyaluronic acid

It is one of the major ECM components, natural non sulfated glycosaminoglycan, biocompatible but present poor mechanical properties. Numerous natural materials and polymers were used to mimic the extracellular matrix and facilitate cellular adhesion. These include alginate, collagen, hyaluronic acid (HA), fibrin, acellular scaffolds.

2.3.2.5 Alginate

Alginate are natural, biocompatible polymers extracted from brown algae or polysaccharide derived from bacteria. This polymer can create ionic binds when exposed to different ions such as calcium, magnesium, barium or strontium (Amorim *et al.*, 2021). Its carboxyl group increases the swelling capability of alginate to induce simple gelation and to be resistant to acid solutions. On the other hand, it presents a poor mechanical property since the rate of degradation is uncontrolled. A wide range of applications has been linked to alginate. Alginate beads were implicated in drug delivery, they encapsulated cells and served as a hydrogel for bone (S. Yang *et al.*, 2020), cartilage (Saygili *et al.*, 2021), liver (Rajalekshmi *et al.*, 2021) and pancreas tissue engineering, as well as vascularization procedures.

Alginate-based hydrogels have gained interest in cell encapsulation and tissue engineering. Due to their availability and non-immunogenicity, many scientists have used them as biomaterials. Researchers have encapsulated MSC into Arg-Gly-Asp-modified alginate microspheres to examine cellular viability and their bone regeneration efficiency. MSC as a result showed high survival in alginate microspheres, where alginate guided their functions and ensured bone regeneration (Ho et

al., 2016). Another study by Ansari *et al.*, demonstrated that periodontal ligament stem cells encapsulated in a hydrogel made up of alginate and HA in combination of TGF-β1, differentiated into chondrogenesis *in vitro* and *in vivo* (Ansari *et al.*, 2017). Jin et Kim has reported that also alginic hydrogels may suppress dedifferentiation of chondrocytes. They used 3 different gels: alginate, collagen and a combination of both, considering that maybe combination of these gels can enhance growth of chondrocytes and lower their dedifferentiation. Their results have suggested that chondrocytes cultured in Alginate/collagen gel preserved better chondrocyte phenotype and significantly suppressed dedifferentiation, compared to those in alginate or collagen gel alone, shedding light on the importance of optimizing hydrogel conditions for successful cartilage-tissue engineering (Jin and Kim, 2018). A novel approach was published by Visscher *et al.*, where they printed an auricular implant model that was easy to inject with hydrogel. They combined both polycaprolactone (PCL) and alginate and created a two-part biodegradable 3D-printed mold. First, this mold was made from PCL and was injected later on with chondrocyte-laden alginate that supported cell survival after 21 days. Their model can be easily printed and injected with any type of cell source, providing possibility of fabrication of tissue and organs (Visscher *et al.*, 2019).

2.3.3 Synthetic scaffolds

2.3.3.1 Metals and polymers

Although these biomaterials presented natural ECM, however, some products weren't really desirable since they were produced from animals and carried diseases and pathogens (Hughes *et al.*, 2010). Due to their physical and chemical properties, synthetic polymers are of high interest in regenerative applications. These biomaterials are more reproducible and more conformable compared to natural biomaterials. They are designed in simple, degradable matrices, controlled by different polymers, crosslinks, and organizations. Among the most frequently used synthetic scaffolds for tissue engineering are Poly (ethylene glycol) (PEG), poly (vinyl alcohol) (PVA), polycaprolactone (PCL) and poly (lactic-co-glycolic acid) (PLGA), that showed a great impact on directing stem cells fate and supporting their adhesion and proliferation (Wasyłeczko *et al.*, 2020). Many studies have reported the use of these synthetic materials in directing cells towards a specific lineage. Mirzaei *et al.*, showed that the addition of an optimized PEG into polylactic acid (PLA) solution enhanced the hydrophilicity as well as the mechanical properties of the nanofibrous meshes. Besides, the addition of glucosamine in the scaffold promoted cell adhesion and

differentiation of MSC towards chondrocytes (Mirzaei *et al.*, 2017). Others have designed a 3D PEG-based hydrogel crosslinked with collagen I, that provided easy support without affecting cell differentiation and proliferation. Also, the encapsulation of human adipose-derived stem cells in ECM PEG hydrogel enhances the lipid formation and thus adipose regeneration after 2 weeks (Li *et al.*, 2018).

2.3.3.2 Ceramics

Apart from metals and polymers, bioceramics have been recognized as candidates for dentistry and orthopedic application, due to their critical properties and resistance to weight. They are classified into 3 types, consist of bioactive ceramics such as glass and polycyclic aromatic hydrocarbons, bioglass, and high strength ceramics including alumina, zirconia and carbon. Zirconia-based ceramics has been an attraction for bone stem cell differentiation, since it is characterized by a superior mechanical strength and toughness character, to support implants. In their studies, Komine and Kitagawa, found that zirconia was able to induce chondrogenic differentiation of equine BMMSC, that was seeded into the microwells. There was an upregulation of COL II, ACAN and cartilage oligomeric matrix protein (COMP) markers in the microwells supported by the physical properties of zirconia (Inui *et al.*, 2019). Furthermore, alumina has also been attractive in skeletal regeneration application, due to its hardness and firmness properties. As for bioactive glasses, they were formed from glass precursors such as silica, phosphoric oxide and sometime boric acid. Scientists have demonstrated the use of bioactive glasses with stem cells and showed that different ions could be released during the incorporation of glasses with cells and may lead to change their pathway and fate.

2.3.3.3 Nanomaterials

Although hydrogels and porous scaffolds have stimulated stem cell differentiation, however, they still fail to completely mimic the nanoscale of ECM. Various studies have reported the use of nanofibers, nanocues to control stem cell growth and function in cartilage tissue engineering (Chen *et al.*, 2021; Ding *et al.*, 2020). Other studies have provided the possibility of using carbon-based nanomaterials such as carbon nanofibers, diamond-like carbon, graphene and its derivatives and

carbon-based quantum dots. Due to their excellent mechanical, chemical and thermal properties, in addition to their novel structure and unique composition, these materials have attracted interest as carriers of stem cells and delivery of molecules for tissue engineering and cell therapy. (Kim *et al.*, 2016; Menaa *et al.*, 2015). Yao *et al.*, have provided that the incorporation of PLA into PCL nanofibers, enhanced the human MSC osteogenic potential and the differentiation towards bone formation *in vivo* (Yao *et al.*, 2017). Onoshima el al., has utilized quantum dots and incorporated them as bioprobes or biological labels for cell, he used them as fluorescent probes that were used for stem cells labeling (Onoshima *et al.*, 2015). As mentioned above, many nanomaterials can enhance stem cell growth and function, however, some other studies have reported the toxicity that can be imparted from silica nanoparticles. Mouse embryonic stem cells were exposed to four different silica nanoparticles in different concentrations, where they impaired and inhibited the differentiation of stem cells.

In contrast to natural hydrogels, synthetic hydrogels alone permit but don't promote cellular activity, however, when combined with bioactive polymers most commonly PEG, they fine-tune biochemical and mechanical properties. PEG is an interesting bioactive molecule due to its hydroxyl end groups that crosslink with peptide and growth factors. In order to have superior engineering effects, synthetic and natural polymer combine together by conjugating their functional groups together to form hybrid hydrogels. Using their specific reactive groups such as carboxylic groups, thiol groups, polymers form covalent bonding with natural scaffolds such as collagen, chitosan, heparin and others (Hao *et al.*, 2016). Many examples of hybrid hydrogels were investigated by several researchers, for example PEG was coupled to matrigel and was shown to play a specific role of mechanical and adhesive inputs on 3D tumor growth, invasion, and dissemination (Beck *et al.*, 2013). In other reports, PEG was combined to photoinitiator and exposed to UV to form hydrogels to cultivate cells in 3D environment (Almany and Seliktar, 2005; Pradhan *et al.*, 2017), also heparin-based hydrogel showed to be a promising matrix in presence of PEG for encapsulation and differentiation of hepatocytes and stem cells (Kim *et al.*, 2010).

2.3.4 Hydrogels

3D structures have received remarkable attention in the *in vitro* cell culture. Indeed, these 3D structures mimic the natural environment found *in vivo*. So that the cell morphology closely

resembles its normal shape in the body. In cartilage tissue engineering, it has been shown that chondrocytes encapsulated in 3D hydrogels, sustain and conserve their phenotypic stability, that limit their dedifferentiation (Gz and Hw, 2018). Many 3D natural and synthetic scaffolds were evaluated for their chondrogenic properties, however there is an increasing demand for other substitutes scaffold that may enhance cartilage tissue engineering. 3D hydrogel models are illustrated in **Figure 13** where they present porous hydrogels, fibrous scaffolds, cellular encapsulated systems, microwells and microfluidics, and sandwich scaffolds until reaching 3D bioprinting.

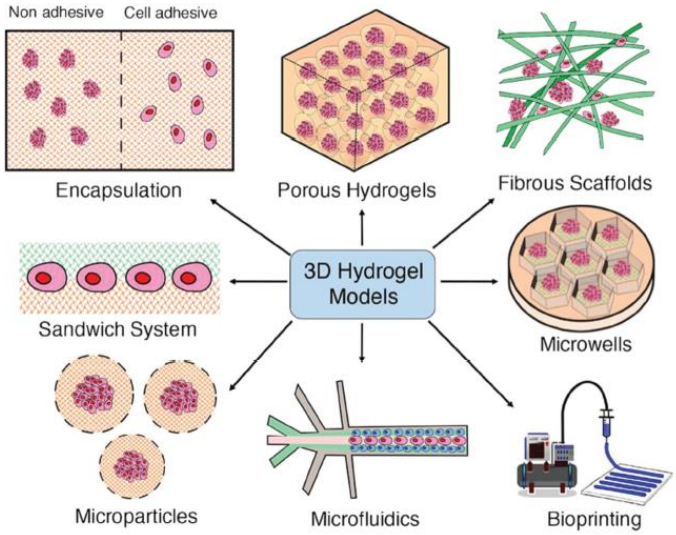

Figure 13: Scheme illustrating different types of hydrogel models (Liaw *et al*., 2018) .

Porous scaffolds are mainly produced by lyophilization. Leaching and sometimes gas foaming. The pore size is larger than cells to permit attachment and migration of cells, as well as the facility of nutrients and oxygen transport.

Fibrous scaffolds are usually prepared by self-assembly, phase separation, and electrospinning technique. Researchers have investigated self-assembly when producing amphiphilic peptide that assembled into nanostructure that was highly bioactive in tissue-engineered and spinal cord therapy (Cui *et al.*, 2010). Other studies have mentioned electrospinning technique and thermal phase separation of nanofibrous collagen into a nanostructure that improved cell adhesion and promoted

bone tissue formation, and PCL/PLA electrospun technique for cartilage regeneration (Holzwarth and Ma, 2011; Yao *et al.*, 2017). Gelatin was also blended with natural or synthetic polymers and showed increased biomechanical and biocompatibility properties, attractive for bone, cartilage and vascular tissue engineering (Aldana and Abraham, 2017).

Microencapsulation of cells has also been used in different fields. Cells are encapsulated and immobilized in 3D environment by hydrogels that isolate them from the outside environment, enhancing their cell-cell interaction and differentiation and secretion properties. Extrusion, emulsion and microfluidics systems were most common for cellular encapsulation. Not only this microencapsulation system enhances growth and development of cells, but also serves to regulate cellular physiology. To produce this system, cells are first seeded on the surface of the hydrogel, cultured to let cells attach on to the surface of the hydrogel. Next, a second layer of the hydrogel is placed on top of seeded cells, producing a sandwich model where cells are in the middle of two layers of hydrogels.

Microwell is another way to trap cells and induce them to form spheroids. It is a multi-step process, where a mold is created usually from poly(dimethylsiloxane) PDMS, using the soft lithography technique. The hydrogel is then introduced and crosslinks with PDMS in microwells. Hydrogel-based microwells can be further modified by the incorporating of different proteins using their bottom surfaces to enhance cell-matrix adhesion. Zhang *et al.*, have engineered 3-based PDMS microniches using soft lithography technique for regulating the phenotype and function of chondrocytes in native cartilage. Chondrocytes were cultured in these micro niches that enhanced their mechanical properties and the functionality of the chondrocytes (Kavand *et al*., 2019; Q.-Y. Zhang *et al*., 2020) and osteoconductive regeneration of bone tissue (Kiyama *et al.*, 2018).

2.3.5 Decellularized scaffolds

Due to the challenges associated with preparing synthetic matrices that can mimic cell microenvironment, there has been an increasing demand for the use of the naturally-derived ECM obtained with the help of decellularization processes. Decellularization is the elimination of cells and genetic materials from a native tissue while conserving its structural, biochemical and mechanical properties (Keane *et al.*, 2015). These bio-derivative scaffolds could then be used either

as personalized tissue when repopulated by the patient own cells, or an allogenic or xenogeneic biological support for developing engineered tissues or organs (**Figure 14**).

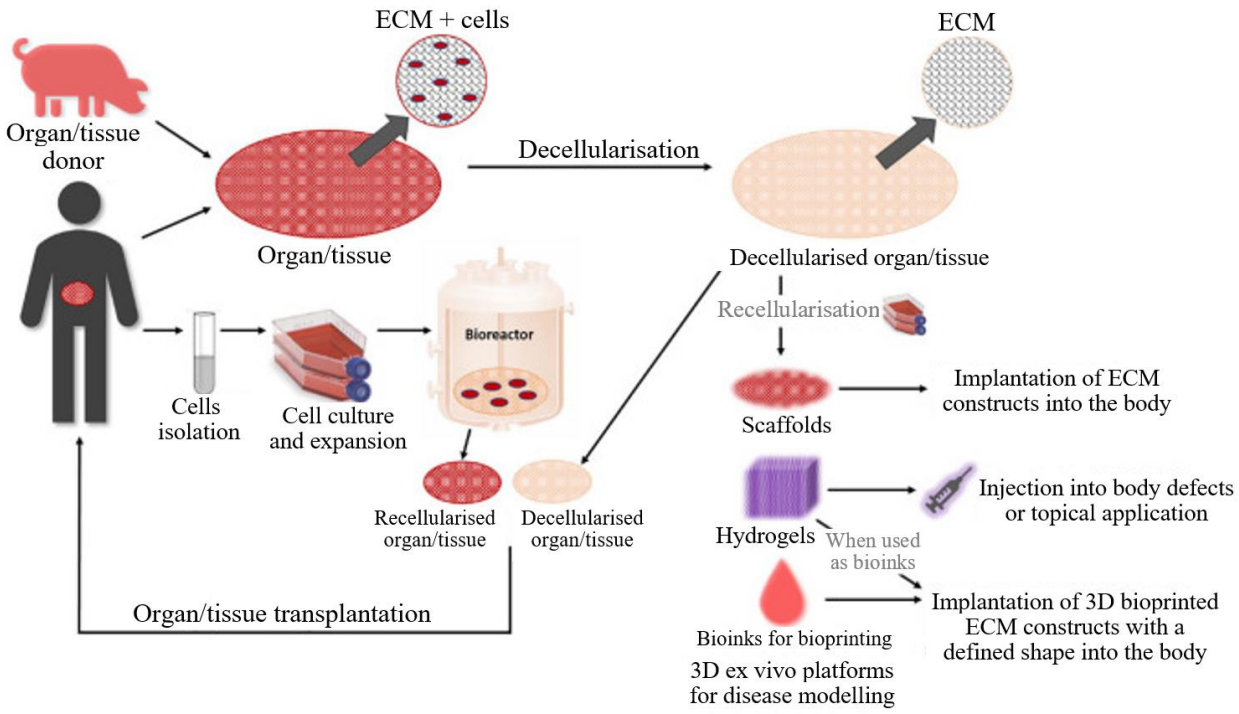

Figure 14: Decellularization of animal or human tissue and its recellularization by implanting extracellular matrix (ECM) into the body or evaluating the tissue using a bioreactor then transplanting it back to the patient Adapted from (Fu *et al*., 2014)

Extracellular matrices provide a niche for cells, architecture for tissues, in addition to some proteins and growth factors that can drive cellular differentiation and sustain development of tissues and organs. To characterize and asses the quality of the decellularized matrix, three different factors should be measured: A complete removal of cellular materials and total elimination of genetic materials to prevent immune rejection of the scaffold after repopulation of cells (**Figure 15**).

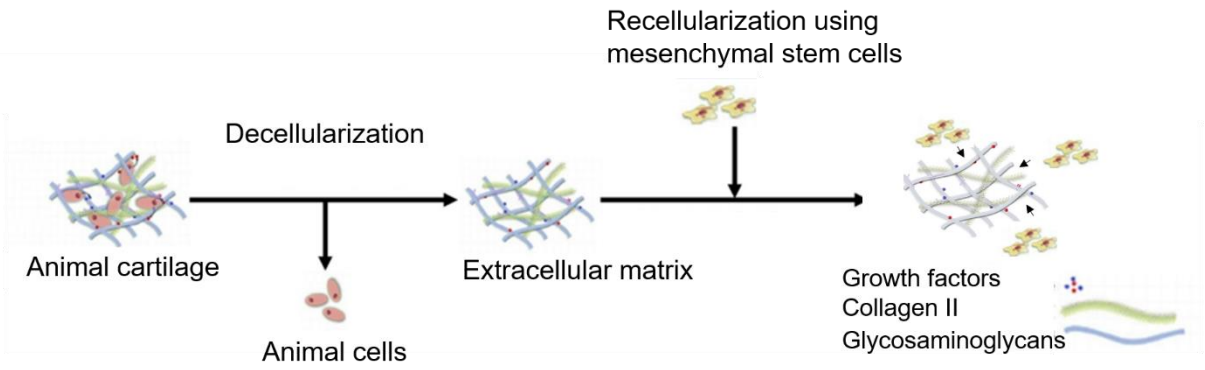

Figure 15: Cell-free tissue can be generated by decellularization of native tissue. The remaining ECM can then be seeded with different cell types adapted from (Bourgine *et al*., 2013).

The criteria for producing good, efficient scaffold is that the decellularized ECM should have less than 50ng double-stranded DNA (dsDNA) per mg of ECM dry weight, less than 200bp DNA fragment length and no visible nuclear material when staining with 4'6-diamidino-2-phenylindole (DAPI). ECM proteins such as fibronectin, collagen, GAGs should be conserved during decellularization processes as well as the structure and integrity. Finally, the decellularized scaffold should be able to attain its biomechanical properties in order to restore its function after transplantation (García-Gareta *et al.*, 2020).

Reducing the scaffold's immunogenicity is a critical factor for the use of a decellularized scaffold in clinical applications. The factors capable of inducing immunogenicity are genetic materials such as DNA, RNA and antigens. Specific epitopes must be measured such as alpha-gal epitopes which can induce the complement cascade immune response and major histocompatibility complexes located on the cell membrane. Next, restoring mechanical properties is an essential characteristic to ensure optimal scaffolding.

Due to the cartilage high density, native tissue should be disrupted in order to allow chemicals and reagents to increase their efficiency of decellularization. This could be performed by first exposing tissue to physical and mechanical treatments such as freeze-thaw cycles, osmotic pressure, this would increase cell lysis and thus exposing tissue less to chemical reagents, which is very important for the retention of microstructure and preservation of ECM proteins. Decellularization has been performed using different strategies and methods.

2.3.5.1 Chemical and enzymatic techniques

Several chemical and enzymatic agents have been used in the decellularization process: Surfactants are most common as decellularizing agents. Their mode of action is to lyse cells by disarranging the phospholipid membrane, which facilitates the elimination of cells and genetic material. These surfactants are classified according to their charges. They can be ionic, nonionic and zwitterionic. Sodium dodecyl sulfate (SDS), is the successful most used surfactant due to this ability to efficiently remove cells and genetic material. It was the major and agent used in decellularization of the whole rat heart perfusion by (Ott *et al.*, 2008) that showed a revolution in decellularization processes (**Figure 16**).

SDS was also used to decellularize human heart and valve (Guyette *et al.*, 2016). Not only did SDS maintain and preserve the ultrastructure of whole organs via perfusion, but also it prevented deformation of certain vessels and organelles in perfusion of human and porcine lungs (Gilpin *et al.*, 2014), porcine kidneys (Sullivan *et al.*, 2012), porcine cornea (Pang *et al.*, 2010) and tubular small intestine protocols (Syed *et al.*, 2014).

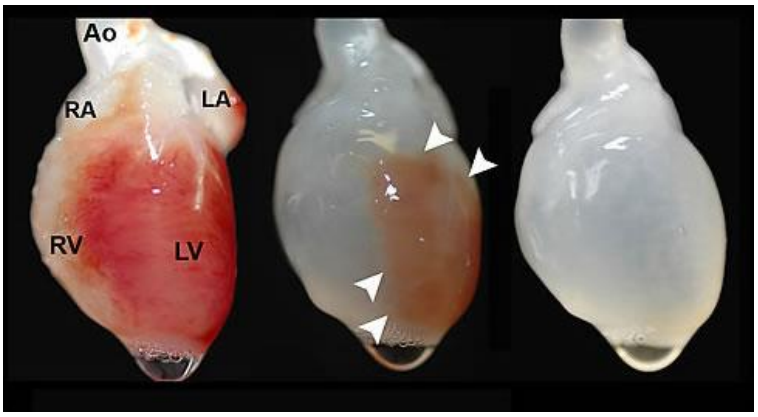

Figure 16: Perfusion decellularization of whole rat hearts. SDS perfusion yielded full removal of cellular consituents after 12hrs. Ao: Aorta; LA: left atrium; RA: right atrium; LV: left ventricle; RV: right ventricle (Ott *et al.*, 2008).

Despite the advantages of using SDS for decellularization, some problems lie behind the use of SDS, where it may be also damaging to the structure and signaling protein. For instance, GAGs were decreased upon SDS treatment, which prevented the full retention of mechanical properties of the decellularized tissues.

Sodium deoxycholate (SD) is another ionic surfactant that works by solubilizing the cell membrane and produces highly biocompatible scaffolds. To avoid DNA agglutination on surface of tissue, this latter is combined with deoxyribonuclease I (DNase I) enzyme, to breakdown DNA. SD was used to retain structural proteins necessary for the tissue's function such as myosin after decellularization of lungs (Kuevda *et al.*, 2017), as well as the preservation of collagen and elastin in heart valves (Namiri *et al.*, 2018). Cells have also shown a high metabolic activity when seeded on SD-decellularized matrices.

On the other hand, Triton X-100, a nonionic detergent, less damaging to the structure of tissue and was used sometimes to remove traces of SDS. Also, it was used to decellularized many whole organs such as heart (Ramm *et al.*, 2020), lungs (Hashimoto *et al.*, 2019), liver (Zhao *et al.*, 2020) and cartilage (Vas *et al.*, 2018) . Moreover, when Triton X-100 was combined with ammonium hydroxide, it preserved ultrastructure, mechanical properties and a greater amount of collagen I that maintained after decellularization compared to SDS treatment (Sullivan *et al.*, 2012).

As for zwitterionic detergents, 3-[(3-cholamidopropyl)dimethylammonio]-1-propanesulfonate (CHAPS), has been applied to many decellularization processes. Wang and his colleagues used decellularized autologous ECM-based grafts using CHAPS, to regenerate neoartery in minipig model (T. Wang *et al.*, 2019). CHAPS helped in a complete acellular conduit with excellent performance in mechanical properties.

2.3.5.2 Acids and bases

These agents solubilize the cell membrane by utilizing charged properties. For instance, Ethylenediaminetetraacetic acid (EDTA), decreases salt and acid-soluble ECM proteins. It is used alone to replace non-ionic detergents to form an ECM scaffold with high biocompatibility, low cytotoxicity and good mechanical properties (Xu *et al.*, 2017). Also, it creates a denser, more compacted matrix with well conserved microarchitecture of ECM in the decellularization of hepatic tissue (Maghsoudlou *et al.*, 2016). Moreover, EDTA can be combined to Triton X-100 and trypsin in some decellularization protocol to enhance the lower DNA contents and to achieve high GAG preservation and good biocompatibility.

2.3.5.3 Enzyme-assisted Decellularization

It was mentioned before that DNase I is usually added to SDS treatment to prevent the agglutination of DNA on the surface of tissue. Similarly, many enzymes have been used to supplement the activity of chemical properties. For example, trypsin which breaks cell-matrix adhesions was used with EDTA to decellularize human corneal lenticule. The hypotonic solution was added to trypsin/EDTA and this treatment resulted in transparent, biocompatible where ECM proteins were preserved and the tissue looked like the native corneal tissue (Huh *et al.*, 2018). Trypsin was also used in decellularization of porcine pulmonary valves to completely remove cell material after 24 hours of incubation. However, this long exposure led to decrease in the amount of ECM proteins such as GAG's, collagen, elastin and eventually limited the mechanical strength of the tissue (Schenke-Layland *et al.*, 2003). In another study and for the aim of heart valves decellularization, Triton X-100, DNase I and RNase I were added after trypsin/EDTA treatment. This step allowed the complete removal of cell remnants and preserved elastin fibers (Zhou *et al.*, 2010). Therefore, chemical approaches can be enhanced by adding enzymes, and chelating agents. Although chemical and enzymatic decellularization may result in good cell removal and biocompatibility of scaffold, cytotoxicity can be encountered easily after such treatments. That's why various studies have introduced mechanical and physical approaches depending on temperature and pressure. Freeze-thaw cycles can vary from -80°C to 37°C, they involve the rapid change of temperature that can cause lysis of cells but not complete removal of cellular materials (Xing *et al.*, 2015). High pressure, is another option to destroy cell membranes, but it is harsh on ECM where it can denature ECM proteins such as collagen and elastin. Although this treatment sterilizes the tissue by destruction of bacterial and viral membranes, it can affect structural and mechanical properties.

To achieve a biocompatible, non-immunogenic scaffold, mechanical approaches should be combined with chemical approaches to completely remove cellular material with less damage to the tissue structure. Indeed, the construction of perfusable, functional organs requires a vascular optimized ECM. Thus, flow-controlled and pressure perfusion are the two suitable perfusion systems to completely decellularize whole organs.

Recellularization is the repopulation of decellularized, acellular scaffolds of tissues and organs with specific cell types to reconstruct their microstructure, thereby restoring their function. Cells populated on ECM scaffold requires support and guidance by specific growth factors and signals

from ECM for their maturation and differentiation. Thus, the preservation of these proteins and signals during decellularization is essential for obtaining an optimal recellularization process (W. Yang *et al.*, 2018).

Recellularization is performed using two different ways. The first technique uses perfusion in the vascular network of organs, while the second is via direct injection of cells. And sometimes both techniques are combined to optimize outcomes (Robertson *et al.*, 2014).

The first successful perfusion decellularization and recellularization were done on a cadaveric rat heart, where Ott and his colleagues used SDS for 12 hours to produce a complex, biocompatible perfusable cardiac ECM scaffold with vascular valves. This latter was reseeded with rat neonatal cardiomyocytes and rat endothelial cells. This bioengineered heart showed contractile responses upon electrical stimuli and developed a functional ventricle (Ott *et al.*, 2008). After that, many other decellularization techniques of mouse, porcine and human heart has been performed. Lu *et al.*, for instance, used xenogeneic cell scaffold combinations of mice ECM and human cells, they created heart constructs by repopulating decellularized mouse hearts with human induced pluripotent stem cells derived from cardiac progenitors and showed that these cells migrated and proliferated towards cardiomyocytes and endothelial cells reseeding decellularized heart. They also realized that after 20 days of perfusion, the heart constructs generated contractions and mechanical forces (Lu *et al.*, 2013). Furthermore, human hearts have also been decellularized, producing acellular cardiac scaffolds with preserved ECM material properties, that were functionally regenerated upon seeding with human iPS-derived cardiac myocytes. As a result, heart constructs presented contractile and functional myocardial tissue (Guyette *et al.*, 2016). Regenerated pulmonary vasculature was achieved by repopulating the vascular system of decellularized human lung with human derived iPS (Ghaedi *et al.*, 2018). They were later on optimized using a bioreactor. Various studies have also investigated recellularization of liver (Wang *et al.*, 2015) and the kidneys (Hu *et al.*, 2020).

2.3.6 Vegetal matrices

Cellulose is most abundant source of organic matter in nature. It exists as a structural component for plant cell walls and also produced by bacteria itself as a protective envelope. Cellulose is the

preferred choice for biomaterial fabrication because of its natural source and availability. Being bioactive, biocompatible and biomechanical, as well as its representation of a low-cost platform for engineering tissue. Cellulose fibers strengthen plant cell walls and comprise a matrix of hemicellulose containing pectin or lignin. Cellulose is arranged in microfibrils and organized in an orderly structure. Hydrogen bonds form between cellulose and the polysaccharide hemicellulose to sustain and interconnect the matrix (arabinoxylans, xylans) and the stiff cellulose microfibers. Plants offer a unique transport system, where it possesses a branching system that consists of highly interconnected pores and vessels to ensure a feasible transport system of oxygen, water and nutrients(Courtenay *et al.*, 2018).

Different plant species were tested for their ability to retain a substantial amount of water after their decellularization. Vanilla and parsley stem maintained their porosity after decellularization, this enlarged their pore size. Stiffer stems like bamboo were able to retain almost four times their weight in water, however, softer stems (vanilla and parsley) retained 20 times their weight. Due to their ability to conserve ultrastructure's hierarchy and hydrophilicity, they were interesting scaffolds for mammalian cells. The highly hydrophilic characteristic of plant tissue and their efficacy in transport of fluids enabled efficient expansion of human cells. Decellularized plants were coated with RGD- dopamine conjugate that supported the adhesion of human dermal fibroblasts as well as maintaining plant's topographical features. Human MSC and fibroblasts were seeded on different stems. Significant MSC expansion was shown in parsley stems compared to vanilla and calathea stems that presented significant decrease in cell number Different plant species were tested for their ability to retain a substantial amount of water after their decellularization. Vanilla and parsley stem maintained their porosity after decellularization, this enlarged their pore size. Stiffer stems like bamboo were able to retain almost four times their weight in water, however, softer stems (vanilla and parsley) retained 20 times their weight. Due to their ability to conserve ultrastructure's hierarchy and hydrophilicity, they were interesting scaffolds for mammalian cells. The highly hydrophilic characteristic of plant tissue and their efficacy in transport of fluids enabled efficient expansion of human cells. Decellularized plants were coated with RGD- dopamine conjugate that supported the adhesion of human dermal fibroblasts as well as maintaining plant's topographical features. Human MSC and fibroblasts were seeded on different stems. Significant MSC expansion was shown in parsley stems compared to vanilla and calathea stems that presented significant decrease in cell number (Fontana *et al.*, 2017). Human cells efficiently attached to the

plant network, where they totally aligned in the plant microstructure. For instance, human dermal fibroblasts preferred to grow in plants stomata and within grooves. This alignment direct cell differentiation and proliferation. It should be noted that many plant types can cause or secret toxic materials, so the use of these plants as a scaffold should be avoided, since when in contact with cells, these plants can accumulate heavy metals and elements that can interfere with the proliferation and expansion of cells. Furthermore, it has been proved that high crystalline celluloses provoke no immune complication and thus are safe to use in designing scaffolds. Interestingly, the tightly packed structure of crystalline cellulose chains protects cellulose enzymes to degrade cellulose over time. In their study, they conserved the complexity of plant structure after decellularization and by a simple biofunctionalization, they managed to support the adhesion and proliferation of human cells. The hydrophilic property of plant tissue helped the fluid transportation into conduits and vessels to nourish cells and support its growth for a period of time. Human cells were well aligned into the topography of plant structure and sensed the topographic features of plants and this offer the potential to shorten and economize the time and cost of scaffold production (Dutta *et al*., 2019).

In this context, many studies have investigated whether plants and their vasculatures could serve as scaffolds to engineer human tissue and organs. Plants are composite materials, composed of hard and soft materials arranged hierarchically. Plant cell walls reinforce a variety of cellulose, pectin and lignin polymers. Cellulose, on one hand, which is the main component of plants that gives rigidity to cells, has been playing a role in wound healing processes (Blasi-Romero *et al.*, 2021). Cellulose microfibrils form hydrogen bonds with hemicelluloses, such as xylans, to increase their stiffness. Together they cross-link with polymers of pectin, a group of polysaccharide rich in galacturonic acid units, using intramolecular hydrogen bonds and low-inter molecular attractive forces, to combine strength and flexibility. Plant materials may offer good transport properties due to their pores and vessels that maintain hydraulic continuity achieved in parallel by the branching system ranging from wide conduits into small vessels. From this point of view, plants would provide the desired biomaterial for tissue engineering, by applying decellularization principles. This will result in a sophisticated and biofunctionalized scaffold, supporting human cell attachment and expansion (J. Lee *et al.*, 2019).

Furthermore, cellulosic scaffolds derived from decellularized apples, have shown feasibility and good cellular proliferation *in vitro* (Modulevsky *et al.*, 2014) as well as *in vivo* where decellularized

apple scaffolds were implanted subcutaneously in wild-type immunocompetent mice for 4 to 8 weeks, where they retained much of their original shape and demonstrated biocompatibility (Modulevsky et al., 2016). Cellulose fibers strengthen plant cell walls and comprise a matrix of hemicellulose containing pectin or lignin. Cellulose is arranged in microfibrils and organized in an orderly structure. Hydrogen bonds form between cellulose and the polysaccharide hemicellulose to sustain and interconnect the matrix (arabinoxylans, xylans) and the stiff cellulose microfibers. Plants offer a unique transport system, where it possesses a branching system that consists of highly interconnected pores and vessels to ensure a feasible transport system of oxygen, water and nutrients.

One of the major limitations of tissue engineering is the lack of an organized and functional vascular system that permits the transfer and diffusion of oxygen and nutrients. The difficulty in creating such network of perfusion vessels and conduits, has shifted researchers to focus more on plants and vegetal tissues (Jahangirian *et al*., 2019). Plants and animals exploit different approaches of chemicals, and fluid transportation, however they share high similarities in their vascular network. Plant structure possesses similar mechanical properties, similar to human tissue, and presents a multi-functional tissue. Knowing that cellulose is most abundantly present in plant cell walls, it was also studied as a natural biocompatible compound and has been shown to promote wound healing and was used in a wide range of tissue engineering applications (summarized in **Table 1**), bones, cartilage.

Table 1: Plant-derived scaffolds and their use in tissue engineering approaches

Plant Scaffold	**Cell sources**	***In vitro***	***In vivo***	**References**
Tobacco BY-2 cells Rice cells Tobacco hair roots	Human foreskin fibroblast (hFF)	Scaffolds support attachment and growth of hFF after 14 days of culture	-	(Phan *et al*., 2020)
Green-onion	C2C12 human skeletal muscle cells (HSMCs)	Microstructure of the outer white section of the green onion guided C2C12 cell differentiation into myotubes and engineered aligned human skeletal muscle	-	(Y.-W. Cheng *et al*., 2020)
Apple Carrot Celery	Murine cell lines MC3T3-L1 cells Mouse l929 fibroblastic cells	Lipid droplets accumulation on apple scaffolds promoted adipogenic differentiation. Increased ALP activity and inorganic matrix deposition on carrot scaffolds drived osteogenic differentiation. Orientation of fibroblast cells mimicking anisotropic connective tissue of tendons. Good mechanical strength of these scaffolds	-	(Negrini et al., 2020)
Cabbage leaves	HUVEC	Human Endothelial cells highly proliferated cabbage scaffolds Generation of ROS malondialdehyde and catalases antioxidants, that enhanced metabolism of these cells.	-	(Walawalkar and Almelkar, 2020)

Apples	hiPSC	Osteoblastic differentiation in apple scaffolds, mineralized bone-like tissue after 21 days	Successful engraftments of bone organoids, Collagen type I deposition and blood-vessel like structures. Bone-organoids promoted defect healing and provided bone tissue with blood supply.	(J. Lee *et al*., 2019)
Baby spinach leaves plus gelatin coating	HDMEC hDF	Gelatin-coating enhanced the attachment and growth of hDF on acellular spinach	HDMEC Induced neovascularization and angiogenesis after 7 days of implantation	(Dikici *et al.*, 2019)
Apples	C2C12 mouse myoblast cells	Apple scaffolds whether tested alone, combined to collagen, or gelatin, presented high biocompatibility	Increase of Collagen matrix deposition, extensive cell invasion and vascularization, no calcification, nor fibrosis	(Hickey *et al.*, 2018)
Spinach and parsley leaves	HUVEC MSC hPS-CM	HUVECS aligned vascular wall and remained viable. MSC adhered to the surface, hPS-CM attached to the surface of leaf scaffolds and contracted after 5 days. This was continued over 21 days	-	(Gershlak *et al.*, 2017)
Parsley stems Calathea Orchid Vanilla	MSC hDF	MSC highly expanded in parsley stem cells and to a low degree in Calathea and vanilla stems. Metabolic activity of hDF highly increased in parsley and to a lesser degree in Orchid. Parsley presented highest hydrophilicity and larger pore size	-	(Fontana *et al.,* 2017)

Apples	Human ADSC Human CB-MSC	Proliferation was induced through ASC production of VEGF and IL-6	-	(Lee *et al*., 2016)
Apples	C2CI2 mouse myoblasts NIH3T3 mouse fibroblast	-	Apple constructs implanted subcutaneously in immunocompetent mice, shape retained, ECM deposition, good biocompatibility, angiogenesis and vascularization of scaffolds	(Modulevsky *et al.*, 2014)
Apples	C2CI2 mouse myoblasts NIH3T3 mouse fibroblast	Cells invade, proliferate and remain viable after 12 weeks of culture	-	(Modulevsky *et al.*, 2014)

Recently, it was also used in cell attachment when extracted from decellularized apples and proved to be biocompatible when implanted *in vivo* in animal models. These similarities accumulated and inspired researchers more towards investigating plants and their vascular system after perfusion-techniques to decellularize these tissues. Decellularization, as mentioned before, removes cellular material, while preserving the intact vascular network. These techniques were applied to various plant species to give rise to acellular, tissue engineering scaffolds. Multiple plants from different botanical groups have undergone decellularization. Among these, spinach, parsley stems, peanut hairy roots. Spinach was chosen due to its high availability and dense vascularity. Both quantitative and qualitative analyses have shown the loss of nuclear material, though conservation of the structure and native composition of the plant tissue. Gershlak and his team decellularized spinach (**Figure 17**) and then they recellularized the plant scaffold with human umbilical vein endothelial cells (HUVEC), that adhered into the inner vascular wall of the leaf. MSC progressively adhered to the surface of the leaf, and human pluripotent stem cell-derived cardiomyocytes (hPS-CM) contracted for a period of 21 days and kept attached to the surface of the leaf. They effectively used

the highly vascularized natural architecture of spinach leaves to engineer mammalian cardiac constructs (**Figure 18**).

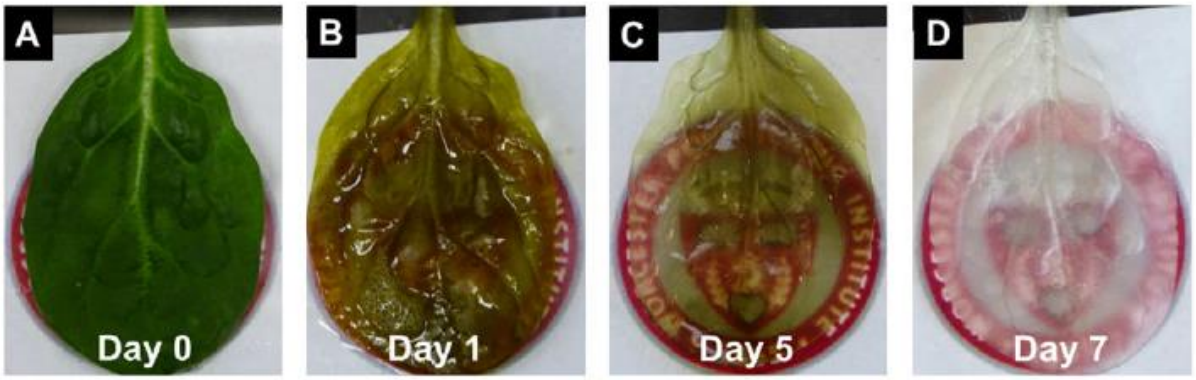

Figure 17: (A) Leaf is dark green and opaque prior to decellularization at Day 0. **(B)** At Day 1, the leaf loses some of its dark coloring and begins to appear translucent. **(C)** By Day 5, the leaf is completely translucent while maintaining a light green hue. **(D)** After being treated and sterilized with sodium chlorite, the leaf loses the remainder of its coloring and becomes completely decellularized on Day 7 (Gershlak *et al*., 2017).

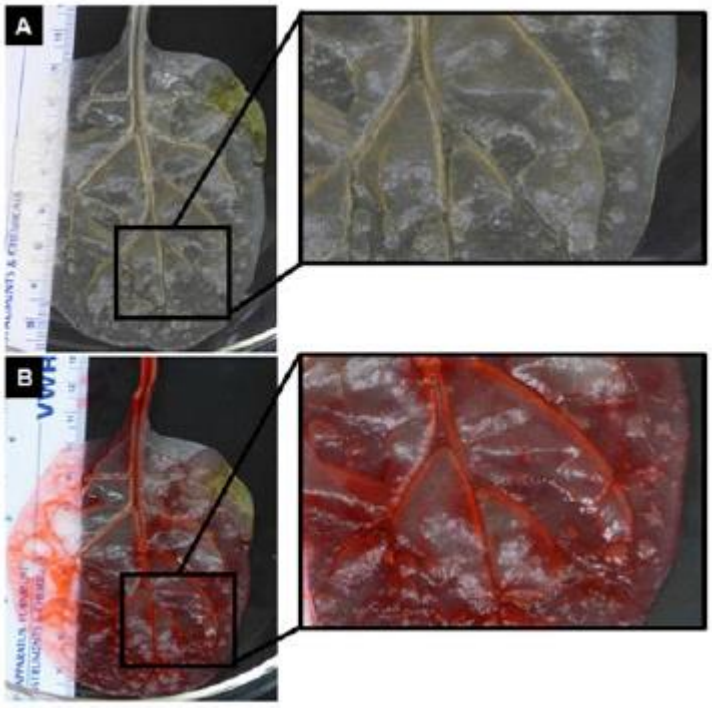

Figure 18: Spinach leaves retain perfusion capabilities after decellularization (Gershlak *et al.*, 2017).

Plant-derived cellulose, complementary to bacterial-derived cellulose offers a straightforward, potential approach to produce biocompatible, implantable scaffold that retains shape and produces ECM proteins, as well as promoting angiogenesis. Previous work has shown that scaffold can also be fused with proteins before culture.

Apart from plants, certain bacteria, algae, and fungi produce cellulose as well. Because of their specific supramolecular structures, these cellulose forms are frequently used as model substances for further research on cellulose structure, crystallinity, and reactivity, as well as for the development of new materials and biomaterials (Carvalho *et al*., 2019). Although identical to the cellulose of plant origin in terms of molecular formula, bacterial cellulose is quite different. The degree of polymerization is very high, with DP values of 2000–8000. Crystallinity is also high, with values of 60–90%. Bacterial cellulose is characterized by its high purity with no association with accompanying substances like hemicelluloses, lignin, or pectin and by extremely high water content of 90% or more. Upon complete removal of water by air drying, the bacterial cellulose will only rehydrate to the same low extent as that of plant celluloses after re-exposure to water: about 6%. After gentle freeze-drying, however, it can absorb up to 70% of the original water content by re-swelling Through a stepwise exchange of water for other solvents, it is possible to introduce methanol, acetone, or n-hexane, for example, at the same volume as water in bacterial cellulose, while maintaining the hollow space and network structure (Palaninathan *et al.,* 2018).

2.3.7 Cell sheets

Scaffolds are successful means to regenerate tissues and organs, but may induce some undesirable inflammation responses once degraded. This can hinder cell viability and therapeutic effects in sensitive organs. On the other hand, one of the key challenges of tissue engineering is vascularization. Isolated cell injection presents a non-homogenous seeding efficiency and a low cell survival rate when transplanted *in vivo*. Therefore, a new cell sheet technology has been engineered to increase cellular survival rate in tissue. Cells proliferate and grow on culture surface until they reach confluency. These cell sheets maintain their cell-cell junctions and protein-ECM, facilitating the adhesion to the host's tissue. This layer of cells is then transplanted as a single sheet or stacks of cell sheets on top of each other to regenerate damaged tissues and organs.

With the continuous advance in cell sheet technology, a variety of systems was used to construct and prepare these cell sheets. These include temperature-responsive dishes, electro-responsive, pH-responsive, photo-responsive, magnetic, and finally mechanical systems.

2.3.7.1 Temperature-responsive systems

The first introduced system to form cell sheets was using temperature-responsive dishes, which are currently the most used nowadays for cell sheet preparation (Lee *et al.*, 2021; Thorp *et al.*, 2020). In 1990, Yamada *et al.* and Okano *et al.* have successfully grafted Poly (N-isopropyl acrylamide) PIPAAm on commercially available tissue culture polystyrene by electron beam irradiation. This polymer has reversible soluble/insoluble temperature-responsive character depending on temperature changes (Okano *et al.*, 1993). It undergoes a reversible phase transition with a low critical solution temperature (LCST) of 32°C in aqueous solutions. When the temperature of these plates are above LCST, intra and inter-molecular hydrophobic interactions form between group of PIPAAm's isopropyl groups, enabling cell adhesion and proliferation on the immobilized matrix. On the contrary, upon temperature decrease, hydrogen bonds between hydrophilic parts of PIPAAm and water increases, causing a rapid detachment of the whole cell sheet with its cell-cell junction and ECM proteins (**Figure 19**).

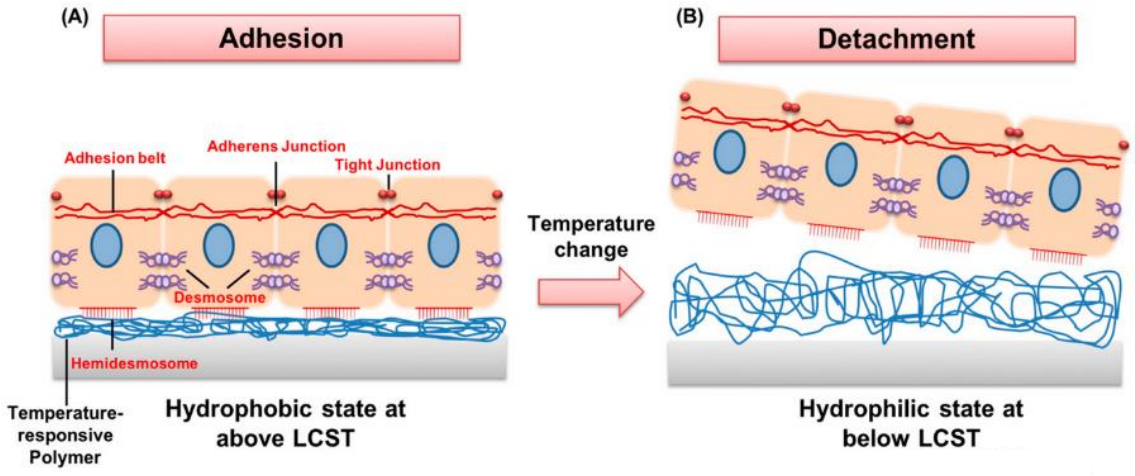

Figure 19: A temperature-responsive matrix showing the attachment and detachment of cell sheets while preserving cell–cell junctions. (**A**) At 37 °C, the cells attach to the surface that is hydrophobic (above lower critical solution temperature). Cells connect to each other by various cell-to-cell junctions and deposit ECMs. (**B**) At values below LCST, cells detach from the hydrophilic surface. Temperature-responsive culture surfaces are able to preserve the pre-existing cell-to-cell junctions and cell-secreted extracellular matrices (ECM) (H. Kim *et al.*, 2019).

To accelerate the harvesting procedure of cell sheet, several approaches have been developed by modifying either physical properties of the surface or chemically adapting the structure to overcome the long exposure of cell sheet to low temperature and to shorten the duration of cell sheet detachment, thus preserving the viability of cell sheet. Integration of PIPAAm to a porous membrane (PM), on one hand was performed using an electron beam irradiation on surface of the culture plates (PIPAAm-PM). This showed a decrease in cell sheet detachment time from 75 to 30min, compared to the traditional PIPAAm dishes. A more significant decrease in time was shown when PEG was co-grafted with PIPAAm on the same porous membrane. This changed detachment time to 20min at 20°C. This is due to the hydrophilic PEG chains, which possess flexible terminals and form a number of channels for water diffusion, increasing the hydration of PIPPAm layer.

The heterogeneous cell environment plus the 3D structure is a key role in the survival of tissues and organs. The incorporation of specific structures in cell sheets is very important to mimic the complex architecture of native tissue. To construct such tissues, a micropatterning technology has been applied to cell sheet preparation. Micropatterning comprises the fabrication and use of a culture substrate with microscopic features that impose a defined cell adhesion pattern. A patterned, dual temperature-responsive substrate using two different cell types, was fabricated by polymerizing n-butyl methacrylate into PIPAAm in presence of electron beam irradiation Another temperature-responsive system was used to fabricate ADSC spheroids directly on adhesive PIPAAm substrates. Cell-cell interaction within these spheroids was then evaluated and cell viability was increased (Kim *et al.*, 2020).

2.3.7.2 Electroresponsive systems

Guillaume-Gentil *et al.* proposed a new method to prepare cell sheets by using a system of electrochemical polarization. The cell sheet was formed by growing cells to reach confluency on a thin polyelectrolyte film. Positive potential for electrochemical polarization was applied to detach cell sheet from the film (Guillaume-Gentil *et al.*, 2008). This was achieved by grafting poly (L-lysine) on a monolayer of PEG on metal oxide surface when positive potential was applied, the monolayer desorbed and the cells lost their attachment points and detached. A range of cell types has been cultured to confluence and detached as cell sheets from these surfaces including hepatocytes, endothelial cells and fibroblasts (Qiao *et al.*, 2018)Another group of researchers

presented another electrochemical system involving gold as a substrate modified with a monolayer of alkanethiol and Arg-Gly-Asp peptides. Cell sheets are formed on the surface and then harvested by applying a negative electrical potential for 10min. (Inaba *et al.*, 2009). Also, the micropatterning technique was used in this system to create gold substrates modified with cell-adhesive and cell-repulsive oligopeptides. To examine the detachment of cells adhering to a gold surface, relatively few cells detached from the gold surface after 3 min. almost all cells detached within 2min from surfaces modified with cell-adhesive zwitterionic that was rapid.

2.3.7.3 Photo-Responsive Systems

Light illumination is another approach to stimulate cell harvesting. This strategy uses ultraviolet light that can mediate changes in hydrophobicity and hydrophilicity of culture substrates. Hong *et al.* studied substrate wettability by using 2 metals, zinc oxide (ZnO) and titanium dioxide (TiO2), due to their biocompatibility and wettability at a safe range of wavelength (365nm). Mouse pre osteoblastic cells were first cultured on TiO2 nanodot films, coated with quartz substrate to form cell sheets. By applying 365nm ultraviolet beam for 20min, the osteoblastic cell sheet detached. This is caused by the release of adsorbed adhesive protein when the surface becomes more hydrophilic under luminosity. To more preserve cell sheet integrity, TiO2 nanodot film was immobilized to RGD that promoted cell sheet adhesion and proliferation (Hong *et al.*, 2013). Another role of photo-responsive molecules is that they can also control adhesion and detachment of cells. Spiropyran is a photosensitive molecule. When stimulated by UV light, it undergoes a reversible confirmation from hydrophobic to hydrophilic state accompanied by a change in color Gold is a photoresponsive material investigated for cell attachment and detachment. Gold nanoparticle exhibits a strong photoabsorption that lies in the green spectral range. After irradiation of the nanoparticles-based surface with a specific wavelength of about 532nm, reactive oxygen species (ROS) are produced that causes some damages to the cell membrane, stimulating the detachment of the cell sheets (Kolesnikova *et al.*, 2012). This technique presents an advantage where the surface is able to recover, allowing the reattachment of new cells, thus creating a co-culture cell sheet system using only a single surface.

2.3.7.4 PH-responsive systems

Polymers with acidic or basic groups can accept or release protons according to the surrounding environment, and thus change their structural and confirmation due to different solubility of the medium. Cell sheets could be controlled by different pH-responsive substrates such as polylactic acid and their derivatives. A study used a combination of cationic and anionic layer of polystyrene sulfonate, that has adhered to the conductive surface of culture. Guillaume and his colleagues seeded placenta-derived stem cells till reaching confluency on polyelectrolyte surfaces and managed to detach the whole-cell sheet with matrix, when using a pH of 4 in specific culture media. And thus, cell sheet detached due to the drop in pH at cell-substrate level. The viability and differentiation capability was retained when this latter was added in acidic medium (Guillaume-Gentil *et al.*, 2011). Chitosan is another pH-responsive polymer, exhibiting a pH of 7.4. When cells are attached to the surface of chitosan and upon lowering its pH, this latter exhibits a positively charged surface that attracts the negatively charged fibronectin, secreted by cells. When the pH of the medium is raised to 7.65, the chitosan reverses its charge and fibronectin resorbs, allowing the detachment of the cell sheets as shown in the **Figure 20** below.

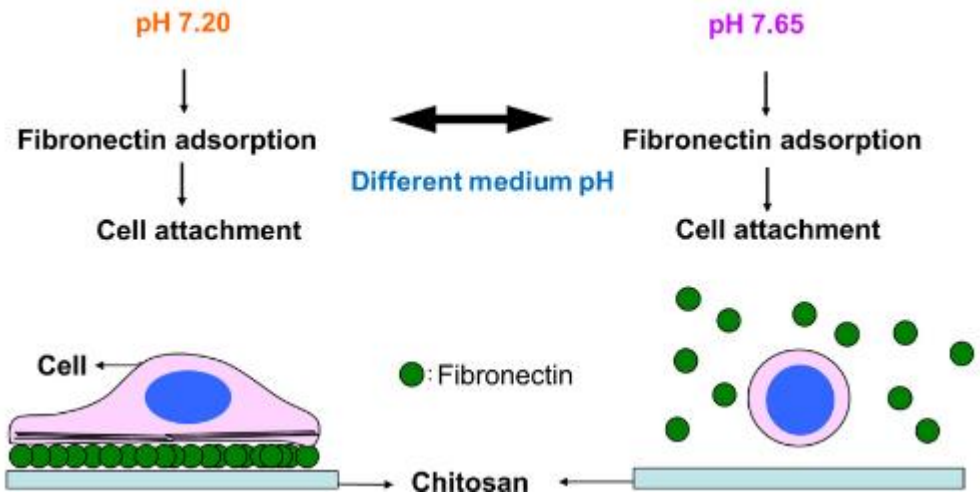

Figure 20: Schematic representation of the relationship among medium pH, fibronectin adsorption, and cell attachment on chitosan (Chen *et al.*, 2012).

2.3.7.5 Magnetic systems

Magnetic systems rely on interactions between positively charged nanoparticles and negatively-charged cell membranes. This technique was used for human MSC when incubated with magnetic nanoparticle-containing liposomes that were used to reduce apoptosis and increased expression of endothelial growth factor. Magnetized MSCs formed thick multilayered cell sheets according to magnetic force and were harvested from magnets and layered on top of each other and implanted in mice (Ishii *et al.*, 2011). Recent studies have investigated the remarkable outcomes of magnetic system to develop a hierarchical 3D construct for bone tissue engineering. The culture of magnetite labeled human ADSC and umbilical vein endothelial cells (HUVECs) that were bound that were organized in triple sheet conformation (**Figure 21**). Cells within sheets were able to interact by secretion of growth factors and proteins that increased cellular proliferation and viability. With the aid of a magnetic force, cell-cell interactions were enforced and thick and collagen-enriched matrices was developed that successfully promoted a stratified 3D constructs for bone tissue engineering applications (Silva *et al.*, 2020).

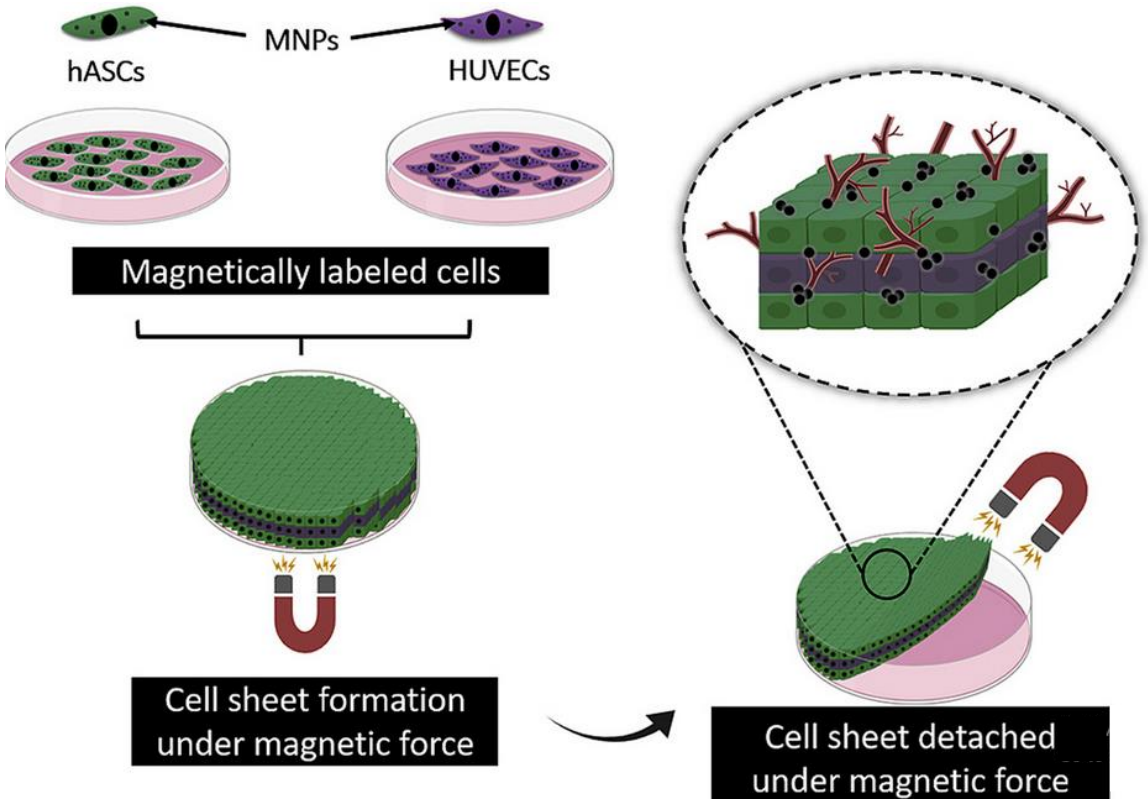

Figure 21: Multi-layer pre-vascularized 3D construct formed and detached by using magnetic force (Silva *et al.*, 2020).

2.3.7.6 Mechanical system

Vitamin C is an antioxidant that improves the expression of different cellular markers that maintain the undifferentiated state of cells. Many studies have reported the importance of vitamin C or L-ascorbic acid in formation of cell sheets. Wei *et al.*, were first to suggest a method for MSC sheet engineering based on the addition of vitamin C without the use of thermoresponsive plates (Wei *et al.*, 2012). The addition of vitamin C in cell sheets induced the increased expression of human telomerase reverse transcriptase (h-TERT) that enhanced cellular longevity.

Pedroni *et al.*, have also introduced the use of vitamin C in the formation of dental pulp stem cell sheets, that improved the expression of cellular markers related to longevity and maintenance of the undifferentiated state of cells (Pedroni *et al.*, 2018). Shotorbani *et al.*, have also investigated the formation of adipose cell sheets by the addition of vitamin C that enhanced the overall results of adipose cell sheets and induced a better performance and harvesting of the intact sheet in terms of viability and anti-aging functions of cell sheets (Shotorbani *et al.*, 2018). On the other hand, ascorbic acid has also been essential in exerting beneficial effects in stem cell culture where it increases proliferation and DNA synthesis of mesenchymal stem cells *in vitro* (Wu *et al.*, 2020). Furthermore, upon comparing different methods of preparing cell sheets, ascorbic acid method was found the most rapid and effective methods to obtain cardiac cell sheets (Kaynak Bayrak and Gümüşderelioğlu, 2019). Ascorbic acid stimulated the deposition of collagen upon culturing MSC at a confluent density on culture plates with supplementation of ascorbic-acid from bone marrow origin (Kaukonen *et al.*, 2017), and synovium that highly deposited ECM proteins (Yan *et al.*, 2020).

2.4 Application of cell sheet technology in cartilage regeneration

With the rapid development of cell sheet technology, cell sheet technology has been implicated in a wide range of tissue and organs, specifically cartilage regeneration. This approach overcomes different problems linked to conventional tissue engineering. For instance, tissue engineering constructs lack spatial complexity in tissue organization, and chondrocytes sources are still key factors restricting large scale cartilage engineering and limiting their success. For that, it is imperative to define the characteristics and phenotype of cell sheets compared to native cartilage structure. Compared with monolayers, multilayered chondrocyte sheets showed increased

expression level of chondrogenic and adhesive related markers and proteins, showing that multilayered chondrocyte sheets regenerate cartilage defects by closely mimicking native structure and secreting growth factor such as transforming growth factor beta (TGF-β) and prostaglandin (Takizawa *et al.*, 2020). As compared to scaffold with isolated cells, chondrocyte cell sheets regenerated partial and full-thickness lesions with well-integrated between native and engineered articular cartilage. Besides, many researchers have applied cell sheet technology to treat bone-cartilage defects. For instance, Ebihara *et al.* prepared multilayered chondrocyte sheets using temperature-responsive elements and transplanted them into condylar cartilage defects in mini pigs. 3 months later, articular defects repaired fast, while subchondral bone was poorly repaired (Ebihara *et al.*, 2012). Ito *et al.*, on the other hand, combined chondrocyte layered sheets with synovial cells and transplanted them into femoral groove of rabbits(Ito *et al.*, 2012). These results showed an increase in repair in both articular and osteochondral defects in rabbits. To confirm these results, Takaku *et al.*, prepared cell sheet from both chondrocyte and synovial cells and transplanted them in osteochondral joints of rats. He suggested that these cells could be left for 21 months in rats with a complete reparation and regeneration of bone-cartilage defects (Takaku *et al.*, 2014). Another group explained that higher expression of TGFβ-1 is contributing to osteochondral cartilage repair, they fabricated chondrocyte and synovial cell sheets and transplanted these allogenic cell sheets to cover an osteochondral defect in a rat model. Green fluorescent proteins (GFP) were used to track cells *in vivo*. Results showed that cartilage repair was significantly enhanced in the group implanted with a chondrocyte cell sheet, then in that with synovial cell sheet and cell tracking experiments showed that regenerated cartilage was largely composed of cells derived from transplanted chondrocyte sheets (Shimizu *et al.*, 2015). Moreover, Zhang and his colleagues constructed microtissue using growth-factor-immobilized cell sheets. They used magnetically labeled molecules to bind several growth factors that help mimic cartilage-bone interface. Osteogenic growth factor BMP-2, in addition to the chondrogenic growth factor TGFb-3 were bound to a magnetic nanoparticle coated with nanoscale graphene oxide that has no influence of cell viability. Magnetic nano particle-labelled cells can be organized via magnetic force to from multilayered cell sheets in different patterns. The advantage of graphene oxide is that this coating provides plenty of carboxyl groups to bind and deliver growth factors. Thus, a double-layered osteochondral complex was formed that mimics cartilage-bone interface where the upper chondrogenic cell sheet was immobilized by TGFb-3 and the lower bone sheet with BMP-2, after transplantation into nude mice

(Zhang *et al.*, 2017). Chondrocyte microtissue have also been combined with chondrocyte cell sheets that fabricated a 3D auricular mold that highly resembled and retained human auricle after 8-week of subcutaneous implantation (Yue *et al.*, 2020).

Due to their limited proliferation capability and dedifferentiation nature, chondrocyte sources are still limiting factors for large scale cartilage engineering. For this reason, somatic stem cells have been good candidates and achieved much attention during recent years because of their self-renewal abilities and their capability to differentiate into many lineages. Engineered cartilage from MSC cell sheets has been shown to induce a good integration between regenerated and native surrounded cartilage. Wang *et al.*, compared the feasibility of cartilage cell sheet derived from chondrocytes and BMSCs, with bone-phase scaffolds formed from PGA/PLA to regenerate mandibular condyle in nude mice. The bone-phase scaffold fused well with surrounding native bone and induced new bone formation, however, the disc adhered firmly to the artificial condyle, since there was no cartilage repair. Whereas when multilayered cartilage cell sheets were combined with bone-phase scaffolds, integration between cartilage and bone was tighter. Thus this combination enhances osteochondral defects and avoids inflammation during fiber degradation (F. Wang *et al*., 2017). A recent study has also shown the potential of allogeneic BMSC sheets in reconstructing rabbit osteochondral defects. These sheets were transplanted into defect site and quickly mixed with bone marrow blood to repair knee joints (Z. Wang *et al.*, 2020). Similarly, a transplantable hyaline-like cartilage construct was fabricated by MSC cell sheets that adhered directly to cartilage surfaces where they maintained cartilage characteristics, thus scaffold-free hyaline cartilage constructs that well regenerated articular cartilage (Thorp *et al.*, 2020). Novel bioscaffolds have also been evaluated using ADSC sheet-derived ECM. These scaffolds high preserved 3D architecture of ECM and retained its mechanical properties. This allowed a much easier recellularization and less immunological response upon transplantation into *in vivo* models, thus promoting a good application for cartilage regeneration (S. Zhou *et al.*, 2020).

2.5 Growth factors and hypoxic environments

A wide range of growth factors and signaling molecules play a vital role in cell growth, proliferation and differentiation. Mostly used growth factors include insulin-like growth factors (IGF), basic fibroblast growth factors (bFGF, bGFG-2), vascular epithelial growth factors (VGEF),

bone morphogenic proteins (BMP) and transforming growth factor-beta (TGF-β). These growth factors are delivered via different ways including carriers where DNA plasmids encode the gene of the desired growth factors.

2.5.1 Insulin-like growth factors

Are circulating cytokines that exist in circulation and in many biologic fluids associated with the specific IGF-binding proteins. IGFs are produced in the bone marrow and liver in response to growth hormones. It is present in serum and synovial fluid of cartilage and chondrocytes, and required to maintain cartilage integrity and facilitates maturation by increasing the production of sulfated glycosaminoglycans in cartilage and preserving these materials in the pericellular matrix.

2.5.2 Basic fibroblast growth factor (bFGF)

The basic fibroblast growth factor (bFGF) is a part of the family of growth factors. During embryology, it promotes the differentiation of MSC into chondrocytes. It also induces chondrogenic nature of adipose stem cells.

2.5.3 BMP-2

(The bone morphologic protein-2 is a molecule that is part of the transforming growth factor superfamily. It was proved that BMP-2 can promote osteoblastic differentiation of mesenchymal stem cells, along with bone formation regeneration in the early phase. Studies by Yin *et al.* demonstrated that a combination of multiple growth factors exerts a synergic effect facilitating bone regeneration (Yin *et al.*, 2018). Another study has investigated the coating of hydroxyapatite on titanium surfaces with the addition of chitosan and BMP-2 that was encapsulated within coatings. Their *in vitro* tests showed that all coatings accelerated cell adhesion, and when adding BMP-2 within chitosan, BMP-2 successfully enhanced cell adhesion, bioactivity and biocompatibility (Qiu *et al.*, 2020; X. Wang *et al.*, 2019).

2.5.4 TGF-β

It is a growth factor involved in essential physiological processes such as embryonic development, tissue repair, differentiation and control of cell growth. At the level of cartilage, it is considered as a powerful anabolic factor since it increases the deposition of ECM by promoting synthesis of COL2 and ACAN proteins.

2.6 Hypoxia

Hypoxia is one of the most remarkable factors that affect cells in multiple ways. It plays an important role in different cellular features, where it affects cell migration, proliferation, and metabolism. Hypoxia, mediates these cellular modifications by the HIF pathway, by inducing of the hypoxia-inducible factor 2α (HIF2α), to stimulate chondrogenesis via increasing of the SRY (sex-determining region Y) - box 9 (SOX 9) transcription factor, as well as COL2A1 (**Figure 22**).

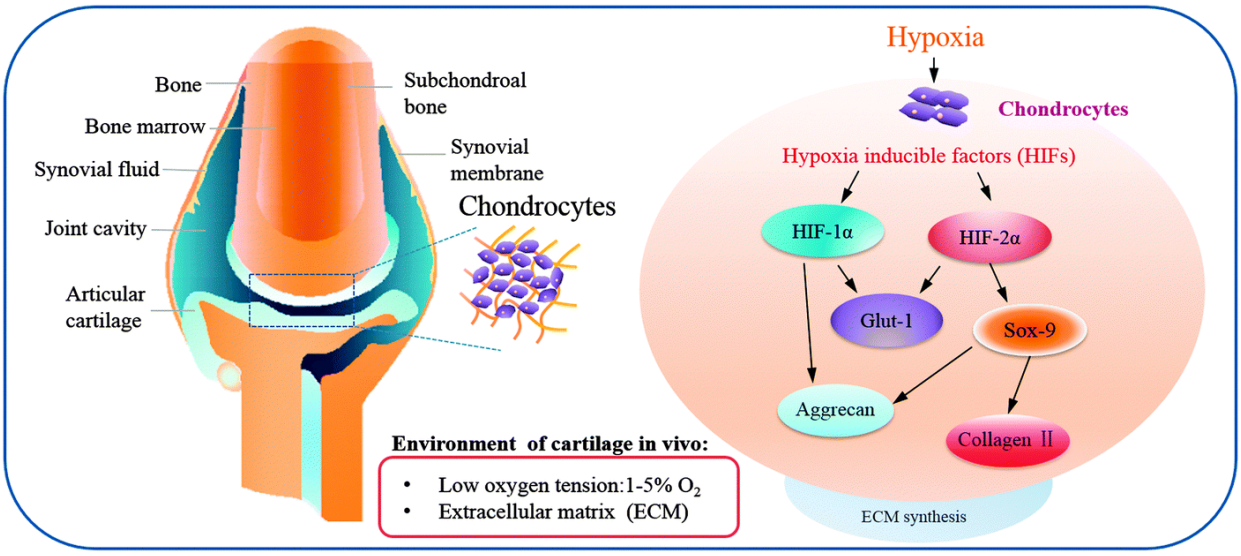

Figure 22: The schematic representation of an *in vivo* articular cartilage environment in 3D and it its ECM proteins regulated by hypoxia inducible factor (HIF) signaling pathway (Shi *et al.*, 2015).

HIF possess more than 1000 target genes that can be either regulated or suppressed by hypoxia. The process of hypoxia in promoting the decrease of hypertrophic markers such as collagen X (COLX) and Runt-related transcription factors (RUNX2), can be contributed to the addition of parathyroid hormone-related peptide hormone (PTHrP) that maintain homeostasis and play a vital

role in the regulation of skeletal development by suppressing the hypertrophy effect of chondrocytes. Studies conducted by Browe *et al.*, showed that not only does (PTHrP) decrease collagen and hypertrophic genes, but also it has negative effects on GAG synthesis. However, when combining hypoxia with the addition of exogenous PTHrP, they observed a high and accumulative expression of GAG synthesis, whereas a reduction was observed in alkaline phosphate assay (ALP) activity. This suggests that in absence of oxygen tension, hypoxia induces the expression of the PTHrP receptor that increases cellular response to limit the expression of PThrP. Hypoxia also regulates myocyte-specific enhancer factor 2C (MEF2C) that is responsible to express COLX gene. So in low oxygen levels, PTHrP levels are high, subsequently protein kinase A (PKA) activates protein phosphatase 2A (PP2A) that dephosphorylates histone deacetylase 4 (HDAC4), which in turn attenuates the levels of MEF2C (Browe *et al.*, 2019). Foyt *et al.*, suggested that soft hydrogels with a hypoxic environment promoted hMSC to have more spreading morphology, and stimulate the increase in molecular markers of chondrogenesis, such as COL2A1 and SOX9 to develop cartilage tissue engineering (Foyt *et al.*, 2019). Anderson and his colleagues cultured MSC and auricular chondrocyte progenitors similarly in hypoxic medium (2%). These two cell types have undergone chondrogenic differentiation and hypertrophic gene were then analyzed. Results suggested that although MSC significantly downregulated hypertrophic chondrocytes, however, they still secreted COLX. On the other hand, articular chondrocyte progenitors significantly decreased cartilage hypertrophy and expression of COLX was not detected in any clones of these cells (Anderson *et al.*, 2016). Furthermore, DPSC were also tested for their stemness in hypoxic environment. A new hypoxic system was introduced by Ahmed *et al.*, suggesting a supply of 5% O2 tension in culture that provided a good culture condition for DPSCs. They compared different oxygen percentages (21%, 5% and 3%) to see which is the optimal expansion culture condition that more suits dental stem cells. Many studies have shown that smaller cells exhibit better differentiation potential. Their results confirmed these studies and showed cells that have undergone hypoxic conditions, were smaller and promoted a better morphology compared to cells cultured in normoxia. Thus, these cells expressed stem cell markers way more than normoxic cells. By comparing 5% and 3% oxygen tension, specific stem cell markers such as granulocyte colony-stimulating factor receptor (G-CSFR) and C-X-C chemokine receptor type 4 (CXCR4) were significantly higher in 5% than 3% hypoxia, indicating the optimal level of oxygen for migration of dental stem cells. Moreover, proliferation was also tested and results suggested that the first 4

days, proliferation rate of normoxic and hypoxic culture were the same, whereafter cells cultured in 5% oxygen tension proliferated rapidly compared to 3% and 20% O2. Also, pluripotency markers in presence of hypoxia were upregulated, where expression of SOX9, octamer-binding transcription factor 4 (OCT4) were higher in hypoxic MSC (Ahmed *et al.*, 2016).

Diverse reports have reported the importance of hypoxia in the physiological processes of MSC since it is similar to the natural environment of bone marrow. Many studies have conducted hypoxic-induced MSC. MSC can survive by adjusting to changes in their microenvironment and displaying several biological responses. For instance, MSC cultured in hypoxic conditions grew slowly until 1st passage and increased afterward. MSC are adapted to hypoxic conditions where they express common surface markers and possess the ability to differentiate into the three lineages. Different studies have shown that adipogenic and osteogenic genes are more stimulated in hypoxic cells than normoxic cells (Husak and Dworzak, 2017). Binder *et al.*, suggested that combining serum reduction and low oxygen levels would boost the osteogenic differentiation of MSC. They incubated MSC in media containing different FBS concentrations and they varied the oxygen levels and measured ALP activity in each case, as well as the mineralization and calcium secretions. Their data showed that serum concentration and oxygen levels synergistically influenced MSC differentiation, increased Wnt signaling and improved osteogenesis. Thus a superior level of osteogenesis was achieved when culturing cells in hypoxic environment and reducing serum amount in culture media (Binder *et al*., 2015).

Due to the lack of vascularization system in articular cartilage, this latter takes and absorbs oxygen and nutrients from synovial fluid. Therefore, the oxygen concentration was estimated to be somehow low in the joint surface, ranging from 7% to reach the subchondral bone at 1%. This is responsible for HIF transcription factors that play roles in the development of endochondral bone *in vivo*. Many studies have tested the hypoxic culture *in vitro* and its effect regarding chondrogenesis. Phenotypical changes and molecular changes were observable usually after several days of culture.

Meretoja and his colleagues investigated the co-culture of human chondrocytes with mesenchymal stem cells *in vitro*, when cultured on porous polymer scaffolds under hypoxic conditions. Their 3D structure showed increased collagen content and hypoxia increased matrix synthesis. Besides, COLX and ALP activity were induced by hypoxic co-culture, however, hypertrophy was

suppressed with no calcifying phenotype was observed. Co-cultured 3D constructs use fewer chondrocytes to produce the same end results compared to pure articular chondrocyte constructs. In other words, co-cultures of MSC and chondrocytes showed enhancement of cartilaginous matrix in porous scaffolds, which gives some advantages for cartilage tissue engineering in decreasing the amount of harvesting of cartilage and obtaining a more stable chondrogenic profile (Meretoja *et al.*, 2013).

In the last several years, many scientists have focused on the effects of hypoxia on stem cells derived from several tissues and origins. In this context, the overexpression of HIF-1α in bone marrow-derived MSC on COL1 scaffold promoted cartilaginous repair of chondylar osteochondral defect in a rabbit model (M.-S. Cheng *et al*., 2020). Hypoxia effects have also been investigated on MSC differentiation potential of these cells. Not only did low oxygen levels downregulated the expression of genes involved in lipid metabolism, but also osteoclast and osteoblast mineralization were highly decreased in these cells (Camacho-Cardenosa *et al*., 2020).

A gene expression profile was analyzed by a microarray to study the effects of hypoxia on MSC properties. Hypoxia was found to increase the expression of different growth factors involved in cellular proliferation and angiogenesis (Hung *et al.*, 2007). Moreover, mesenchymal stem cells-derived conditioned medium (MSC-CM) and hypoxic environment have shown significantly high levels of VEGF and interleukin 6 (IL-6), angiogenic factors that stimulated fracture healing and angiogenesis in diabetic rats (Wang *et al.*, 2012). Incubation of MSC for 48 hours in 1% oxygen level mediates some metabolic changes that promoted *in vivo* and *in vitro* survival of MSC. Studies have shown that low oxygen levels can affect lipids in MSC, which in turn are responsible for different regulatory and signaling functions in cellular processes. Lakatos *et al.*, reported that MSC responds to hypoxia by secreting high amounts of lipids, specifically diacylglycerol (DG) that is responsible for mediating angiogenic factors in cells (Lakatos *et al.*, 2016).

Some studies reported high chondrogenic potential when human synovial membrane mesenchymal stem cells were cultured in hypoxic medium (Bae *et al.*, 2018; Li *et al.*, 2011), other found a small insignificant effect on chondrogenesis (Neybecker *et al.*, 2018), however Ohara *et al.*, suggested that no effects of hypoxia were observed when analyzing chondrogenesis profiles (Ohara *et al.*, 2016). In this study, SOX 9 and COL2 were increased in both synovial-membrane mesenchymal stem cells and BMMSC when cultured in hypoxia. Enhanced cartilage repair was

observed in the case of bone marrow-derived mesenchymal stem cells, while synovial membrane-derived mesenchymal stem cells did not show high chondrogenic capability under a hypoxic environment (Gale *et al.*, 2019).

3. Auricular cartilage engineering

3.1 Background

In order to eliminate the use of large tissue harvests and the complications that result from auricular reconstruction techniques, auricular tissue engineering provides the means of using small biopsies to generate cartilage-like structures in the shape of an auricle. However, to be able to bioengineer such constructs, there are many criteria that need to be evaluated. Scaffolds, should maintain an adequate environment and good structural and mechanical properties for supporting tissue growth and development. Besides, for a successful auricular cartilage engineering, the scaffold should maintain long-term integrity and strength with a porous architecture that supports neo-cartilage formation (Li and Sun, 2019). Efforts have been devoted to engineering auricular cartilage, until the first successful transplantation was carried out by the two Vacanti brothers. This was illustrated by a human ear grown on the back of a mouse using methods of tissue engineering. This mouse was known as 'auriculosaurus' or the Vacanti mouse named after Joseph Vacanti who developed it. This goes back to 1986 where Robert Langer of the Masschusetts Institute of technology and Joseph Vacanti of Harvard children's hospital in Boston designed and performed the first successful transplantation experiment using bio absorbable artificial polymers as 3D matrices. Since ears are very hard to create surgically, due to their peculiar and complicated shape, they decided to make a scaffold in the shape of a human ear. A biodegradable human ear-shaped mold was created and cow cartilage cells were seeded in it, followed by a subcutaneous transplantation in an immunocompromised mouse (Cao *et al.*, 1997). The cartilaginous ear was implanted under the skin layer of the mouse, but over the muscle layer. After 3 months, the mouse grew extra blood vessels that nourished the cow cartilage cells, that then grew and infiltrated into the biodegradable scaffolding, which had the shape of a human ear presented in **Figure 23**.

Figure 23: The Vacanti mouse (Langer and Vacanti, 2016).

By the time that the scaffolding had dissolved away, the cartilage had enough structural integrity to support itself. However, this cartilaginous structure that looked like a human ear was never transplanted onto a human, because it was full of cow cells and would have been rejected by a person's immune system. For ensuring non-immunogenicity and good biocompatibility, the choice of cell sources should be carefully and slowly examined. Cells from the auricles are the gold standards since they already produce elastin, however this choice is not easily accessible, especially if patients have small or no auricle. For these reasons, the choice of other cell sources should be slowly examined to enhance the quality of auricular cartilage tissue generated. Early research has investigated mature cells such as chondrocytes or epithelial cells, for their capacity of generating new tissue.

3.2 Cell sources

Von Bomhard *et al.*, have used goat auricular chondrocytes to evaluate a new resorbable chondro conductive biomaterial. They investigated the use of a biomaterial produced from decellularized porcine septum cartilage, seeded with auricular chondrocytes in order to evaluate a new scaffold for nasal septum regeneration. Their results showed that the rate of proliferation of auricular

chondrocytes was lower than that of nasal chondrocytes, however, the production of a cartilage-like matrix was more in auricular chondrocytes since they showed an expression of anabolic growth factors such BMP 5 and IGF1(Von Bomhard *et al*., 2019). Rosa *et al.*, investigated rabbit auricular chondrocytes that were grown in culture mold in presence of IGF-1 and TGFβ-1 as 3D ear-shaped constructs. Increased expression of elastic fibers and the deposition of cartilaginous ECM was shown and a thick stable construct was then produced with good mechanical properties after 4 weeks of bioreactor growth (Rosa *et al.*, 2014).

A chondro-supportive scaffold from auricular cartilage has been produced and repopulated with different cells. Nurnberger and his colleagues proposed the "AuriScaff", derived from auricular cartilage, decellularized and investigated its potential to be seeded by various cell sources. Elastic fibers had selectively been removed to create a traversing network for cells to pass and migrate deep into the matrix. Bovine and human articular chondrocytes, were cultured on one hand, and co-cultured with human adipose-derived stromal cells on the other hand. Cells migrated and differentiated into chondrogenic cells that uniformly repopulated the scaffold (Nürnberger *et al.*, 2019).

Chiu *et al.*, engineered tri-layered auricular tissue in two different ways. They first used a bi-layered construct done from thousands of cells that were seeded into the polypropylene wells of a continuous flow bioreactor, provided by a flow of fresh medium supplemented with sodium bicarbonate and ascorbic acid. The first method of developing a tri-layered construct consisted of using ficol separation that isolated perichondrial cells from auricular tissues and seeded them into the bi-layered construct. This method produced thin perichondrial layers compared to the native rabbit auricular perichondrium, and GAG content was also reduced. However, when they used the second method that involved the growth of the bi-layered constructs in osteogenic culture medium without addition of cells, another layer of perichondrium was formed on top of the bi-layered construct, resulting in a formation of a tri-layered auricular tissue (Chiu *et al*., 2019).

Microtia chondrocytes were used as cell sources for regenerating auricular cartilage. These cells have been considered as promising sources since they possess abilities to form elastic cartilage. He *et al.*, in their work, demonstrated that microtia chondrocytes are appropriate cell candidates for regeneration of tissue-engineered auricle. Microtic chondrocytes when cultured in 3D chondrogenic culture system, restored their phenotype and generated mature cartilage with rich

cartilage-specific ECM and appropriate mechanical properties (He *et al*., 2020). Besides, insulin growth factor-1 stimulated the induction of concentrated growth factor that significantly synthesized auricular chondrocyte ECM proteins (Chen *et al*., 2019). Moreover, when co-cultured with BMMSC, microtic chondrocytes successfully generated robust cartilage tissue similar to auricular cartilage tissue, conserved their chondrogenic potential and elasticity and produced stable chondrogenesis with a homogenous distribution of lacuna structures without any calcification or fibrogenesis (Zhang *et al*., 2014).

Akbari *et al.*, also generated human scaffold-free auricular cartilaginous constructs. Cells were collected from pediatric auricular cartilage and cultured as high-density micro masses for 8 weeks. Their results showed that the engineered constructs structurally resembled native auricular tissue, with good GAG and collagen II content compared to the native auricular cartilage, in addition to a cellularized neo-perichondrium like layer surrounding the inner cartilage (Akbari *et al.*, 2017).

A Recent study has reported the use of auricular chondrocyte progenitor cells from perichondrium tissue. Layering and rotational culture methods were realized to form a stiff 3D multilayer cartilage tissue that resembled human auricle with a high COL 2 expression. This created an autologous scaffold-free elastic cartilage (Enomura *et al*., 2020). Similarly, adipose derived stem cells have shown to be a promising cell source for auricular cartilage repair (Oh *et al*., 2020; Ziegler et al., 2021).

3.3 Scaffolds

Finding a suitable scaffold is the key to successful reconstruction of auricular cartilage. This latter supports the growth of cells and maintain their phenotypes and deliver signals that can induce cells to secrete ECM and thus regenerate and reconstruct tissue. Furthermore, biomaterials should adhere to the surrounding native tissue and provide mechanical integrity associated with the function of reconstructed tissue. Different options have been used to mimic cartilage extracellular matrix. Many studies have investigated natural polymers where a combination of natural material was used to optimize fabrication of a porous scaffold. Xia and his colleagues, prepared a hydrogel composed of gelatin with hyaluronic acid, and 3D printing was performed to ensure pore structure and shape. Methacrylic anhydride was then added to induce a photocrosslinking reaction, and lyophilization was used to enhance mechanical strength by transforming scaffolds into solid biomaterials to improve cell seeding procedures. Then scaffolds were seeded with goat-auricular chondrocytes and

constructs were cultured in chondrogenic medium in *in vitro* and then *in vivo* models. Their study has demonstrated that photo-cross liked gelatin and hyaluronic acid could form porous scaffold with good internal pore structure, high mechanical strength and weak immunogenicity for cartilage regeneration (Xia *et al.*, 2018). Also, another group used an ear-scaffold composed of porous collagen, supported with titanium wire framework. This biomaterial supported chondrocytes attachment and matrix deposition where glycosaminoglycan content was high and elastin fibers were formed. The embedded titanium wire associated to the scaffold, prevented shrinkage and distortion and withstood mechanical forces during wound healing and neocartilage maturation (Pomerantseva *et al*., 2016). Other studies have also designed 3D ear model resembling human ear that was implanted in a rabbit model. Auricular mesenchymal progenitor cells derived from rabbit perichondrium were seeded on silk-alginate scaffold and the whole construct was implanted in rabbits for 2 months. Although silk alginate model diminished slightly over time, however, it maintained shape and flexibility and supported extracellular matrix production such as collagen II and proteoglycans (Sterodimas and de Faria, 2013). Synthetic polymers were also investigated in auricular cartilage engineering where a group of researchers developed a biocompatible poly gamma-glutamic acid hydrogels, that presented excellent elasticity and withstood 70% mechanical strain. Not only it mediated cell proliferation, but also played an important role in inducing gene expression of cartilage markers. Gamma-PGA hydrogels regenerated the phenotype of auricular chondrocytes that were consistent with the native chondrocytes and facilitated the production of extracellular matrix protein (R. Yang *et al.*, 2020). Furthermore, it has been proved that polyurethane biodegradable matrix was used to treat surgically created auricular and perichondrial defects (Chetty *et al.*, 2008; Iyer *et al*., 2016).

3D Scaffolds made from polycaprolactone based-polyurethane were widely used in auricular engineering. However, the supply of oxygen and nutrients remains a challenge in reconstructive engineering. This is due to the absence of the perichondrium layer that is responsible for this transfer. Thus, microsurgical implantation of the arteriovenous loop can present ameliorated neovascularization of the 3D cell construct. Bomhard *et al.*, investigated this idea by using auricular cartilage biopsies, as cell sources and seeded them in 3D polycaprolactone scaffolds implanted with vascular loops subcutaneously under the skin. After implantation, the 3D auricle was well integrated under the skin and with a stable well-vascularized structure that resembled that of the native cartilage. ECM formation was detected even in the center of the construct and newly-formed

collagen II was also demonstrated, however, when analyzing the control group without an implanted loop, they realized that the center didn't contain any vital cells, but necrotic regions (von Bomhard *et al.*, 2013). They reported that the supply of oxygen and nutrients could be enhanced by using a vascular pedicle implanted with the cartilage construct, that better vascularize and integrate it with the surrounding tissue. Repair of ear cartilage was also done using scaffold made up of PLGA with chitosan non-woven cloth. This was achieved by harvesting bone marrow mesenchymal stem cells that developed into functional cartilage that supported chondrocyte distribution and perfectly repaired defects in rabbit ears. A new approach of using bacterial nano cellulose (BNC) scaffold has been used by (Martínez Ávila *et al.*, 2015). He used (BNC) that possesses excellent biocompatibility and tissue integration capability. BNC is a natural biopolymer derived from different bacterial species. It is mainly composed of water, that's why it is an interesting component in forming a hydrogel. This bilayer BNC scaffold integrates a high porosity and mechanical stability for *in vitro* and *in vivo* auricular cartilage tissue engineering. Furthermore, BNC with alginate has provided support for nasoseptal chondrocytes alone and combined with human mononuclear cells to form neocartilage *in vitro* and *in vivo.* Lately, it has been confirmed that decellularized natural ECM has proved a regenerative capability *in vitro* and *in vivo* and has become an emerging approach where host cells are eliminated, leaving behind a natural functional ECM to be used as a support. Numerous studies have been reported on acellular xenogeneic scaffolds, for instance, tracheal, articular, nasal, intervertebral discs and to a lower degree acellular ear cartilage. This latter is composed of thick elastic fibers and collagen I and II, rendering it dense to be decellularized. Different methods have been used to decellularize auricular cartilage, for instance, freeze-thawing methods can help disrupt the cell membranes as well as causing apoptosis. Trypsin was also used in different protocols as an effective reagent to decellularize elastic cartilage (Rahman *et al*., 2018)

Chiu *et al.*, engineered tri-layered auricular tissue in two different ways. They first used a bi-layered construct done from thousands of cells that were seeded into the polypropylene wells of a continuous flow bioreactor, provided by a flow of fresh medium supplemented with sodium bicarbonate and ascorbic acid. The first method of developing a tri-layered construct consisted of using ficol separation that isolated perichondrial cells from auricular tissues and seeded them into the bi-layered construct. This method produced thin perichondrial layers compared to the native rabbit auricular perichondrium, and GAG content was also reduced. However, when they used the

second method that involved the growth of the bi-layered constructs in osteogenic culture medium without addition of cells, another layer of perichondrium was formed on top of the bi-layered construct, resulting in a formation of a tri-layered auricular tissue (Chiu *et al.*, 2019).

Other studies have investigated the implantation of biodegradable polyurethane matrix in pig models to assess this matrix as support for cartilage. Iyer *et al.*, for instance, have surgically created auricular cartilage and perichondrial defects and filled up these defects with biodegradable polyurethane matrix. The matrix was able to integrate into auricular defects, however, a poor regenerative activity was achieved, this was due to the limited migration of cells that were trapped within the extracellular matrix, and their slow metabolic rates. It has been shown that not all successful *in vitro* experiments can be replicated *in vivo,* Since, biological and regulatory mechanisms are not the same (Iyer *et al*., 2016). Pomerantseva *et al.*, on the other hand engineered successfully a human ear-shaped cartilage in an immunocompetent sheep model. They produced disk and human ear-shaped scaffolds from porous collagen, similar to the work of Bichara *et al.*, but with superior neocartilage quality (Bichara *et al*., 2014). Since Pomerantseva supported the construct with a titanium wire to conserve the shape of the ear. These scaffolds were then seeded by sheep chondrocytes, cultured for 2 weeks *in vitro*, and implanted subcutaneously in sheep. They demonstrated the first stable, engineered ear that was implanted where it was rich in high GAG content and elastic fibers. The surrounding wireframe withstood mechanical forces and protected the engineered ear from retention and ameliorated the quality and stability of neocartilage (Pomerantseva *et al*., 2016).

Acellular matrices in auricular cartilage have received a great attention, in the recent years. This was due to their excellent biocompatibility and biodegradability. Also, these matrices were characterized by robust intrinsic bioactive components, mimicking their microenvironment (Weiming Chen *et al*., 2020; Xu *et al*., 2020). Pore size and 3D structure are crucial elements for cell proliferation, adhesion and ECM production in cartilage engineering. Silk fibroin has used 3D printing techniques to repair cartilaginous defects *in vitro* and *in vivo* (Wei Chen *et al*., 2020; Shi *et al*., 2017). Furthermore, fish collagen has recently been considered as alternative to mammal-derived collagen, where Li *et al.*, have shown that this natural source was characterized by excellent biocompatibility and degradability with a significant increase in water absorption and mechanical strength. The porous fish collagen promoted cartilage repair when evaluated *in vitro* and *in vivo* in

rabbit models (H. Li *et al.*, 2020). Many studies have investigated the biological potential of acellular cartilaginous matrix and dermal matrix as scaffolds for auricular cartilage tissue engineering. Wang *et al.*, in their studies have demonstrated that acellular dermal matrix showed higher cell adhesion, neocartilage formation and more stable mature cartilage, with low immune response compared to acellular cartilage matrix when implanted in goat models, indicating that dermal matrices are more suitable for cartilage engineering (Y. Wang *et al.*, 2020).

The application of cell sheet technology used in cartilage tissue engineering may resolve the limitation of using a non-porous acellular scaffold where cells are inhibited from proliferating and differentiation and sometimes causing structural collapse. This technique should a superior adhesion and enhanced regeneration. It is also imperative to characterize chondrocyte sheets and evaluate its similarity to native cartilage. Mitani *et al.*, showed in 2009 that chondrocyte sheet produced cartilage markers and expressed SOX9, collagen type II, and some fibronectins, in addition to that, these sheets efficiently regenerated partial and full-thickness cartilage, resembling native tissue physiology (Mitani *et al.*, 2009).

Gong *et al.*, established a sandwich model for cartilage engineering, porcine cartilage was cut into circular sheets, decellularized, and lyophilized. Acellular sheets were stacked layer by layer with chondrocytes forming a sandwich model of about 20 layers. This model was cultured *in vitro* for 4 weeks and *in vivo* in nude mice for 12 weeks, after then analyzed and showed cartilage characteristics with no inflammatory response (Gong *et al.*, 2011).

Auricular and articular scaffold-free system constructs were compared for their ECM stiffness and production *in vitro* when coupled to porous tantalum and upon *in vivo* implantation. Auricular constructs produced more and stiffer ECM compared to articular ones. Upon *in vivo* implantation, auricular chondrocytes produced thicker constructs and by attachment to porous tantalum by cellular ingrowth to the pores (Whitney *et al.*, 2012). Studies by Tani *et al.*, have described the preparation of auricular sheets that were looped around a silicon tube and cultured for several weeks. Their results showed a proper level of flexibility and rigidity in an engineered trachea (Tani *et al.*, 2010).

Auricular cartilage tissue was highly fabricated using fibrin gel auricular scaffold resembling human auricular anatomy shown in **Figure 24.** This was achieved by extracting rabbit auricular chondrocytes from ear cartilage and culturing them to form cell sheets. These sheets were then

successfully laden with chondrocytes and constructing a fibrin gel auricle scaffold that highly resembles human ear. This scaffold highly maintained ear morphology after 1 week *in vitro* and became firmer since chondrocytes secreted cartilage-like matrices that substituted the initial fibrin gel. After implantation of the auricular-shaped tissue in animal models for 8-weeks, newly formed cartilaginous tissue showed mature cartilage tissue with protein rich ECM, however with a low mechanical strength (Yue *et al.*, 2020).

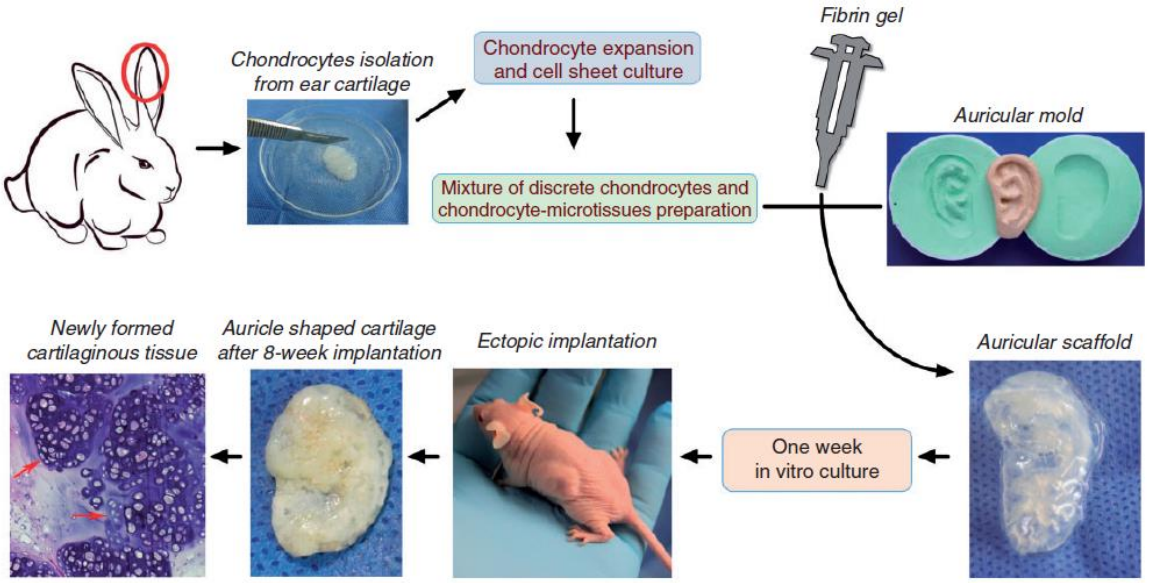

Figure 24*:* Scheme showing the fibrin gel auricular scaffold fabrication process and its *in vitro* and *in vivo* evaluation (Yue *et al*., 2020).

3.4 Growth factors used for enhancing auricular tissue engineering

Growth factors are biologically active molecules, stimulating cell division, growth, and differentiation into specific niches. The anabolic factors can also stimulate production and synthesis of extracellular matrix. In cartilage, many growth factors regulate development and homeostasis, thus offering a key factor in treatment and regeneration of cartilage.

3.4.1 Insulin-like growth factors

They look like growth factors and physiologically stimulate growth of cartilage by stimulating already differentiated chondrocytes and promoted their multiplication. Also, IGF-1 was shown to

induce chondrogenesis of MSC from bone marrow (Zhou *et al.*, 2016). Studies have shown a significant increase in IGF-1 expression when ADSC were transplanted *in vivo* to fill defects of auricular cartilage. The high expression of collagen II and IGF-1 at 8 weeks post-injection, was due to the high ECM matrix and the presence of IGF-1 that induced the maturation of these cells to produce more and more collagen and IGF-1 (Oh *et al.*, 2020). Also, IGF-1 released by concentrated growth factor-stimulated the synthesis of the auricular chondrocyte extracellular matrix via the activation of IGF-1R/PI3K/AKT pathway. This was confirmed by silencing IGF-1 using siRNA. As a result, the amount of GAG, proteoglycans, collagen and ACAN in CGF-treated groups were significantly higher than that of the auricular cartilage in presence of DMEM and of silenced IGF-1. This indicated that IGF-1 plays an important role in CGF-induced ECM synthesis in auricular chondrocytes (Chen *et al*., 2019). In addition to that, these growth factors were investigated to stimulate elastogenesis in auricular chondrocytes. Rabbit auricular chondrocytes that were cultivated and supplemented with insulin and IGF-1, showed after 4 weeks of growth, increased deposition of ECM, and good mechanical properties as well as a thick structure comparable to native tissue. Furthermore, IGF-1 increased expression and localized elastin within the matrix of the tissue (Rosa *et al.*, 2014).

Injection of IGF-1 on rabbit auricular cartilage autografts implants were performed every 2 weeks to investigate the viability of cartilage. It was revealed that IGF-1 increased the viability of the implanted auricular cartilage and suppressed immune modulation effect (Beriat *et al.*, 2012; Okubo *et al*., 2019).

Chiu *et al.*, have engineered a tri-layered auricular tissue to reconstruct external ear anomalies. They combined chondrocytes with perichondrocytes in a bioreactor system with osteogenic medium supplemented with both insulin and insulin-like growth factor (IGF-1). They showed that combining IGF-1 and insulin improved the development of a bi-layered construct (Chiu *et al*., 2019).

3.4.2 Basic fibroblast growth factor (bFGF)

It has been proved that bFGF is a growth factor present in the bovine extract. It induces proliferation and differentiation, as well as migration and angiogenic potential. Studies by Miyanaga, reported that when bFGF was integrated into the inner layer of the perichondrium, auricular perichondrial

cell markers are activated by bFGF, becoming active chondrocyte precursor cells, where they start proliferating and differentiating into functional chondrocytes, reforming the perichondrial membrane. He added that chondrogenesis was bFGF concentration-dependent since the highest concentration of bFGF yielded the highest level of cartilage formation and also confirmed that proliferative nature of human ear chondrocytes increased when these chondrocytes were treated in bFGF (Miyanaga *et al.*, 2018). Not only IGF-1 induced elastic cartilage, but also bFGF can be supplemented in medium to enhance elastic chondrogenesis after 8 weeks of autologous implantation (Lou, 2020).

3.4.3 BMP-2

This transforming growth factor promotes stem cells differentiation into chondrocytes, as well as the redifferentiation of chondrocytes when encapsulated in 2D and 3D culture models (alginate beads) with an increased synthesis of collagen type II. However, if the chondrocytes are exposed to BMP-2 for a longer period of time, they will differentiate towards a bone phenotype. When BMP-2 was loaded on nanoparticles and distributed into 3D PCL scaffold and implanted in vivo, results showed that bone formation was highly significant and compressive strength was improved in coated group in presence of BMP-2 compared to the uncoated group (Kim *et al.*, 2018). Moreover, BMP-2 was also implied in cartilage tissue engineering, where the combination of BMMSC and BMP-2 repaired completely the osteochondral defects in rabbits (Vayas *et al.*, 2017).

3.4.4 TGF-β

TGFβ-1 was most commonly used for in vitro culture and has stimulated the synthetic activity of chondrocytes. It enhanced GAG's synthesis and adipose-derived stem cells regenerative effects in rabbits (Oh *et al.*, 2018). TGFβ-3 has recently been shown to have the best chondrogenic activity of the three isoforms. When incubated with adipose-stem cells, TGFβ-3 induced and displayed chondrocytes-like cells with typical lacunae which is similar to the native cartilage (Goh *et al.*, 2017). Furthermore, when TGFβ-3 was transfected into BMSC using an adenovirus, stable expression of this protein was observed and BMSC differentiation into chondrocytes was enhanced and Combination of TGFβ-3 with bFGF synergically increased the potential of porcine chondrocytes to enhance and regenerate autologous elastic cartilage (Wang *et al.*, 2014). Recently,

a new study demonstrated that TGF-β modulated pSmad3 cells levels in tissue that increased growth of neo cartilage tissue. Moreover, fibrosis was mediated by TGFβ signaling that enhanced the differentiation of cartilage during ear-hole regeneration (Abarca-Buis *et al*., 2020).

3.5 3D printing

3D printing creates and manufactures objects using different layers of materials stacked on top of each other to design the specific shape required, using a software and specific bioinks. 3D printing technology is nowadays popular in tissue engineering, due to its easy fabrication of scaffolds with or without living cells. The choice of ink has always been a challenge, since specific biochemical and mechanical requirements are critical for mimicking biomechanics of soft tissue.

Moreover, 3D printing techniques have been shown promising results in auricular cartilage engineering. Methacrylated Gelatin (GelMA) and Hyaluronic acid (HAMA) were combined together, as well as Polycaprolactone (PCL) to print 3D scaffolds that highly increased the viability of human MSC. As a result, 3D scaffold produced mimicked human auricular cartilage and presented excellent support and porosity of cells with good mechanical strength (Chung *et al.*, 2020). 3D-PCL auricular scaffolds shown in **Figure 25**, printed in two-stages with high fidelity and interconnected pores that helped to increase viability of MSC and induced robust tissue ingrowth and angiogenesis when implanted *in vivo* in rat models (Brennan *et al.*, 2021). Other studies have investigated 3D printed chitosan that stimulated differentiation of chondrocytes (Sahai *et al*., 2020). By combining chitosan to poly(ethylene glycol) diacrylate (PEGDA), induced excellent mechanical properties and enhanced flexibility and elasticity of 3D auricle (Deng *et al*., 2020). Elasticity was also achieved by adding gelatin to hyaluronic acid (HAMA)/alginate hydrogel that constituted a good functionalized bioink, thus improving cytocompatibility and cellular proliferation (Y. Zhou *et al.*, 2020).

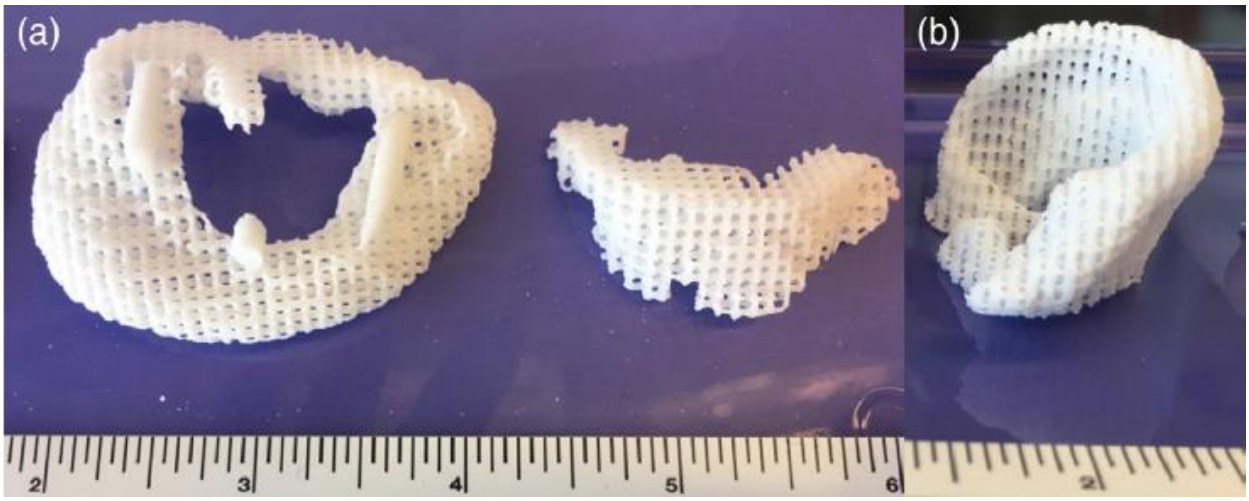

Figure 25: 3D-printed auricular cartilage scaffolds (Brennan *et al*., 2021).

3.6 *In vivo* and clinical applications

The identification and comparison of auricular perichondrocytes were reported in some previous studies. However, the *in vivo* chondrogenesis of these cells has not yet been well studied and characterized. A recent clinical study has shown that stem cells from auricular cartilage exhibit better chondrogenesis compared to perichondrium progenitors. After 6 weeks of *in vivo* incubation, their results showed an upregulation of cartilage genes and the formation of a mature cartilage with a good mechanical property (X. Zhang *et al*., 2019). Cartilage stem progenitor cells expressed more GAG and collagen II levels than perichondrium stem progenitor cells, indicating that auricular cartilage progenitors can serve as an ideal cell source *in vitro* and *in vivo*.

Not many studies have investigated clinical *in vivo* auricular cartilage reconstructions. Iyer *et al.*, have investigated a polyurethane matrix seeded with porcine chondrocytes and perichondrocytes and incubated afterwards in a porcine allogenic model. This matrix favored the integration of granulation tissue filling perichondrium defects. There was no difference between constructs seeded with chondrocytes alone or combined to perichondrocytes, both expressed GAGs and collagen II, and a good integration of the matrix to the site of injury (Iyer *et al.*, 2016).

Many researchers have also examined cartilaginous defects in rabbit models, where Yue *et al.*, developed a 3D microtissue from rabbit chondrogenic cell sheets and chondrocytes. This 3D structure retained its anatomical properties after 8 weeks in allogenic rabbit models (Yue *et al.*, 2021).

Other researchers introduced bioreactor cultivated constructs to reconstruct cartilaginous and perichondrium-like defects with different alteration of medium, for instance, Duisit *et al.*, in their studies perfused human auricular ears to prepare decellularized human auricle that retained their complex shape and were able to host new viable cells and vascularization upon implantation in animal models (Duisit *et al.*, 2018).

Recent high fidelity 3D-printed bioscaffolds have successfully enhanced auricular cartilage reconstruction. Combination of PCL material and cartilage remnants promoted better regenerated quality of auricular cartilage. For instance, Brennan *et al.*, in their studies have fabricated 3D-printed auricular cartilage scaffolds that were implanted subcutaneously in rat models for several week and significantly increased tissue growth and angiogenesis as shown in **Figure 26**.

Figure 26: Ear scaffolds implanted on the dorsum of rat models (a). Angiogenesis and vasculature in-growth of 3D-printed auricle scaffold (b) (Brennan *et al.*, 2021).

To conclude, I summarize the different sources and scaffolds that have been used in the recent 5 years for *in vitro* and *in vivo* auricular cartilage regeneration (**Table 2**).

Table 2 : Table summarizing cell sources, scaffolds, experiment conditions and growth factors for *in vitro* and *in vivo* auricular cartilage engineering.

Cell sources	Scaffolds	Experiment Conditions	Growth factors	*In vitro*	*In vivo*	References
Rabbit auricular chondrocytes	Fibrin gel-based scaffolds Chondrocytes cells sheet	Chondrocytes mixed with chondrocyte cell sheet to from chondrocyte microtissues		3D structure and auricular anatomy was retained after 1 week	Cartilaginous tissue regenerated after 8 weeks of implantation in rabbit models, auricular anatomy maintained	(Yue *et al*., 2021)
	Auricular cartilage +(PCL)	3D-printing			Maintenance of integrity, of anterior and posterior auricular surfaces, robust tissue ingrowth and angiogenesis (5 weeks in rat models)	(Brennan *et al*., 2021)
ADSC and their secretome		Direct injection of ADSC in defects		ADSC improved auricular cartilage regeneration, expression of collagen II, TGFβ-1 and IGF-1 (4-8 weeks in rabbit models)		(Oh *et al*., 2020)
	Scaffolds with or without autogenous minced auricular cartilage				Minced cartilage scaffolds regenerated better auricular cartilage	(Min *et al*., 2020)

ADSC Rabbit articular chondrocytes	PCL framework and cell-laden alginate hydrogel	3D printing		PCL sustained sustain the structure and enhance the mechanical properties, alginate inhibited ADSCs from osteogenesis, leading to chondrogenesis	More native-resembling auricular cartilage with no donor site-morbidity	(Jang *et al.*, 2020)
	3D-printed auricular bioscaffold with or without porcine cartilage tissue inserts in an athymic rodent model with PCL	3D printing			Grossly visible tissue ingrowth and angiogenesis, robust soft tissue infiltration and vascularization in both seeded and unseeded scaffolds, maintenance of viable cartilage in cartilage-seeded scaffolds	(Chang *et al.*, 2020)
Rabbit BMMSC	Methacrylate-PGA and cysteine functionalized ϒ-PCA			Outstanding capacity of anti-compression and shape recovery, matrix production and 3D chondrogenic formation of BMSC		(R. Yang *et al.*, 2020)

Canine auricular chondrocytes	atelocollagen	3D-cultured with four types of media	IGF-1, FGF-2, insulin	High gene expression of type II collagen was detected in the construct cultured with the differentiation medium whereas cell apoptosis were suppressed in the proliferation medium.	Abundant cartilage matrices, high cell viability	(Okubo *et al*., 2019)
Human chondrocytes perichondrial cells	Scaffold-free bi-layered auricular tissues	Bioreactor	IGF-1 insulin	Tri-layered auricular tissue for ear reconstruction		
Cow auricular chondrocytes	Auricular cartilage discs	Enzymatic treatment of elastase	BMP-6 TGFβ-3	Repopulation of auricular cartilage scaffold		
Human auricular chondrocytes	(PLA)/ (PLGA) with collagen	Chondrocytes were put in scaffolds and implant-type tissue-engineered cartilage	BMP-2 TGFβ IL-1β	TGFβ stimulates hypertrophic maturation, IL-1β promotes angiogenesis and cartilaginous formation		
Goat auricular chondrocytes	PCL scaffold and alginate beads	3D printing	TGFβ	high-compressive moduli that were 100 higher than that of native cartilage		(Visscher *et al.*, 2019)

Rabbit auricular chondrocytes Nasal chondrocytes	Decellularized porcine nasal septum			Auricular chondrocytes produced more cartilage-like matrix higher expression of anabolic growth factors BMP5 and IGF1		(Von Bomhard *et al.*, 2019)
Rat ADSC Human aortic endothelial cells	12 human ears	Perfusion decellularization using SDS/polar solvent	TGFβ VEGF bFGF	Extra vascular rigidity, high vascular resistances	Preservation of the ECM structure, rich in collagen, mild immune response, Vascularized and complex auricular scaffolds	(Duisit *et al.*, 2018)
Rodent adipose-derived stem cells	Porcine ear	Decellularization		Vascularization, high viability of the different cells	High vascularization, normal blood pressure, architecture and biochemical components retained	(Duisit *et al.*, 2018)
Autologous microtic chondrocytes	PCL mesh as an inner core, wrapped with PGA unwoven fibers and coated with PLA	3D printing		Engineered ear cartilage retained its original 3D shape, decreased stiffness and increased elasticity after 2 years	Regenerated cartilage itself without PCL frame with mechanical properties similar to those of native cartilage	(Zhou *et al.*, 2018)

Human auricular chondrocytes	Remnant, normal pediatric auricular cartilage samples	Micromass cultures		Mechanical stability and structurally resembled native auricular tissue, with a perichondrium-like layer of cells surrounding the inner cartilaginous zone after 8 weeks	-	(Akbari *et al*., 2017)
Rabbit auricular chondrocytes	PCL framework with alginate bioink	3D printing		-	Cell printed structure showed complete cartilage regeneration	(Park *et al.*, 2017)
Sheep auricular chondrocytes	Collagen (disk-shaped) scaffolds + ear-shaped scaffold	Titanium wire to support scaffolds			Wire frame withstand mechanical forces during neocartilage maturation and prevented shrinkage	(Pomerantseva *et al.*, 2016)

II-Aims

Auricular cartilage reconstruction remains one of the most challenging techniques for otolaryngology head and neck surgery. Tissue engineering is an alternative and promising approach, that uses cells, scaffolds and growth factors to assemble functional constructs that can improve, restore or replace damaged tissues and organs. Despite significant progress in this field, many confronts remain unsolved.

Several Scaffolds have been used, however, no material that perfectly mimics the nature of elastic cartilage has been investigated yet. Despite the significant progress of tissue engineering approaches, optimization is still needed to enhance cellular growth, differentiation and integration during *in vivo* implantation.

A variety of scaffolds have been engineered and used to replace surgical reconstructions, however, these scaffolds degraded over weeks or months, and space was then replaced by proliferated cells leading to fibrosis. Cell suspension injections are also an option but not really suitable for large tissue reconstruction, since few percent of injected cells are integrated into host tissues.

My thesis project aims to investigate new approaches of auricular cartilage repair through the use of decellularized scaffolds and to evaluate them *in vitro* and *in vivo*. Animal (native cartilage) or vegetal (apple) scaffolds were tested after characterization of different cell sources for their ability to regenerate cartilage. Alternatively, we highlighted and investigated the use of new matrices, namely cell sheets, as potential support for auricular cartilage engineering.

In order to contribute to a better recellularization and reconstruction potential, the main objective was divided into several tasks:

- Characterization of best cellular sources that can express chondrogenic and elastic markers, and enhance cartilage formation to be used in reconstructing auricular cartilage defects.
- Developing an animal model of cartilage defect and reconstruction

- Investigation of cell sheet technology from auricular perichondrocytes for cartilage production *in vitro* as well as cellularized scaffold to be introduced into the site of injury to regenerate *in vivo* cartilaginous defect in rabbits.
- Development of several *in vitro* uses of cell sheets as allogenic and xenogeneic cellular patches that result from decellularized cell sheets as a replacement of intact scaffolds. These investigations, also led us to develop an innovative use of cell sheets, after decellularization and lyophilization.
- Designing and engineering of new cellulosic matrices from apple tissue for auricular cartilage engineering.

III-Results

1-Effects of hypoxia on chondrogenic differentiation of progenitor cells from different origins

Cartilage tissue engineering approaches are highly controlled by cell sources. Whether directly seeded on transplanted scaffolds or expanded *in vitro*, choice of cellular material has a major and very important role in affecting biological processes of cartilage tissue. In the first part of my thesis, we were interested in producing and regenerating auricular cartilage tissue work was to choose the cellular source that best produce and engineer auricular cartilage tissue. For engineering ear tissue, it was necessary to investigate progenitors from head area that derive from different embryological origins. For this reason, we chose auricular perichodrocytes (AuP), nasal perichondrocytes (NsP) and dental pulp stem cells (DPSC) that were compared to BMMSC. The cells were encapsulated in a well mastered model of chondrogenesis, namely 3D alginate beads. Moreover, in this study we aimed also to study the effect of hypoxia on cell's chondrogenic potential to form auricular cartilage tissue. This was performed by encapsulating the four cell sources in alginate beads and culturing them in normal (21% O2) and low oxygen levels (3% O2).

Our results suggested that after 2 weeks of culture, all cell types were able to produce cartilaginous ECM as shown in histological staining. More clearly auricular perichodrocytes presented the highest significant expression of cartilaginous genes in chondrogenic normoxic environment. Interestingly, apart from the remarkable increase of elastic cartilage generation, the relatively low expression of COL X in auricular progenitors indicates the preservation of the phenotype in these cell types under *in vitro* chondrogenic conditions, compared to other progenitors. On the other hand, hypoxic environment highly stimulated BMMSC to express significantly high results of cartilaginous markers, except for COL1 and COLX genes that were relatively low in these cells.

Altogether, these results indicate that among our tested cells, AuP highly produce cartilaginous elastic extracellular matrix and that hypoxia is not needed and didn't affect their chondrogenesis, in contrast to BMMSC results. This could be explained by the different mechanisms of action of low oxygen levels on different cells and progenitors.

To conclude, auricular perichondrocytes are the best candidates for engineering elastic cartilage tissue in normal oxygen levels. Nevertheless, hypoxia, turns to be ineffective and unbeneficial for these cells. Our results spotlight on the role of oxygen in promoting and enhancing the quality of engineered elastic cartilage. To deepen our results, *in vivo* studies in animal models should be designed in the same conditions for a clear investigation of cells to regenerate and repair auricular cartilage.

Effects of hypoxia on chondrogenic differentiation of progenitor cells from different origins

Mira Hammad[1,2], Sylvain Leclercq[1,3], Vincent Patron[4], Alexis Veyssiere[1,2,5], Catherine Baugé[1,2], Karim Boumédiene[1,2]

[1]Normandy University, UNICAEN, EA 7451 BioConnecT, Caen, France, [2]Fédération Hospitalo Universitaire SURFACE, (Amiens, Caen, Rouen), France, [3]Clinique Saint Martin, Service de Chirurgie Orthopédique, 14000, Caen, France, [4]Service ORL et chirurgie cervico-faciale, CHU de Caen, [5]Service de chirurgie Maxillo-faciale, CHU de Caen, Caen, France,

Abstract

Ear cartilage malformations, resulting from congenital anomalies, trauma or cancer, are commonly encountered problems in reconstructive surgery, since cartilage has low or no self-regenerating capacity. Malformations that impose a psychological and social burden on one's life are currently treated using ear prosthesis, synthetic implants or autologous flaps derived from rib cartilage. These approaches were challenging, not only they do request high surgical expertise, but also because they face progressive resorption, lack of flexibility and severe donor-site morbidity. Through the last decade, a newly approach of tissue engineering gained attention. It aims at replacing, regenerating human tissues or organs in order to restore or establish normal function. This technique consists of three main elements, cells, growth factors, regulating cellular activity and above all, a scaffold that support cells and guide their behavior. Several studies have investigated different scaffolds prepared from both synthetic and natural materials, and their effects on cellular differentiation and behavior. In this study, we investigated natural scaffold (alginate), as three-dimensional (3D) hydrogel where it was seeded with progenitors from different origins such as bone marrow, perichondrium, and dental pulp. In contact with the scaffold, these cells remained viable and were able to differentiate into chondrogenic lineage when cultured *in vitro*. Quantitative and qualitative results show the presence of different chondrogenic markers as well as elastic markers for the purpose of ear cartilage, upon different conditions of culture. Here, we confirm that auricular perichondrocytes outperform other cells to produce chondrogenic tissue in normal oxygen levels and we report for the first time the effect of hypoxia on these cells. Our results provide some updates for cartilage engineering and regeneration for future clinical applications.

Introduction

External ear anomalies describe a wide range of birth defects such as microtia and anotia, as well as amputation and burns that can result from animal bites, surgery and sometimes cancer (Wernheden *et al.,* 2019). Different clinical approaches are used to correct such anomalies. Reconstruction was first done by harvesting autologous cartilage from ribs and carving it in the shape of the ear (Firmin and Marchac, 2011). However, this technique possesses some

disadvantages such as donor-site morbidity and poor elasticity of the cartilage. On the other hand, synthetic scaffolds and prosthesis have been widely used and created a proper shape for ear reconstruction. These latter were also shown to produce undesirable effects, where they induced inflammation and tissue irritation. This explain the ever-lasting demand for tissue engineering, investigating multiple scaffolds. Significant advances have been successfully accomplished in regenerative medicine, with various innovative approaches and scaffolds that have been introduced to replace current treatments (Li and Sun, 2019). Many studies have investigated fabricated constructs, were cells were seeded in scaffolds or encapsulated into polymers of cross-linked monomers to be injected later on into ear molds (Bernstein *et al.,* 2018; Cohen *et al.,* 2016). Successful engineering of a clinically auricular implant necessitates a biomaterial, providing 3D system to control and support cellular growth and chondrogenesis. 3D systems are biologically more relevant and thus using these kinds of systems, add biological relevance to cells and optimize their response to their environment. Among them, alginate has been proved to successfully maintain chondrogenic profile and neocartilage regeneration (Yang *et al.,* 2018). Recent research highlighted that alginate-hydrogels serve as a stable, cytocompatible, high integrity scaffold in chondral regeneration (Gentile *et al.,* 2017) and auricular 3D printing (Visscher *et al.,* 2019). In addition to alginate, oxygen level also plays a key role in chondrogenesis. Hypoxia was shown to enhance nuclear accumulation of HIF-1alpha levels that promotes mesenchymal stem cells (MSC) to follow a chondrogenic pathway by activating SRY-Box Transcription Factor 9 (SOX 9) promoter activity in mesenchymal stem cells and promoting chondrogenic differentiation (Bae *et al.,* 2018; Foyt *et al.,* 2019). Regarding the cells used for cartilage reconstruction, chondrocytes were used as native autologous sources, from desired tissues. However, the low cell density of biopsies, the possible donor-site creation and the propensity of chondrocytes to dedifferentiate upon subculturing, led to the widely use of progenitor cells that are characterized by a good proliferation rate. Their differentiation is mastered under specific conditions (3D culture, differentiation media, and environment).

Tissues and organs are rich with a certain number of progenitors that can replace cells or restore injured tissues and organs. Cartilage is mainly targeted with bone marrow-derived stem cells (BMMSC). Interestingly, several studies have reported the high proliferative rate of tissue progenitor stem cells identified in auricular perichondrium of different species (Shinji Kobayashi *et al.,* 2011; Togo *et al.,* 2006). This cell population was characterized by multiple differentiation potential as well as the expression of cell surface markers and colony forming units (Xue *et al.,* 2016). Perichondrial derived porcine progenitors were shown to induce cartilage-like matrix (Derks *et al.,* 2013), both *in vitro* and *in vivo*. Furthermore, monkey-derived perichondrial cells transplanted in subcutaneous autologous craniofacial injuries developed mature elastic cartilage after 3 months (Kagimoto *et al.,* 2016). Another recent study has also suggested the importance of the use of auricular perichondrial cells in mice that produced mature elastic cartilage under chondrogenic conditions (Zhang *et al.,* 2019).

Dental pulp stem cells (DPSC) have also been investigated for cartilage regeneration and repair. Nemeth *et al.,* have demonstrated that DPSC when encapsulated in nanopatterned polyethylene glycol, gelatin methacrylate hyaluronic acid (PEG-GelMA-HA) 3D spheroids, upregulated the chondrogenic gene markers and enhanced cartilage tissue engineering (Nemeth *et al.,* 2014).

Encapsulated in a nanoscale thermosensitive scaffolds, DPSC presented a stable biocompatible construct *in vitro* and *in vivo* where it showed a proliferative capacity similar to MSC and retained mechanical strength (Talaat *et al.,* 2020). In other report, DPSC were evaluated in animal models and their chondrogenic potential was proved to repair hyaline cartilage (Fernandes *et al.,* 2018; Mata *et al.,* 2017) as well as fibrous cartilage (Longoni *et al.,* 2020).

Recent literature has also shown that nasal chondrocytes have similar structural composition as articular chondrocytes, however a greater chondrogenic ability since they possess greater cell density and higher amount of glycosaminoglycans (GAGs) (Mumme *et al.,* 2016). They also reported that nasal chondrocytes and neural-crest derived cells successfully repair articular cartilage with a greater chondrogenic capacity than mesenchymal stem cells (Li *et al.,* 2020). Moreover, Amaral *et al.,* characterized chondrogenic cell population from human nasal septal cartilage tissue and showed their potential to differentiate into osteogenic and chondrogenic lineages where they observed a high expression of the master gene SOX 9 and also presented cartilage-like extracellular matrix (ECM) in pellet culture system (Amaral *et al.,* 2012). Other reports have also compared the chondrogenic potential of nasal septal chondrocytes to perichondrial cells and establishes a novel process to ensure effective and safe clinical use of these cells (Asnaghi *et al.,* 2020). In this study, we wanted to determine the best cell candidate to use in order to engineer auricular cartilage for cartilaginous graft preparation. Auricular and nasal perichondrocytes (AuP and NsP) were chosen as well as DPSC to compare their chondrogenic potential to the goal standard BMMSC. Due to the different embryological origins of these cells from ear cartilage which is mainly derived from neural crests, it was therefore, necessary to investigate and compare progenitors from head area.

Materials and methods

Isolation and cultivation of human cell sources

Cells were obtained from several sources. BMMSC were derived from bone marrow aspirates that were collected during arthroplasty. Patients have signed the consent form according to local legislation. Bone marrow was separated by ficoll gradient and the intermediate ring containing peripheral blood mononuclear cells (PBMC) was plated and cultured in alpha-MEM containing basic fibroblast growth factor (bFGF). Medium was changed twice per week and cells were freezed when they reached passage 3.

Dental pulp tissue was obtained from freshly-extracted teeth of young donors (16-20 years). These latter were transferred into hypotonic phosphate buffered saline solution and were disinfected by a solution of antibiotics. Then pulp tissue was isolated from the pulp chamber where the tissue was minced into small pieces and sequential enzymatic treatment was carried out by collagenase I (3mg/ml) and dispase (4mg/ml) for 30-45min, at 37°C. After enzymatic digestion, cell suspension was centrifuged at 2000 rpm for 10min, and the cell pellet was resuspended with cultivation media (alpha-MEM + 10% FBS + 1% penicillin/streptomycin + bFGF 0.5µg/ml) and seeded into cultivation dishes, and freezed when reaching passage 3.

Nasal perichondrocytes samples were collected after septoplasty to remove a part of nasal cartilage and its perichondrium. Cartilage was dissected and separated from perichondrium layer that was transferred to a tube of PBS and antibiotics. Perichondrium was then washed with a diluted solution of antibiotics, tissue was cut into small section and digested with pronase and collagenase for 45min to collect cells. Cell suspension was centrifuged at 1500 rpm for 10min and the remaining cell pellet was resuspended using the same cultivation media as above. Medium was changed twice a week cell were expanded until reaching passage 3, after which they were freezed at -150°C.

Auricular perichondrocytes were obtained from fresh-human auricular cartilage biopsies after 12-year old children rhinoplasty. Perichondrium was separated from cartilage by dissection and sliced into small pieces. Cells were collected by sequential enzymatic digestion using pronase for 45-60 min at 37°C and collagenase II overnight at 37°C. The next day cells were seeded in T75 flasks and amplified till reaching passage 3, which then freezed for further use.

Trilineage differentiation

The four progenitors were tested for their ability to differentiate *in vitro* towards osteogenesis, adipogenesis and chondrogenesis. Cells were then plated in 6-well plates at a density of 12.5x10^4 cells/cm^2. After 24hrs, they were incubated with appropriate differentiation media. Osteogenic medium (Alpha-MEM, 0.1% antibiotics, 10% fetal bovine serum, 100nM dexamethasone, 50µg/ml ascorbic acid-2 phosphate, β-glyceraldehyde 10µmol/L. Adipogenic medium (alpha-MEM, 0.1% antibiotics, 10% fetal bovine serum, 100nM dexamethasone, 0.5mmol/L Isobutylmethylxanthanine. Chondrogenic medium (DMEM initially with glutamine, 0.1% antibiotics, 100nM dexamethasone, 50µg/ml ascorbic acid-2 phosphate, 40µg/ml proline, 1mM sodium pyruvate and ITS+1 (Insulin transferrin solution selenite media supplement (100x) and transforming growth factor beta-3 (TGFβ-3).

Cells were incubated for 14 (osteogenic medium) and 21 days (adipogenic and chondrogenic medium) and then fixed with 4% PFA and prepared for cytological specific stainings with Alizarin red, Oil red and Alcian Blue for osteogenesis, adipogenesis and chondrogenesis, respectively.

Tridimensional culture and chondrogenic conditions

Cells were used after the forth passage, collected by centrifugation and mixed with (1%) alginate solution (5x10^6 cells/ml). The suspension was extruded into calcium chloride solution (0.1M) to produce gel beads that were kept in calcium chloride solution for 10min, then rinsed with NaCL (0.15M). The beads were then separated into desired conditions and cultured in 6 well-plates dishes. Cells were tested in both normoxic (21% O2) and hypoxic (3%) conditions with or without chondrogenic medium for 2 weeks.

Cytology

After 2 weeks, alginate beads were fixed in 4% PFA for 30min and rinsed overnight with 30% sucrose solution. The next day they were embedded in Optimal Cutting Temperature (OCT) mounting medium and cryosectioned (Leica CM 3050S) at -21°C. Sections of 10µm were collected on super frost® plus microscopic slides (Fisher scientific) and air-dried before

histotology and immunostaining. Safranin O and Alcian blue staining were applied to stain glycosaminoglycans and proteoglycans, respectively.

Immunohistochemistry

Sections on super frost slides were rinsed in PBS and incubated overnight at 4°C with ELN (1:100, ab21607 abcam, Cambridge, UK), collagen II (1:100, ab34712 abcam, Cambridge, UK) and ACAN (1:200, ab3773abcam, Cambridge, UK) primary antibodies. A negative control was performed by replacing primary antibody solutions with PBS. The next day, slides were rinsed five times in PBS to remove traces of primary antibody, and a secondary antibody (Alexa Fluorophore 594 conjugated anti-rabbit) diluted (1:800) was used to incubate slides for 1.5 hour. Rinsing with PBS was done to remove excessive secondary antibody. Slides were then rinsed three time with PBS before mounting for microscopic observation by EVOS cell imaging system microscope, Thermo fisher scientific).

RNA extraction and real time RT-PCR

Alginate microspheres were dissolved in a solution of sodium citrate (0.1M) and total RNA was extracted by Qiagen kit (RNeasy® mini kit 250), according to the manufacturer's protocol. 1µg of total RNA was treated with DNAse before retrotranscription into cDNA using MMLV enzyme (28025-013, Invitrogen by thermofisher scientific) and oligodT primers. Specific transcripts were then amplified by real time PCR using the following primer sequences:

Gene	Forward primer	Reverse primer
ELN	CCAGGTGTAGGTGGAGCTTT	CCATAGCCATAGGGCAGTTT
SOX9	CCCATGTGGAAGGCAGATG	TTCTGAGAGGCACAGGTGACA
COL1	CACCAATCACCTGCGTACAGAAC	CAGATCACGTCATCGCACAAC
ACAN	GTGCCTATCAGGACAAGGTCT	GATGCCTTTCACCACGACTTC
COL2A1	CCAGATGACCTTCCTACGCC	TTCAGGGCAGTGTACGTGAAC
COLX	CCTGGTATGAATGGACA	CCCTGAGGGCCTGGAAGA
GAPDH	ATGGGGAAGGTGAAGGTCG	TAAAAGCAGCCCTGGTGACC
RPL13	GTTCGGTACCACACGAAGGT	CTGGGGAAGAGGATGAGTTTG
B2-MG	GAGGCTATCCAGCGTACTCCA	CGGCAGGCATACTCATCTTTT

The relative expression was determined with the 2^{ddCT} method, using 3 (GAPDH, RPL13 and β 2-MG) housekeeping genes for normalization.

Statistical analyses

Data are presented as mean ± standard deviation. Statistical data were performed by two-way ANOVA with Tukey's multiple comparison test, to compare different sets of data, using GraphPad prism 7 software, significance level was set at $P<0.005$.

Results

Cell choice and characterization

In this study, we wanted to compare the potential of different progenitors to produce cartilaginous and elastic matrix in comparison to MSC isolated from human bone marrow as a gold standard for chondrogenesis. Progenitors were derived from head and neck area, i.e. nasal and auricular perichondrium and dental pulp. They were tested first for their ability to trigger chondrogenesis, osteogenesis and adipogenesis *in vitro*. Cytological stainings showed their potential to evolve towards the trilineage, indicating an undifferentiated status (Fig. 1). Difference in staining intensity was shown depending on cell types. Although, these differences were not quantitative, however, they suggested some differentiation tendencies towards cartilage and bone tissue.

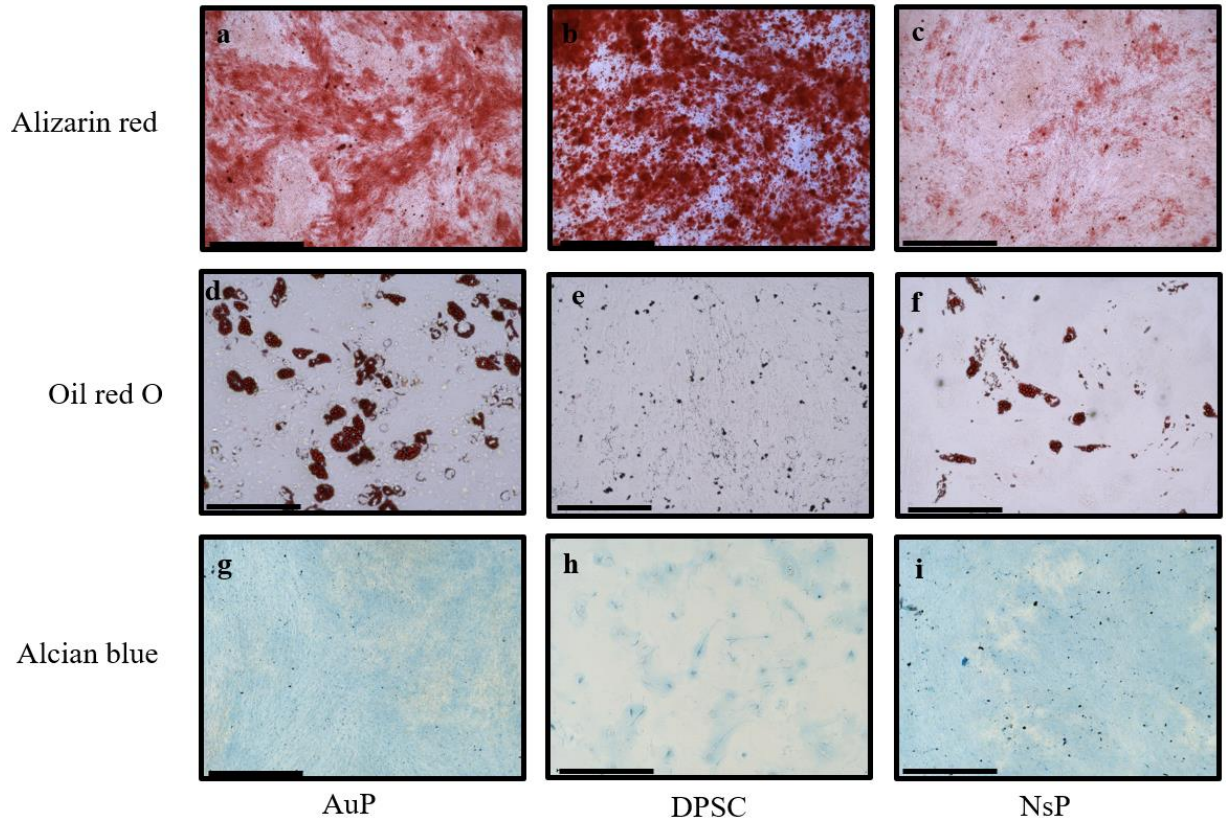

Fig. 1 Multilineage differentiation potential of human progenitors. AuP, DPSC and NsP were assayed for trilineage differentiation and stained with Alizarin red (a, b, c,), oil red O (d, e, f), and alcian blue (h, i, j), respectively. Control samples were stained after 24 hrs (supplementary data). Scale 500µm.

Chondrogenic differentiation in alginate microspheres and cytochemistry

Next, a comparative chondrogenic study of different cells was performed in a well mastered 3D hydrogel model (alginate) against BMMSC. Cellularized beads were cultured under chondrogenic media in normoxic (21% O_2) or hypoxic environment (3% O_2) for 2 weeks. Beads were then analyzed by cytological staining for ECM production and cell morphology (Fig. 2). Alcian blue is known to stain proteoglycans while safranin O stains cartilage and mucins. After 2 weeks of

culture, all cell types were able to produce cartilaginous ECM as shown in histological staining. Except in BMMSC, where the effect was not clear.

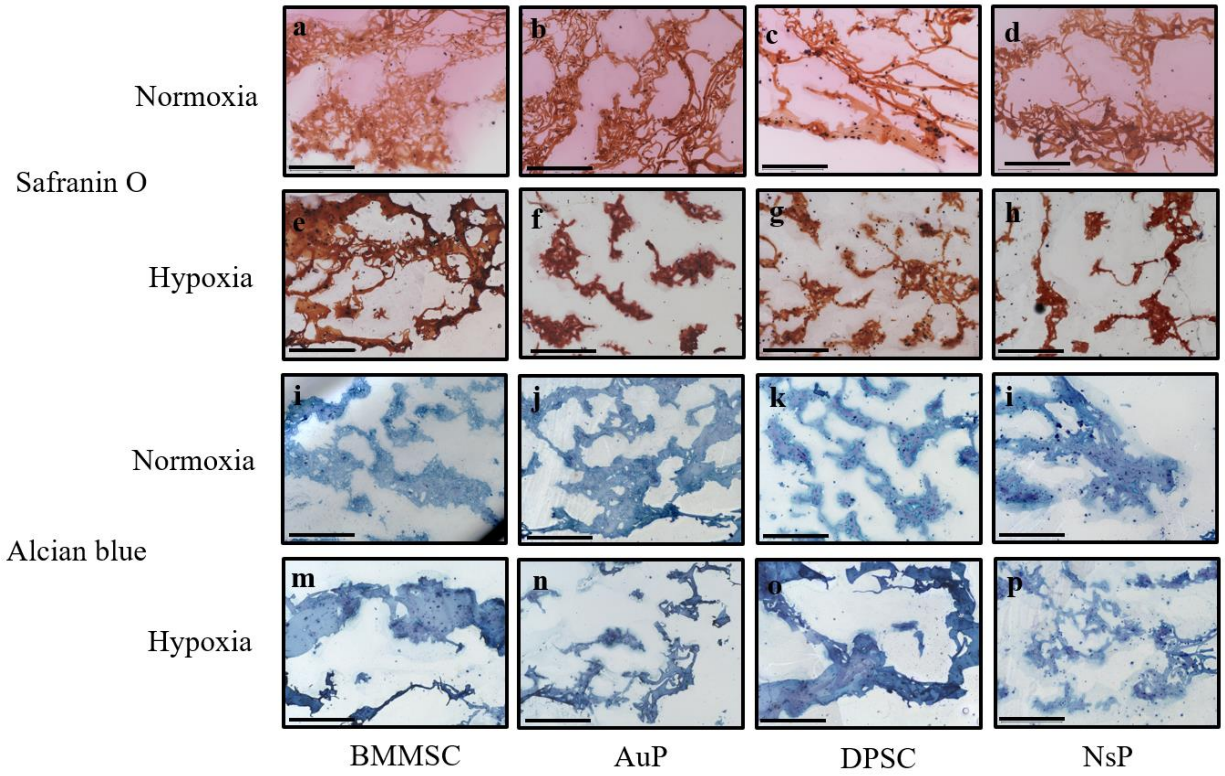

Fig. 2 Histological staining after chondrogenesis in alginate microspheres. Safranin O and alcian blue staining were respectively performed for illustrating the positive production of proteoglycans (red) and glycosaminoglycans (blue). These were shown in bone marrow-derived mesenchymal stem cells (BMMSC) a, e, i, m, auricular perichondrocytes (AuP) b, f, j, n dental stem cells (DPSC) c, g, k, o, and nasal perichondrocytes (NsP) d, h, l, p, encapsulated in 3D alginate microsphere in normoxic and hypoxic conditions, respectively, after 2 weeks of culture in chondrogenic medium (scale bar 500µm).

Gene expression by real-time RT PCR

Gene expression analysis was also conducted after the same treatment, targeting cartilaginous matrix markers. The expression of cartilage markers (COL2A1, ACAN, SOX9), elastin (ELN) and unspecific collagen type I (COL1) as well as hypertrophic marker (COL X) was analyzed by real-time RT-PCR after normalizing data against three housekeeping genes (RPL13, GAPDH and beta 2-MG) (Fig. 3-A). After 2 weeks of chondrogenic differentiation, all cell types were able to enhance the expression of cartilage markers (COL2A1, ACAN, SOX9) and ELN. Progenitors from auricular perichondrocytes (AuP) demonstrated the highest significant expression of these gene that were upregulated in these cells. AuP showed more interesting results regarding undesirable genes, since expression of COL1 and COLX were not regulated by chondrogenic medium, compared to other progenitors.

Hypoxia also induced chondrogenesis and was used in our study. As expected, it enhanced cartilage gene expression (COL2A1, ACAN, SOX9, ELN) and did not regulate COL1 and COLX except in dental progenitors. Although hypoxia appears as a potent stimulator of BMMSC, it did not improve chondrogenesis of dental progenitors, nasal perichondrocytes and most of all auricular

perichondrocytes (Fig. 3-B). This suggests that hypoxia has different mechanisms of action in controlling chondrogenesis depending on the cell progenitor source used.

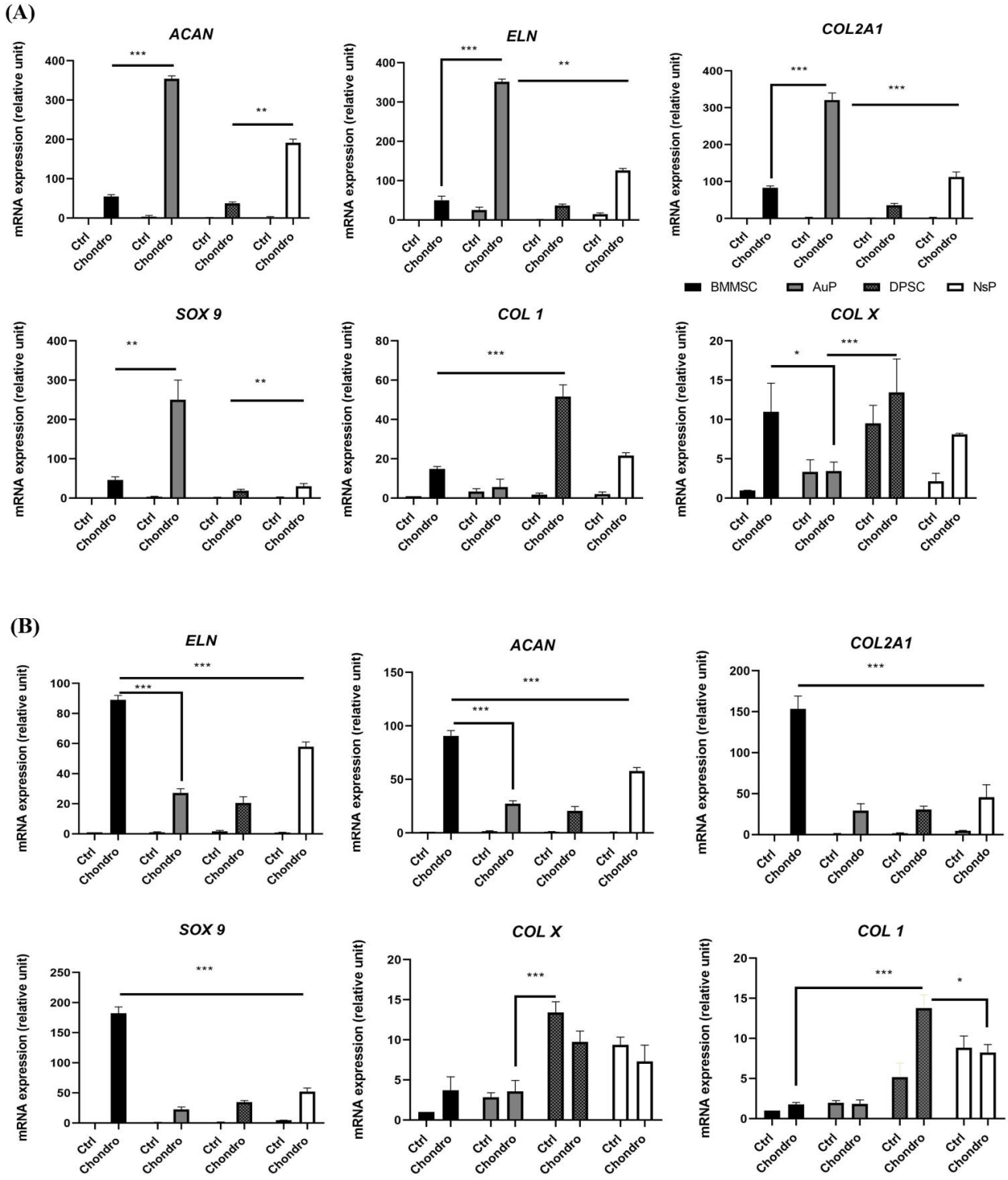

Fig. 3 Expression of cartilage genes in four different cell sources in normoxic and hypoxic environments. RT PCR analyses were performed to examine cartilaginous markers in 4 different cell lines in normoxic (**A**) and hypoxic (**B**) conditions. The expression of these markers was normalized to the average of the 3 housekeeping genes.

Taken together, these results indicate that among our tested cells, AuP highly produce cartilaginous elastic extracellular matrix and that hypoxia is not needed and did not affect their chondrogenesis.

Immunohistochemistry and cartilage-markers expression

To confirm gene expression study, immunohistochemistry of COL2A1, ACAN, ELN was performed on sections of cellularized alginate beads. We limited the test to AuP and compared them to BMMSC which presented significantly high results in real-time RT-PCR analyses. Negative controls were performed to ensure that secondary antibody binding is specific (Fig. 4-A). As expected both cell types were able to produce cartilage specific proteins (COL2A1, Fig. 4-B and ACAN, Fig. 4-C and ELN, Fig. 4-D). Here again, we noticed that hypoxia doesn't beneficially impact chondrogenesis of AuP, as in the case of BMMSC. This is particularly glaring when regarding COL2A1 expression.

(A)

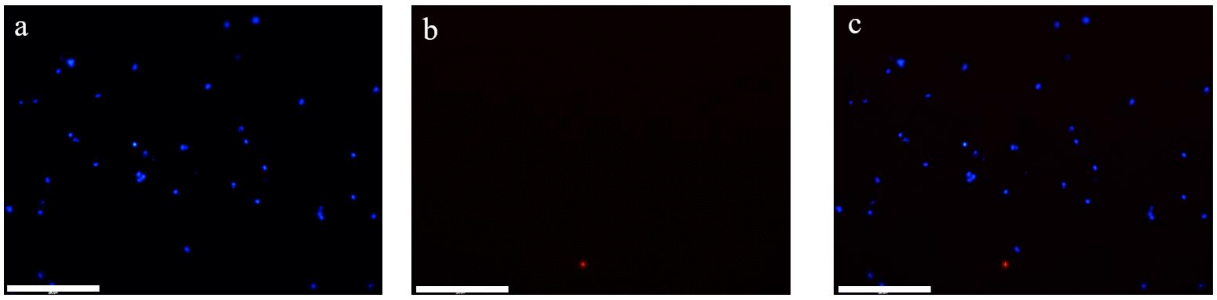

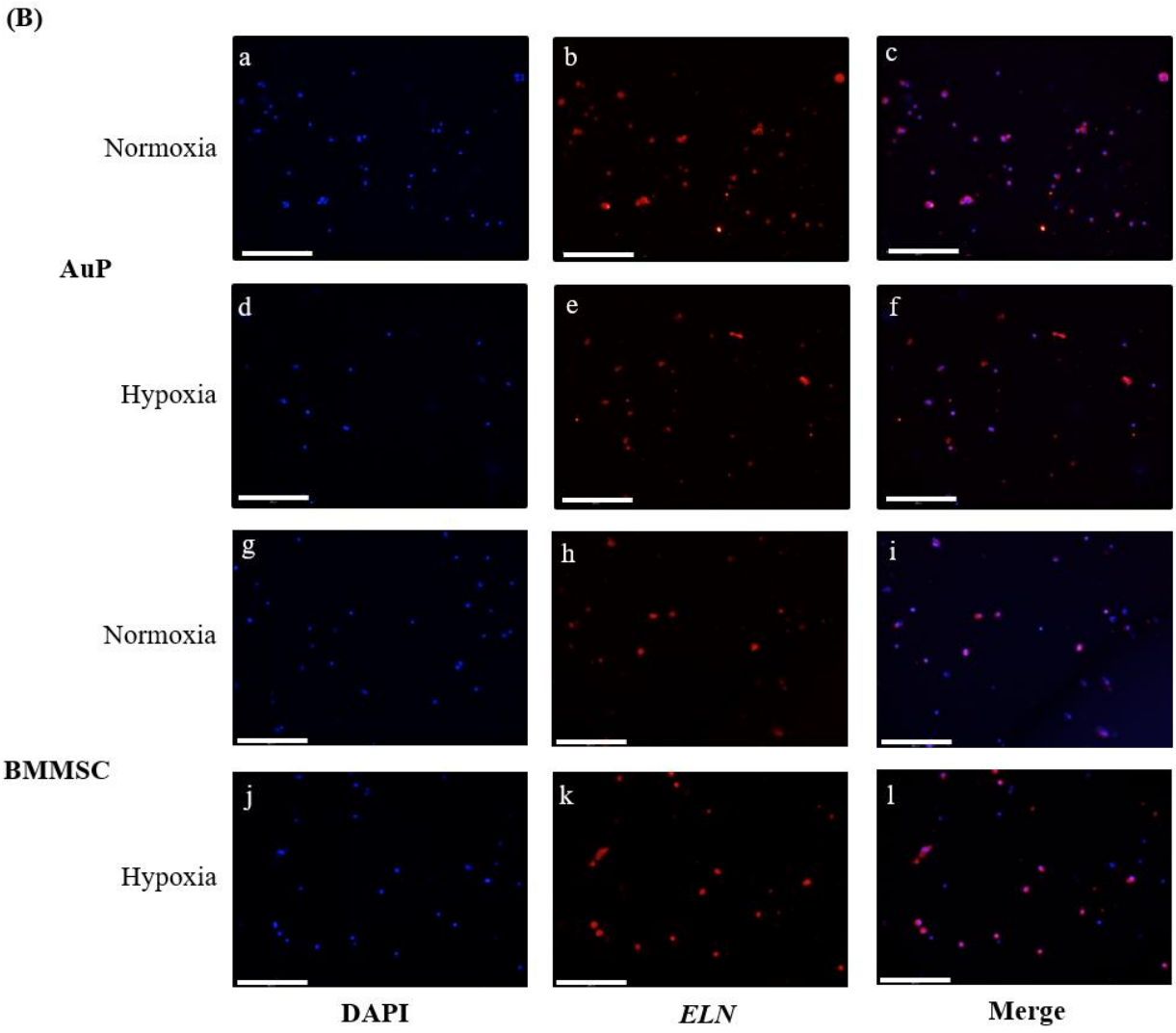
(B)
a
b
c
Normoxia
AuP
d
e
f
Hypoxia
g
h
i
Normoxia
BMMSC
j
k
l
Hypoxia
DAPI
ELN
Merge

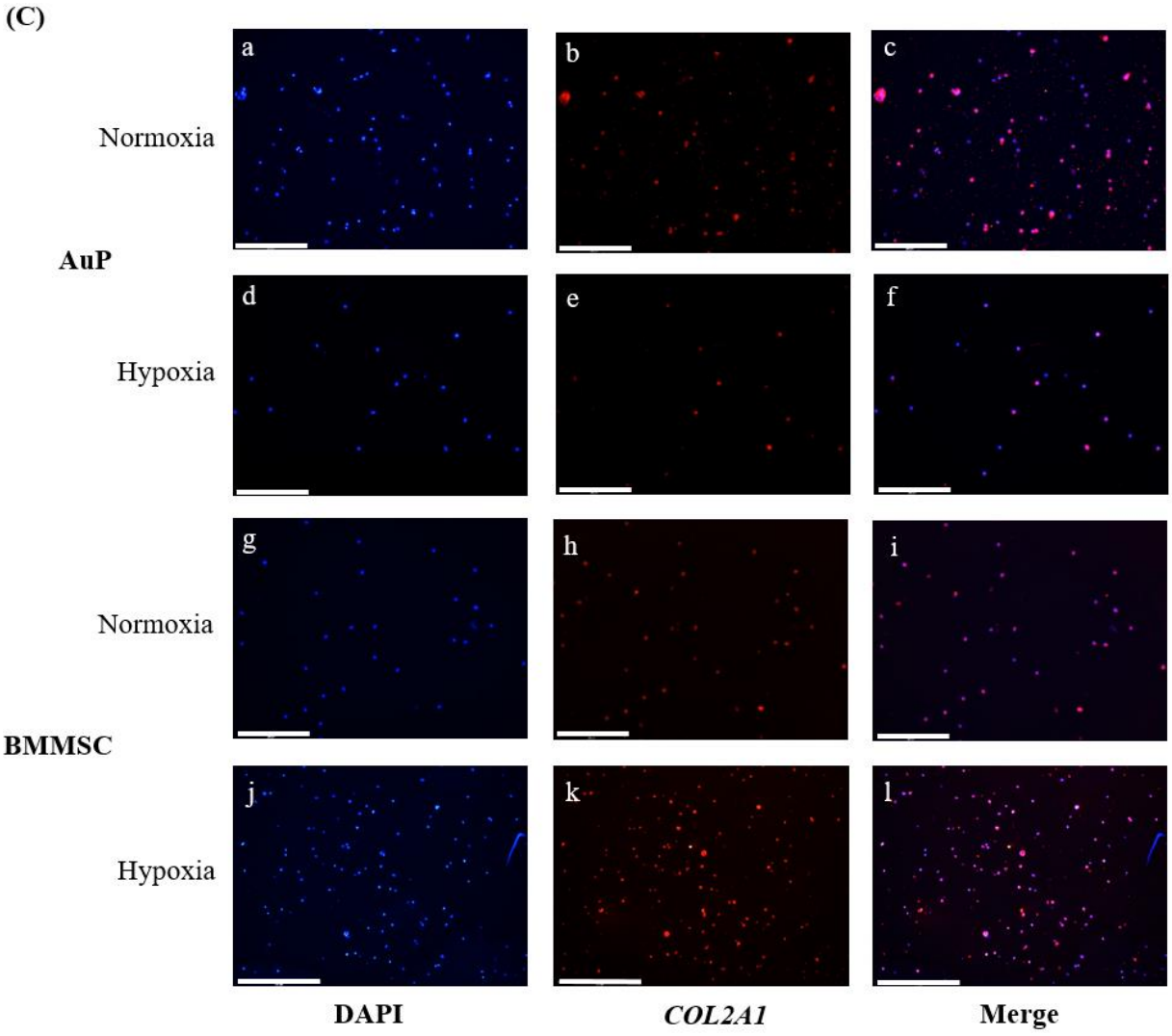
(C)
a
b
c
Normoxia
AuP
d
e
f
Hypoxia
g
h
i
Normoxia
BMMSC
j
k
l
Hypoxia
DAPI
COL2A1
Merge

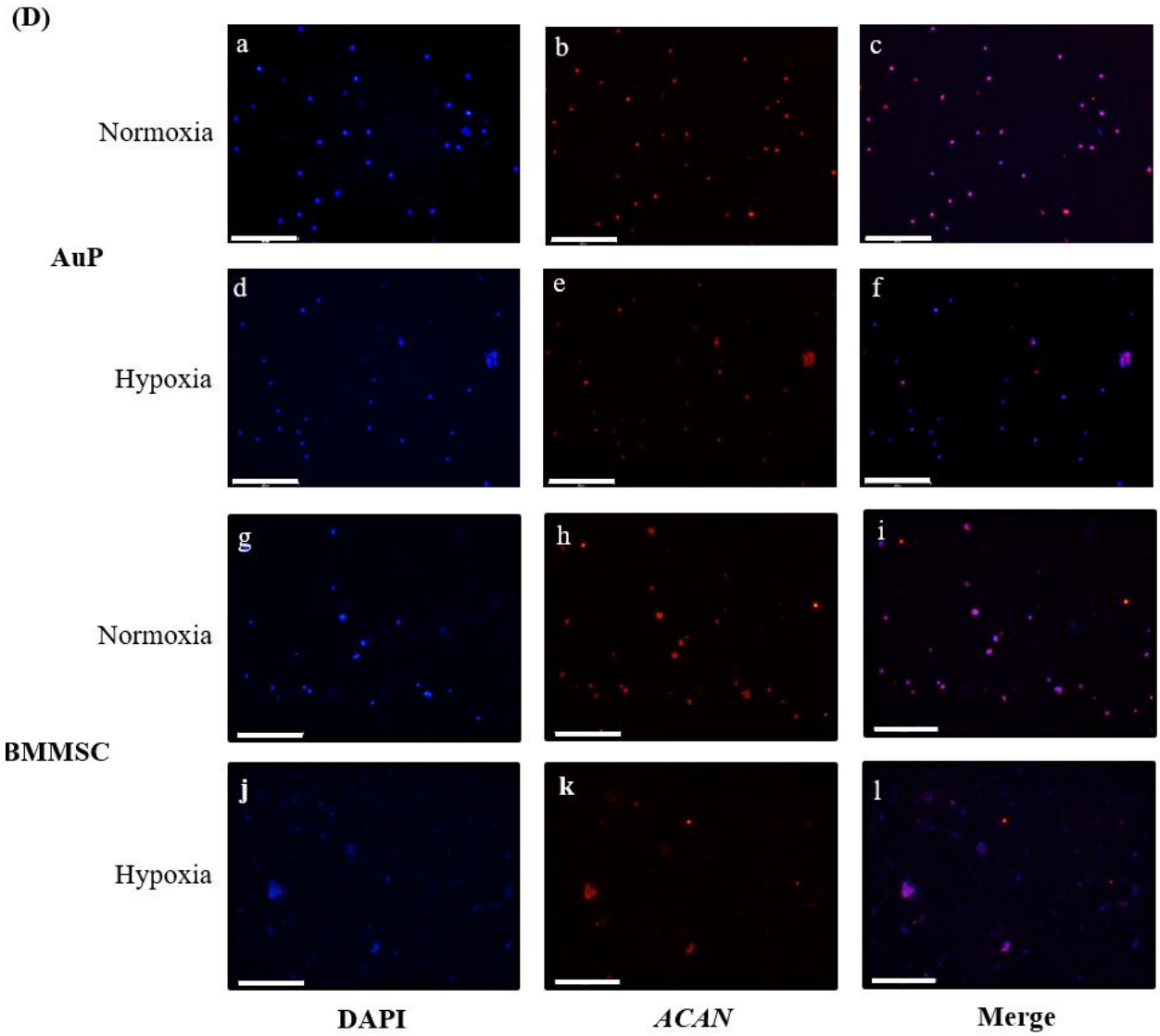

Fig. 4 Immunohistochemistry of ELN, COL II and ACAN. (**A**): Negative control was illustrated where primary antibody was replaced by PBS (a, b, c). (**B-C-D**): represent ELN, COL II and ACAN expression, respectively. This expression was detected in auricular perichondrocytes and bone marrow-derived mesenchymal stromal cells in presence of high (a, b, c, g, h, i) and low oxygen tension (d, e, f, j, k, l), respectively (scale bar 200µm).

Discussion

The aim of this study was to evaluate the ability of different cellular sources to form and better express cartilage genes and to investigate whether hypoxia can affect their chondrogenesis. The cells progenitors were chosen for their ability to differentiate into cartilage and their origin area. The comparison was made against human bone marrow derived mesenchymal stem cells as gold standard for chondrogenesis. They were used regarding several previous studies and as expected, when encapsulated in 3D alginate microspheres they presented the highest expression of cartilaginous genes in 3% hypoxic environment and a dense proteoglycans aggregates, which is correlated with previous studies that demonstrated that hBMMSC grown in 3D with extended

hypoxia increased the expression of cartilaginous genes (Ma *et al.,* 2009). It also corroborates our previous studies showing that hypoxia induced the differentiation of BMMSC into cartilage-like cells, with an upregulated expression of COL2A1, ACAN and SOX transcription factors with no hypertrophic markers in both *in vitro* and *in vivo* conditions (Duval *et al.,* 2012). Other groups have also investigated that immortalized murine MSC incubated in 1% oxygen increased the levels of chondrogenesis markers SOX 9, ACAN, COL2A1 (Robins *et al.,* 2005). Effect of hypoxia on MSC from different sources has been demonstrated where hypoxic culture of BMMSC enhanced *in vitro* and *in vivo* chondrogenesis capacity, proliferation and tissue formation (Chen *et al.,* 2020; Contentin *et al.,* 2020; Pattappa *et al.,* 2020).

The choice of alginate hydrogel to recapitulate 3D environment, was based on the porosity, flexibility and elasticity of alginate material. It is biocompatible and easily injectable in minimal invasive manner, which leave it very interesting in tissue engineering applications. In addition, this biomaterial support chondrogenesis and stem cell differentiation into cartilage cells (Sahai *et al.,* 2020; Weizel *et al.,* 2020).

Knowing that hBMMSC are the gold standard cells and well mastered source for chondrogenesis, their embryological origin is different from auricular cartilage. To fully engineer auricular tissue, progenitors from head and neck area should investigated for their chondrogenic ability to form robust cartilage. Hence, we used cartilage-derived progenitors from ear and nose perichondrium, since can generate large number of cells and represent a promising source for in tissue engineering based cell therapy (Otto *et al.,* 2018).

Human nasoseptal derived perichondrium were also tested for their ability to form cartilage. Staining results showed a better proteoglycans and collagen amount at standard oxygen tension compared to other cell sources. Also, these cells presented a good expression profile of elastic cartilage. Although nasal perichondrocytes expressed ELN, SOX 9, ACAN and COL2A1, but still expression of these genes were significantly lower than those of auricular perichondrocytes. A similar pattern of results was obtained when Hellingman *et al.,* in their studies evaluated the potential of culture-expanded human auricular and nasoseptal chondrocytes as cell sources for regeneration of cartilage. Chondrocytes originating from both nasal septum and auricles showed potent proliferation in either monolayer or 3D condition. Their results suggested that auricular chondrocytes produced large pellets with more cartilage-like matrix and had a higher expression of anabolic growth factors than nasoseptal chondrocytes (Hellingman *et al.,* 2011). However, both cell types didn't produce COLX, in agreement with our results.

AuP were also compared to progenitors from dental pulp. Recent reports have described the potential of dental stem cells as stem cell therapies for articular cartilage repair (Fernandes *et al.,* 2020). These cells contained microvilli-like structures on their surfaces, permitting a good attachment to the specific scaffold (Fernandes *et al.,* 2018). Once grown in chondrogenic medium, dental stem cells presented a rounded morphology that was correlated with ACAN and COL2A1 expression (Mata *et al.,* 2017). Another study reported that formation of collagen fibers by dental stem cells, confirming their ability to effectively differentiate into chondrocyte within matrices (Westin *et al.,* 2017). In our experiment, their chondrogenic differentiation was weaker compared to BMMSC and AuPs. These results have been suggested by other studies where they found that

3% hypoxia suppressed differentiation of dental stem cells (Iida *et al.,* 2010). Also, Ahmed *et al.,* compared the different low oxygen tension concentrations and reported that 3% O_2 has a positive effect on *in vitro* survival and cell-renewal of BMMSC, 5% O_2 induced a significant increase in expression of CXR4 that controls stem cell trafficking and migration. 5% O_2 enhances proliferation of DPSC better than 3% O_2 and 20% O_2. 5% O_2 significantly increased the expression of pluripotency marker SOX9 compared to 3% and 20% O_2 in dental stem cells (Ahmed *et al.,* 2016). In line with previous reports, that suggested that dental stem cells boosted bone healing process and promoted increase in VEGF expression by hypoxia, as well as bone formation, collagen ECM arrangement and numerous mineralization modules (Novais *et al.,* 2019). Our results showed that after 14 days of culture in normoxic and hypoxic conditions, dental stem cell showed the highest expression of COL 1, which could more a profile of bone tissue. These were consistent with finding that showed that hypoxic condition promoted mineralization and differentiation of dental pulp cells of the odontoblastic layer (Wang *et al.,* 2017) . Hypoxia was shown to be an effective treatment to amplify numbers of progenitor cells and to enhance angiogenic potential and affect the differentiation ability of odontoblasts (Ito *et al.,* 2015).

Auricular progenitors behave similarly to MSC in terms of multipotency, and possess the ability to differentiate towards multiple lineages. Auricular progenitors from perichondrium were described to be good candidates for ear cartilage production (Otto *et al.,* 2018; Zhang *et al.,* 2019). However, to date, no study has evaluated the effect of hypoxia on AuP.

In this study, auricular perichondrocytes presented good results of chondrogenesis where they highly produced elastic cartilage genes (ELN, COL2A1, ACAN, SOX9) with low expression of COL1 and COLX. It is also noteworthy that the best effect is obtained in normoxic conditions even though hypoxia strongly modulated the chondrogenesis of several progenitors, including hBMMSC (Peck *et al.,* 2019).

Aside to the remarkable increase of elastic cartilage generation, the relatively low expression of COLX in auricular progenitors indicates the preservation of the phenotype in these cell types under *in vitro* chondrogenic conditions. This was also proved by Gale *et al.,* who reported that hypoxic culture of MSC downregulated hypertrophic markers such as COLX and increased chondrogenesis (Gale *et al.,* 2019). Several studies have reported the expression of COLX in cartilage tissue engineered from auricular chondrocytes, indicating that the low expression of this gene, preserved the phenotype in these cells.

Similarly, the chondrocyte dedifferentiation marker, COL1 was also mostly reduced in auricular perichondrocytes both in normoxic and hypoxic conditions. It is widely known that human perichondrium tissue initially contains COL1. When these cells were encapsulated in alginate 3D beads, COL1 expression significantly decreased where a small expression was confirmed by our results in normoxia as well as hypoxia. This indicated that 3D encapsulation of auricular perichondrocytes suppressed the expression of COL1and increased elastic cartilage phenotype.

On the contrary, Xue *et al.,* has shown that cell derived from the cartilage tissue appear more apt to differentiate towards the chondrogenic and osteogenic lineages, whereas perichondrium-derived progenitor cells differentiate more into adipose tissue (Xue *et al.,* 2016). This wasn't the case in

our work since auricular derived perichondrium cells showed the best cell source to produce healthy elastic cartilage non hypertrophic when cultured in alginate beads in normoxic conditions. Also, MSC from both bone marrow and adipose tissue, despite a high proliferation capacity, appear not to be the optimal cell source for cartilage due to limited chondrogenic differentiation development of hypertrophic cartilage (Derks *et al.,* 2013).

To validate the results of real-time RT-PCR, immunohistochemistry was performed and results were consistent with real-time RT-PCR results, where auricular perichondrocytes expressed more COL 2, ACAN and ELN, in normoxia and the lower expression of these genes in hypoxia. Hypoxia suppressed cartilaginous activity of auricular perichondrocytes on one hand, and stimulated the significant increase of BMSC on the other hand. Overall, these finding are in accordance of results by Kobayashi *et al.* who identified a human progenitor auricular perichondrium cells that are highly proliferative and able to differentiate into multiple lineages and can differentiate and produce an elastic mature cartilage rich with elastic fibers and proteoglycans, when subjected to bFGF and IGF1(S. Kobayashi *et al.,* 2011).

Conclusion

In conclusion and as previously described, auricular perichondrocytes are the best candidates for elastic cartilage. Although these cells highly present elastic cartilage markers in normoxic conditions, hypoxia, on the other hand, turns to be ineffective and useless for these cells. Our results highlight the importance of these cells to be cultured in normal oxygen levels to promote and enhance elastic cartilage formation. In order to profoundly evaluate our *in vitro* results, *in vivo* studies in animal models should be carried out in same conditions for further investigation of the potential of these cells to regenerate and repair elastic cartilage.

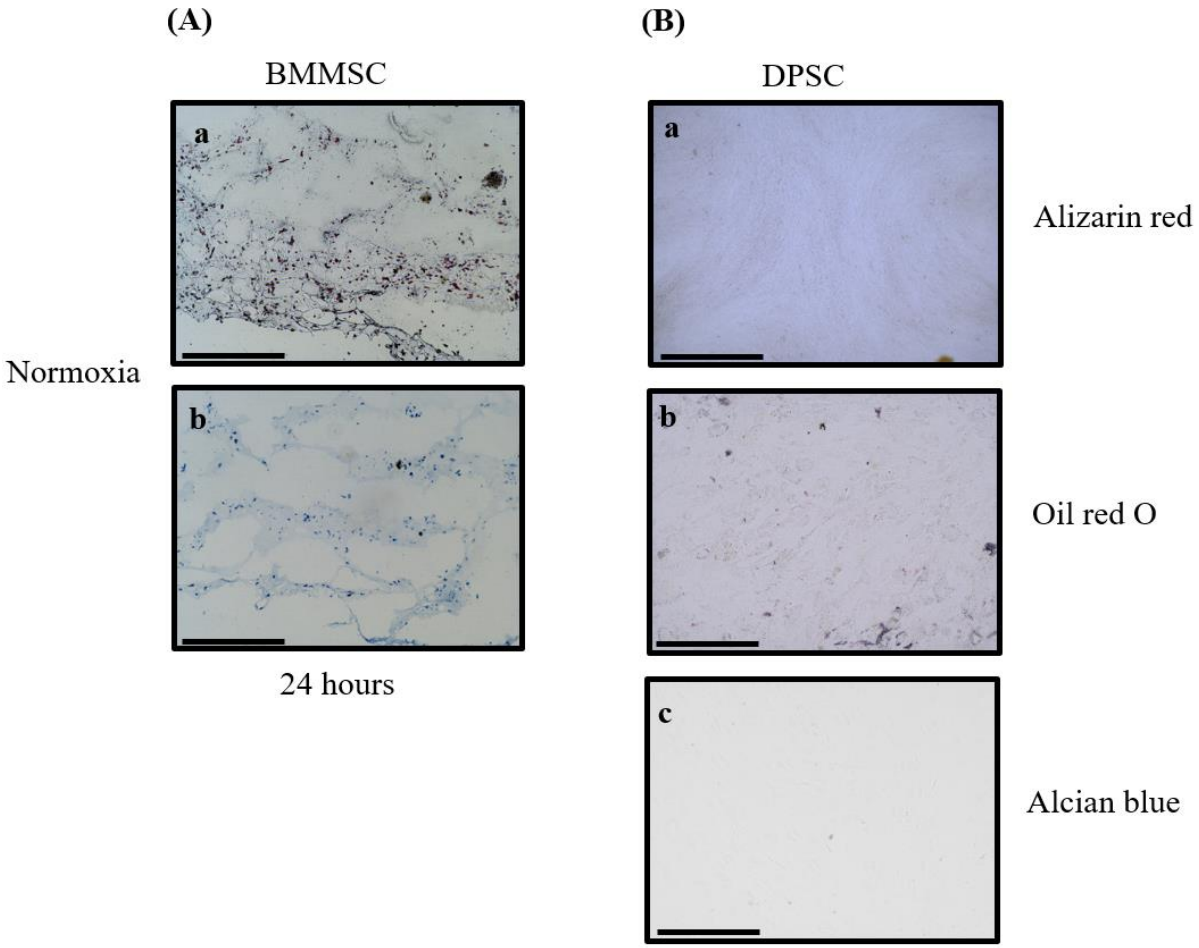

Supplementary figure 1 Control Staining (A): Safranin O (a) and alcian blue (b) staining of BMMSC in normoxic condition in normal medium after 24 hours. (B): DPSC were tested for the trilineage differentiation (a, b, c). Scale: 500µm.

2-Cell sheets as tools for ear cartilage reconstruction *in vivo*

Many researchers are still using 2D approaches, since they provide efficiency and simplicity to cell culture applications. However, recent research focuses more on self-assembly and 3D culture to reproduce cell-cell interaction *in vitro* and to mimic *in vivo* environment. Cell sheet technology is based on cell harvesting without any proteolytic enzymes or chelating agents, thus, preserving cell-cell junctions and ECM secreted by cells. It is based on the cultivation and recovery of the layer of cells as an intact sheet of cells that can be used later on in cell therapy applications.

We have already shown in our first part of the thesis that auricular perichondrocytes presented the best chondrogenic potential compared to the different cell sources tested. From this point, we tested our different cellular sources for their potential to form cell sheets and mainly focused on auricular perichondrocytes and their tendency to regenerate cartilage *in vitro* and *in vivo*. Despite the high ability of stem cells and progenitors to produce cell sheets, rabbit auricular perichondrocytes were the best to form an intact, pliable, flexible cell sheet after one month of culture. These latter were then characterized and revealed a similar ECM composition closely related to native auricular cartilage.

Cell sheets were investigated in different *in vitro* and *in vivo* applications. First of all, they were used as carriers, in order to recellularize porcine decellualrized cartilage. Two different culture methods were examined and results showed that wrapping decellualrized cartilage with cell sheets, promoted better recellularization. This is shown by deep penetration of cells that advocated a homogenous distribution throughout the whole cartilage tissue after 2 weeks of culture.

To better expand cell sheet biocompatibility and cartilage repair, we proceeded to examine these cell carriers by creating *in vivo* allogenic animal models. Cartilaginous defects were created in rabbit ears and filled with cell sheets, previously cultured in chondrogenic medium *in vitro* for several weeks. After 2 months of *in vivo* implantation in rabbit models, these cell sheets presented good integration of host tissue and a suitable good defect filling that highly repaired cartilaginous defects.

In short, our rabbit auricular cell sheet provides a novel tool for cartilage engineering approaches, promoting and enhancing *in vitro* cartilage regeneration as well as *in vivo* cartilage repair.

Cell sheets as tools for ear cartilage reconstruction *in vivo*

Mira Hammad[1,2], Alexis Veyssière[1,2,3], Didier Goux[4], Eric Maubert[5], Catherine Baugé[1,2], Karim Boumédiene[1,2]

[1]Normandy University, UNICAEN, EA 7451 BioConnecT, Caen, France, [2]Fédération Hospitalo Universitaire SURFACE, (Amiens, Caen, Rouen), France, [3]Service de chirurgie Maxillo-faciale, CHU de Caen, Caen, France, [4]CMA bio3, UFR des sciences, SF4206 ICORE, Caen, France, [5]UMRS1237 PhIND, INSERM, Normandy University, Institut Blood and Brain @ Caen-Normandie, Université de Caen, Caen, France.

Abstract

Cartilage reconstruction and repair has always been a challenge in both tissue engineering research and clinical practices. Tissue engineering approaches for cartilage regeneration presented promising results when cells were seeded into scaffolds. However, many obstacles such as scaffold biocompatibility and cellular viability interfered in the clinical application. Due to these reasons, a new cell sheet technology has gained increasing interest because it can provide a naturally occurring, complex set of physiologically functional signals required for cellular growth. Cells are cultured to reach hyperconfluency and are harvested without utilizing proteolytic enzymes, such as trypsin, thus their endogenous extracellular matrix (ECM) and cell-cell junctions are effectively preserved, allowing the constructed tissue to have a high cell density and a uniform cell distribution to mimic native tissue more closely. As a consequence, cell sheet offers features that retain the microenvironment of cells. In this study, we used cell sheets as carriers to colonize and restore a xenogenous decellularized cartilage and to repair a defect in rabbit model of auricular cartilaginous defect *in vivo*. First, native ear porcine cartilage was decellularized and then firmly wrapped by cell sheets that recellularized porcine cartilage after 2 weeks in chondrogenic medium. Moreover, to validate their ability of regeneration, cartilaginous defects were produced in auricular area of rabbits and were filled with cell sheet pre-cultured with chondrogenic medium. After 2 months of transplantation to the site of injury, we observed good integration in host tissue and total regeneration of cartilage defects. Our results show that this natural scaffold could be used as a cell carrier for recellularization *in vitro* and regeneration of cartilage *in vivo*. Therefore, it holds great and promising potential for cartilage tissue engineering and regenerative medicine.

Introduction

Tissue engineering is widely used for regenerative medicine, where it combines cells, scaffolds providing structural support, signals and growth factors that help cellular growth and differentiation to reconstruct or regenerate damaged tissues or organs. One of the major challenges of this field is to find the best scaffold that can mimic the native microenvironment of the cells. (Wang *et al*., 2021).

A Lot of tissues are subjected to reconstruction and among them, cartilage that is frequently targeted due to a lack of innervation and vascularization. It has also poor cell content, nutrients and oxygen supply (Jiang and Tuan, 2015). These characteristics limit its potential of self-repair and intrinsic regeneration capacity. Several repair techniques are utilized, especially in orthopedic or plastic surgery, such as microfracture, mosaicsplasty, autologous chondrocyte implantation, costal cartilage harvesting for ear reconstruction (Nixon *et al*., 2017). They often result in insufficient functional cartilage with fibrocartilage apparition and donor site morbidity. Therefore, tissue engineering hopes to solve these problems through the investigation of new cell and scaffolds combinations.

In the last decade, a natural cell-free scaffold has emerged, namely decellularized tissues. These types of scaffold are obtained by removing the cellular part of a tissue, leaving only an ECM (Serban *et al.*, 2008). Several decellularization protocols have been used to eliminate cells while conserving the structure and function of ECM, organized as in a native tissue. Such matrices appears as good standards that provide cell adhesion, bioactive molecules regulating cellular differentiation and migration (Duisit et al., 2018; Rahman *et al*., 2018; Schwarz *et al.*, 2012; Utomo *et al*., 2015; Zheng *et al.*, 2011). Once decellularized, they can be repopulated by different cell types, either specialized or progenitors. This step could be achieved with many techniques, including static culture, pulsatile perfusion, ultra sonication and centrifugal force. However, all of them failed to attain homogeneity of recellularization of tissue. Usually, the seeded cells formed only a monolayer over the scaffold with no deep penetration ability in matrix, and therefore, this step is still one of the technological limitations for using decellularized tissues.

Different cell sources can been used for cartilage engineering, including, primary chondrocytes (Luo *et al.*, 2016), mesenchymal stem cells (MSC) and adipose-derived stem cells (ADSC) (Martinello *et al*., 2014). Bone marrow derived MSC (BMMSC) are widely used owing to the advantage of easy obtainment, high proliferative rate and differentiation capacity (Reboredo *et al*., 2016).

Recent progression in this field, aimed to investigate new approaches to treat cartilage disorders, by introducing cell sheet technology to overcome all conventional acellular tissue problems, thus increasing migration ability of cells deep into tissues (N.-C. Cheng *et al.*, 2020).

Cell sheet technology is based on cell harvesting without any proteolytic enzymes or chelating agents, thus, preserving cell-cell junctions and ECM secreted by cells. It is based on the cultivation and recovery of the layer of cells as an intact sheet (S. Zhou *et al*., 2020). This technology was applied to many tissues and organs, including heart (Ito *et al*., 2020; Kc *et al*., 2020), skin (Merrilees *et al.*, 2021; Yu *et al.*, 2018), liver (Sakai *et al.*, 2018), nerves (Junka and Yu, 2015) periodontal ligament and also bone (F. Wang *et al.*, 2017) and cartilage (Thorp *et al*., 2020; Xue *et al*., 2018). In this context, cell sheet would be used either alone, replacing bone and cartilage scaffolds, mimicking more native tissue, or in combination with other scaffolds as a source of cells, to better way of recellularization than using scaffolds seeded with cell suspensions. Engineered cartilage cell sheet from chondrocytes or MSC has been shown effective regeneration promoting partial and full thickness lesions where they present satisfactory results, especially upon the integration between regenerated cartilage and native surrounded cartilage (Zhou *et al.*, 2021).

Moreover, cell sheet avoids the inflammation caused by exogenous scaffold (Matsuura *et al.*, 2014). Hence, this promising cell sheet technology which is rich in ECM can be innovatively used as both scaffold and cell source.

In this study, we investigated different cells sources for their ability to form cell sheets. Thereafter, we used them as cell carriers both *in vitro* an *in vivo*. First, after cellular and genetic material removal from porcine cartilage, we set up a wrapping model with cell sheets to drive rabbit cells to colonize the decellularized tissue. In a second step, we developed an auricular cartilaginous defect *in vivo* in rabbit and proceeded to its filling by cell sheets from allogenic auricular perichondrocytes. In both cases, the resulting tissues showed a deep cell penetration and repopulation of decellularized cartilage *in vitro* and an appropriate filling defect *in vivo*.

Materials and methods

Isolation and cultivation of human cell sources

Human cells were obtained from several sources. Bone marrow samples were collected from patients undergoing arthroplasties who have signed the consent form according to local legislation. To obtain mesenchymal stem cells, bone marrow was separated by Ficoll gradient and cultured in alpha-MEM medium containing basic fibroblast growth factor (bFGF), with medium changes, twice per week, and freezed after passage 3. For dental stem cells, freshly extracted teeth (from young patients, average age of 17 years) were transferred into hypotonic phosphate buffered saline solution and were disinfected by a solution of antibiotics. Then pulp tissue was isolated from the pulp chamber where the tissue was minced into small pieces. Enzymatic treatment was carried out by collagenase I (3mg/ml) and dispase (4mg/ml) for 30-45min, at 37°C. After enzymatic digestion, cell suspension was centrifuged at 2000 rpm for 10 min, and the cell pellet was seeded into cultivation dishes and resuspended with cultivation media (alpha-MEM). For nasal samples, a surgery was performed to remove a part of nasal perichondrium that was transferred to a tube of PBS and antibiotics. Nasal perichondrium was digested with pronase and collagenase for 45min to digest tissue and to collect cells. Fresh human auricular cartilage was harvested from 12-year old children undergoing plastic surgery. Perichondrium was separated, mechanically from connective tissue, washed in phosphate buffered saline, and cells were extracted by enzymatic digestion using pronase for 45-60 min at 37°C. After that, 0.2% collagenase II was added overnight at 37°C. The next day, cells were seeded in T75 culture flasks and cultured in alpha-MEM medium containing bFGF. Cells were passaged twice and then freezed at -150°C. All patients were informed and signed the consent form according to local law.

Rabbit perichondrocytes and bone marrow-derived MSC

Rabbit ears were obtained from a 3 weeks-old rabbit. Animal procedures were approved by animal care ethical committee. Perichondrium tissue was harvested and cultured as a primary outgrowth culture for one month. After that, cells were cultured in alpha-MEM medium until reaching passage 3 and were then freezed at -150°C until further use. Rabbit bone marrow was harvested from femoral heads and separated afterwards using ficoll reagent. BMMSC were seeded in alpha-

MEM, medium with supplemented bFGF. Medium was changed twice a week, passaged until reaching passage 3 and freezed for further uses.

Progenitors from both humans and rabbits, were assayed for their ability of trilineage differentiation, i.e. chondrogenic, osteogenic and adipogenic, before storage and use.

Cell sheets production

Cells were cultured to reach hyperconfluency in 6-well plates with appropriate media containing concentration of 100µg/ml of L-ascorbic acid. After one month of culture, cell sheets were then harvested as an intact single sheet with tweezers and processed for further use.

Scanning electron Microscopy

The ultrastructure of the cell sheets was analyzed by scanning electron microscopy (SEM). For that, upon harvesting, the sheets were fixed with 2.5% glutaraldehyde sodium cacodylate 0.1M, pH 7.4 for 24 hours, and rinsed with sodium cacodylate 0.1M, pH 7.4. Then they were incubated with 1% osmium tetraoxyde for 1h post fixation, and rinsed with sodium cacodylate and dehydrated with alcohol. Thereafter, they were embedded in Epon 812 resin and sectioned into ultra-thin sections using Ultra Cut R microtome (Leica). Observation were done using on SEM microscope (JEOL 1011) equipped with Orius 200 GATAN camera.

Cell sheets characterisation

Fastin elastin kit was used to detect and quantify elastin, Sircol collagen kit to quantify total collagen in samples and Blyscan kit for glycosaminoglycan content. All these kits were purchased from Biocolor (life science assays, UK).

Animal surgery and cartilage defect model

Animal experiments in this study were approved by the institutional animal care. The operative procedure and care of rabbits were performed in accordance with the institutional guidelines of ethical committee. General anesthesia was induced before surgery through an intravenous injection of ketamine hydrochloride (60mg/kg) and xylazine (6mg/kg). Cartilaginous defects were performed on auricular regions, by removal pieces of perichondrium and cartilage. After defects were made, cell sheets previously prepared from allogenic rabbit were stacked into the defects. On average one sheet harvested from one well in 6-well plate (9.5cm^2/well) was used for filling one cartilage defect. For negative control experiments, defects were created but kept unfilled. Postoperatively, all rabbits were housed in separate cages and allowed to move freely immediately after surgery. No animal showed any evidence of infection and all wounds healed well.

Histological analysis

Harvested samples were fixed in 4% PFA for 8 hours, then they were rinsed in 30% PBS-sucrose overnight. The next day they were embedded with Optimal Cutting Temperature (OCT) and flash-freezed in liquid nitrogen. These samples were then sectioned into slices of 10µm thickness, and stained with safranin O to analyze glycosaminoglycan distribution, as well as hematoxylin-eosin for cell nuclei and extracellular matrix

Porcine Cartilage

Auricular cartilage was harvested from 3-month-old Piglets. Animal procedures were approved by the animal care ethical committee. Piglets were sacrified and perichondrium was removed, and cartilage was harvested and cut into fragments of 2x2cm, washed with PBS in presence of ciprofloxacine and stored at -80°C.

Decellularization of porcine cartilage

Decellularization of porcine cartilage was performed by an enzymatic protocol from our laboratory consisting of several steps. First, 0.2% of collagenase I was added to cartilage pieces at 37°C, under agitation (200 rpm for 2hr). Thereafter, samples were rinsed thoroughly with distilled water at 4°C. After that, cartilage pieces were incubated with 0.2% pronase under the same conditions for 2 hrs, before washing again with water to remove traces of pronase. The final stage of decellularization protocol was digestion of DNase for 30min at 37°C and a final wash in distilled water overnight at 4°C.

Recellularization of porcine cartilage

After decellularization, porcine cartilage was recellularized using rabbit cell sheets. On one hand, cell sheets were firmly deposited on top of porcine cartilage, on the other hand, the entire porcine cartilage was covered and wrapped firmly using cell sheets. These two constructs were then cultured for 2 weeks in chondrogenic medium, in presence of TGFβ-3 at 37°C. After 2 weeks, traces of cell sheets were removed and recellularized cartilage was analyzed.

Fluorescence Microscopy

Recellularized cartilage was fixed with 4% PFA for 4 hrs and then rinced overnight with 30% PBS-sucrose, then embedded with OCT, flash freezed in liquid nitrogen and stored at -80°C. Sections of 10µm were produced using Leica cryostat. Porcine cartilage stained with DAPI and was observed under EVOS FL Auto 2 (Invitrogen, Thermofisher Scientific) microscope.

Immunohistochemistry

Sections on super frost slides were rinsed in PBS and incubated overnight at 4°C with ELN (1:100, ab 9519 abcam, Cambridge, UK), collagen II (1:100, ab 185430 abcam, Cambridge, UK) primary antibodies. A negative control was performed by replacing primary antibody solutions with PBS. The next day, slides were rinsed five times in PBS to remove traces of primary antibody, and a secondary antibody 715-166-150 Cy3 conjugated Affini pure $f(ab)_2$ fragment donkey anti-mouse (Jackson Immuno Research) diluted (1:800) was used to incubate slides for 1.5 hour. Rinsing with PBS was done to remove excessive secondary antibody. Slides were then rinsed three time with PBS before mounting for microscopic observation by EVOS cell imaging system microscope, Thermo fisher scientific).

RNA extraction and RT-PCR

Total RNA was purified according to the RNeasy® Mini Kit protocol (Qiagen) Quantity and purity was determined by 260/280absorbance. RT was carried out using a mixture composed of 1µg of

RNA, 2.5 µM of oligodT, 0.5 mM of dNTP, 1X First Strand Buffer and 10 U / µL of Moloney Murine Leukemia Virus reverse transcriptase (M-MLV-RT, Invitrogen) for each RNA condition. Amplification was carried out on a StepOnePlus ™ Real-Time PCR System thermocycler (Applied Biosystem) for 40 cycles which consist of a denaturation step at 95 ° C for 15 seconds and a hybridization and polymerization step of one minute at 60 ° C. The specificity of the amplification products was checked by analysis of the melting curve. The relative expression of the gene studied using real time RT-PCR primers are listed in the table below. Results were compared to normalized to three housekeeping genes (GAPDH, RPL13, HPRT1).

Gene	Forward primer	Reverse primer
ELN	GCTGCTCAGTTTGGGTTAGG	CCTTCGCAGCAGACTTGG
SOX9	TGGAGACTGCTGAACGAGAG	CCTTGAAGATGGCGTTGG
COL1	CGGTGGTTACGACTTTGGTT	GAGCCTTCAGGAGTGAGGAG
ACAN	GGAGCAGGAGTTTGTCAACAACAAC	CCAGTTCTCAAATTGTAGGGGGTGT
COL2A1	CGGTGGTTACGACTTTGGTT	GAGCCTTCAGGAGTGAGGAG
COLX	GTTCATGGAGTGTTCTACGCTGAG	ACCTTGTTCTCCTCTCACTGG
GAPDH	CAGTTTCCATCCCAGACCCC	TGCTGTCGAGACTTTATTGATGGT
RPL13	TCCAAGCTGGTCCTCTTCC	CAGCTTCCTTGGCTCTTTTT
HPRT1	CAATGCAGACCTTGCTTTCC	AGTCAAGGGCATATCCTACAACA

Results

Several sources of cells and their potential to form cell sheets

Several cell types were tested to investigate their potential to form cell sheets. Hence, we used BMMSC and auricular perichondrocytes (AuP) from both rabbit and human as well as human nasal perichondrocytes (NsP) and human dental pulp stem cells (DPSC). The cells were cultured under specific culture media and concentrations of L-ascorbic acid as shown in table 1. Even all of them used were able to form cell sheets, it was more or less rapid, depending of the cell type. Rabbit auricular perichondrocytes were the best to form an intact, pliable, flexible cell sheet after one month of culture. This cell type divided rapidly and at a higher rate than all other types, so we used it in our further experiments.

Table 3: Several cell sources have been tested for their potential to form cell sheets.

Cell sources	Species
BMMSC	Rabbit
AuP	Rabbit
NsP	Human
AuP	Human
DPSC	Human

BMMSC	Human

Recovery and characterization of cell sheets

After seeding and culturing rabbit AuP until confluency (approximately 1 week), the cells were kept in the dishes for 3 more weeks with frequent medium change (twice a week). Thereafter, the cell sheets were recovered as a layer of cells (Fig. 1-A-a) using tweezers where cell-cell and cell-ECM junctions were conserved. The extracellular matrix produced and deposited by the cells under L-ascorbic acid treatment is maximized and facilitate the recovery of cell sheet (Fig. 1-A-b). Cell sheets were then proceeded to be examined using electron microscopy. They showed several cell layers that were distributed on top of each other on different levels and separated by a great amount of extracellular matrix secreted by the cells during cell culture (Fig. 1-A-c). This showed that our AuP cell sheets present a multi-layered structure. This was also observed during the recovery of cell sheets since we were able to obtained at least 3 of them separately from the same culture dish (data not shown). To best characterize these cell sheets, quantification of extracellular proteins was performed and showed a significant upregulation of these proteins compared to a native auricular rabbit cartilage (Fig. 1-B). These results signify that rabbit AuP produced high collagen, elastin and glycosaminoglycans, and have a composition similar to that of the native auricular cartilage.

(A)

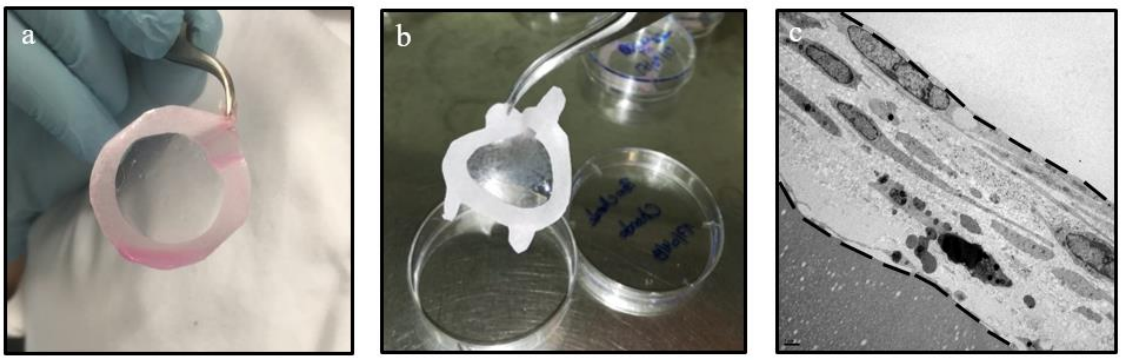

(B)

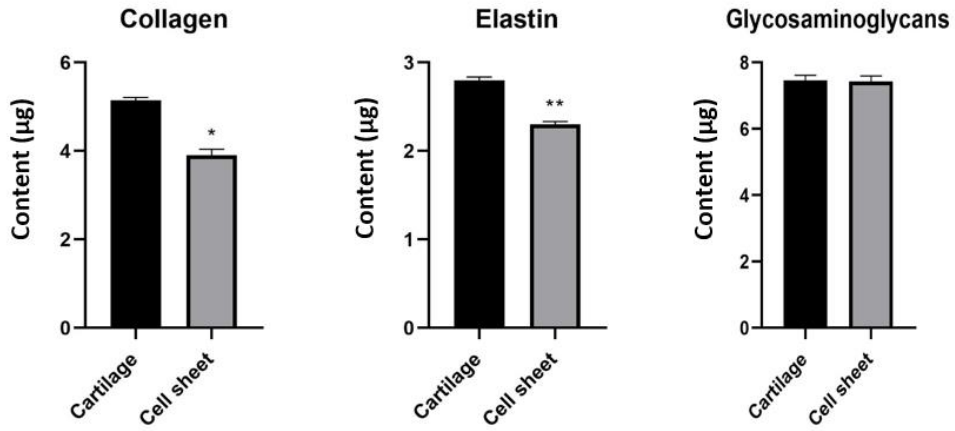

Fig. 1-A (a, b) Macroscopic views of rabbit cell sheet recovery. (c) Scanning electron microscopic view of the cell sheet section showing a multilayered structure (between the 2 dashed lines). **(B):** Quantification of collagen, elastin and glycosaminoglycans in rabbit auricular cell sheet compared to native cartilage.

Decellularization of porcine cartilage and its recellularization using cell sheets

In order to evaluate some applications of using cell sheets as cell carriers for recellularization, we investigated them in a protocol of decellularization/recellularization of cartilage. Native porcine auricular cartilage (Fig. 2-a) was decellularized using a 1-day enzymatic protocol developed by our laboratory (Fig. 2-b). Our decellularization protocol resulted in more than 90% reduction in DNA content of cartilage tissue (data not shown). Thereafter, this decellularized natural scaffold has undergone recellularization by cell sheets using two different approaches. First, the sheet was simply deposited to cover decellularized cartilage (Fig. 2-c). For the second approach, the cartilage was entirely wrapped with the cell sheet, to create more contacts (Fig. 2-d). These two models were cultured for 2 weeks with chondrogenic medium and then analyzed. With the DAPI staining, we showed that decellularization actually led to removal of cellular nuclei through the depth of tissue (Fig. 2-f), when comparing to native porcine auricular tissue, where cell nuclei were detected through blue fluorescence (Fig. 2-e). The use of cell sheets allowed to recellularize the cartilage pieces. Simple deposition of cell sheets showed some degree of recellularization from the part that was in direct contact with cell sheets and examining the blue fluorescence, we could see that cells migrated slowly from the part in contact with cell sheet and a little bit further in scaffold (Fig. 2-g). When observing the wrapping model, blue fluorescence was observed on both sides of the scaffold and also deep in the center which indicates that cells had deeply migrated and penetrated the scaffold after 2 weeks of culture (Fig. 2-h). The same observations could be done using hematoxylin-eosin where native cartilage presented violet cells in lacunae (Fig. 2-i) while eliminated after decellularization steps, where lacunae were empty and the remaining extracellular matrix was staining in pink (Fig. 2-j). Recellularization of cartilage was shown in both techniques where cells were stained in violet (Fig. 2-k, l). To detect cartilage formation and glycosaminoglycan secretion, safranin O staining was performed and was directly proportional to the amount of proteoglycans in native cartilage tissue (Fig. 2-m), that was decreased after decellularization (Fig. 2-n). Cartilage reformation was confirmed by the production of proteoglycans in the simple deposition model and a partial recellularization of scaffold (Fig. 2-o), as well as the wrapping model, where cartilage cells integrated the whole scaffold and recellularized it completely (Fig. 2-p).

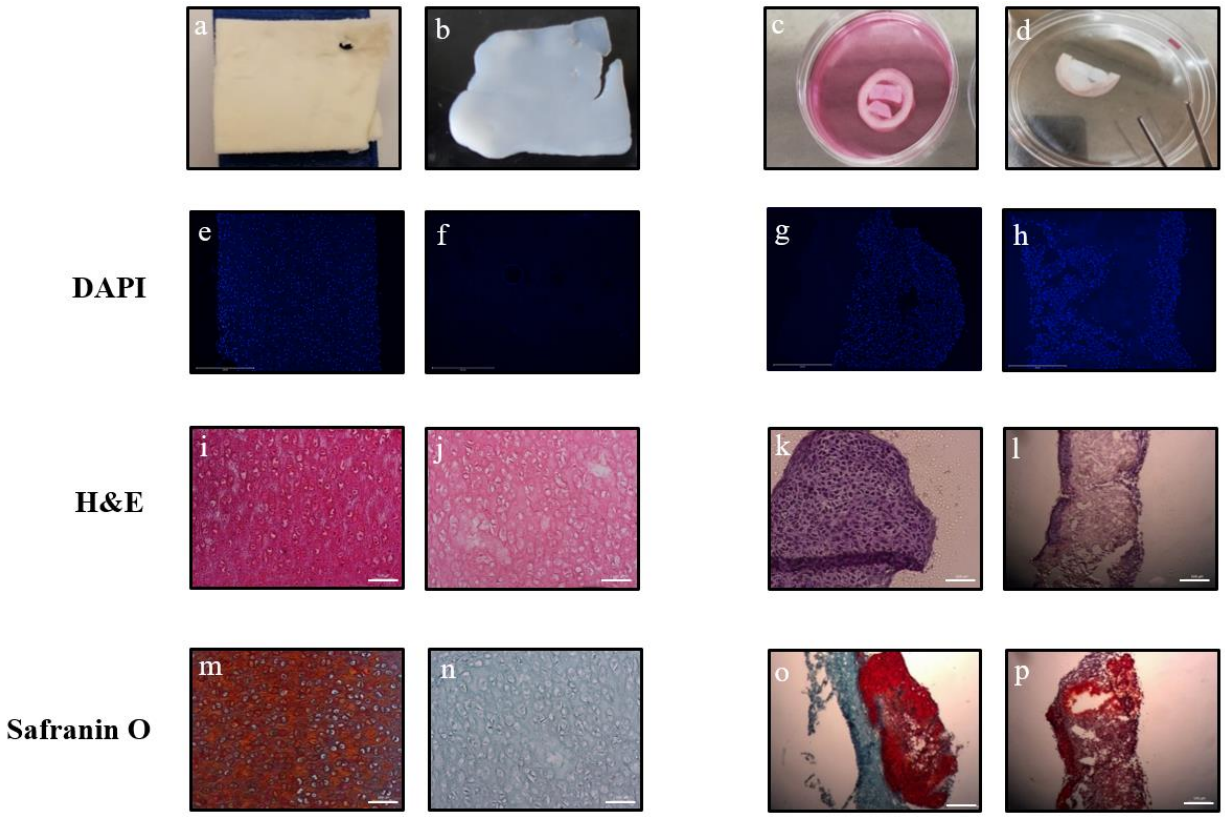

Fig. 2 Decellularization of porcine cartilage and recellularization with cell sheets. Native porcine cartilage (a), was decellularized (b) and recellularized by cell sheet simple deposition on its top (**c**) or entirely wrapped with cell sheet (d). After, 2 weeks of culture, corresponding samples were stained with DAPI (c, d, e, f), hematoxylin-eosin (h, i, j, k) and safranin O (l, m, n, o), respectively. Scale bar: 500µm (DAPI) and 100µm (H&E, Safranin O).

Cell sheets regenerates cartilaginous defects in rabbit models

Furthermore, we wanted to investigate the ability of cell sheets as carriers of cells *in vivo*in a rabbit model of cartilage defect as shown in the experimental procedure (Fig. 3-A). Cell sheets created from rabbit AuP were cultured with chondrogenic medium for 3 weeks before harvesting as described in materials and methods. Cartilaginous defects were surgically created at the level of auricular cartilage (Fig. 3-B-a, b), and cell sheets were then transplanted to the defect site before suturing (Fig. 3-B-c). After 2 months of *in vivo* incubation, no sign of infection or inflammation nor graft rejection were observed (Fig. 3-B-d). After rabbit sacrifice, the ears that received the grafts were dissected to extract biopsies. Macroscopic view of regenerated cartilage is shown and indicates glossy appearance and good integration of cell sheet graft into the host cartilage (Fig. 3-e). However, fibrous-like tissue was observed in the experimental group. These biopsies were then analyzed for their expression of cartilaginous markers. Just before implantation in rabbit models, rabbit cell sheets were grown for 3 weeks *in vitro* and their expression level of cartilage markers was analyzed compared to the cell sheets harvested after 2 months of implantation. *In vivo* cell sheets highly produced cartilage markers where expression of ELN, ACAN, SOX 9 was highly

increased after 2 months of implantation. COL2A1 presented the highest cartilage marker in these biopsies. COL1 expression was increased after 2 months, however, this increase wasn't significant compared to the massive increase of elastic cartilage markers, presenting a stable cartilage tissue (Fig. 3-C). Moreover, we didn't detect any hypertrophy of this regenerated tissue since very low expression of COLX was detected after implantation of these cell sheets. These implanted cell sheets were able to enhance and upregulate cartilaginous markers and significantly regenerate auricular defects in rabbits.

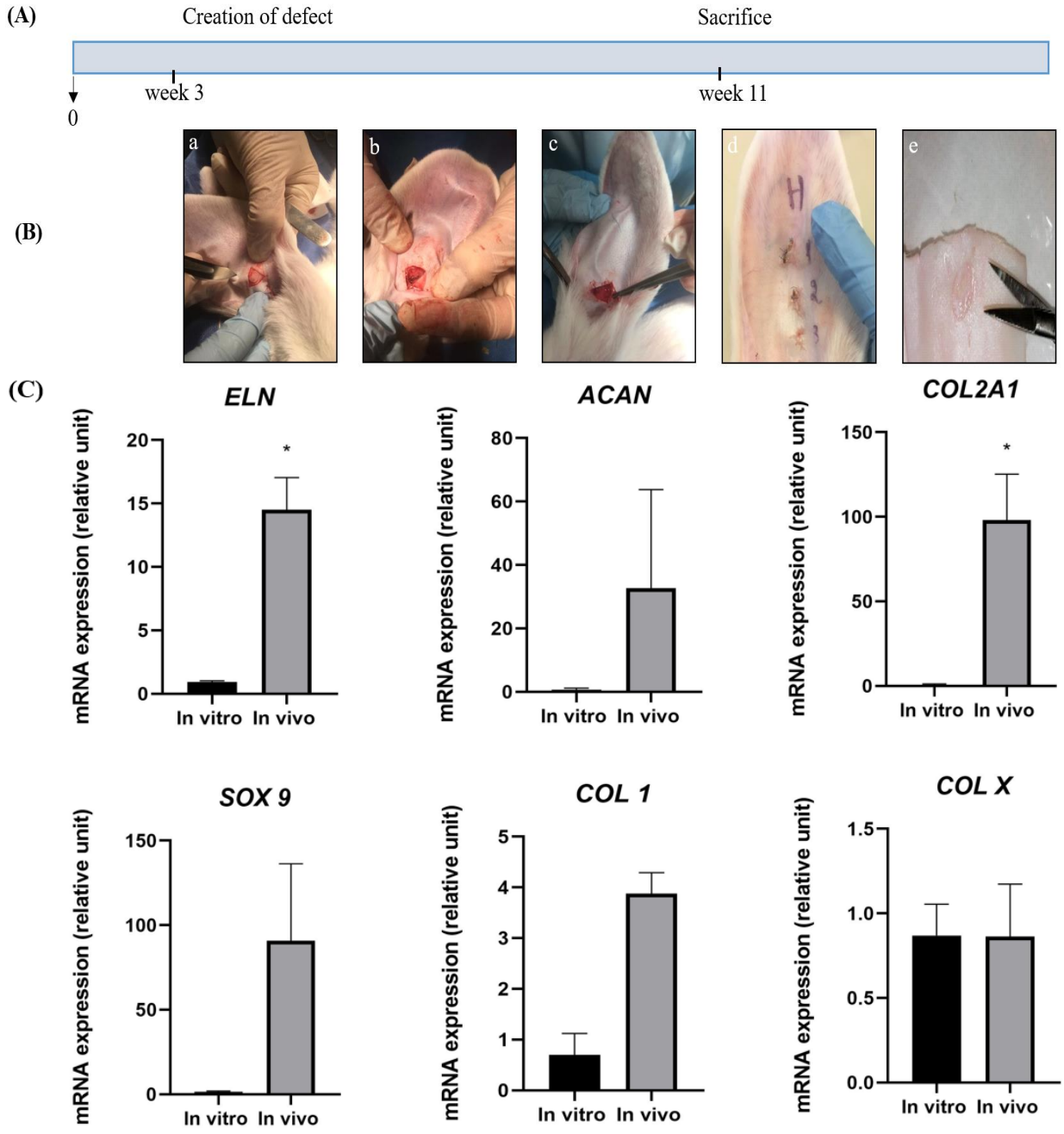

Fig.3. ***In vivo*** **use of cell sheets as cell carriers**. (**A):** Cells sheets were used to fill a defect in rabbit ear cartilage model according to the experimental procedure described. **(B):** Macroscopic observations of procedure and methods: Perichondrium-cartilage incision using an ophthalmic scissors and a scalpel in a semi-sharp direction (a). Cartilaginous defect was created in the rabbit ear (b). Filling with rabbit cell sheet pre-cultured with chondrogenic medium (c). The skin is reclosed and sutured. Sacrifice after 2 months of transplantation and ear harvesting and identification (d). Glossy white appearance of defect filled with cell sheet resembling at native cartilage (e) **(C):** Cartilage gene expression markers of rabbit cell sheets before and after *in vivo* implantation for 2 months.

Consequently, biopsies from native cartilage, unfilled defect and a defect filled with cells sheets were stained with safranin O and examined by immunohistochemistry of COL2A1 and ELN. Native cartilage is stained in red showing the native alignment of proteoglycans and cell distribution (Fig. 4-a). The negative experimental group where the defect was sutured unfilled shows an attempt of tissue cartilage restoration. However, it seems limited and appears unable to produce enough tissue to completely replace the lacking tissue (Fig. 4-b). When the defect was filled with cell sheets, the cell distribution and staining is more likely resembling native tissue. The neo-cartilage shown in red was regenerated in continuity with the native cartilage remnants, indicating a good restoration of the hierarchical structure (Fig. 4-c). To confirm these results immunohistochemistry of COL2A1 and ELN, revealed that the neocartilage was successfully generated since cell sheets exhibited an important expression of COL2A1 and ELN observed in the cartilaginous region (represented by white dashed lines), when defects were filled with cell sheets (Fig. 4-f, i), almost resembling the native tissue structure (Fig. 4-d, g). On the other hand, neither COL2A1 nor ELN was observed in the region of unfilled defect, respectively (Fig. 4-e, h). These results corroborate with the above real-time PCR results and confirm that cell sheets implanted in defects site highly regenerated elastic cartilage tissue in rabbit models.

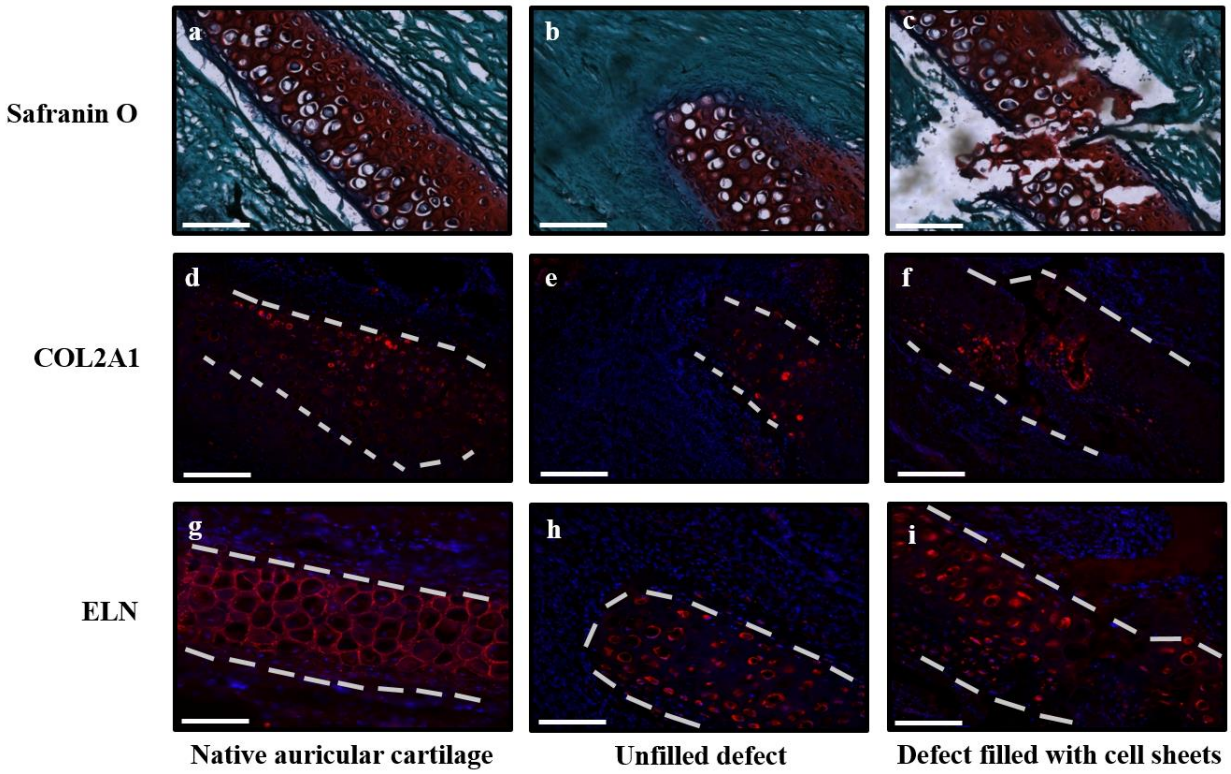

Fig. 4 Safranin O staining and immunohistochemistry of collagen II and elastin proteins in cartilaginous defects of rabbit after 2 months of transplantation. Cartilaginous region is represented by the white dashed line. Positive control showing the rabbit native cartilage (a, d, g). Experimental negative control where defect was created but unfilled (b, e, h). Defect was filled with cell sheet pre-cultured with chondrogenic medium (c, f, i), respectively. Scale bar: 200µm.

Discussion

In this study, we aimed to investigate different approaches and applications of cell sheets *in vitro* and *in vivo*. Cell sheets can be produced from a range of cell types, including chondrocytes (Takizawa *et al*., 2020; Toyoda *et al*., 2019; Wongin *et al*., 2020; Xue *et al.*, 2018), MSC (Kuramoto *et al.*, 2020; Thorp et al., 2020), fibroblasts, endothelial and epithelial cells (Alio del Barrio *et al*., 2015), cardiac (Araki *et al.*, 2020; Kainuma *et al.*, 2021) and periodontal (Farag et al., 2017, 2014), tendon, adipocytes (Chen et al., 2021; Y. Zhang et al., 2019) and bone *(Fan et al.*, 2020; Ren *et al*., 2017; Silva *et al.*, 2020). No studies have yet tested auricular perichondrocytes ability to form sheets for their application in cartilage tissue engineering. From this point, we tested several cell types shown in Table 1, and mainly focused on perichondrocytes and their tendency to form cell-secreted matrices, implicated in cartilage tissue engineering.

Many researchers are still using 2D approaches, since they provide efficiency and simplicity. However, recent research focuses more on self-assembly and 3D culture to reproduce cell-cell interaction *in vitro* and to mimic *in vivo* environment. Scaffold-free approaches create cell sheets for instance, can also be layered creating a 3D structure. A porous 3D scaffold is challenging to seed with cells because the distribution of the cells tends to be homogenous, especially in large constructs. This technology evolved and instead of using biodegradable scaffolds, they are

progressively substituted by cell sheets that avoided the limitation of scaffold degradation and maintained cell-cell junctions and the complete secretion of ECM proteins. The preservation of these cell-cell interactions that is guaranteed without any proteolytic enzyme, preserve quality and quantity of these cells and ensure their homogenous distribution (Imashiro and Shimizu, 2021). Furthermore, the use of cell sheets reported greater cell survival and suppressed the immunological intervention related to scaffolds (Asadi *et al*., 2020; Takeuchi *et al*., 2016). Besides, our study affirms that cell sheets retains native cartilage composition when cultured in chondrogenic medium.

Many cell sheets produced a multi-layered structure when cultured on temperature-responsive culture dishes. Sakai *et al.*, for instance, produced a double to triple cell sheet when 2 types of hepatic cells were cultured on top of each other (Sakai *et al*., 2013). Co-culture of both periodontal ligament stem cells combined to bone marrow mesenchymal stem cells also created a natural 3-layered cell sheet to reconstruct and regenerate periodontal ligament tissue (Safi *et al.*, 2019). Apart from tissue responsive dishes, multi-layered skeletal muscle sheets were formed when seeded within collagen microgrooves (Chen *et al.*, 2015). Our results, were consistent with those presented in literature, however, it is important to mention that auricular cell sheet presented multi-layered structure and didn't require any cell sheet stacking to create 3D structure, nor cellular or scaffold combinations. This was controlled by only cell seeding density and L-ascorbic acid concentration.

One approach for cartilage engineering is the use of native decellularized tissue, seeded with cells. This cell-derived extracellular remaining matrix has emerged in recent years as a safe, natural, alterative extracellular matrix source that reduce the potential risk of pathogen transmission and immune response. However, the recellularization of cartilage remains an issue and was investigated by several researches. Luo *et al.*, for instance, introduced channels in cartilage in an attempt to facilitate recelluarization (Luo *et al*., 2016), others removed elastic fibers by digesting them with elastase to allow rapid recellularization of auricular cartilage tissue (Z. Huang *et al*., 2017). To overcome the cell seeding problems and to reduce the number of cells required to recellularize tissues and organs, cell sheets were used to better mimic and enrich the natural structure with ECM. Gong *et al.*, on the other hand, seeded porcine chondrocytes on decellularized porcine cartilage sheets and stacked them layer by layer, in a sandwich model of 20 sheets and successfully engineered cartilage *in vitro* (Gong *et al.*, 2011). Our results of wrapping cartilage showed a deep penetration of cell into porcine cartilage showing a homogenous distribution of cells. It is important to note that this method, overcomes the cell-seeding problems during recellularization and maintains the original structure of auricular cartilage.

It has been shown that cartilaginous extracellular matrix derived from decellularized cartilage favored cell recruitment and enabled construction of osteo-chondral defects in rabbits *(Z. Wang et al.*, 2018), as well as in mini pig models (Ebihara *et al*., 2012). Chondrocytes when encapsulated in printed 3D scaffolds (Park *et al*., 2017) promoted auricular rabbit cartilage repair, as well as when combined with synovial cells that repaired partial thickness defects of articular cartilage (Xue *et al*., 2018). Adipose-derived stem cells have been shown to highly promote auricular cartilage regeneration in rabbits when injected directly in defect sites (Oh *et al*., 2020, 2018) or

encapsulated in alginate beads (Leslie *et al*., 2018). Importantly, these cells successfully vascularized and repopulated perfused-decellularized human ears, that were implanted afterwards in mice for 60 days without any rejection, promoting functional properties (Duisit *et al.*, 2018). In our study allogenic auricular perichondrocyte sheets were transplanted for the first time into auricular defects in rabbit models. Apparently, these cell sheet did not elicit any immune response and promoted regeneration of auricular cartilage defects in rabbit ears. Our study present encouraging work, however, the biomechanical function of these cell sheets should be deeply assessed to evaluate transplant stability and performance in order to be applicable for larger cartilage defects.

Cell sheets not only supported *in vitro* recellularization of xenogenic porcine cartilage, but also these sheets acted as cell carriers that induced and regenerated auricular cartilage defects in allogenic rabbit models.

Conclusion

Our results casts new light on regenerating auricular cartilage using auricular progenitor cells. Indeed, we show that cell sheets made from rabbit auricular perichondrocytes are capable to form a multi-layered and complex structures that can be recovered for further use. These sheets are useful as cell carriers for colonization of decellularized cartilage. This open a route for engineering pieces of cartilage from biopsies. Moreover, such sheets can also be used *in vivo* for filling a cartilage defect and thus, regenerating elastic auricular cartilage in an allogenic model in rabbit Altogether, these findings bring new insights in the use of cell sheets and particularly in cartilage engineering.

3-Cartilage tissue engineering using apple cellulosic scaffolds

To a wide range of scaffold materials for cartilage tissue engineering, and due to the recent advance of using plants-derived tissues, we were interested in investigating apple hypanthium scaffolds as biomaterials for cartilage tissue engineering.

In this study, we show that decellularized apples provide cellulosic scaffolds for 3D culture of different human progenitors, when seeded with different progenitors.

Apple matrices showed high proliferation rate and viability after 21 days of culture when seeded with human NSP, as well as rabbit auricular GFP transfected perichondrocytes after 2 weeks of culture, illustrating the cellular growth and proliferation.

Moreover, these cellularized apples were then stimulated by chondrogenic induction in normal or low levels of oxygen and induced cartilage-like tissue. Chondrogenic medium is sufficient to trigger high tissue formation in AuP and to a lesser extent in DPSC, while BMMSC and NsP necessitate an additional hypoxic condition to secrete more ECM production.

Cartilage tissue formation was also confirmed by high levels of mRNA expressed by chondrogenic differentiation. Cartilaginous genes such are COL2A1, ACAN, COMP, SOX9 and ELN, were differently expressed in different cellular types. NsP, AuP and BMMSC successfully reported chondrogenic potential in apple-derived tissue, however, dental stem cells presented a more osteogenic profile.

In our hands, apple scaffolds showed a higher tendency and surpassed alginate potential to direct chondrogenic differentiation into cartilage tissue. This highlights the beneficial of apple scaffold potential to promote proliferation and chondrogenic differentiation encouraging its use for cartilage or other tissue engineering approaches, considering its ease of use and wide availability.

In conclusion, we here demonstrate the advantageous effects of apple matrices on proliferation and migration of different progenitors. Interestingly, our data show that decellularized apple hypanthium tissue provides a natural and porous scaffold that guide chondrogenic differentiation of different progenitor cells *in vitro. In vivo* evaluation of chondrogenic potential of these scaffolds would be interesting in future experiments.

Cartilage tissue engineering using apple cellulosic scaffolds

Mira Hammad*[1,2], Justin Dugué*[1,2,3], Catherine Baugé[1,2], Karim Boumédiene[1,2]

[1]Normandy University, UNICAEN, EA 7451 BioConnecT, Caen, France, [2]Fédération Hospitalo Universitaire SURFACE, (Amiens, Caen, Rouen), France, [3]Service ORL et chirurgie Cervico-faciale, CHU de Caen, Caen, France

**Authors equally contributed to this work.*

Abstract

There is a growing clinical need for exploring new biomaterials that support and promote integration and proliferation of different cells for various regenerative medicine applications. Decellularization of tissues have widely been accepted as an alternative to the use of synthetic polymeric scaffolds. Due to preservation of morphology and biochemical composition after cellular removal, animal-derived tissues present good choice for obtaining extracellular matrix (ECM), with an intact vascular network that delivers oxygen and nutrients for cells. Despite their advantages, animal-derived tissues have presented some limitations concerning ethical issues and their variability among donors. For that, plant-derived tissues have recently been selected since they possess a wide range of architecture and have reported good cytocompatibility and biocompatibility. In this study, we prepared decellularized, porous apple scaffolds to promote cellular growth and proliferation. We aimed to generate cartilage-like structure by seeding different progenitors, stimulated by chondrogenic medium and cultured in normal or reduced oxygen level environment. Cell viability experiments showed high proliferation of these cells. Histological staining, as well as real time RT-PCR results revealed the deposition of new cartilaginous ECM in apple cartilage-like tissues. Furthermore, we compared the chondrogenic potential of our decellularized apple scaffolds to alginate beads, as a robust and well mastered model of chondrogenesis. Our results demonstrate that apple scaffolds are superior models in driving chondrogenic differentiation of several human progenitors *in vitro*. Taken together, these results provide promising approaches of plant-derived matrices for tissue engineering and biomedical applications.

Introduction

Advancement of innovative three-dimensional (3D) scaffolds for tissue engineering has gained wide attention over the past decade. These 3D systems present several morphological and biochemical differences compared to 2D culture, that makes them better representatives of the nature of ECM environments that can be used in multiple applications (Baker and Chen, 2012; Puschmann *et al.,* 2013). Creating 3D culture systems require a multidisciplinary understanding and experience in different parameters to choose the best material, cell type and culture method that best suits the desired tissue.

The utmost aim of the scaffolds is to bring proteins and molecules present initially in the ECM in order to mimic native tissue and restore their physiological functions. This is where decellularized

matrices become an essential choice, since they inherit the specific intrinsic signals from a native ECM (Huh *et al.,* 2018).

Most current bioengineering approaches have shifted more towards decellularized derived matrices (Ott *et al.,* 2008; Xing *et al.,* 2015). Decellularization is the elimination of cellular material from tissue and organs, leaving behind a functional ECM, inheriting a non-immunogenic character. This latter would be repopulated later on with patient cells to engineer and create autologous grafts for damaged and injured tissues and organs (Mazza *et al.,* 2015; Robertson *et al.,* 2014; Zhou *et al.,* 2010). Many animal-derived tissue were decellularized with a complete preservation of their vascular structure such as human skin that was used as a potential soft tissue replacement (Brouki Milan *et al.,* 2020), retinal matrix to produce retinal thin films (Kundu *et al.,* 2016), bone constructs (Smith *et al.,* 2017), cartilage constructs (Galuzzi et al., 2018; Y. S. Kim *et al., 2019)*, and vascular grafts (Mallis *et al.,* 2018; Yang *et al.,* 2019).

Nevertheless, whole organ decellularization techniques have also gained attention in the last decades where they enabled the fabrication of scaffolds to generate new organs. They included liver (Maghsoudlou *et al.,* 2016), pancreas (Elebring *et al.,* 2017; Kuna *et al.,* 2018), kidney (Mayorca-Guiliani *et al.,* 2019; Tajima *et al.,* 2020), heart (Hülsmann *et al.,* 2018; Timchenko *et al.,* 2017) and lungs (Urbano *et al.,* 2017; Wrenn *et al.,* 2018). Although they showed interesting results, however animal and human sources present undesirable clinical aspects and limitations, where we have shortage of these tissues that can decrease but without a complete elimination of xenogeneic reactions. Moreover, ethical concerns lie behind their use, rendering them controversial (Kaw *et al.,* 2016).

Recently, many studies are more focused on using cellulose as a biomaterial in tissue engineering. It is the major constituent of plant cell wall. Not only produced by plants, but also from bacterial and animal origin. A number of studies have been published during the last decades that investigated cellulose biocompatibility as well as its biodegradability. Studies by Carvalho *et al.,* have investigated bacterial cellulose (BC) in healing and regeneration of rapid wound healing in skin models. These used as injectable microspheres scaffolds that enhanced 3D cell culture and proliferation rate of chondrocytes (Carvalho *et al.,* 2019), also chondrocytes proliferation was enhanced when lotus root starch was incorporated with BC (Wu *et al.,* 2019). BC was also used for cartilage engineering where it was coupled to methacrylated gelatin, resulting in supported chondrocytes proliferation and cell growth (Gu *et al.,* 2020). Colonization of cells was achieved by using 3D laser perforation that facilitated the passage of chondrocytes into the bacterial cellulose scaffolds, thus increasing cell quantity and gradually matrix deposition towards cartilage regeneration. Taking into consideration the structural and mechanical similarities of both ECM and BC, Wang *et al.,* proposed natural bionic nanofibrous microcarriers that mimic natural ECM by crosslinking bacterial cellulose. This showed a great ability to repair articular cartilage defects (Y. Wang *et al*., 2018).

Apart from bacterial cellulose, plants have gained special attention in recent years, since they cover a wide range of features and similarities with mammalian vasculature, whether morphologically, physically or even mechanically. Due to their availability, biocompatibility and affordability,

plant-derived tissues have been used as an alternative to mammalian and animal tissues and organs (Fontana *et al*., 2017; Gershlak *et al*., 2017).

Many studies have demonstrated the ability of plant tissues to be decellularized, leaving behind a cellulosic scaffold that in turn can be a support for *in vitro* 3D culture as well as a biocompatible *in vivo* implantable scaffolds. Spinach leaves, for instance, remained patent and permitted transportation of microparticles, after their decellularization. Human endothelial cells populated the inner surface of the scaffold and stem cells-derived cardiomyocytes colonized the outer part, thus generating a contractile function (Gershlak *et al*., 2017). For a better understanding, Dikici *et al.,* then explored the proangiogenic activity and enhanced the survival of endothelial cells on small spinach leaves, promoting vascularization and angiogenesis within 1 week of culture (Dikici *et al.*, 2019). Not only small leaves supported endothelial cells, but also decellularized cabbage leaves best preserved vascularity and better fabricated pre-vascularized large sized scaffold that supported mammalian cell functionality (Walawalkar and Almelkar, 2020). Onion green leaves also provided a simple and low-cost biomaterial for skeletal muscle tissue engineering where its microstructure guided CaCl2 cell differentiation into aligned myotubes (Y.-W. Cheng *et al*., 2020).

In fact, plant-derived scaffold not only exhibited a functional scaffold but also both good cyto-biocompatibility (Modulevsky *et al.,* 2014, 2016). Interestingly, decellularized apples have supported mammalian *in vivo* cell culture and interestingly, showed high biocompatibility when implanted *in vivo* in mice models (Modulevsky *et al.,* 2016, 2014). Hence, we used decellularized apples as a scaffold and tested their ability to drive different cell progenitors towards chondrogenesis when subjected to different culture environments.

Four different cell sources were used. Progenitors of auricular and nasal cartilage (AuP and NsP), dental pulp stem cells (DPSC) and bone marrow-derived mesenchymal stem cells (BMMSC). BMMSC possess high proliferative and vast chondrogenic potential, where it is reported as the gold standard for cartilage repair and regeneration (Bae *et al.,* 2018; Khatab *et al.,* 2020). Recent reports have also reported the cartilage-forming ability of AuP (Otto *et al.,* 2018). These cells can be expanded up to a large number without losing their differentiation potential. We have already proved in our previous work the potential of these cell to produce healthy elastic cartilage (Hammad *et al.,* to be submitted).

Many studies have investigated the potential of nasal-septal derived chondrocytes in cartilage tissue engineering. Lim *et al.,* evaluated the encapsulation of nasal chondrocytes in COL1 hydrogel that significantly repaired osteochondral defects in rat models (Lim *et al.,* 2020). These cells also demonstrated safe and feasible regeneration of traumatic knee injuries in clinical trials (Mumme *et al*., 2016). However, no studies have yet demonstrated nasal progenitors (NsP) in elastic cartilage regeneration.

Many cartilaginous tissues were engineered from DPSC. Recent studies have described the potential of DPSC as stem cell therapies for articular cartilage repair (Fernandes *et al.,* 2020). These cells are characterized by microvilli-like structures on their surfaces, permitting a good attachment to the biomaterial of interest (Fernandes *et al.,* 2018). Once grown in chondrogenic medium, DPSC presented a rounded morphology that was correlated with ACAN and COL2A1

expression when encapsulated in nanocelluose-chitosan hydrogels (Mata *et al.,* 2017; Talaat *et al.,* 2020). Another recent study have reported the potential ability of DPSC to exert an anti-apoptotic effects to treat osteoarthritis (Lin *et al.,* 2021).

To assess potency, the above cellular sources were seeded on our apple scaffolds to investigate their chondrogenic ability in cellulosic 3D models.

Materials and Methods

Preparation of apple hypanthium tissue

Granny smith apples (*Malus domestica*) were commercially purchased from an organic farm. They were used directly with no preservation in our laboratory. Apple slices were cut homogenously using a mandolin slicer. This made it possible to obtain standardized slices with a thickness of 1mm and of a diameter of 11mm, that were also carved in their center with a biopsy punch tool to facilitate cell seeding.

Decellularization protocol

Decellularization was performed by testing different sodium dodecyl sulfate (SDS) concentrations and for different time intervals. Prepared apple sections were immersed in 1% SDS for 24 hrs at 37% with continuous agitation. Afterward, SDS was removed and the slices were rinsed with distilled water for 30min. This step was repeated twice, then left in distilled water overnight. Native samples were freshly cut from apples, and kept at 4°C for further analyses.

DNA extraction and quantification

DNA extraction was carried out following mechanical lysis of the apple tissues with pestle and mortar in lysis buffer consisting of Tris Base, SDS and dithiothreitol (DTT) (100mM). After centrifugation to remove debris, the DNA was precipitated by adding isopropanol and centrifugation. The pellet was then washed with 70% ethanol and centrifuged before being dried and taken up in distilled water. The assay was then carried out by spectrophotometry (Thermo Scientific TM, micro-dropTM and Thermo Scientific TM SkanIt TM software) and DNA concentration determined reading optical densities at 260 nm. The values were normalized to the "wet" weight of the different samples, taken directly after slicing.

Size of DNA fragments

The size of the DNA fragments was evaluated by migration of the genomic DNA on 1% agarose gel (30 minutes at 100V) and staining with Gel Red. The revelation was carried out by exposure of the gel to UV light and photographed under Chemi Doc XRS apparatus (Bio-Rad). DAPI solution 0.5µg/ml was used as a final concentration to stain cells in native and decellularized apple matrices.

Sterilization and seeding of constructs

Before inoculating the decellularized slices, a sterilization process was carried out following the washing phases. It consisted of a 1.5-hour immersion with continuous stirring and at room temperature in a mixture of 1X PBS and 0.2% penicillin / streptomycin. Subsequently, the samples were incubated at 37 °C and 5% CO2 in 2 mL of culture medium for 12 hrs in a 24-well plate. Finally, the next day, the medium was aspirated and samples were left for 2hrs in dry conditions, to eliminate the surplus of medium and to facilitate cell seeding.

The cells were seeded at a density of 7,000,000 per apple section. This was guided after several preliminary assays. The samples thus seeded in the 24-well plates are left for 3 hours without adding medium in order to promote cell adhesion. The medium was then added (2 mL), and the samples are incubated under standard conditions (37 ° C, 5% CO2) for a period of 48 hours before the application of specific culture conditions, in order to have homogeneous cell adhesion of the different samples. After 48 hours, culture plates were changed and sample were transferred to new culture plate to avoid the cells that potentially escape and adhere to plastic. The culture medium was changed every two days and incubated in normoxia (21% O_2) or hypoxia (3% O_2) culture conditions.

Cell viability

Cell viability was first assessed by measuring ATP using the Cell Titer-Glo® kit (Promega). After cell culture, the samples were lysed in Cell Titer-Glo Reagent (150 µL) and culture medium 1:1 and stirring for 45 minutes at room temperature, then the emitted luminescence was measured using a luminometer (Varioskan Lux, Thermo Scientific). This method permits to quantify the ATP present in cell cultures signaling the presence of metabolically active cells. Alternatively, GFP-labeled rabbit AuP were seeded on apple slices for monitoring by fluorescence microscopy.

Histology

After culture, the cultured slices were fixed in 4% PFA for 1 hour at 4°C, rinsed with 30% PBS-sucrose for 2 hrs and cryopreserved in OCT (Optimal Cutting Temperature gel) at -80 ° C. The histological sections (10 to 15µm thick) were obtained using a cryostat (Leica CM3050) and deposited on slides. Different stains were applied i.e. Hematoxylin-Eosin (HE), Safranin-O (SO), Alcian blue (AB) and Masson's Trichrome (MT).

Cellular sources

Different cell types were used. Nasal and GFP stably transfected auricular perichondrocytes from rabbit for the viability assays. They were obtained after animal dissection and conserved in the lab after expansion. For differentiation experiments, human cells were used. Human BMMSC were derived from bone marrow aspirates of patients undergoing hip arthroplasty and having signed the consent form in agreement with the local ethics committee CPP Nord-Ouest III. Bone marrow was separated on a ficoll density gradient (GE Life Science).and the ring of mononuclear cells was collected and then seeded in MSC amplification medium: αMEM with 10% FBS, 1 ng / mL of FGF-2, 200mM of glutamine, 100 IU / mL of penicillin and 100 µg / mL of streptomycin. The medium was changed three times a week, apart from the first medium change after five days of cell adhesion. The cells were incubated at 37°C in an atmosphere containing 5% CO2. They were

cultivated and amplified until the 4th passage before use. At this stage, tests are carried out to verify the absence of hematopoietic markers (CD34-, CD45-) by RT-PCR.

NsP came from surgical waste from various interventions within the otorhinolaryngology or maxillofacial surgery surgical units of the CHU of Caen of patients who signed consent forms. After dissection of the perichondrium, pieces were cut and used for outgrowth cultures. NsP were expanded in αMEM expansion medium. After 6 Passages, they were freezed at -150°C for further use.

AuP were obtained from fresh-human auricular cartilage biopsies after 12-year old children undergoing rhinoplasty. Perichondrium was separated from cartilage by dissection and sliced into small pieces. Cells were collected by sequential enzymatic digestion using pronase for 45-60 min at 37°C and collagenase II overnight at 37°C. The next day cells were seeded in T75 flasks and amplified till reaching passage 3, which then freezed for further use.

DPSC were obtained from freshly-extracted teeth of young donors (16-20 years). These latter were transferred into hypotonic phosphate buffered saline solution and were disinfected by a solution of antibiotics. Then pulp tissue was isolated from the pulp chamber where the tissue was minced into small pieces and sequential enzymatic treatment was carried out by collagenase I (3mg/ml) and dispase (4mg/ml) for 30-45min, at 37°C. After enzymatic digestion, cell suspension was centrifuged at 2000 rpm for 10min, and the cell pellet was resuspended with cultivation media (alpha-MEM + 10% FBS + 1% penicillin/streptomycin + bFGF 0.5µg/ml) and seeded into cultivation dishes, and freezed when reaching passage 3.

RNA extraction

Total RNAs were extracted according to the Rneasy® Mini Kit protocol (Qiagen), based on the binding of nucleic acids to a column of silica. The different samples were mechanically lysed with a mortar and pestle in 600 µl of highly saline buffer containing guanidine thiocyanate. RNA bound to column kit were finally eluted with DEPC treated water and concentration measured by OD 260 reading on Microdrop system (Thermo Scientific Multiskan GO).

Reverse transcription

First, 1 ug of RNA was treated with DNase (Sigma-Aldrich®) to eliminate contaminating DNA that may be present in the samples. After that, reverse transcription was carried out in order to obtain complementary DNAs. Reverse transcriptase was carried out using a mixture composed of 1 µg of RNA, 2.5 µM of oligodT, 0.5 mM of dNTP, 1X First Strand Buffer and 10 U/µL of Moloney Murine Leukemia Virus reverse transcriptase (M-MLV-RT, Invitrogen). The reactions products were then diluted 100 times before being stored for later use in real-time PCR.

Real time PCR

Reverse transcription products are used in a reaction mixture containing 0.2 µM sense and antisense primers of the target gene and 7.5 µL of the Power 2X SYBR Green mix. Amplification was carried out on a StepOnePlus ™ Real-Time PCR System thermocycler (Applied Biosystem) for 40 cycles which consist of a denaturation step at 95 ° C for 15 seconds and a hybridization and

polymerization step of one minute at 60 ° C. The specificity of the amplification products was checked by analysis of the melting curve. The relative expression of the gene studied was calculated by the $2^{-\Delta\Delta CT}$ method. Real time RT-PCR primers are listed in the supplementary table below. Results were compared to normalized to three housekeeping genes (GAPDH, RPL13, β2MG).

Gene	Forward primer	Reverse primer
ELN	CCAGGTGTAGGTGGAGCTTT	CCATAGCCATAGGGCAGTTT
SOX 9	CCCATGTGGAAGGCAGATG	TTCTGAGAGGCACAGGTGACA
COL1	CACCAATCACCTGCGTACAGAAC	CAGATCACGTCATCGCACAAC
ACAN	GTGCCTATCAGGACAAGGTCT	GATGCCTTTCACCACGACTTC
COL2A1	CCAGATGACCTTCCTACGCC	TTCAGGGCAGTGTACGTGAAC
COLX	CCTGGTATGAATGGACA	CCCTGAGGGCCTGGAAGA
GAPDH	ATGGGGAAGGTGAAGGTCG	TAAAAGCAGCCCTGGTGACC
RPL13	GTTCGGTACCACACGAAGGT	CTGGGGAAGAGGATGAGTTTG
β2-MG	GAGGCTATCCAGCGTACTCCA	CGGCAGGCATACTCATCTTTT

Statistical analysis

Data are presented as mean ± standard deviation. Statistical data were performed by two-way ANOVA with Tukey's multiple comparison test, to compare different sets of data, using Graph Pad prism 7 software, significance level was set at $P<0.005$.

Results

Decellularized apples provide cellulosic scaffolds for 3D culture of different human progenitors

To begin with, apple hypanthium disks were decellularized by 1% SDS incubation under agitation, then thoroughly washing, until a pellucid aspect was shown after cell removal (Fig. 1-A). Decellularization was checked by observing the removal of genetic material was significantly removed by DAPI staining (Fig. 1-B) and less than 50 ng of DNA remained per mg of tissue (Fig. 1-C). The remaining fragments were less than 200 bp (Fig. 1-D), suggesting an effective decellularization that achieved the recommended criteria. Apple disks were first tested for cellular viability, where perichondrocytes stably transfected with GFP were seeded on the top of the disks at the density of 2,000,000 cells per apple section and incubated in chondrogenic medium, for several days. They were monitored by fluorescent microscopy that showed multiple clusters with great green staining. (Fig. 2-A). In addition, ATP cell production was measured up to 21 days and suggest good viability and even growth after 2 weeks (Fig. 2-B).

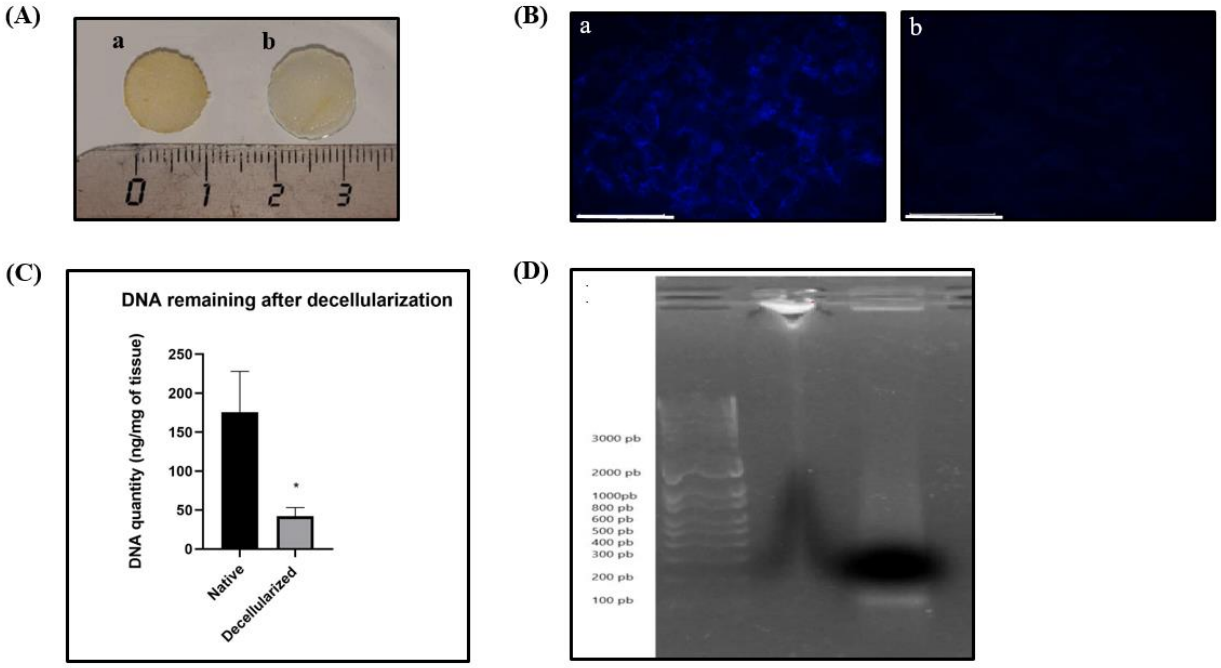

Fig.1 Decellularization of apple hypanthium tissue. (**A**): Macroscopic aspect of apple sections before (a) and after decellularization (b). (**B**): DAPI staining of native (a) and decellularized apple (b). (**C**): Quantification of DNA remaining after decellularization. (**D**): Electrophoretic migration of DNA fragments before and after decellularization of apples.

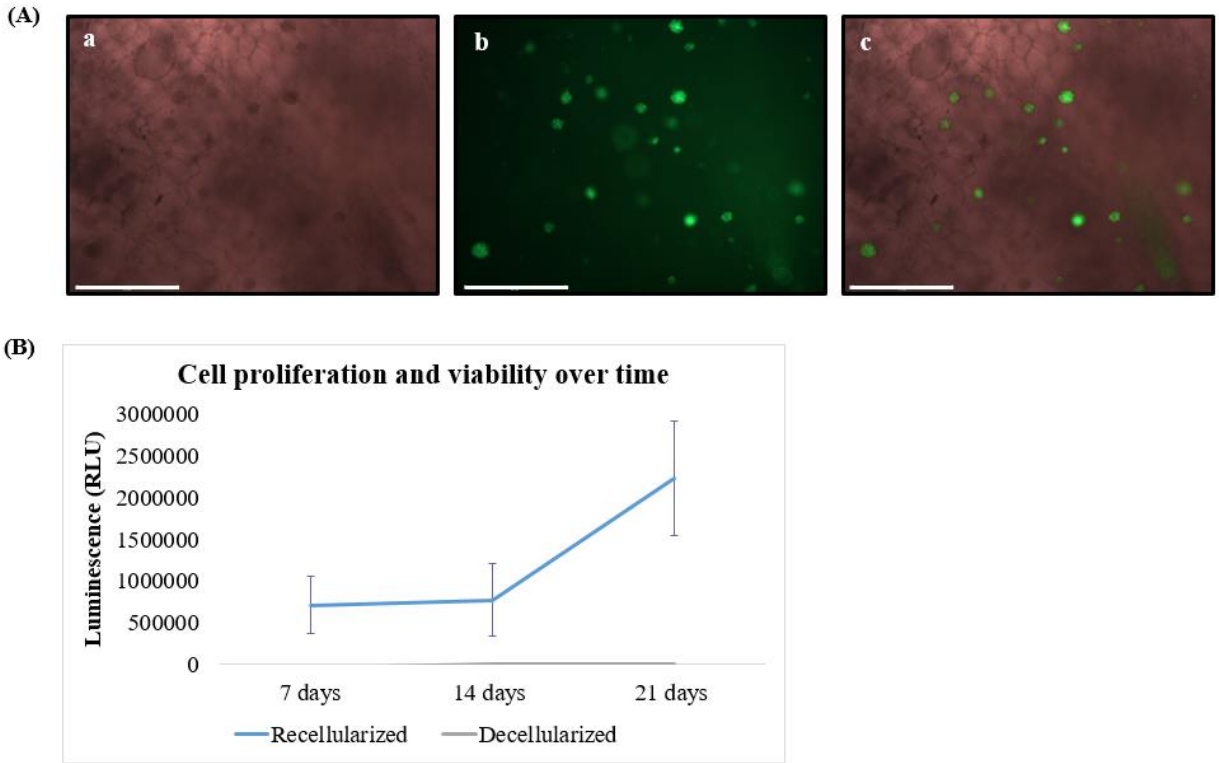

Fig. 2 Viability of nasal perichondrocytes seeded on cellulosic matrix of apples. (**A**): Assessment of GFP expression in cells for 14 days of culture, visualized in phase contrast (a), fluorescence (b) and by

the superposition of two images (c). Scale bar: 500µm. (**B**): ATP quantification of cells as a function of extended culture time in recellularized apples compared to a control (decellularized apple).

Cellularized apple scaffolds induce the formation of cartilage-like tissues

After optimizing cell seeding into apple scaffolds, we performed a comparative chondrogenic potential study of different human progenitors, chosen as described earlier. Cells were seeded at the density of 7,000,000 cells per apple disk in DMEM medium and left for 48h to adhere to the scaffold. After that, they were incubated with DMEM or chondrogenic medium in either normoxic or hypoxic atmosphere, except for auricular perichondrium progenitors. Indeed, for these cells, we previously showed that hypoxia doesn't enhance nor bring benefits for their chondrogenic differentiation. Hence, they were tested only in normoxic conditions. Macroscopic views of cellularized apple scaffolds was shown after 14 days. Attentive examination allows to distinguish whitish and translucent tissue in scaffold center in several conditions. Chondrogenic medium is sufficient to trigger high tissue formation in DPSC and AuP, while BMMSC and NsP required additional hypoxic environment to secrete visible ECM production (Fig. 3). After incubation for 14 days in chondrogenic medium, both in normal or hypoxic atmosphere, the cellularized scaffolds were fixed and prepared for histological staining in comparison to unseeded decellularized apple. Hematoxylin-Eosin (HE), Safranin O (SO), Alcian blue (AB) and Masson's Trichrome (MT) were used for tissue morphology and ECM analysis.

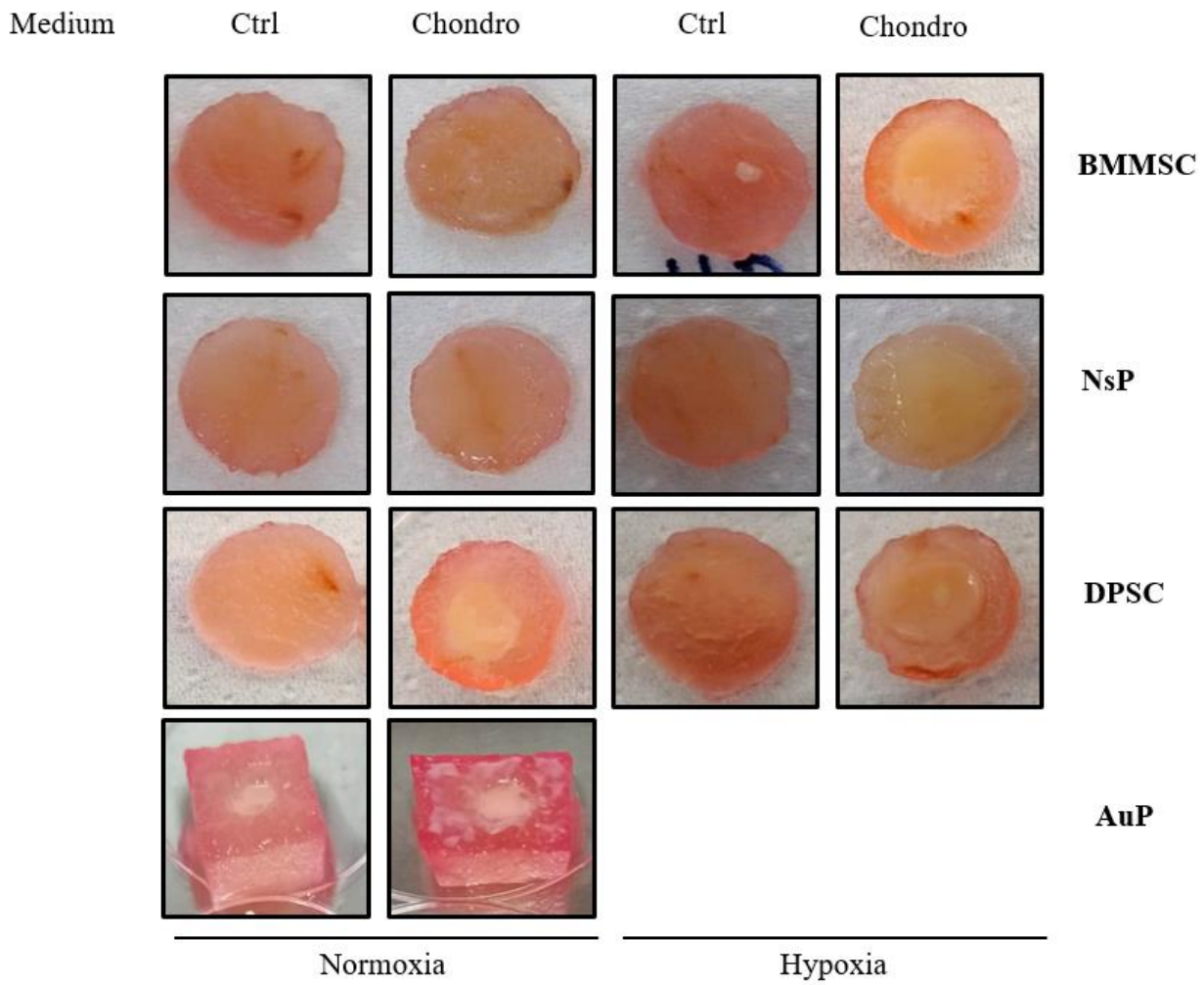

Fig. 3 Macroscopic aspects of apple scaffolds seeded with different progenitors in control and chondrogenic medium for 14 days in normoxic and hypoxic conditions. Apple scaffolds seeded with bone marrow-derived stem cells (BMMMSC), nasal perichonrocytes (NsP), dental pulp stem cells (DPSC), and auricular perichondrocytes (AuP).

Histological staining also showed that when apple scaffolds were seeded with BMMSC, low tissue formation was observed under normoxic conditions. However, this was greatly enhanced upon hypoxic culture as shown by abundant cytoplasmic components and ECM production such as collagen and elastin fibers stained in pink, cartilage proteoglycans and glycosaminoglycans stained in dark red and blue color (using SO and AB staining) respectively. Collagen fibers were more clearly stained when MT was performed, showing a great abundance of these fibers observed in dark blue color (Fig. 4-A).

In parallel, NsP and DPSC were tested in the same conditions. All of them, showed tissue formation with abundant ECM secretion under chondrogenic medium and hypoxia did not significantly enhance this process, as already described for AuP, tested here only in normal oxygen levels (Fig. 4-B-C-D).

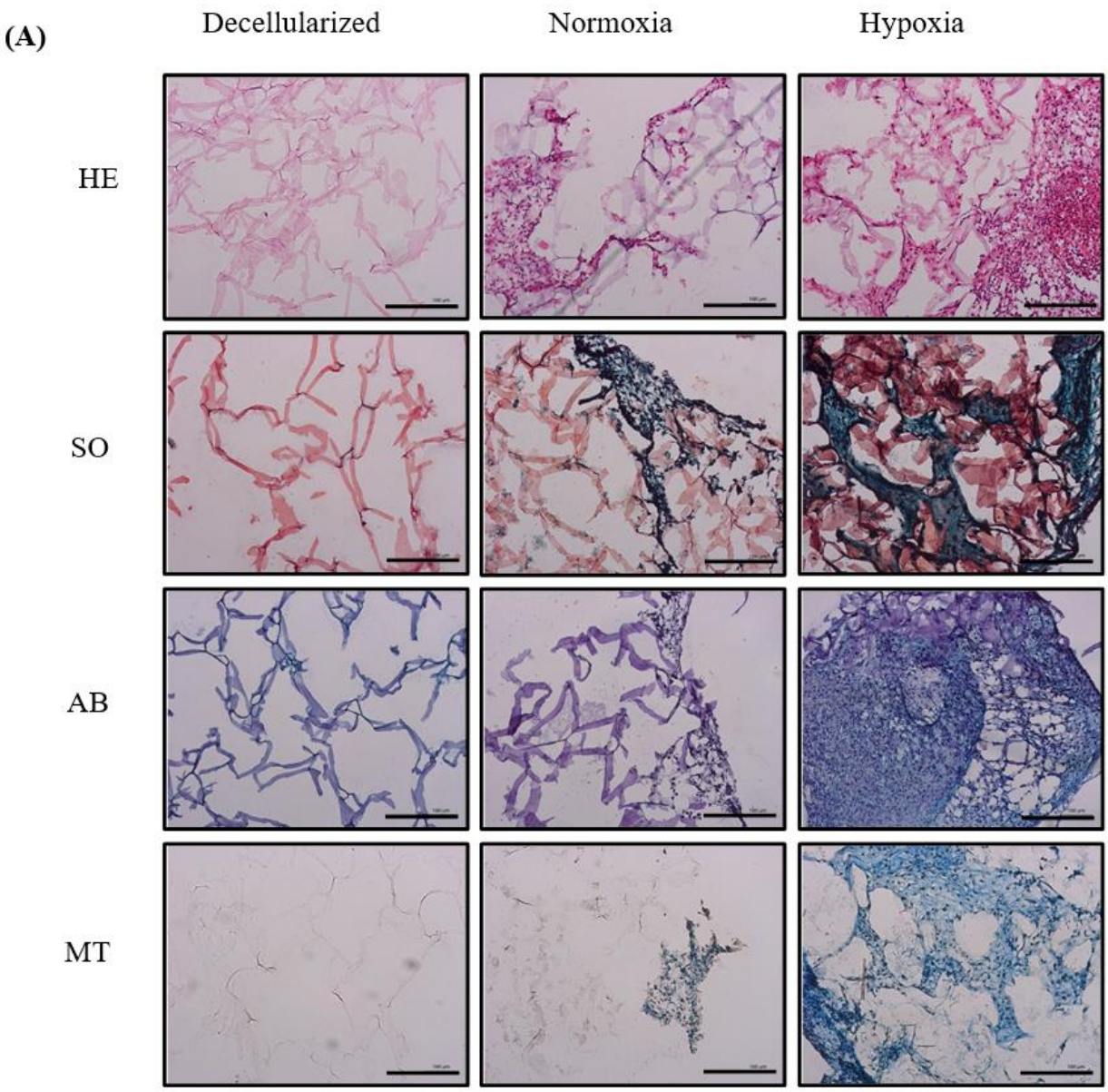
(A)
Decellularized
Normoxia
Hypoxia
HE
SO
AB
MT

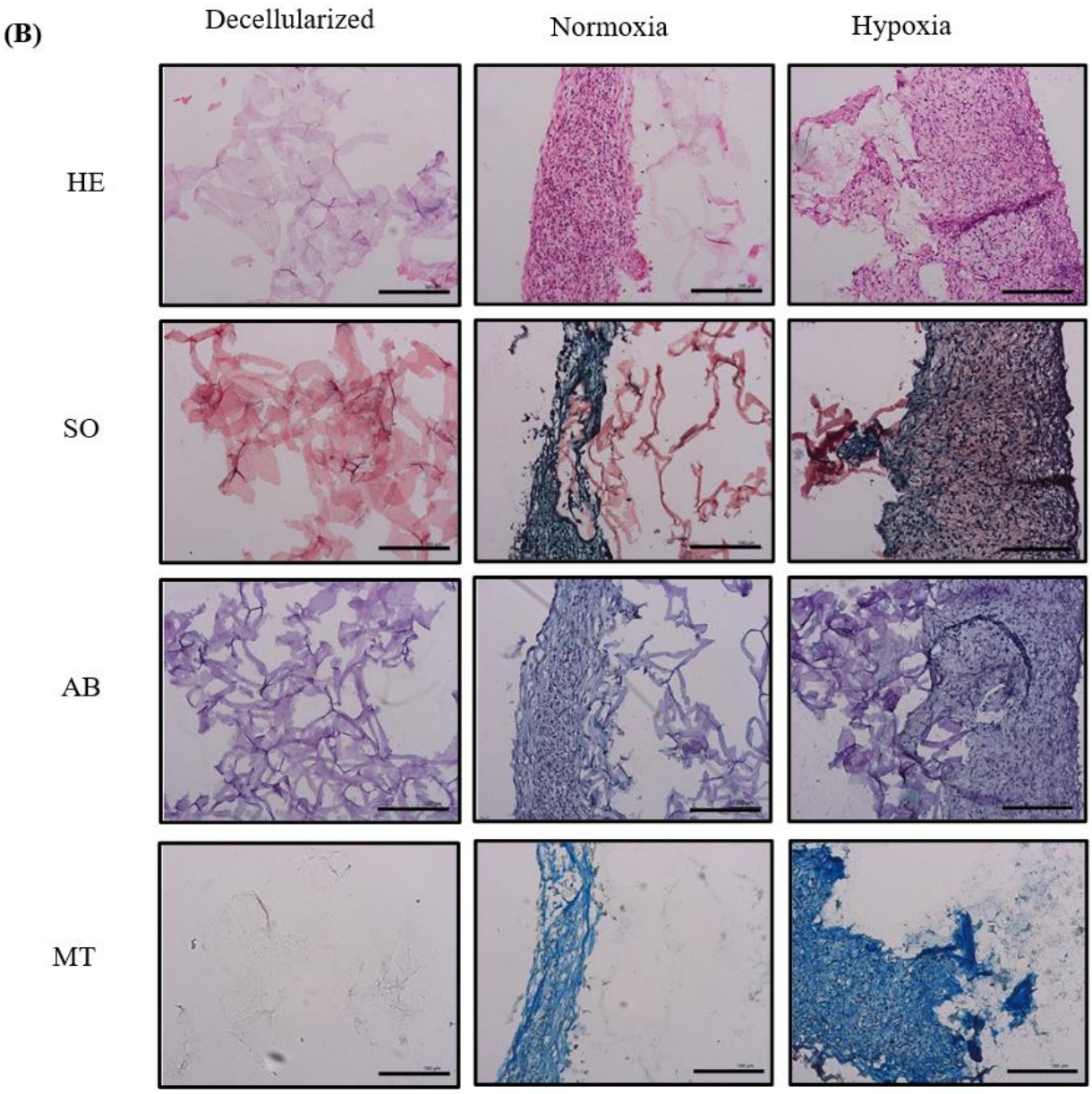
(B)
Decellularized
Normoxia
Hypoxia
HE
SO
AB
MT

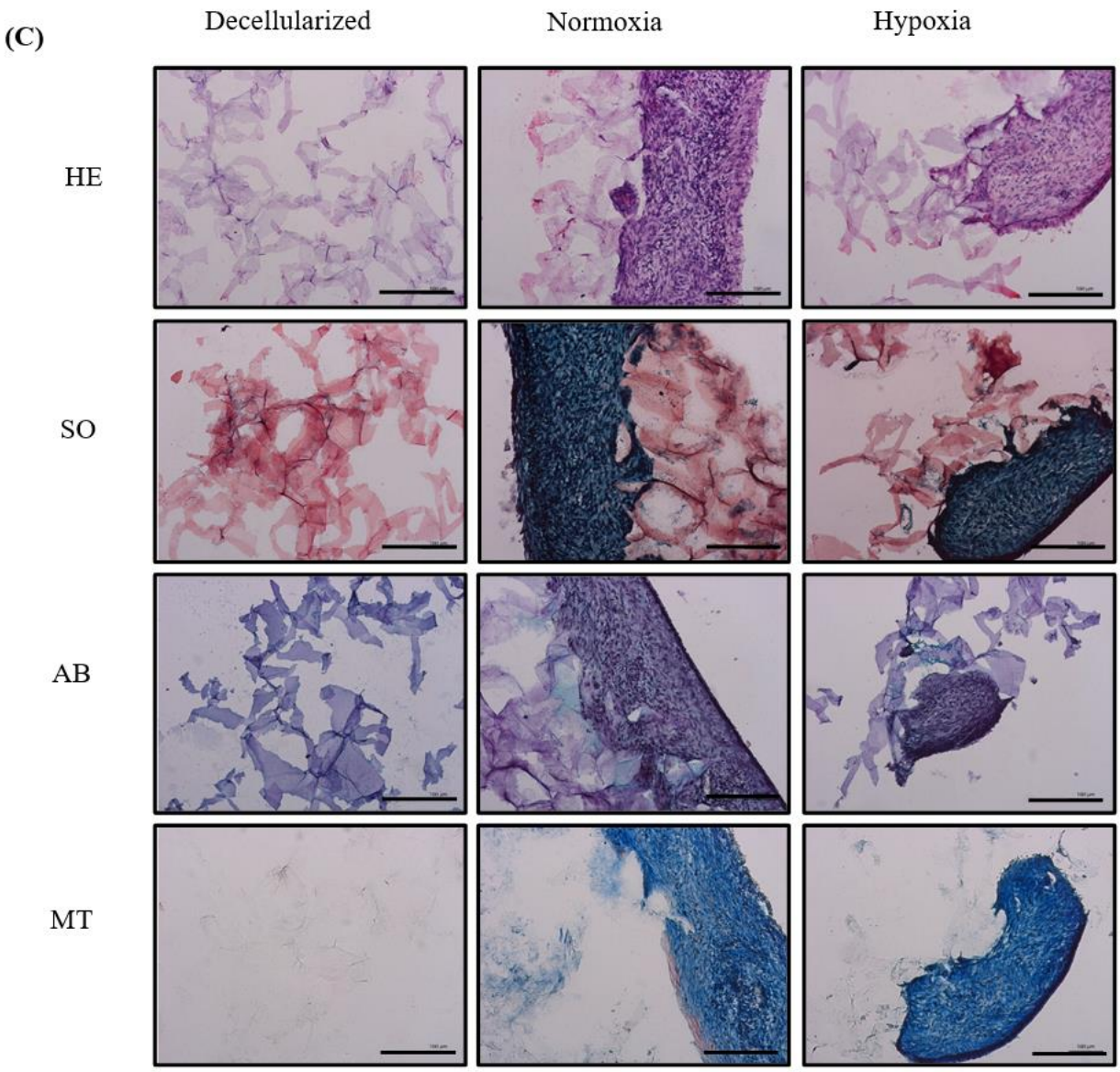
(C)
Decellularized
Normoxia
Hypoxia
HE
SO
AB
MT

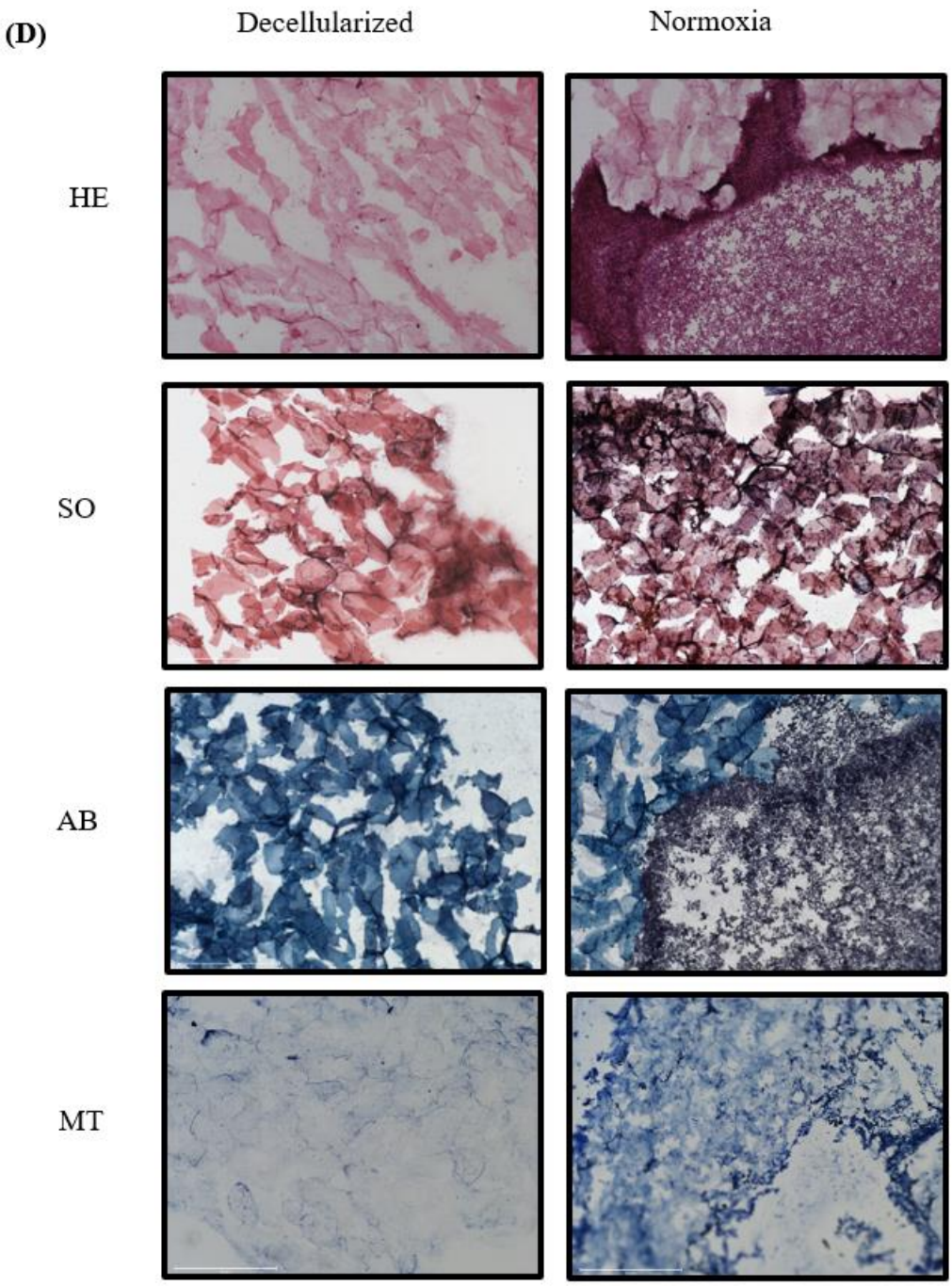

Fig.4 Histological staining of apple sections seeded with BMMSC (A), NsP (B), DPSC (C), AuP (D) under chondrogenic induction in normoxic and hypoxic culture condition for 14 days. HE: Hematoxylin-eosin, SO: Safranin O, AB: Alcian blue, MT: Masson's Trichrome. Scale bar: 500µm

Chondrogenesis differentiation of different progenitors within apple scaffolds

Cartilage tissue formation was also confirmed by high levels of mRNA expressed by chondrogenic differentiation. Cartilaginous genes such are COL2A1, ACAN, COMP, SOX9 and COL1, that is usually unexpected in healthy cartilage, were tested in different progenitors.

When BMMSC were used, chondrogenic genes were up regulated when seeded in chondrogenic medium and as expected, hypoxia enhanced these effects. Furthermore, COL1 was shown to increase in normoxic conditions, once again hypoxia attenuated its expression (Fig. 5-A).

Different expression profiles were observed for nasal perichondrocytes, where COL2A1, ELN and ACAN were induced by chondrogenic medium but not affected by hypoxia. On the other hand, hypoxia influenced SOX9 and COMP expression where these genes were significantly upregulated in low oxygen levels (Fig. 5-B). Surprisingly, COL1 expression was enhanced in presence and absence of oxygen. Furthermore, Dental stem cells analysis showed that the main cartilage markers were highly down regulated (COL2A1, ACAN, SOX9) while COL1 is over expressed (Fig. 5-C). Finally, we also analyzed expression profile in AuP. We have already shown that hypoxia is absolutely not beneficial for chondrogenesis of these cells, so culture of these cells was limited to normoxic chondrogenic conditions. Interestingly, all cartilage markers were enhanced showing a good propensity to chondrogenesis and notably, COL1 is simultaneously down-regulated (Fig. 5-D).

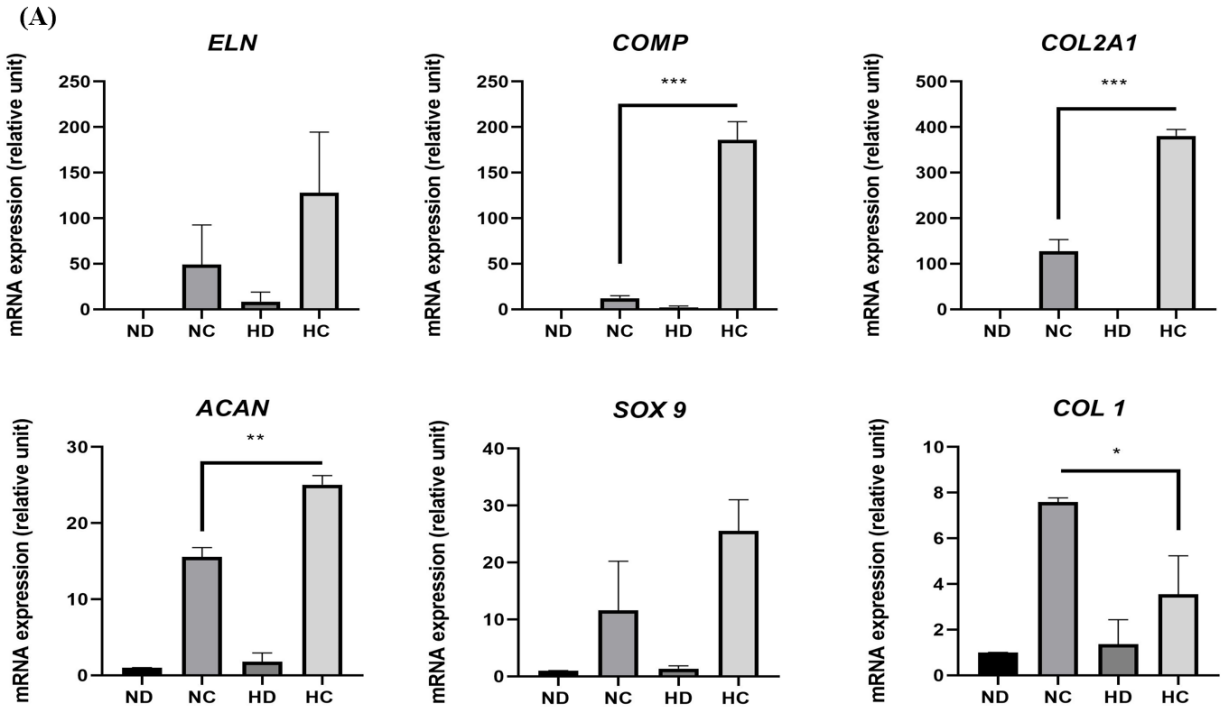

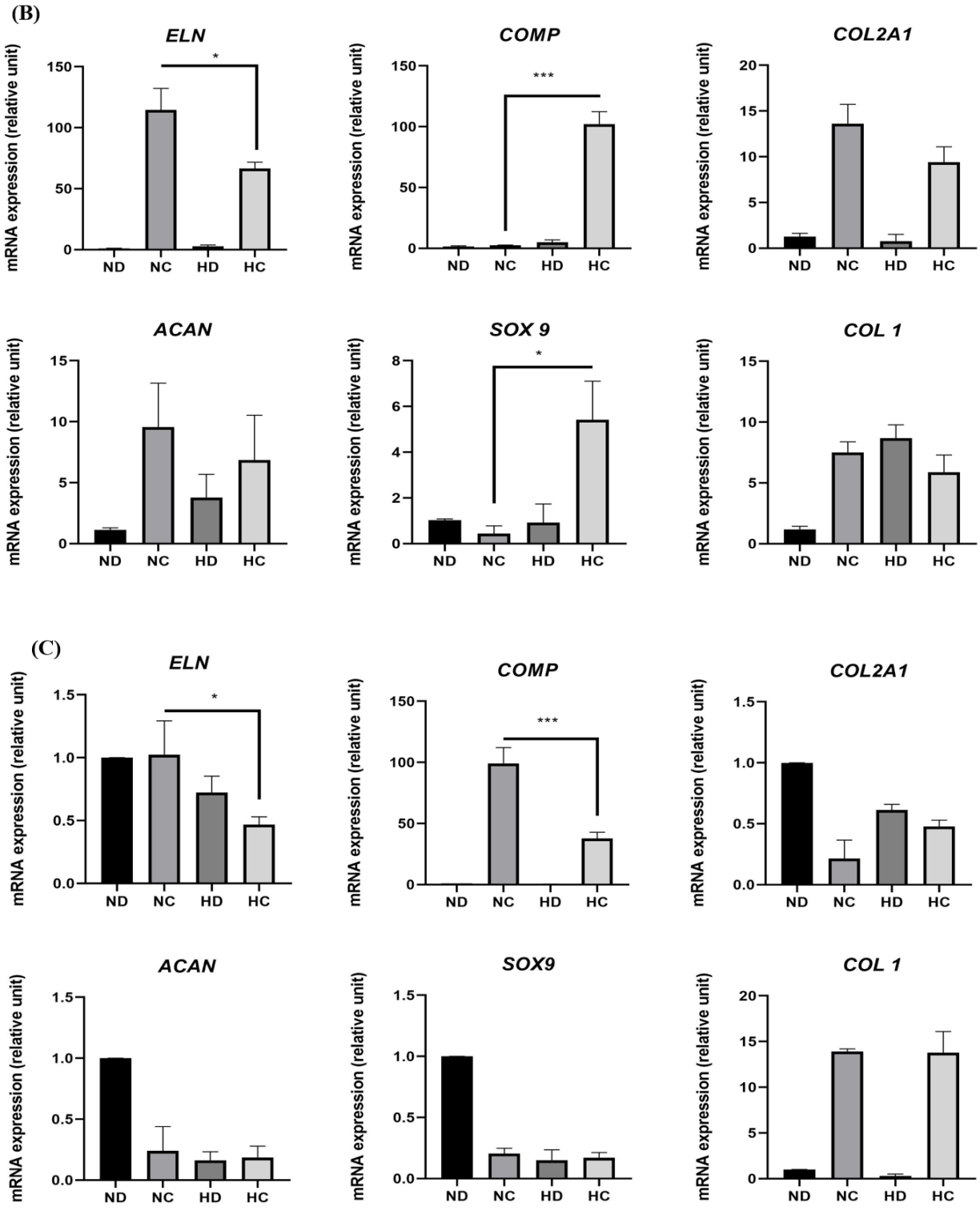
(B)
ELN
COMP
COL2A1
ACAN
SOX 9
COL 1
mRNA expression (relative unit)
ND
NC
HD
HC
(C)
ELN
COMP
COL2A1
ACAN
SOX9
COL 1
mRNA expression (relative unit)
ND
NC
HD
HC

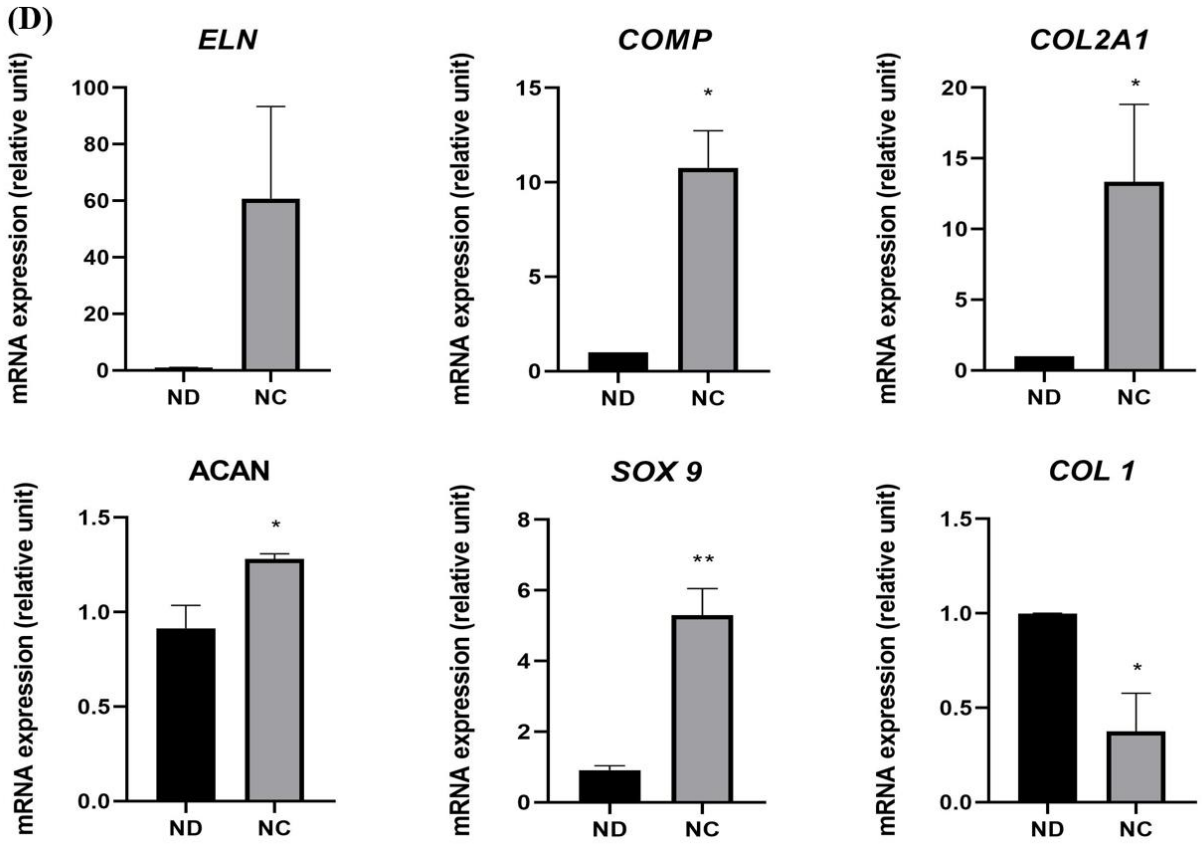

Fig. 5 Expression of cartilaginous markers in different cells BMMSC (**A**), NsP (**B**), DPSC (**C**) and AuP (**D**), expanded in different cell culture conditions after 14 days of culture. ND: normoxia and DMEM (control), NC: normoxic and chondrogenic medium, HD: hypoxia and DMEM (control), HC: hypoxia and chondrogenic medium (n=2, *p<0.05, **P<0.01, ***p<0.005).

Cellularized apple scaffolds surpass chondrogenic potential of alginate beads

It appears that decellularized apples are interesting scaffolds for chondrogenesis since they conduct different progenitors to differentiate properly towards cartilage-like tissues. Upon several scaffolds used in cartilage tissue engineering, we compared chondrogenic potential of decellualrized apples to alginate hydrogels that are recognized as robust models for chondrogenesis. For this purpose, we chose nasal perichondrocytes, seeded in apple scaffolds or encapsulated in alginate beads and cultured with chondrogenic medium for 3 weeks. The expression of chosen genes was normalized to that of alginate condition. Very interestingly, and despite the equal expression of ACAN in both cases, all other critical cartilage genes (COL2A1, SOX9, ELN) were highly significantly upregulated by 2-3 folds in decellularized apple scaffolds (Fig.6). Strikingly, decellularized apple disks provided healthy cartilage profile, due to the significant low expression of COL1 in these scaffolds, compared to alginate hydrogels. This suggest a higher potential of apple scaffolds to drive chondrogenesis.

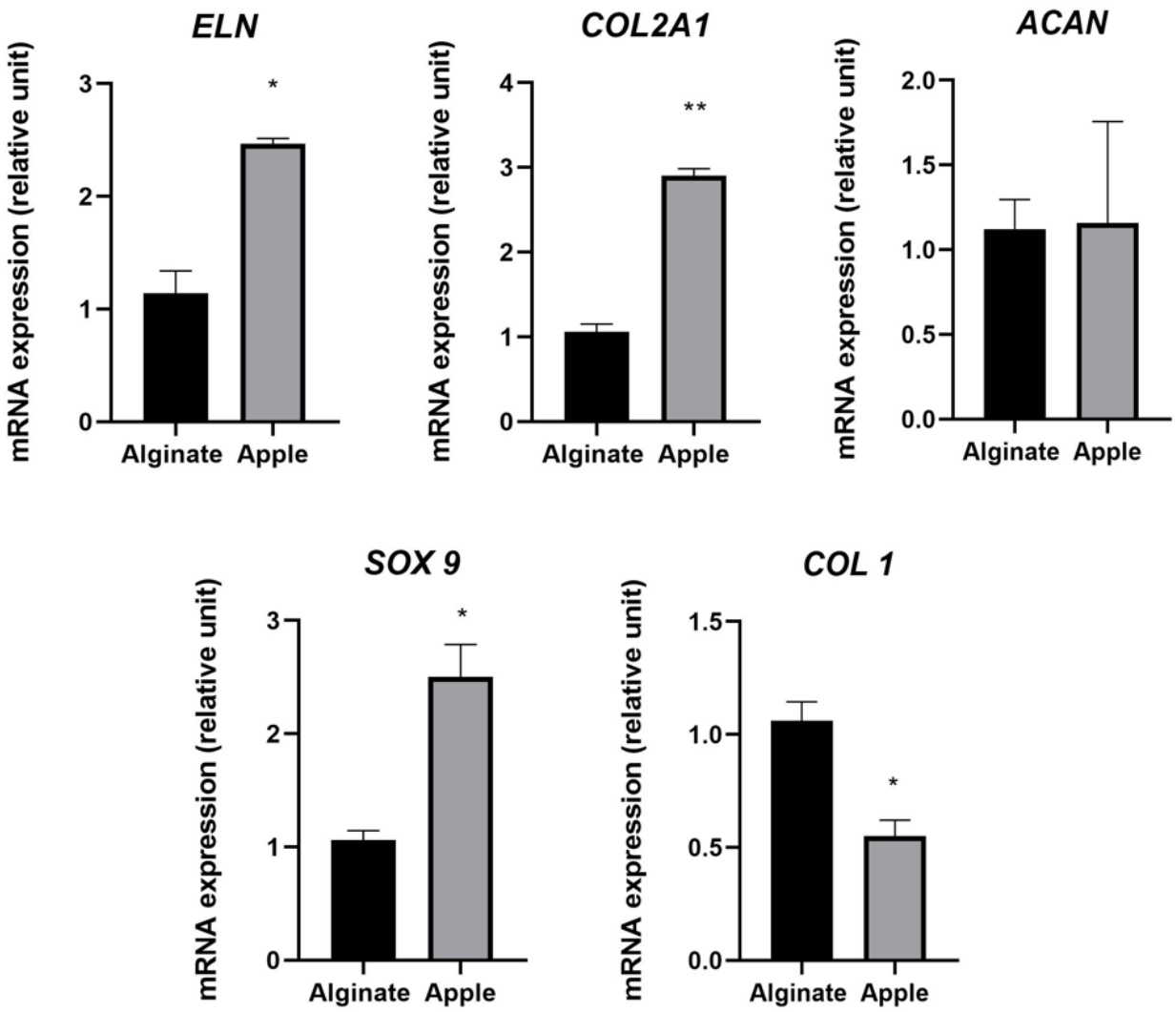

Fig. 6 Comparison of chondrogenesis in apple scaffolds and alginate microspheres. Chondrogenic markers expression in nasal perichondrocytes seeded into apple scaffolds compared to alginate beads after 14 days of culture in normoxic conditions. Their mRNA expression was calculated using 3 housekeeping genes and normalized to alginate conditions (n=2, *p<0.05, **P<0.01, ***p<0.005).

Discussion

Although significant advancement has been made in the field of tissue engineering, there are still no material that fully capture the complexities of the native tissue nor restore its ideal function. As a result, novel composite materials to mimic native tissue, remain a challenge to address.

Decellularized tissue are reliable alternatives for tissue engineering applications because of their 3D structure that offers the potential for cells to exhibit a tissue-like structure, mimicking native tissue and presenting better functionality in a more physiologically relevant manner. Inspite of the successful engineered constructs relying on decellularized animal tissue (Brouki Milan *et al.,* 2020; Ibsirlioglu *et al.,* 2020; Tajima *et al.,* 2020), plant decellularized tissues may overcome

availability of animal tissues with low cost and can eliminate ethical issue related to the use of animal sources (Y.-W. Cheng *et al*., 2020a; Walawalkar and Almelkar, 2020).

Cellulose scaffolds have been shown to design complex materials for different tissue engineering application. This latter was used to trigger the healing and regeneration of skin (Li *et al.,* 2015; Rees *et al.,* 2015), new bone tissue formation (Y. Huang *et al*., 2017; Park *et al.*, 2015; Sundberg *et al*., 2015), neural and neuronal therapeutic enhancement (Kandalam *et al.,* 2017) in addition to blood vessels (X.-Y. Wang *et al.*, 2015; Zhang *et al*., 2015).

Recently, it was shown that plant tissue could be investigated and used for tissue engineering applications. This new insight on biomaterial design, allowed the use of plant biomaterials to be adopted for tissue engineering application that would be optimized for specific biological and mechanical functions (Adamski *et al.,* 2018; Fontana *et al.,* 2017; Modulevsky *et al.,* 2016).

Several recent reports have used the apple as a natural scaffold for adipogenesis (Lee *et al.,* 2016), bone tissue and tendon (J. Lee *et al*., 2019; Negrini *et al*., 2020), but no study has investigated the chondrogenic potential derived by apple matrices. So our study was the first to explore apple matrices as scaffolds for auricular cartilage engineering.

Accordingly, in this study we aimed to explore a natural-derived scaffold for auricular cartilage engineering, and exploit the intrinsic 3D architecture by decellularizing an apple hypanthium tissue and investigating its chondrogenic potential when repopulated with different cell sources at specific culture conditions.

Before studying chondrogenic potential of apple-derived matrices, we first decellularized them to remove apple cells and remnants. Decellularization was effective and met the standard requirements for complete cell removal (Rana *et al.,* 2017).

These matrices were then seeded with different progenitor cells and were tested for their behavior and viability over time. Apple matrices showed high proliferation rate and viability after 21 days of culture with human nasal perichondrium, as well as rabbit auricular GFP transfected perichodrocytes after 2 weeks of culture. This illustrates that cells divided and increased in number after several weeks. These results demonstrate the fact that not only the cartilage progenitors colonized the matrix, but also deeply proliferated and integrated into the decellularized apple scaffold. This corroborate with what is mentioned in previous studies where proliferation maintained for 3 up to 10 weeks in apple scaffolds (Modulevsky *et al.,* 2014). Apple tissue was repopulated by NsP and two stem cells lineages from different origins. Histological and gene expression analyses showed colonization and chondrogeneis of the different cell sources in apple scaffolds. However, colonization was the greatest in the case of BMMSC where cells secreted more ECM than the case of nasal perichondrocytes, and to a lesser degree in dental stem cells, that presented more of an osteogenic profile. Hypoxia was favored for the case of bone marrow, as confirmed in our previous studies (Hammad *et al.,* to be submitted). This created a cartilage-like tissue as observed in macroscopic views of apple matrices after 2 weeks of chondrogenesis. Indicating that these matrices induced cell infiltration and differentiation and a normal functionality of cells as shown in bone and tendon regeneration (Negrini *et al.,* 2020).

Nasal perichondrocytes proliferated and expressed the majority of auricular cartilage genes better in hypoxic environment. This confirms the morphological results where a cartilage-like tissue was formed clearly in hypoxic conditions. This is contrary to what is reported in a recent study where nasal perichondrocytes did not have the capacity to form GAG and collagen II-engineered tissues (Asnaghi *et al.,* 2020). Our results further demonstrate the significant chondrogenic ability of nasal perichondrial cells in producing cartilage genes under chondrogenic induction, that could be enhanced in low oxygen levels. Alternatively, COL1 expression was enhanced upon chondrogenic induction in both normoxic and hypoxic conditions. The upregulation of COL1 could be explained by TGF-beta that stimulated and increased the expression of COL1 in these cells. This idea is reinforced by the work of Jung *et al.* that showed that COL1 expression increased upon TGF beta-1 that stimulated collagen gel and stimulated specific signaling pathways to transform nasal cells into cell-derived fibroblasts (Jung *et al.,* 2018).

On the other hand, dental stem cells weren't able to differentiate into cartilage when seeded on apple scaffolds. This was unexpected since we have previously reported in our work, the chondrogenic ability of these cells when encapsulated 3D alginate models (Hammad *et al.,* to be submitted). Even many research report had shown the multi-potent differentiation of DPSC into 3 lineages (Fernandes *et al.,* 2020; Lo Monaco *et al.,* 2020). The overexpression of COL1 in DPSC on apple scaffolds can be explained by the likely potential of these cells to be involved more in bone tissue repair, since their tendancy is shifted more towards osteogenic potential and thus, bone tissue formation. This is confirmed by various studies that investigated the osteogenic potential of these cells in bone tissue regeneration. Stem cells from human teeth have demonstrated the best cell source for bone regeneration and repair (Y.-C. Lee *et al.,* 2019; Nakajima *et al.,* 2018) with less surgical invasion. Taken altogether, future work should be done to investigate osteogenic differentiation of DPSC on our decellualrized apple scaffolds in order to better explain their mechanism of action, and maybe regenerate bone tissue.

We have already proven that AuP have shown a great potential in auricular cartilage regeneration *in vitro* (Hammad *et al.,* to be submitted) and *in vivo* (Hammad *et al.,* to be sumbitted), where it reconstructed auricular cartilaginous of rabbits, so it was also interesting to see if these cells produce the same results in apple hypanthium matrices. So we chose the normoxic condition since we have already proven in our previous work that hypoxia inhibits chondrogenic potential of perichondrial cells. Otto *et al.,* have already proven that progenitors originating from auricular cartilage demonstrated cartilage forming capacity, and a chondrogenic profile in 3D hydrogels. These results were confirmed by our study where colonized AuP in apple hypanthium scaffolds demonstrated a significant increase in ECM production as indicated by Real time RT-PCR and confirmed by histology.

One common problem of cartilage regenerative tissue is calcification and hypertrophy of newly formed cartilage (Jessop *et al.,* 2016). COLX is a typical marker of hypertrophy, that is highly expressed upon expanding primary chondrocytes through their differentiation process. We have verified that using AuP, COLX was downregulated and the phenotype of these cells was preserved. This correlates with results of Otto *et al.,* where they showed the low expression of COLX in cartilage tissue generated from auricular perichondrocytes (Otto *et al*., 2018).

Mimicking the environment of native cartilage, hydrogels are the gold standard models for chondrogenesis and cartilage regeneration. Thus, it was interesting to compare 3D alginate beads with apple matrices to highlight the importance of using apple scaffold as natural biomaterials. Referring to cartilage-gene expression, ECM production was significantly increased in apple matrices compared to alginate beads. Outstandingly, when comparing the expression of the undesired COL1 in cells seeded on different scaffolds, we can highlight the role of apple scaffolds in promoting and improving quality of elastic cartilage. Our results indicate that apple matrices outperform alginate chondrogenic potential by enhancing colonization and upregulating the cartilaginous expression in cells.

Despite of cartilage generation, the main limitation of the work is the lack of mechanical testing of scaffolds. Young's modulus should be applied to apple matrices to calculate elasticity of these constructs to deepen the facilitate their utilization in clinical trials.

Conclusion

Taken together, we have demonstrated the beneficial effects of apple matrices on proliferation and migration of different progenitors. Specifically, our findings showed that decellularized apple hypanthium tissue provides a natural and porous scaffold that drives and enhance the chondrogenic potential of different progenitors and stem cells *in vitro*. Further research should be done to investigate these scaffolds *in vivo*.

4-Cell-secreted matrices: Novel approaches for cell culture applications

In the last part of the thesis, we have described a novel approach for different cell culture applications. We wanted to investigate the potential of an ECM, naturally secreted and organized by cells, to influence cell growth and behavior through differentiation and dedifferentiation processes. Rabbit auricular perichondrocytes (AuP) were cultured under chondrogenic conditions until overconfluency to favor ECM deposition. The plates were then decellualrized and lyophilized. The cell-secreted matrix (CSM) obtained was characterized by protein contents and proteomics in order to be used later on as a substrate for multiple cell culture applications. Lyophilized CSM showed significant amount of ECM proteins as well as several cellular proteins remaining. Thereafter, we used CSM as supports for allogenic and xenogeneic cells. Further investigation was carried out by evaluating chondrogenic potential of human AuP on rabbit lyophilized CSM. Results showed a high significant increase of cartilaginous markers (COL2A1, ELN, COMP and SOX 9) and a down regulation of COL1 and COLX when cells were seeded lyophilized CSM compared to standard plastic plates.

Cartilage tissue engineering needs, sufficient amount of chondrocytes which unfortunately dedifferentiate upon their expansion. We showed that articular chondrocytes subcultured on lyophilized CSM not only have greater proliferation rate but also keep their phenotype after several passages with higher expression of chondrogenic genes (SOX9, ACAN, COL2A1 and ELN) and low hypertrophy (COLX) and dedifferentiation markers (COL1), compared to culturing on regular plastic plates. Very interestingly, the effect observable on proliferation rate is durable, even if the cells are transferred in regular plastic surfaces later on.

In summary, we have created a simple and affordable cell culture tool, which enhances proliferation, differentiation and preserves chondrocyte phenotype upon *in vitro* expansion and that can be applied to other tissues and screening purpose.

Cell-secreted matrices as cell supports: Novel approaches for cell culture applications

Mira Hammad[1,2], Benoît Bernay[3], Catherine Baugé[1,2], Karim Boumédiene[1,2]

[1]Normandy University, UNICAEN, EA 7451 BioConnecT, Caen, France, [2]Fédération Hospitalo Universitaire SURFACE, (Amiens, Caen, Rouen), France, [3]Proteogen Platform, Normandy University, UNICAEN, SFR ICORE, Caen, France.

Abstract

Tissue microenvironment contributes greatly in regulating cellular profile and function. Understanding cell-matrix interactions is crucial to predict cell fate. In the recent years, extracellular matrices (ECMs) have highly evolved to fill their role in guiding cells through interactions of their proteins and signals and then, offer a great potential and an alternative strategy for tissue reconstruction. Here, we hypothesized that cell-secreted matrices (CSM) produced by rabbit chondrogenic cells could influence cell behavior through different cell-ECM contacts.

CSM was obtained by culturing rabbit perichondrocytes until confluency under chondrogenic environment to highly secrete and deposit cartilaginous ECM. After decellularization and lyophilization, the remaining layer was used as a cell culture support for several assays and compared to traditional plastic plates, after characterization. Such CSM coated substrates were shown to be suitable for allogenic and xenogeneic use. In addition, they promote chondrogenic differentiation of human progenitor cells as well as preserve chondrocytes phenotype and reverse their dedifferentiation process. Finally, the coated CSM enhance the cell growth.

This study offers a novel *in vitro* approach and a suitable model for cell culture aiming at achieving phenotype preservation. The model is also very interesting for differentiation assays. As the phenotype is preserved and the differentiation promoted, the model is likely to be closer to physiological status than culturing in 2D plastic.

Introduction

Cartilage repair remains one of the major challenges in orthopedic surgery field, due to the its limited healing capacity. Different surgical treatment options such as matrix-assisted autologous chondrocytes transplantation (MACT) have been widely used for cartilaginous injuries (Andriolo *et al*., 2020). In recent years, these chondrocyte-based tissue engineering techniques have yielded successful outcomes. In order to perform such surgeries, autologous chondrocytes are needed in large quantities to restore larger cartilage defects. It has been shown that chondrocytes expansion have been highly correlated with dedifferentiation and phenotype loss, that is remodeled more into fibroblast-like structures (Charlier *et al*., 2019). Chondrocyte dedifferentiation results from the unsuccessful metabolic imbalance to achieve equilibrium between catabolic and anabolic of cytokines during extracellular synthesis, and thus this is characterized by a reduction of Collagen

II expression and a significant increase in Collagen I (Duan *et al.*, 2015). To minimize dedifferentiation problems during expansion of chondrocytes, many techniques have been employed. Different growth factors, on one hand, have been involved in cartilage repair and regeneration in the last decade. Fibroblast growth factors (FGF), insulin, bone-morphogenetic protein (BMP-2) and many others have clinically been implicated in multiple cartilage repair mechanisms. Nevertheless, these proteins have reported damage and detrimental side effect, since they lacked efficacy and induced aging of chondrocytes by promoting cartilage mineralization and fibrosis (Ahn *et al*., 2016; Brandl *et al*., 2010; Jeyakumar *et al.*, 2019; Speichert *et al*., 2019). Other groups have investigated co-culture of different cell sources with primary chondrocytes, this approach reduced dedifferentiation, but on the other hand increased donor-site morbidity due to the limited availability of these primary chondrocytes (Huang *et al*., 2018; Zhang *et al*., 2014). Furthermore, dedifferentiation process can be rescued by culturing chondrocytes on non-tissue cultured surfaces (Mao *et al*., 2018), yet it was time consuming. Reversal of dedifferentiation can also be obtained by cell transfer into a scaffold that brings a 3D environment, such as alginate (Bonaventure *et al*., 1994). However, these approaches include several manipulation of cells and are time consuming. So there is an urge to explore novel approaches that can yield functional chondrocytes in a short time.

The ECM is the pivotal and critical element that maintain tissue-specific structure and function. The intrinsic signals and biochemical composition of ECM, guide cell adhesion, migration and tissue formation processes (Zhang *et al.*, 2016). CSM maintains the multiplex network of ECM that direct maturation and differentiation of stem and progenitor cells. Published studies have shed light on the importance of decellularized CSM derived from several cell sources such as adipose-derived stem cells, bone marrow-derived mesenchymal stem cells and their potential to support growth of other tissues including bone (Harvestine *et al*., 2018; Hoch *et al.*, 2016), skin, and cartilage (Kim *et al*., 2012) and muscle tissue (DeQuach et al., 2010). A recent paper has reported the ECM derived from human primary chondrocytes harbors biological signals and cues that supported chondrocytes expansion and reduced dedifferentiation. However, they focused more on monitoring and reducing dedifferentiation and not on promoting expression of other ECM proteins (Mao *et al*., 2019).

In this study, we wanted to investigate the potential of an ECM, naturally secreted and organized by cells, to support cell growth and the way it influences cell behavior, by targeting differentiation and dedifferentiation processes. We used auricular perichondrocytes (AuP) as CSM and after cell removal, the remaining matrix served as a substrate for multiple applications with other cells.

Before use, the substrates were shown to support lyophilization for a versatile use and storage. After characterization, we then assayed expansion and chondrogenic differentiation of progenitors as well as dedifferentiation of chondrocytes. In addition to the fact that these substrates can host allogeneic and xenogeneic cells, we provide evidence for a new plate substrate preparation that can serve for multiple applications in cell culture.

Materials and methods

Preparation of cell-secreted matrices from rabbit auricular perichondrocytes

Rabbit ears were obtained from a 3-week-old rabbit. Animals procedures were approved by animal care ethical committee. Perichondrium tissue was harvested and cultured as a primary outgrowth for 1 month. Auricular perichodrocytes (AuP) were extracted and expanded *in vitro* untill reaching passage 3. Cells were then freezed at -150°C. In a 6-well plates, AuP were seeded at a density of 0.6x10^6 per well and cultured for 2 weeks in chondrogenic medium until reaching confluency and forming a cellular sheet. This sheet was then decellularized within the plate by adding 1% SDS and agitated for 24 hours. Distilled water was added after 24 hours to rinse and remove traces of SDS for 30min. This step was renewed twice and kept overnight on a shaking plate. The next day, the acellular sheet was lyophilized in a freeze-dryer (Leica CHRIST beta-2) for 1 hour at 1 mbar. Plates were then stored at room temperature for further use.

Isolation and cultivation of human cell sources

Human articular chondrocytes were extracted from femoral heads obtained from patients (average age: 55 years). All patients signed the consent agreement approved by the local ethics committee. Cartilage samples were sectioned into small slices, where chondrocytes were isolated by digestion with 2mg/ml protease type XIV (Sigma-Adrich) for 25 min and afterwards kept overnight at 37 °C with 1mg/ml of collagenase type I (Invitrogen). The cell suspension was filtered through a 70µm-mesh nylon membrane, centrifuged, counted and seeded on 6-well plates at a density of 4x10^4 cells/cm^2, and cultured in Dulbecco's modified eagle medium (DMEM) supplemented with 10% fetal calf serum (FCS), 100IU/ml of streptomycin, and 0.25µg/ml of fungizone at 5% CO2. Medium was changed twice a week.

AuP were obtained from fresh-human auricular cartilage biopsies after 12-year-old children undergone rhinoplasty. Perichondrium was separated from cartilage by dissection and sliced into small pieces. Cells were collected by sequential enzymatic digestion using pronase for 45-60 min at 37°C and collagenase II overnight at 37°C. The next day cells were seeded in T75 flasks and amplified till reaching passage 3, which then freezed for further use.

Stably GFP expressing cells

Stably GFP transfected rabbit perichondrocytes were obtained by transfection pEGFP-N1 plasmid and G418 antibiotic selection. Stably transfected human cells were generously given by Pr S. Allouche (CHU, Caen).

Fluorescence and normal microscopy

Plates with cultured cells were fixed in 10% NBF at 4°C for 20 min, and washed twice with PBS, and stained with 4,6-diamidino-2-phenylindole (DAPI, sigma) to identify nuclear components. The stained samples, as well as microphotographs of cells that also taken at different passages were examined using a fluorescence microscope (EVOS cell imaging systems, Thermofisher scientific).

Immunohistochemistry

Plates were rinsed in PBS and incubated overnight at 4°C with collagen II (1:100, ab 34712 abcam, Cambridge, UK) primary antibodies. A negative control was performed by replacing primary antibody solutions with PBS. The next day, slides were rinsed five times in PBS to remove traces of primary antibody, and a secondary antibody secondary antibody (Alexa Fluorophore 594 conjugated anti-rabbit) diluted (1:800) was used to incubate slides for 1.5 hour. Rinsing with PBS was done to remove excessive secondary antibody. Plates were then rinsed three time with PBS before microscopic observation by EVOS cell imaging system microscope, Thermo fisher scientific).

Histological staining

Masson's Trichrome staining was composed of several steps: samples were first incubated for 3 min in Weigert's iron hematoxylin solution, then rinsed with distilled water and incubated in Ponceau Fuchsine solution for 5 min, quickly rinsed with 1% acetic. Phosphomolybdic acid was next added for 5 min, and traces were removed by rinsing with 1% acetic acid. The last step was incubating samples with aniline blue for 1 min, rinsing afterwards with 1% acetic acid. Plates were finaly mounted for analyses. Safranin O staining was performed using 10 min incubation of Weigert's iron hematoxylin, followed by 5 min incubation in Fast green solution (0.05%), 1% acetic acid rising before the addition of Safranin O solution (0.1%) for 5 min. For Hematoxylin Eosin staining, samples were stained with Harris, modified Hematoxylin solution for 2min, rinsed with distilled water and incubated with 1% Eosin for 1min. Plates were mounted and were ready for analyses.

Protein extraction

Protein samples were extracted using RIPA buffer followed by protease inhibitors: 1 mM phenylmethylsulfonyl fluoride, 1 µg/ml of pepstatin A, 1 µg/ml of aprotinin, and 1 µg/ml of leupeptin. After 30 minutes on ice, the supernatants were collected by centrifugation, and the amount of total cellular protein was determined according to the Bradford colorimetric procedure (Bio-Rad). Fastin elastin kit to detect and quantify elastin, Sircol collagen kit to quantify total collagen in samples and Blyscan kit for glycosaminoglycan content. All these kits were purchased from Biocolor (life science assays, UK).

Proteomics

5 µg of each protein extract (extracted by RIPA buffer in absence of any protease inhibitors) were prepared using a modified Gel-aided sample preparation protocol described by (Fischer and Kessler, 2015). Samples were digested with trypsin/Lys-C overnight at 37°C. For nano-LC fragmentation, protein or peptide samples were first desalted and concentrated onto a µC18 Omix (Agilent) before analysis.

The chromatography step was performed on a NanoElute (Bruker Daltonics) ultra-high-pressure nano flow chromatography system. Approximatively 200 ng of each peptide sample were concentrated onto a C18 pepmap 100 (5mm x 300µm i.d.) precolumn (Thermo Scientific) and separated at 50°C onto a reversed phase Reprosil column (25cm x 75µm i.d.) packed with 1.6µm C18 coated porous silica beads (Ionopticks). Mobile phases consisted of 0.1% formic acid, 99.9% water (v/v) and 0.1% formic acid in 99.9% ACN (v/v). The nanoflow rate was set at 400 nl/min,

and the gradient profile was as follows: from 2 to 15% B within 60 min, followed by an increase to 25% B within 30 min and further to 37% within 10 min, followed by a washing step at 95% B and reequilibration.

Mass spectroscopy (MS) experiments were carried out on an TIMS-TOF pro mass spectrometer (Bruker Daltonics) with a modified nano electrospray ion source (CaptiveSpray, Bruker Daltonics). The system was calibrated each week and mass precision was better than 1 ppm. A 1400 spray voltage with a capillary temperature of 180°C was typically employed for ionizing. MS spectra were acquired in the positive mode in the mass range from 100 to 1700 m/z. In the experiments described here, the mass spectrometer was operated in PASEF mode with exclusion of single charged peptides. A number of 10 PASEF MS/MS scans was performed during 1.25 seconds from charge range 2-5.

Before post-process, the samples are analysed using Preview software (ProteinMetrics) in order to estimate the quality of the tryptic digestion and predict the post-translational modifications present. The result, below, is used for the "bank research / identification" part. The fragmentation pattern was used to determine the sequence of the peptide. Database searching was performed using the Peaks X+ software. A UniProt *Oryctolagus cuniculus* database (December 2020) was used. The variable modifications allowed were as follows: K-acetylation, methionine oxidation, Deamidation (NQ) and Methylation (KR). In addition, C-Propionoamide was set as fix modification. "Trypsin" was selected as Specific. Mass accuracy was set to 30 ppm and 0.05 Da for MS and MS/MS mode, respectively. Data were filtering according to a FDR of 0.1%, 2 unique peptides and the elimination of protein redundancy on the basis of proteins being evidenced by the same set or a subset of peptides.

RNA extraction and quantitative reverse-transcriptase polymerase chain reaction

Total RNA was purified according to the RNeasy® Mini Kit protocol (Qiagen), based on the binding of nucleic acids to a column of silica. Quantity and purity was determined by 260/280 absorbance. First strand cDNA was synthesized from a single strand of RNA by means of reverse transcriptase. RT was carried out using a mixture composed of 1 µg of RNA, 2.5 µM of oligodT, 0.5 mM of dNTP, 1X First Strand Buffer and 10 U / µL of Moloney Murine Leukemia Virus reverse transcriptase (M-MLV-RT, Invitrogen) for each RNA condition. Real time RT PCR primers are listed in the supplementary table below. Results were compared to normalized to three housekeeping genes (GAPDH, RPL13, β2MG).

Gene	Forward primer	Reverse primer
ELN	CCAGGTGTAGGTGGAGCTTT	CCATAGCCATAGGGCAGTTT
SOX 9	CCCATGTGGAAGGCAGATG	TTCTGAGAGGCACAGGTGACA
COL1	CACCAATCACCTGCGTACAGAAC	CAGATCACGTCATCGCACAAC
ACAN	GTGCCTATCAGGACAAGGTCT	GATGCCTTTCACCACGACTTC
COL2A1	CCAGATGACCTTCCTACGCC	TTCAGGGCAGTGTACGTGAAC
COLX	CCTGGTATGAATGGACA	CCCTGAGGGCCTGGAAGA
GAPDH	ATGGGGAAGGTGAAGGTCG	TAAAAGCAGCCCTGGTGACC
RPL13	GTTCGGTACCACACGAAGGT	CTGGGGAAGAGGATGAGTTTG
β 2-MG	GAGGCTATCCAGCGTACTCCA	CGGCAGGCATACTCATCTTTT

Cell viability Assay

The colorimetric WST-1 kit was purchased from Roche Diagnostics (Germany). The amount of formazan dye detected is directly related to the metabolic activity of cells. Chondrocytes were initially seeded on 6-well plates. After several days of seeding, medium was removed and a new fresh medium was added with WST1 reagent for 3 hours. Absorbance was measured at 450 and 650 nm. Results are reported as relative WST-1 activity, where 100% corresponds to the absorbance measured in plastic plates (control).

Statistical analyses

Data were presented as mean ± standard deviation. Differences between groups was observed using two-way analysis of variance with Tukeys's multiple comparison tests using Prism software. Other sample groups were subjected to unpaired t-test. Values less than 0.05 were indicated as significant difference between the groups.

Results

Preparation and Characterization of lyophilized cell-secreted matrices

Cell-secreted matrices (CSM) were obtained by culturing rabbit auricular perichondrocytes over confluency. Cell layer was then decellularized by SDS detergent aiming to preserve the remaining ECM. DAPI staining shows a good achievement of this step before and after the process (Fig. 1-A). The plates were then lyophilized, and showed a whitish CSM coating (Fig. 1-B).

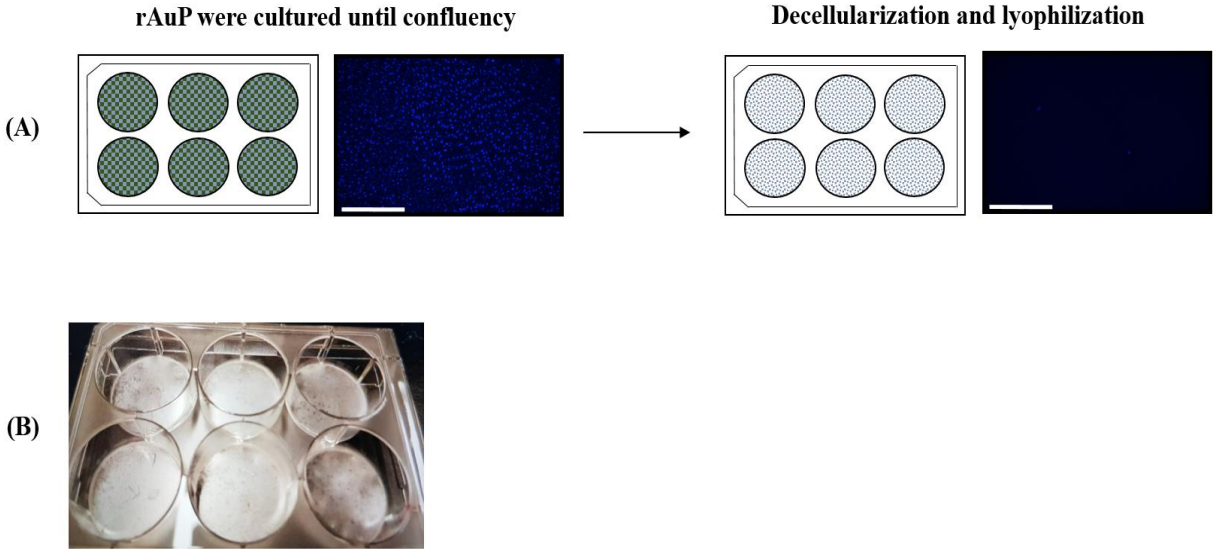

Fig. 1: **Preparation of cell secreted matrices (CSM)**. (**A**): DAPI staining before and after decellularization and lyophilization. (**B**): Macroscopic aspect of lyophilized CSM showing a white coating.

We first characterized the CSM coated plates by several methods. Qualitative analyses shown by cytology staining that confirms the efficacy of the decellularization process, where no nuclei are stained in black when performing different staining patterns (Fig. 2-A-a). Collagen fibers are highly preserved since the dark blue color persisted after decellularization (Fig. 2-A-b) and lyophilization (Fig. 2-A-c). Sulfated glycosaminoglycans (GAG) are detected by Safranin O staining that stained GAG in orange-red color (Fig. 2-A-d). Here, GAG were less conserved than collagen after decellularization and lyophilization processes (Fig. 2-A-e, f). Furthermore, Hematoxylin stained nuclei in dark purple and Eosin detected ECM in pink (Fig. 2-A-g). Extracellular proteins were conserved after decellularization where it shows a good pink color that faded a little after lyophilization (Fig. 2-A-h, i). Elastin fibers were finally low expressed to other ECM proteins since Orcein staining showed a purple color with some aggregates (Fig. 2-A-j). This color slowly faded after decellualrization and lyophilization (Fig. 2-A-k, l).

To further characterize CSM, we analyzed the remaining proteins in the plates after lyophilization in comparison with both native and decellularized cell sheets. Upon observing total proteins, native cell sheet of a 9.6 cm^2 plate contains an average of 14µg of proteins. This amount was reduced by half after decellularization and reached 5µg after freeze-drying process (Fig. 2-B). Different protein types presented in ECM such as ELN, collagen and GAG, were also detected by specific kits. These proteins followed the same reduction rate from native to lyophilized, except for total collagen amount that was reduced to a lesser degree. Furthermore, we wanted to investigate both the protein content in the lyophilized layers and the reproducibility of their preparation. To do so, proteomic analyses were carried out where we compared six protein extracts from lyophilized layers prepared at different dates. Mass spectroscopy analysis and data filtering allowed us to obtain different sets of data. We sorted them by the most abundant proteins (Table 1) and those that are present in all samples (Table 2).

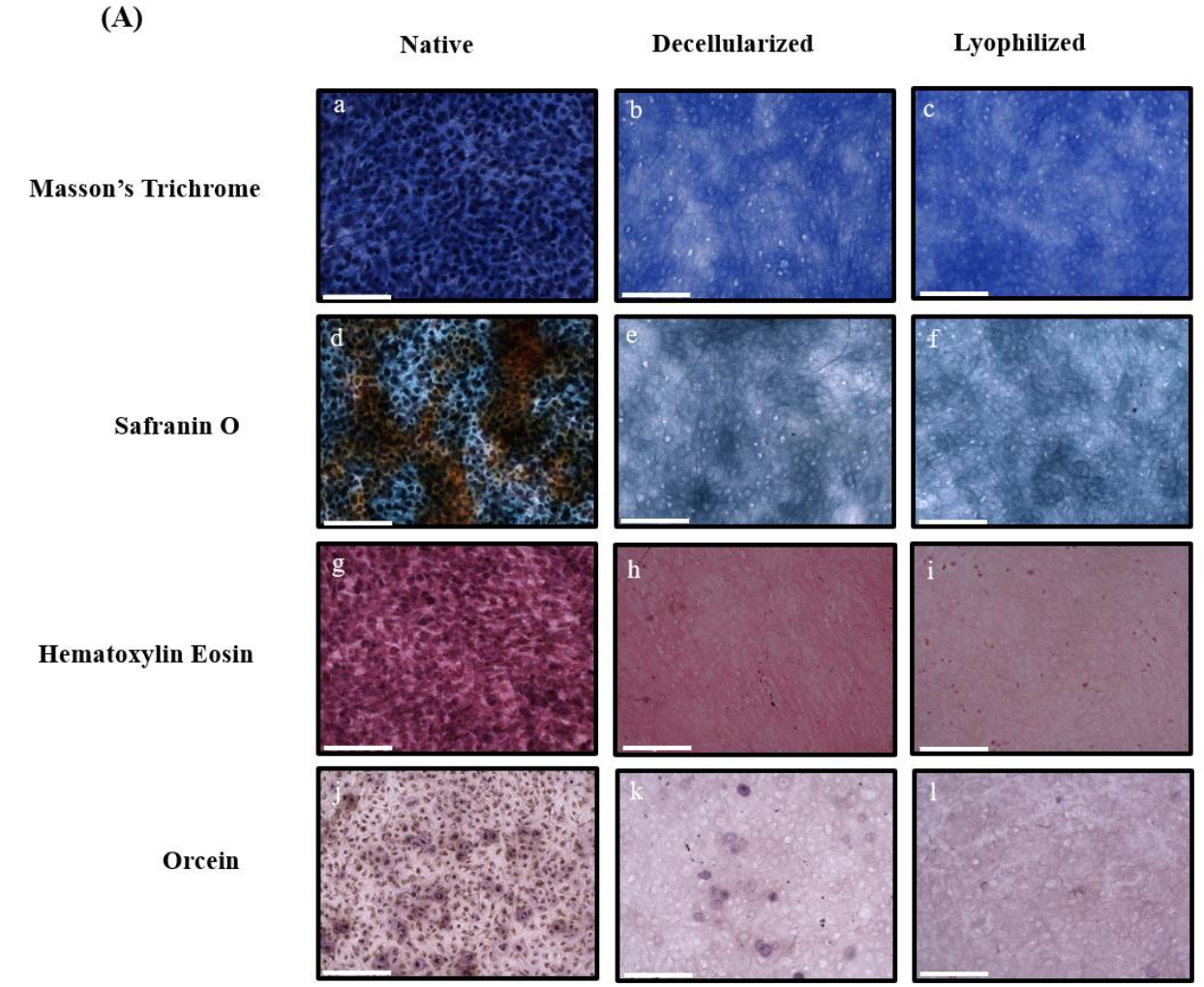
(A)
Native
Decellularized
Lyophilized
Masson's Trichrome
Safranin O
Hematoxylin Eosin
Orcein
a
b
c
d
e
f
g
h
i
j
k
l

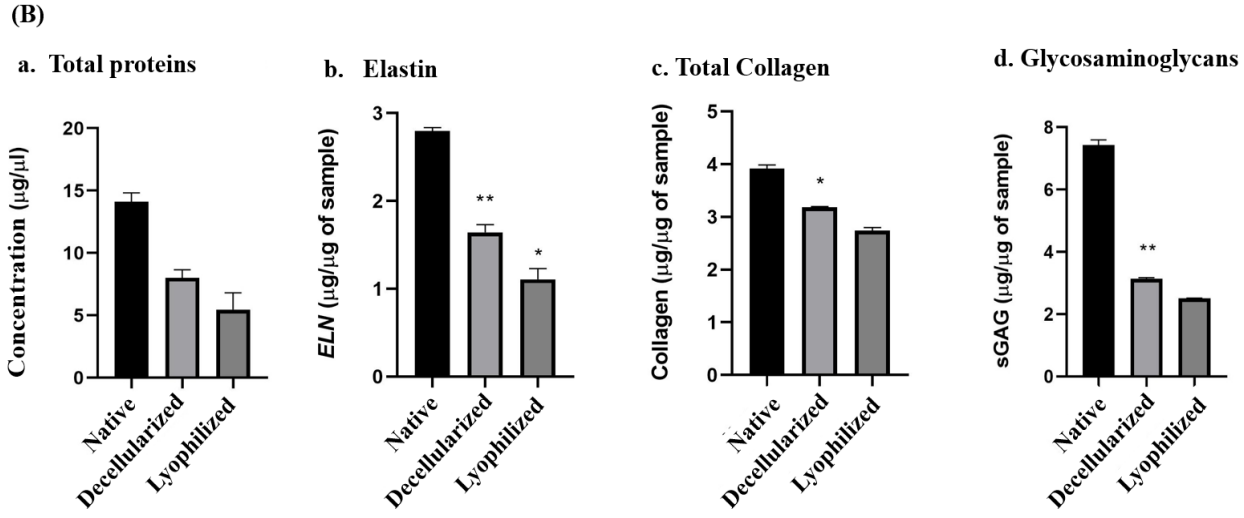
(B)
a. Total proteins
Concentration (µg/µl)
20
15
10
5
0
Native
Decellularized
Lyophilized
b. Elastin
ELN (µg/µg of sample)
3
2
1
0
**
*
Native
Decellularized
Lyophilized
c. Total Collagen
Collagen (µg/µg of sample)
5
4
3
2
1
0
*
Native
Decellularized
Lyophilized
d. Glycosaminoglycans
sGAG (µg/µg of sample)
8
6
4
2
0
**
Native
Decellularized
Lyophilized

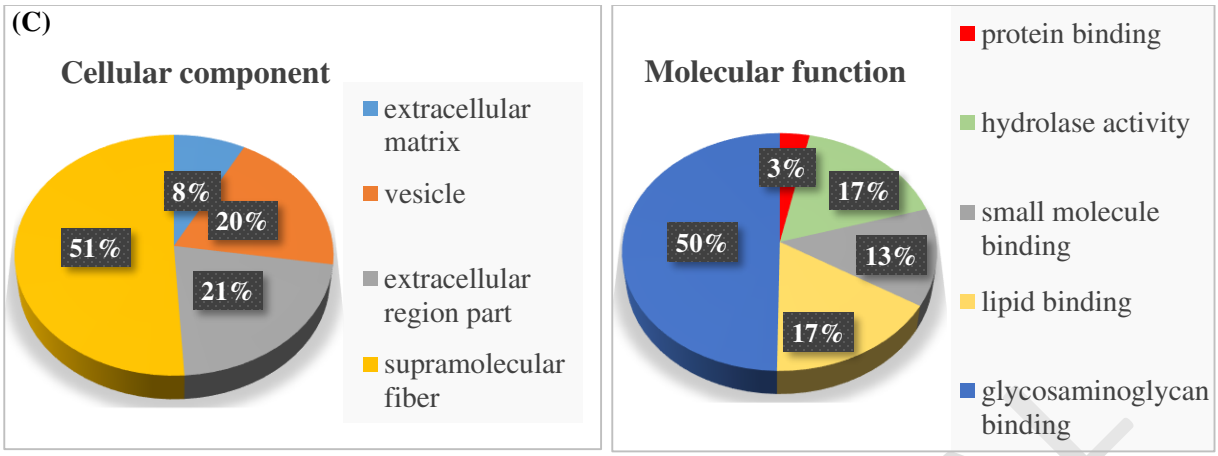

Fig. 2: Characterization of decellularized and lyophilized CSM. (**A**): Histological staining of collagen fibers using Masson's Trichrome (a, b, c), GAG by safranin O staining (d, e, f) and extracellular proteins using Hematoxylin Eosin (g, h, i) scale bar: 200µm. (**B**): Protein concentration was determined by Bradford Assay (a), ELN content by fastin assay (b), total collagen was measured by sircol assay (c) and sulfated GAG by blyscan assay (d). (**C**): Pie chart representing the subcellular localization of the common proteins and their molecular function in CSM.

Table 4: The list of proteins in the lyophilized cell-secreted matrices, sorted by abundancy after normalization to their respective molecular weight (MW).

Description	Accession	Total Area/MW	Description	Accession	Total Area/MW
Histone H4	A0A5F9CMH5	3,95E+03	10 kDa heat shock protein mitochondrial	A0A5F9C1X1	2,52E+01
Histone H2A	A0A5F9D8N0	3,48E+03	Keratin 77	G1SKE3	1,42E+02
Galectin	G1TPZ1	2,08E+03	60S ribosomal protein L31	G1SHG0	3,13E+01
Protein S100	G1SVK5	1,92E+03	Cytokeratin-1	G1U9I8	1,29E+02
Vimentin	G1SWS9	6,59E+03	Helix-destabilizing protein	G1TUI9	5,86E+01
Calpactin I light chain	G1SNE8	1,69E+03	GST class-pi	G1U9R0	8,22E+01
Histone H2B	G1U155	1,02E+03	Actin-depolymerizing factor	G1TMV1	3,06E+01
Hemoglobin subunit alpha-1/2	HBA_RABIT	9,22E+02	Uncharacterized protein	G1TJW3	6,73E+01
Actin cytoplasmic 1	ACTB_RABIT	2,23E+03	Cellular retinoic acid-binding protein 1	G1SDA2	2,14E+01
Protein S100-A6	S10A6_RABIT	4,67E+02	Annexin	G1TED6	4,85E+01
Profilin	G1SER8	5,14E+02	Fibrillin 1	G1SKM2	4,13E+02

Thioredoxin	A0A5F9DIE8	4,78E+02	Collagen-binding protein	G1TV79	2,74E+01
HtrA serine peptidase 1	G1T5H0	7,68E+02	Keratin 2	G1SUH8	6,41E+01
Macrophage migration inhibitory factor	G1U1Q8	2,11E+02	Transforming growth factor-beta-induced protein ig-h3	A0A5F9CTN2	6,99E+01
Biglycan	U3KML1	6,91E+02	Heterogeneous nuclear ribonucleoproteins A2/B1	A0A5F9C6T8	2,60E+01
Annexin	A0A5F9DEV8	6,26E+02	Nucleoside diphosphate kinase	U3KNZ4	2,03E+01
Coiled-coil domain containing 80	G1U4C2	1,35E+03	Collagen type V alpha 2 chain	G1T8L2	1,13E+02
Calmodulin	CALM_RABIT	1,91E+02	Synaptobrevin-2	A0A5F9D3D3	1,48E+01
Elongation factor 1-alpha 1	EF1A1_RABIT	4,91E+02	Collagen alpha-1(XII) chain	A0A5F9C2X4	2,19E+02
40S ribosomal protein S28	G1TIB4	7,47E+01	Phosphoglycerate kinase	G1T7Z6	2,74E+01
2-phospho-D-glycerate hydro-lyase	G1SYJ4	4,51E+02	40S_SA_C domain-containing protein	A0A5F9C7B1	1,60E+01
Hemoglobin subunit gamma	HBG_RABIT	1,38E+02	Protein disulfide-isomerase	PDIA1_RABIT	2,71E+01
Proline and arginine rich end leucine rich repeat protein	G1SXR1	3,68E+02	40S ribosomal protein S19	G1TN62	7,53E+00
Keratin 5	A0A5F9C3E1	4,22E+02	Nucleoplasmin domain-containing protein	A0A5F9DPE8	1,04E+01
Annexin A1	ANXA1_RABIT	1,96E+02	Lamin A/C	A0A5F9DRS0	2,46E+01
Keratin 10	G1T1V0	2,77E+02	L-lactate dehydrogenase	G1TAJ3	1,45E+01
Albumin	ALBU_RABIT	3,10E+02	Lysosomal associated membrane protein 1	A0A5F9CY27	1,29E+01
Decorin	PGS2_RABIT	1,63E+02	Calreticulin	CALR_RABIT	1,40E+01
S100 calcium binding protein A13	G1SI83	4,36E+01	ATP synthase subunit beta	G1SQA8	1,36E+01

Uncharacterized protein	G1TKL2	8,40E+01	Galectin-3	LEG3_RABIT	5,55E+00
Transgelin	G1T2C4	7,01E+01	78 kDa glucose-regulated protein	G1U7L4	9,46E+00
Elastin microfibril interfacer 1	G1SRW4	2,86E+02	Collagen type XIV alpha 1 chain	A0A5F9DVP3	2,25E+01
G1T0Z2	A0A5F9CJW0	6,42E+02	Tenascin C	A0A5F9CFG3	2,19E+01
Tubulin beta chain	G1SH05	1,23E+02	Uncharacterized protein	A0A5F9CTM9	6,82E+00

Table 5: The list of common proteins expressed in the six samples tested.

Accession	Description	Score
G1SKM2	Fibrillin 1	238,45
G1SWS9	Vimentin	235,53
A0A5F9CJW0	Fibronectin	190,5
G1U9I8	Cytokeratin-1	180,28
G1T1V0	Keratin 10	179,87
A0A5F9D471	2-phospho-D-glycerate hydro-lyase	179,45
A0A5F9DEV8	Annexin	176,35
G1U4C2	Coiled-coil domain containing 80	173,26
G1SH05	Tubulin beta chain	164,63
G1SRW4	Elastin microfibril interfacer 1	159,09
P68105	Elongation factor 1-alpha 1	157,59
A0A5F9CJB7	Collagen alpha-1(XII) chain	157,03
A0A5F9DFJ9	Glyceraldehyde-3-phosphate dehydrogenase	150,65
G1TPZ1	Galectin	147,39
A0A5F9CGP0	Histone H4	134,22
G1SXR1	Proline and arginine rich end leucine rich repeat protein	132,9
A0A5F9DUM8	Heat shock protein family A (Hsp70) member 8	129,6
U3KML1	Biglycan	128,56
G1SNE8	Calpactin I light chain	123,95
Q9TTC6	Peptidyl-prolyl cis-trans isomerase A	123,67
G1TKL2	Uncharacterized protein	122,03
G1T5H0	HtrA serine peptidase 1	121,56
A0A5F9D8N0	Histone H2A	120,9
A0A5F9DQH9	Latent transforming growth factor beta binding protein 1	117,33
A0A5F9C804	78 kDa glucose-regulated protein	115,58
G1SER8	Profilin	110,65
G1SVK5	Protein S100	107,81

G1SDA2	Cellular retinoic acid-binding protein 1	106,43
P51662	Annexin A1	105,88
A0A5F9DPN4	Tenascin C	105,73
A0A5F9CXS8	Collagen alpha-1(I) chain	100,85
G1T7Z6	Phosphoglycerate kinase	100,01
A0A5F9CGT7	Heat shock protein HSP 90-beta	99,63
G1U155	Histone H2B	99,53
G1SYD6	Lamin A/C	95,37
A0A5F9D1L2	Transforming growth factor-beta-induced protein ig-h3	94,01
P49065	Albumin	90,24
P01948	Hemoglobin subunit alpha-1/2	88,73
P62160	Calmodulin	84,91
G1T2C4	Transgelin	77
Q28888	Decorin	76,37
P18287	Apolipoprotein E	75,17
P29562	Eukaryotic initiation factor 4A-I (Fragment)	73,71
G1SNC7	Dermatopontin	73,12
U3KNZ4	Nucleoside diphosphate kinase	70,34
P02099	Hemoglobin subunit gamma	62

The abundancy of proteins was normalized to their respective molecular weight (MW). As expected, several ECM and secreted proteins are present (galectin, biglycan, decorin, fibulin, elastin-linked proteins, serine protease HTRA1, collagens) but surprisingly, we noticed a significant part of cellular proteins, especially those linked to cytoskeleton (actin, profilin, tubulin, vimentin) and particularly nuclear proteins like histones. Proteins that are important in cartilage metabolism are also present but to a lesser degree (COLXI, ACAN, COL2 LTBP, etc).

Successively, we listed the proteins that are present in all samples and sorted them by abundancy (Table 2). A total of 46 proteins were recorded as ubiquitous and sorted by KEGG Pathway database according to their cellular localization and function. Apart from extracellular proteins, we observed a significant moiety of proteins involved in supramolecular fibers, which is in accordance with cytoskeleton proteins presence (Fig. 2-C). Interestingly, among the proteins found in all samples, a great part (51.72%) are linked to glycosaminoglycan binding, which is consistent with the cartilaginous nature of the lyophilized CSM.

Lyophilized CSM as a support for allogenic and xenogeneic culture models

To investigate whether different cell types are capable of expanding and proliferating on rabbit-derived CSM, we used both rabbit allogenic and human xenogeneic cells transfected with GFP proteins. These cells were then seeded on Lyophilized CSM plates and fluorescence was monitored. Good adhesion and shape evolving was observed on thess scaffold (Fig. 3). Depending on the cells, we also observe a really good ability to proliferate in some cases (data not shown).

Our results indicated that lyophilized rabbit ECM could advantageously serves as a support for allogenic and xenogeneic culture tests.

Lyophilized CSM influences chondrogenic differentiation of human progenitor cells

Next, we investigated the ability of the lyophilized CSM to drive or influence a proper differentiation. Since the CSM derived from perichondrogenic cells, we tested the chondrogenic potential of human AuP by seeding them on rabbit lyophilized CSM and stimulating chondrogenic differentiation using chodrogenic medium. The same experiment was conducted on regular plastic plates that served as a control. Cells were cultured for 2 weeks and gene expression of cartilaginous markers and undesirable genes was monitored and analyzed by real time RT- PCR. Results showed a high significant increase of cartilage markers (COL 2A1, ELN, COMP and SOX 9*)* and a down regulation of COL1and COLX when cells were seeded on rabbit CSM compared to standard plastic plates (Fig. 4).

The effect is clearly more pronounced when the differentiation is triggered by chondrogenic medium. On the other hand, interestingly, the effect is seen even when the cells were incubated in control medium suggesting that the lyophilized CSM contains sufficient signals to drive chondrogenesis of xenogeneic human cells.

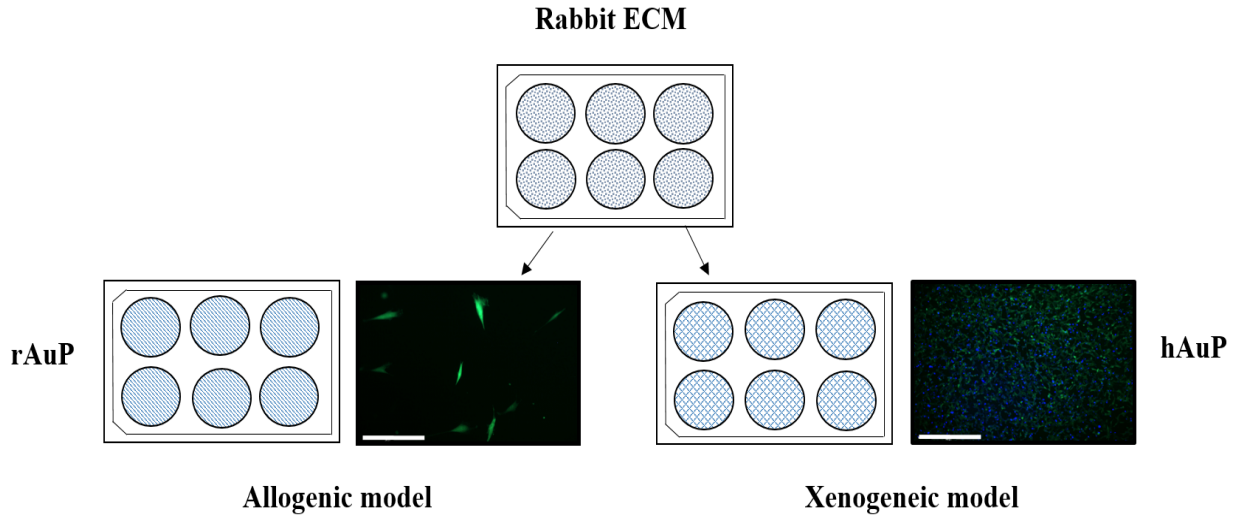

Fig. 3: Lyophilized CSM as a support for allogenic and xenogeneic culture models. Scheme showing rabbit auricular perichondrocytes (rAuP) cultured until confluency. The plates were then decellularized and lyophilized. CSM were then seeded with GFP-transfected rAuP and human GFP-expressing cells. Fluorescent imaging of DAPI and GFP were performed after 7 days to monitor cell spreading.

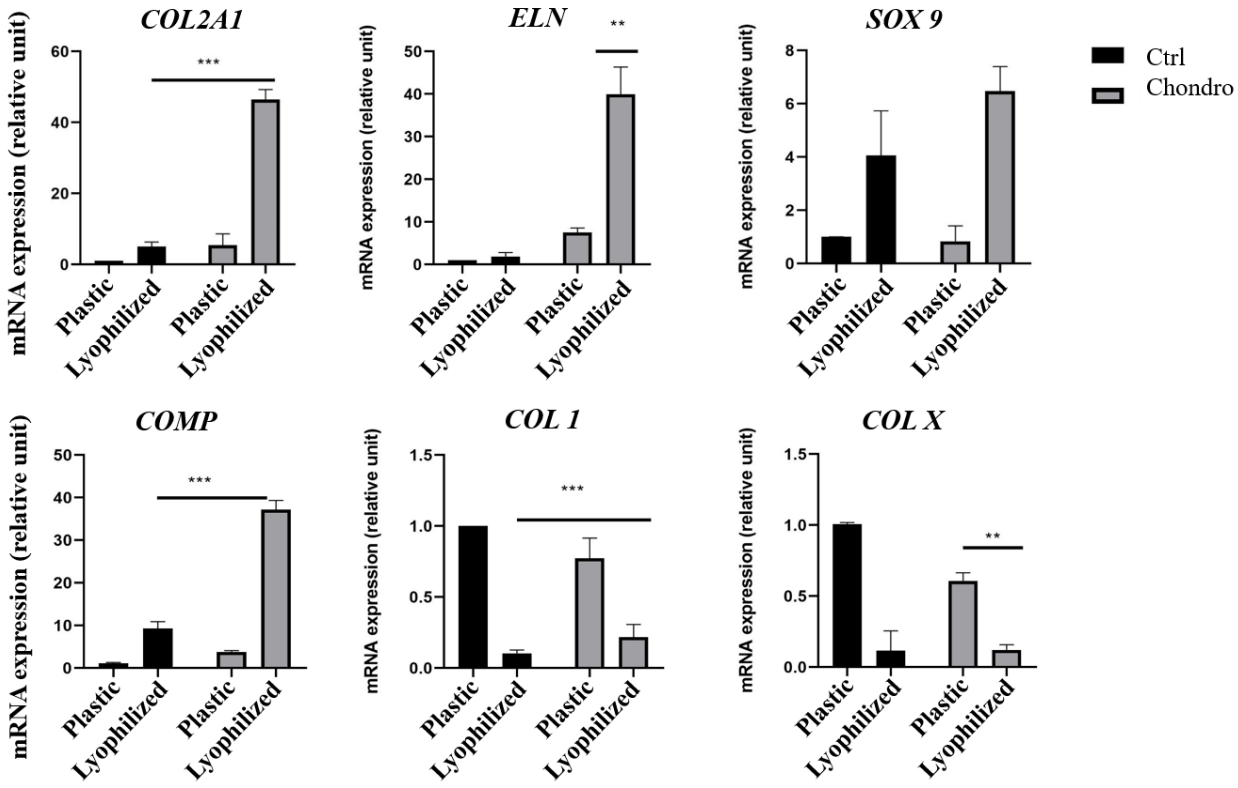

Fig. 4: Lyophilized CSM allow chondrogenic differentiation of progenitors. Human auricular perichondrocytes were seeded on both lyophilized CSM and regular plastic wells. They were then cultured in presence or absence of chondrogenic medium for 14 days. Gene expression analysis was conducted after RNA extraction targeting important cartilage genes, by real time RT-PCR. The expression is normalized to the mean of the 3 housekeeping genes. n=2 (*p<0.05, **P<0.01, ***p<0.005).

Rabbit lyophilized CSM preserve human chondrocyte's phenotype

Chondrocytes are well known to dedifferentiate by losing their phenotype upon *in vitro* expansion after several passages. To investigate whether our lyophilized CSM could improve cell phenotype and chondrocyte stability, primary human articular chondrocytes from three different donors were subcultured on lyophilized CSM as well as plastic standard plates that served as a control. The cells were expanded until reaching passage 5 (Fig. 5-A). Throughout the assay, cells were photographed and RNA was extracted at different times followed by gene expression analyses. Microphotographies showed faster proliferation of cells on lyophilized plates compared to plastic ones (Fig. 5-B). Dedifferentiation of chondrocytes is characterized by an increase of fibroblast markers such as COL1 and a sharp decrease of COL2A1 and ACAN. In order to detect the stability of chondrocytes phenotype, we performed real time RT-PCR for cartilage related genes.

Very interestingly, cells cultured exclusively on lyophilized CSM present a significant higher expression of ACAN, ELN, COL2 and SOX9 while that of COL1 and COLX is still limited (Fig. 5-C). After passage 5, the effects are more evident. We calculated the chondrogenic ratio (COL2/COL1) after the different passages. The culture of chondrocytes on lyophilized CSM

clearly improved this ratio and this value is increased throughout the passages. Immunocytochemistry of COL2A1 was performed on P0 cells and P5 cells. The positive staining of COL2A1 increased to show a great staining after passage 5 compared to plastic wells (Fig. 5-D), correlating with the above real time RT-PCR results for COL2A1 expression.

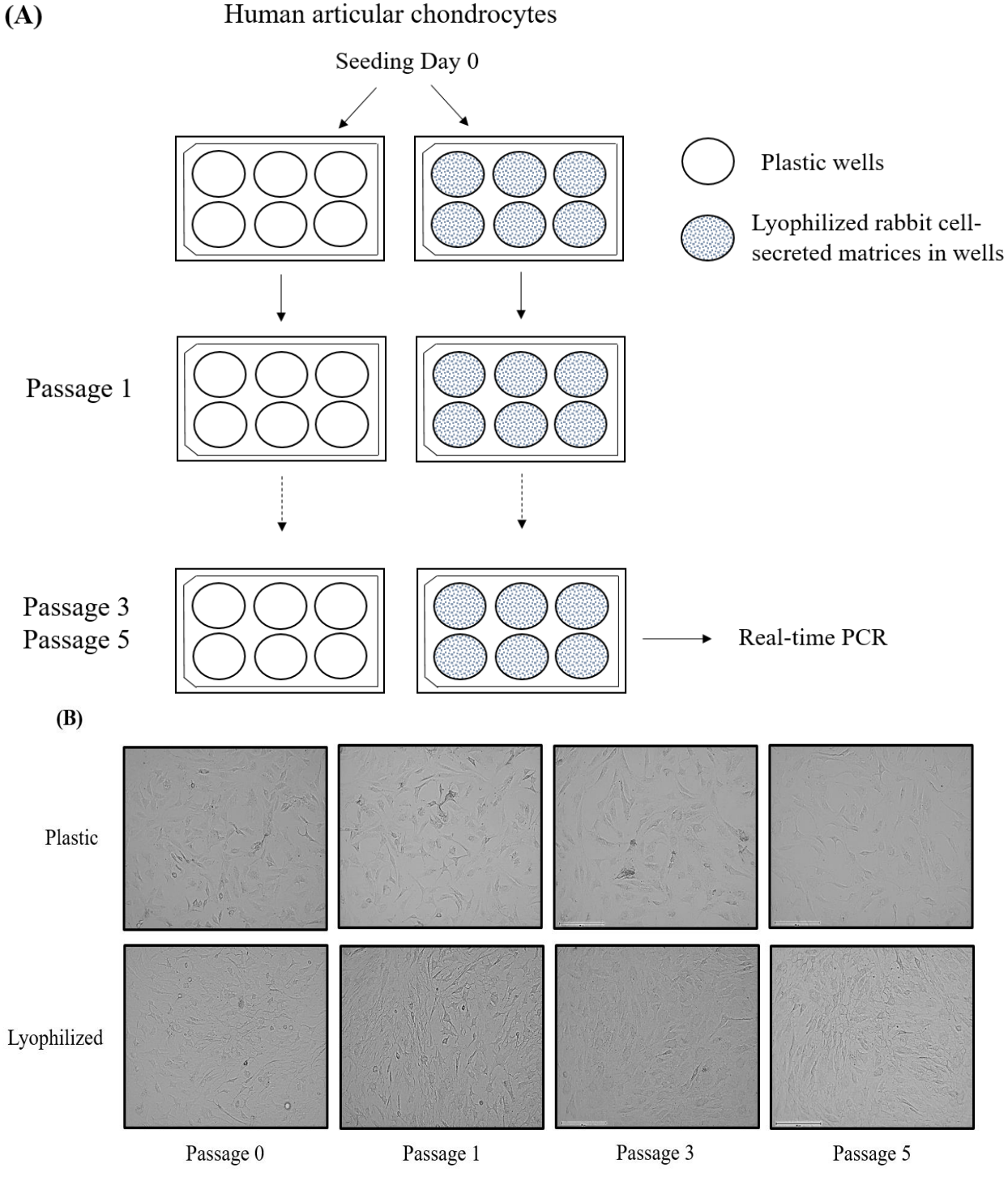

(C)

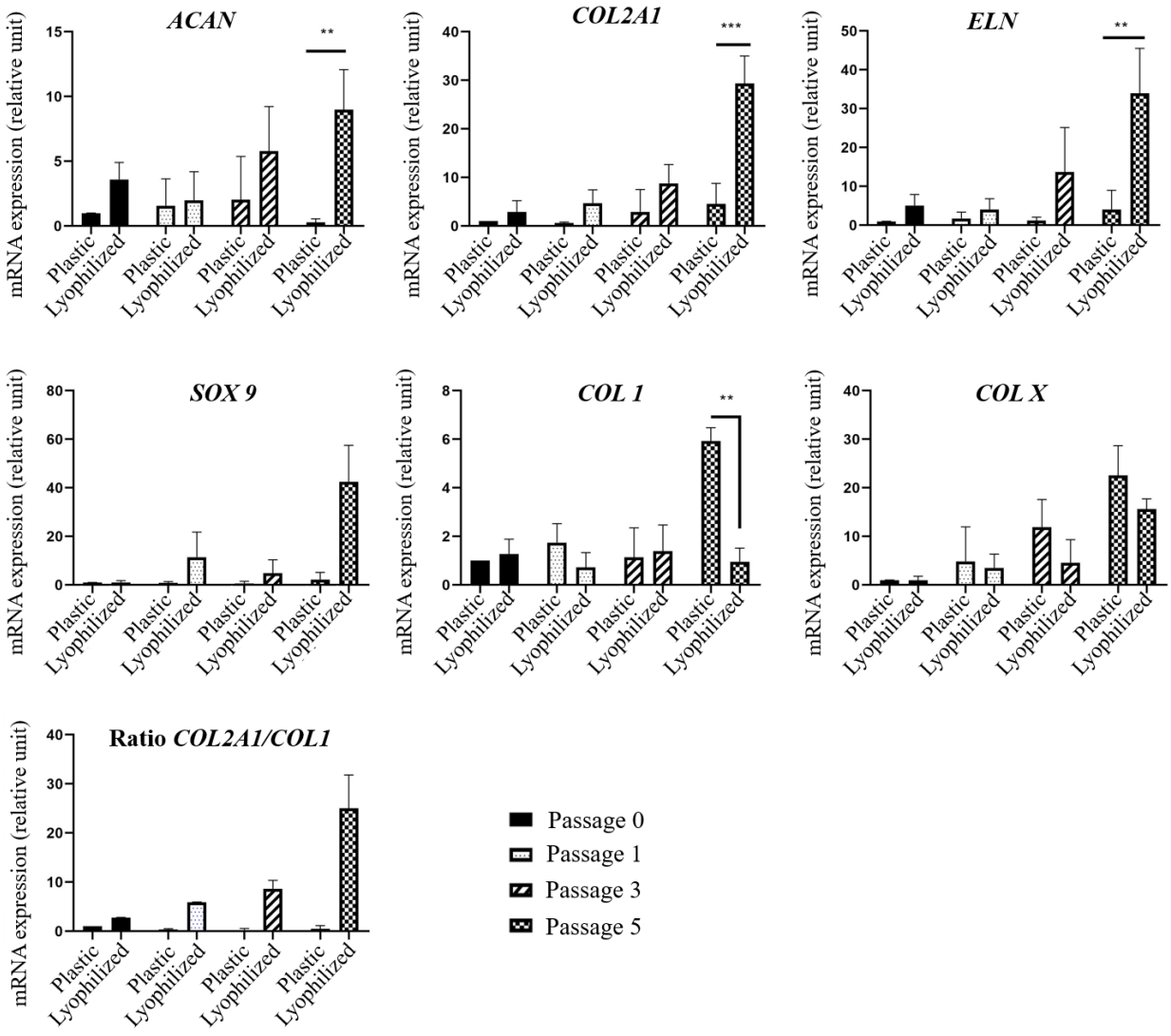
ACAN
COL2A1
ELN
SOX 9
COL 1
COL X
Ratio COL2A1/COL1
mRNA expression (relative unit)
Plastic
Lyophilized
Passage 0
Passage 1
Passage 3
Passage 5

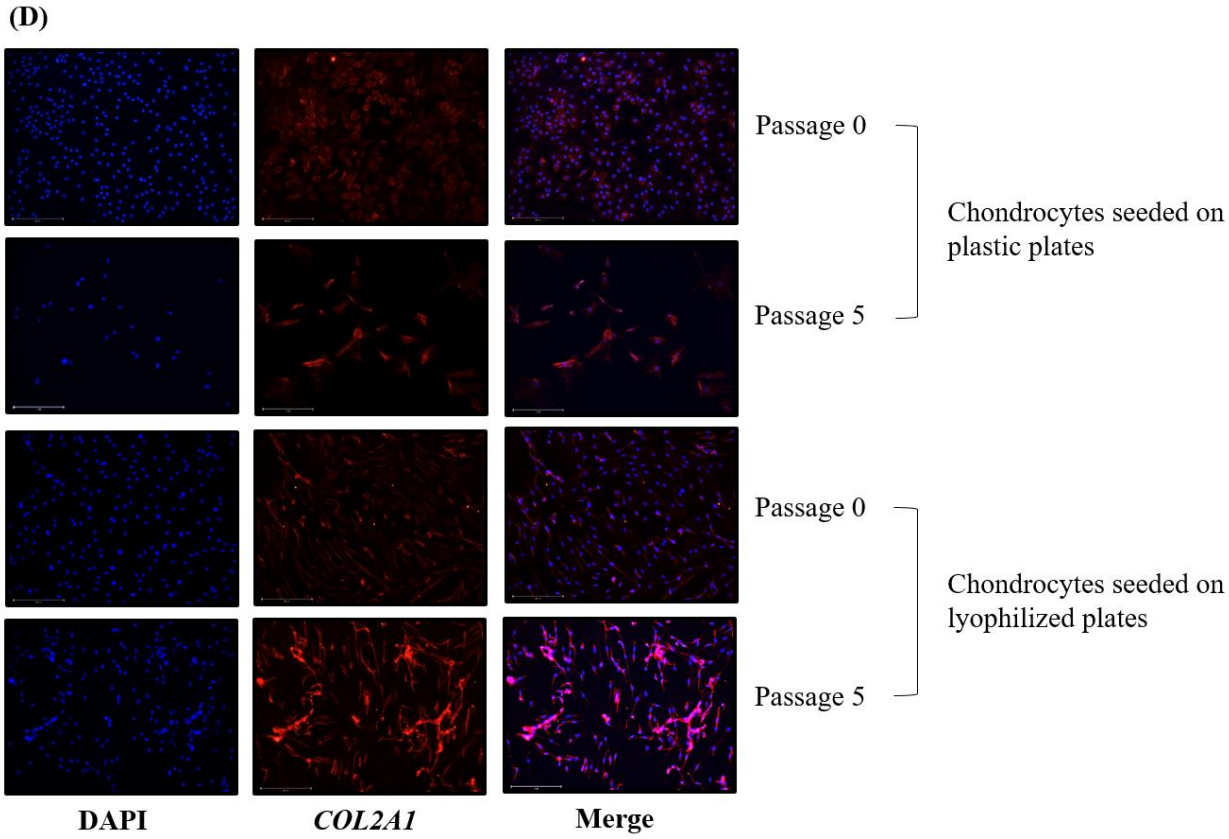

Fig. 5: Expansion on lyophilized CSM preserve human chondrocyte's phenotype. (**A**): Freshly isolated human articular chondrocytes were culture and passaged on either plastic or lyophilized plates until passage 5. (**B**): Microphotographs showing chondrocytes at different passages cultured on plastic vs lyophilized plates. (**C**): At passages 0 ,1 ,3 and 5, RNA was extracted and used for real time RT-PCR analysis of cartilage gene markers (n=3, *p<0.05, **P<0.01, ***p<0.005). (**D**): Immunohistochemistry of COL2A1, comparison between passage 0 and 5 of plastic vs lyophilized plates. Scale bar: 200µm.

Lyophilized CSM reverse the dedifferentiation of chondrocytes

In order to further explore the potential benefits of culturing cells on lyophilized CSM, we investigated the reversibility of dedifferentiation. For this purpose, we cultured human articular chondrocytes on plastic plates until passage 3 (Fig. 6-A). After that, they were trypsinized, divided into 2 fractions seeded either on plastic or lyophilized CSM and cultured for 1 or 2 weeks before gene expression analysis. The expression of cartilage related genes is significantly increased when cells were maintained on lyophilized CSM, especially after 2 weeks. Again, COL1 and COLX expression is counteracted in such substrate (Fig. 6-B). This suggest that the dedifferentiation that occurs upon subculture by passages can be reversed after 1 passage on lyophilized CSM coated plates.

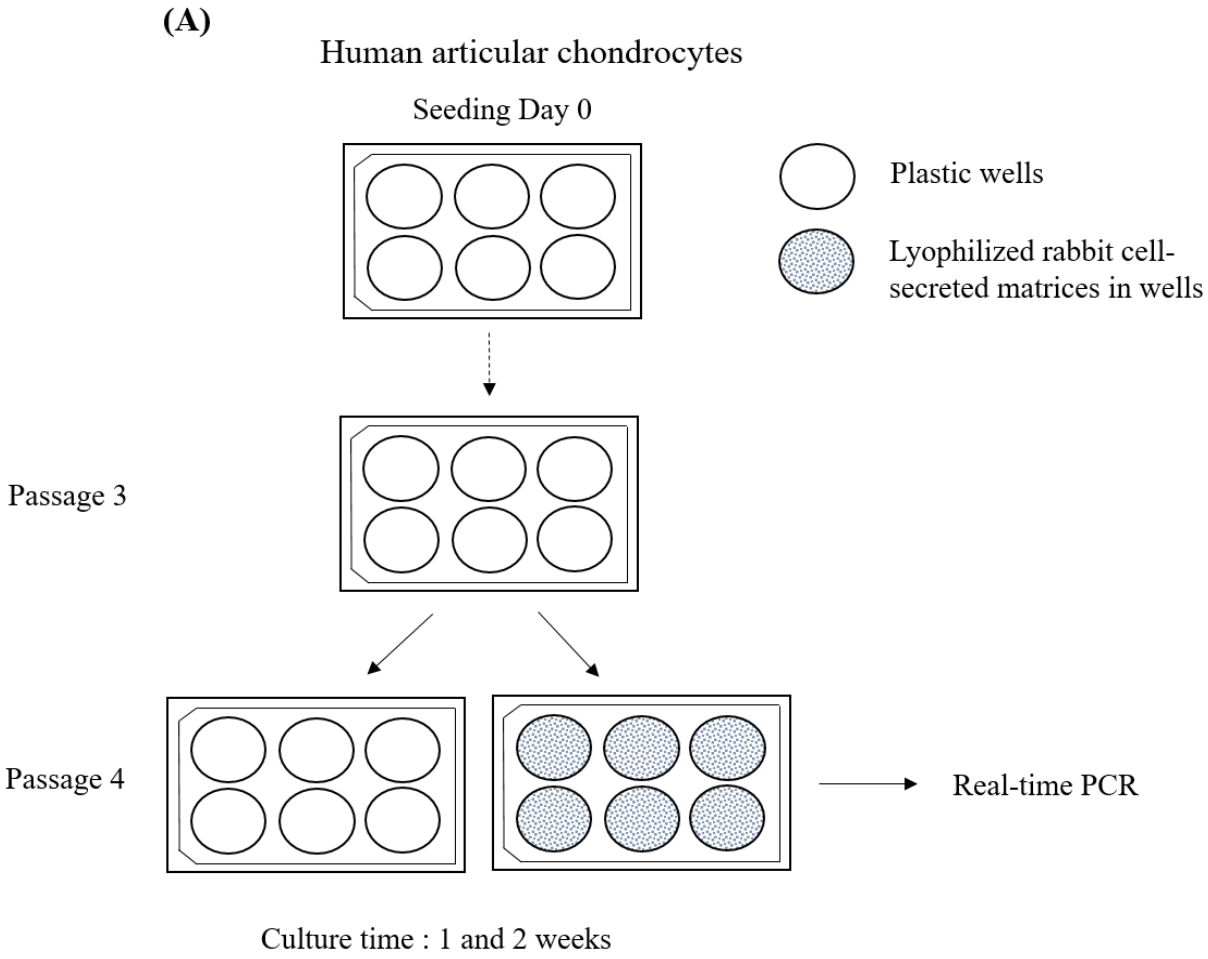
(A)
Human articular chondrocytes
Seeding Day 0
Plastic wells
Lyophilized rabbit cell-secreted matrices in wells
Passage 3
Passage 4
Real-time PCR
Culture time : 1 and 2 weeks

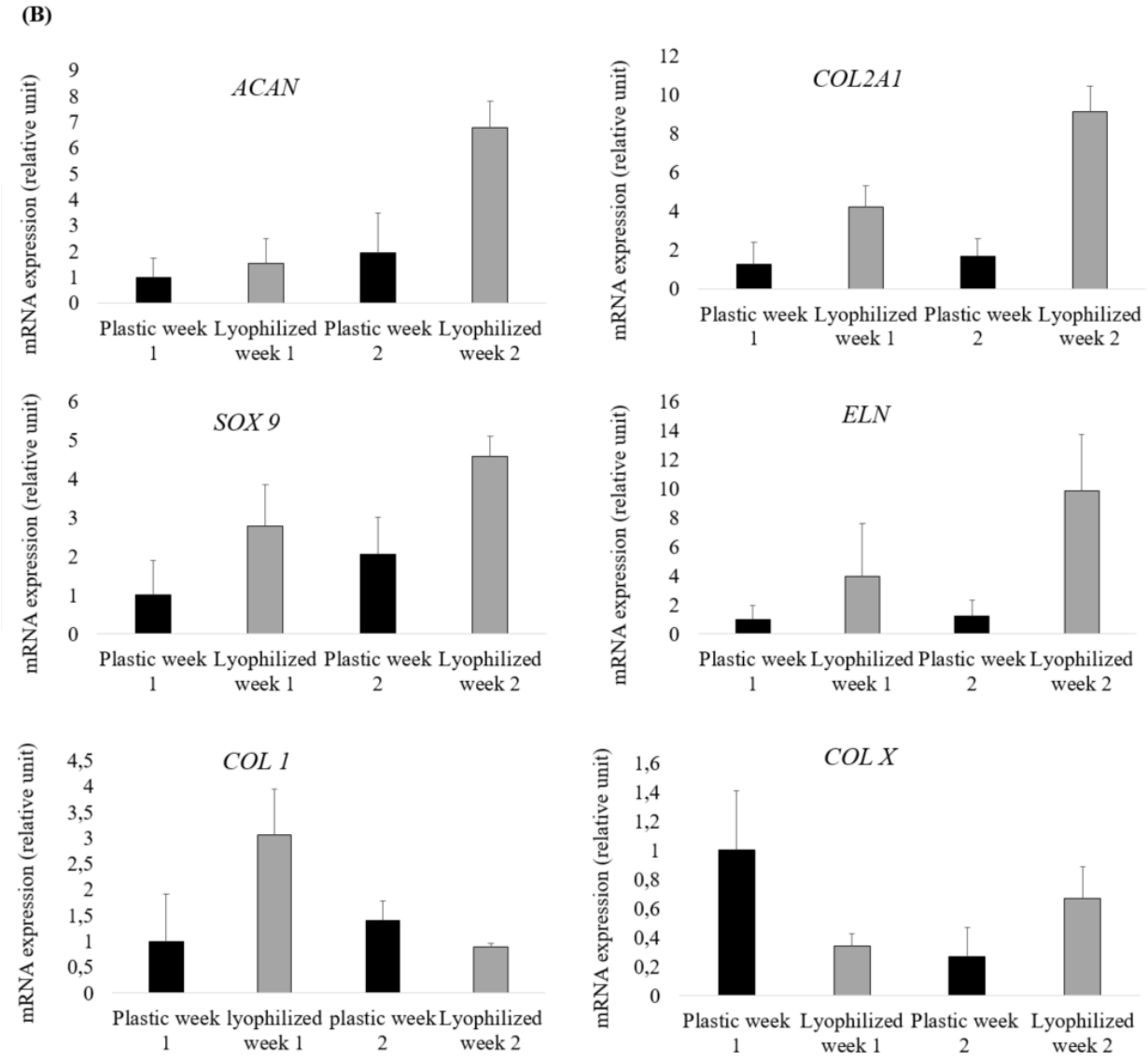

Fig. 6: Lyophilized CSM reverse the dedifferentiation of chondrocytes. (**A**): Human articular chondrocytes were subcultured on plastic plates until passage 3. Thereafter, they were separated into 2 fractions: one seeded again on plastic and another switched to lyophilized matrix. (**B**): After 1 and 2 weeks in culture, RNA was extracted and used for real time RT-PCR analysis of cartilage gene markers. Cartilage gene markers expressed by chondrocytes seeded on lyophilized rabbit matrix compared to plastic plates.

Lyophilized CSM coated plates increased proliferation of articular chondrocytes

Previous experiments suggested a positive effect on cell proliferation induced by lyophilized coated CSM. In order to obtain quantified data and to investigate how the coated substrate could influence cell behavior durably, we conducted a parallel experiment on both plastic and lyophilized CSM coated plates, as illustrated in (Fig. 7-A). Briefly, human articular chondrocytes were subcultured on both plates until passage 3, after they were harvested and divided for seeding on either plastic or lyophilized CSM coated plates. Cells were seeded equally after each passage.

Several days after, WST-1 metabolic tests were performed to monitor cell growth and viability. Cells were microphotographed after 5, 6 and 8 days of culture in both culture conditons. As expected, when compared to plastic plates, the cellular growth is clearly enhanced when chondrocytes are maintained on lyophilized CSM coated plates (PP Vs LL, Fig. 7-B-a). Cell growth was higher when the cells were subcultured on plastic until passage 3 then seeded on CSM coated plates (PL Vs PP, Fig. 7-B-b). Finally, when the cells were initially cultured on CSM coated plates for 3 passages before seeding on plastic, we recorded also a higher growth (LP Vs PP, Fig. 7-B-c). All together, these data suggest that lyophilized CSM coated plates enhance chondrocytes growth and proliferation, more interestingly, these signals are likely persistent even after seeding on plastic.

Microphotography's taken at day 8 corroborate with the viability assay. Indeed, in addition to differences in cell morphology, clear variations are visible in cell densities depending on the condition tested and the same hierarchical order of viability assessment is reported, i.e. where LL cells (most viable) than PL>LP>PP, respectively (Fig. 7-C).

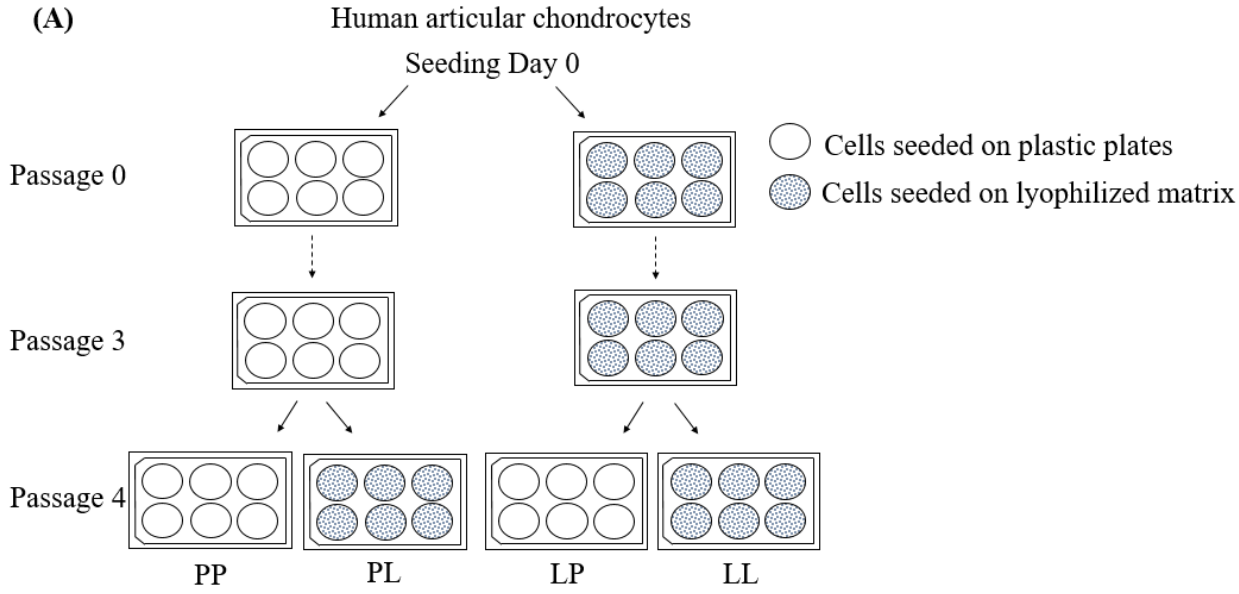

WST 1 assay after 5,6 and 8 days of culture

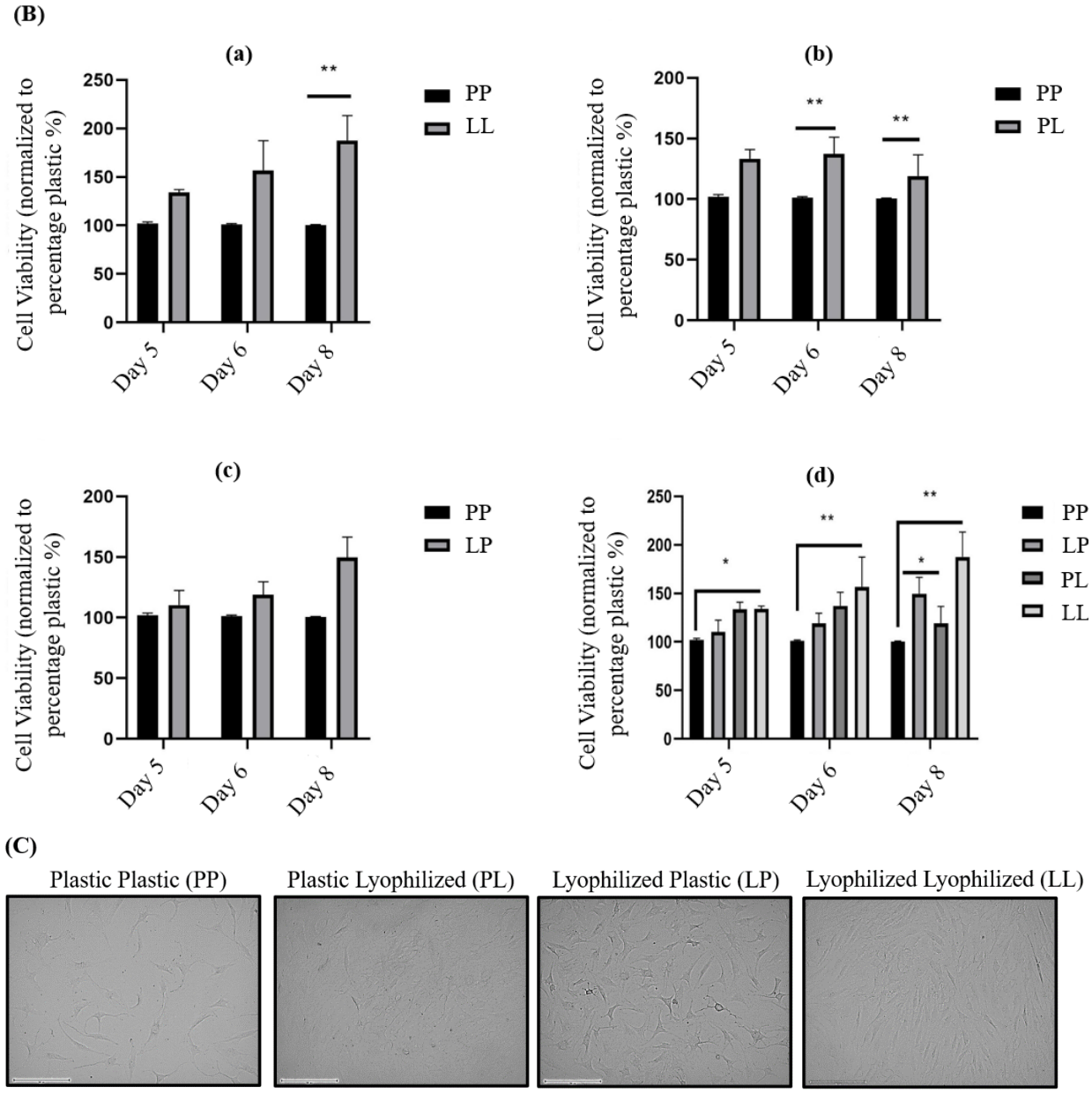

Fig. 7: Lyophilized CSM increases chondrocyte proliferation. (**A**): Human articular chondrocytes were cultured on plastic and lyophilized CSM plates from passage 0 until passage 3, then different seeding methods were performed. Cells initially seeded on plastic were kept on plastic (**PP**), Cells initially seeded on lyophilized CSM plates then switched to plastic plates (**LP**) and vice versa. Cells initially seeded on plastic were switched to lyophilized CSM plates after passage 3 (**PL**) and cells seeded all time on lyophilized CSM plates (**LL**). (**B**): Cell proliferation status of different samples was examined by WST1 assay *p<0.05, **P<0.01 (**C**): Macroscopic images showing chondrocytes seeded on different plates after 8 days of culture.

Discussion

ECM is highly specific and a complex dynamic structure providing support and bioactive signals to cells and their microenvironment. Many strategies are being explored to produces ECM mimics for different tissue engineering applications. In order to achieve a closely related ECM of native tissue, multiple cell types should collaborate to attribute and recapitulate tissue activity and functions. Cell-secreted matrices (CSM) represent a promising approach to fulfill and produce a biomimetic remodeled biocompatible ECM that could be used to study interaction between cells and matrix (H. W. Cheng *et al*., 2020). CSM have been recently evolved and appeared to be promising substrates to MSC expansion and proliferation.

In our study, we have used rabbit auricular perichondrocytes (AuP) to produce CSM. These cells were cultured post-confluence and under chondrogenic conditions. CSM were then decellularized, lyophilized and analyzed for their protein content. These presented good amount of proteins such as elastin, collagen and glycosaminoglycans. Although, we lost some proteins during SDS washing, however, a sufficient amount of proteins remained after decellularization and lyophilization.

In order to investigate the detailed ECM composition of lyophilized CSM, proteomic analyses were carried out. Although large amount of extracellular proteins was present, some intracellular proteins remained in these matrices. Our substrate was a complex between ECM secreted proteins and a mixture of cellular components attached to the ECM. This was surprising since SDS effectively removes host cells and DNA content. However, this could be explained by the possibility of SDS to create cross-links between ECM and cellular proteins, thus trapping some of these proteins in ECM. This could be explained by the sticky histones that remained despite the cell removal. Despite some traces of histones, our decellularization protocol was accepted according to decellularization criteria where DNA fragments were less than 200 bp. This protocol may be enhanced when adding acidic or high-salt conditions to be more suitable for histone cleaning.

Alternatively, high amount of ECM proteins was present and important proteins for cartilage metabolism was also found, but with low quantity. This shows that it is not necessary to have a huge amount of cartilage proteins in the matrix to be effective and exert its chondrogenic differentiation.

Moreover, we have also noticed the remaining of some cytoskeleton proteins, such as actin and tubulin after decellularization and lyophilization. Focal adhesions are dynamic protein complexes that anchor different proteins to ECM through their cytoskeleton in order to inform cells about ECM conditions (Burridge, 2017). Our results suggest that the presence of these cytoskeleton proteins was due to their interactions with some adhesion proteins that persisted despite SDS washing. This can affect ECM integrity in a way or more, since these proteins could still gain their activity and influence other proteins that can in turn impact ECM integrity and stiffness. For that, employment of a multi-step decellularization process involving both chemical enzymatic treatments combined to mechanical approaches is critical for better removal of these persisted proteins.

When have compared protein content in 6 protein samples (lyophilized CSM). These plates were produced and prepared the same way, but not the same time. Despite the low reproducibility of results, biological effect of these CSM was constant. The low reproducibility may be due to dealing with living cells that possess different variability. It also could be due to our heterogeneous cell population, composed of different cells that acts differently to culture conditions.

ECM guides cell fate through a complex of signals and cues that constitute cell microenvironment. CSM may retain tissue specific signals and cytokines that drive specific cellular pathways and functions. MSC cultured on these coatings exhibited high proliferation and integrity, by maintaining their phenotype and enhancing their differentiation potential. These CSM have favored increased colony forming units of MSC and enhanced osteogenic differentiation *in vitro* and *in vivo* in mice models (Larochette *et al*., 2020). Subsequently, these decellularized CSM have been potentially used to coat other surfaces where they were able to be transferred from one plate to another to coat new cell culture surfaces, while maintaining their osteogenic potential (Decaris *et al.*, 2012). On the other hand, different matrices were modeled by MSC that inhibited matrix proteases, that in turn directed MSC to induce a microenvironment conductive to chondrogenesis (Han et al., 2016; Ozguldez *et al*., 2018). Also, CSM have succeeded to import biological properties of native tissue when transferred to different scaffold surfaces to generate bone repair (Kim *et al.*, 2015).

Our study presented encouraging approach for auricular progenitor cells, where chondrogenic profile was significantly enhanced compared to plastic plates. Our CSM stimulated a more significant elastic cartilage profile. This would be also interesting to test other progenitors and stem cells that could remodel CSM into different lineages.

For successful cartilage tissue engineering, sufficient amount of chondrocytes is required for engineering human auricle. However, this is faced with a problem since chondrocytes dedifferentiate upon their expansion. Many techniques have been used in the recent years to limit this dedifferentiation. Dedifferentiated chondrocytes were restored when encapsulated in 3D chondrogenic system (Caron *et al*., 2012). According to previous studies, different pathways are involved in redifferentiation of chondrocytes. Ozturk *et al.*, have shown that hypoxia inhibited Wnt/β-catenin, that in turn enhances the expression of chondrogenic proteins and markers in 3D culture systems (Öztürk *et al*., 2017). Inhibition of MEK-ERK1/2 pathway activity also prevented articular chondrocyte dedifferentiation and thus fibrocartilage formation (Duval *et al.*, 2016; X. Wang *et al.*, 2018).

In addition, many studies have shown that TGF-β may control and modulate phenotype of chondrocytes. For instance, Jahr *et al.*, confirmed that 2.5% physoxia was optimal for key chondrogenic markers expression and an important regulator for TFGβ-2 that increased ECM synthesis in chondrocytes (Jahr *et al*., 2019). Moreover, TGFβ-2 suppresses collagenase that mediates degradation of collagen II in human chondrocytes, thus preserving chondrocyte phenotype in *in vitro* expansion (Khaghani *et al*., 2018; Tan Timur *et al*., 2019). Even when different growth factors were combined in a cocktail mix, nasal septal chondrocytes were shown to exhibits a significantly high proliferative capacity when expanded, this growth factor cocktail reduced nasal chondrocytes of tumorigenic effects up to passage 6 (Al-Masawa *et al.*, 2020).

Co-culture systems, on the other hand were also shown to limit dedifferentiation of chondrocytes. Autologous microtic chondrocytes when combined to MSC, showed a strong chondro inductive ability to promote stable chondrogenesis of BMMSC that were seeded in ear scaffold and subcutaneously implanted for 12 weeks (Zhang *et al*., 2014). In addition, co-culture of ATDC5 and genetically modified chondrocytes stimulated TGFβ-3 that in turn promoted robust expression of cartilaginous ECM, inducing chondrogenesis (Yao et al., 2020). This co-culture system provides potential strategy for the repair and redifferentiation of chondrocytes that regeneration of cartilage where human umbilical cord wharton's jelly-derived MSCs were co-cultured with primary chondrocytes (Y. Zhang *et al.*, 2020).

All the above methods reduced chondrocyte dedifferentiation, but each method has its own limitation. Due to the multipotency of MSC, it was risky to predict the fate of these cells during co- culture techniques. Growth factor used for chondrocyte culture were sometime fetal to cells and presented many side effects (Speichert *et al*., 2019). Besides, chondrocytes when seed on non-tissue culture treated surface, was time consuming (Mao *et al.*, 2018). By using our CSM coated plates, we expanded articular chondrocytes on these plates and demonstrated that these latter formed mature stable cartilage with rich expression of cartilage markers and low hypertrophy and dedifferentiation markers (COL1). Chondrogenic markers such as SOX9, ACAN, COL2A1 and ELN were promoted when chondrocytes were seeded on CSM compared to plastic plates. These cell exhibited an elongated shape, with highly significant COL2A1 expresssion after passage 5. This indicates that rabbit CSM protected chondrocyte profile and enhanced their chondrogenic profile.

Another important point is that chondrocytes initially seeded on plastic culture plates for several passages retained their chondrogenic profile when switched to lyophilized ECM plates for one week or two. Our current results revealed that 1 week was enough for retaining chondrocytes profiles and limiting dedifferentiation. This suggested that chondrocytes rapidly regained their profile, in contrast to 3D alginate models where redifferentiation was time consuming and took 3 to 6 weeks to effectively restore auricular chondrocytes function and profile (He *et al*., 2020).

We have tested different seeding methods of articular chondrocytes where some were initially seeded on plastic then switched to lyophilized CSM coated plates, and other seeded on lyophilized CSM coated plates and then transferred to plastic plates. Interestingly, we found that cells seeded on lyophilized CSM coated plates showed the highest cellular viability compared to cell seeded on plastic plates. This is correlated with a recent study where chondrocytes seeded on chondrocyte-derived matrices presented a high viability compared to chondrocytes seeded on plastic plates (Mao *et al*., 2019). Subsequently, when articular chondrocytes were initially seeded on plastic plates then shifted to lyophilized CSM coated plates, viability of these cells also increased compared to chondrocytes seeded on only plastic plates. Surprisingly, when analyzing chondrocytes seeded on lyophilized CSM coated plates and then switched to plastic plates, these cells revealed high proliferation rates compared to chondrocytes on plastic plates, suggesting that these cells recalled the effects of lyophilized CSM coated plates and exhibited a memory that was later on used to drive proliferation that was highly significant to plastic seeded cells.

Conclusion

We have created a simple and affordable cell culture tool, that enhances chondrogenesis and increases cellular proliferation of different cell sources. Preparation of these plates should be optimized and automated for better reproducibility of results. This model is also used to culture and expand chondrocytes *in vitro* using a short time, limiting their dedifferentiation. These coated CSM plates are efficient to maintain phenotypes, safe cell profile quality with improved safety to overcome challenges in cell therapy strategies and cartilage repair.

IV-Discussion

Due to the poor vascularity of cartilage tissue, cartilage defects heal poorly and lead to many degenerative cartilage diseases. Numerous clinical strategies have been employed to repair cartilaginous defects to achieve a tissue similar to the native one. However, these surgical processes remained challenging. For the reason of limited availability of autologous cartilage donor tissues and their main association with donor site morbidity, and in order to better regenerate cartilaginous defects, a great importance has been attributed in the recent years to cartilage tissue engineering.

The utmost important feature is creating an inert scaffold material, highly porous with interconnected pores to allow nutrient and waste transport. It should also be biodegradable and most of all shapeable and adaptable to the defect. Furthermore, the biomaterial chosen should speed up cell infiltration and attachment to achieve cell migration and proliferation (Wasyłeczko *et al*., 2020).

In addition, to a well-designed scaffold material, cellular sources play a pivotal role in the quality of regenerated tissue engineered constructs. The goal is to select a cell source that could be easily isolated, expanded and able to express cartilage-markers. These sources range from chondrocytes, stem cells to different progenitors.

Chondrocytes are the only cells presented in cartilage tissue. Although these cells have been mostly used in cartilage reconstruction processes, where autologous chondrocytes were the best to regenerate patient own tissue. However, upon expanding of these cells, their tendency of expressing collagen II decrease and an expression of collagen I increase in parallel, causing these cells to become ineffective to produce stable cartilage tissue (Yang *et al.*, 2018).

MSC have a higher stable proliferation rate than chondrocytes, and several studies have reported the potential of these cells to repair cartilaginous defect (Buzaboon and Alshammary, 2020; Rorick *et al*., 2020). Cell selection for cartilage-tissue generation remains one of the remarkable challenges in tissue engineering strategies.

As a first step in our work, we aimed to choose the best cell candidate to better express cartilage genes when encapsulated in 3D alginate beads. It is mostly known that bone marrow-derived mesenchymal stem cells (BMMSC) encapsulated in 3D alginate beads and in low hypoxic conditions express high cartilage markers (Duval *et al*., 2012, 2016 ; Peck *et al*., 2019; Schmidt *et al*., 2020). Alginate hydrogels were chosen due to their high potential to support cellular proliferation, ability to retain larger amount of fluids and water. They are also characterized by high biocompatibility and biodegradability (Ansari *et al*., 2017; Gentile *et al*., 2017). Being a powerful hydrogel, alginate have proved to induce the formation of cartilage-like tissue *in vivo* in many reports (Jin and Kim, 2018; Khatab *et al.*, 2020). To prepare such hydrogels, it is enough to crosslink them with calcium for 10 min and they will be ready to use.

By referring to the head region, we were very interested to see if progenitors from different embryological origin, possess similar chondrogenic potential when encapsulated within hydrogels under different oxygen levels in culture.

Auricular progenitor cells (AuP), nasal progenitor cells (NsP) and dental pulp stem cells (DPSC), were compared to the gold standard BMMSC upon their encapsulation with 3D alginate beads. First, these cell sources were tested for their trilineage formation. Chondrogenic potential of cells were differently presented by each cell source. It is important to mention that no studies have investigated yet, the effect of hypoxia of AuP. So we encapsulated these cells in alginate 3D model in presence and absence of oxygen tension and showed that hypoxia was not beneficial and didn't effect chondrogenic potential of AuP. Normoxic conditions, on the other hand enhanced cartilage forming capacity of perichondrocytes with an increase with cartilage markers.

Our results were complementary to the results of Otto *et al.*, that compared the chondrogenic ability of equine AuP to BMMSC when encapsulated in gelatin-based 3D hydrogels (Otto *et al*., 2018). Similarly, to the above results, AuP in normoxia outperformed BMMSC where ELN increased, cartilage markers increased and hypertrophy presented by COLX decreased. 3% hypoxia was unbeneficial since cartilage expression genes weren't enhanced by low oxygen levels, indicating that BMMSC remains the gold standard to produce cartilage in hypoxic medium. Thus, AuP were chosen as the best cell source for our second series of experiments. The second step was to choose the best scaffold for cartilage tissue engineering, by investigating multiple biomaterials.

Diverse synthetic scaffolds have been shown to produce various shapes and sizes that provided good mechanical and chemical properties of scaffold to improve quality of engineered cartilage. However, most of these polymers degrade upon implantation, and can be metabolized in the body, resulting in toxic side-effects. In addition, these synthetic scaffolds lack biological properties and may elicit immune responses (Liu *et al.*, 2016).

Despite their limited reproducibility, natural scaffolds present a superior biological response and better biocompatibility compared to synthetic scaffolds. In spite of these advantages, both natural and synthetic scaffolds lack characterization and detailed processing of tissue micro organization and structure (Perez-Puyana *et al*., 2020).

Due to their natural microenvironment and their preservation of tissue cues and proteins, natural ECM derived scaffolds, have become popular in recent years. Removal of cells from native tissue offer many advantages with respect to artificial scaffolds. This includes improved biocompatibility, enhanced ability for cellular repopulation and this increased biomechanical strength. The use of recellularized tissue appears to be attractive. The goal of any decellularization protocol is to efficiently remove all cellular and nuclear material, thereby minimizing adverse effects on composition and mechanical integrity. Utomo *et al.*, gave an example of auricular cartilage full decellularized using SDS (Utomo *et al*., 2015).

In this study, we proposed auricular cartilage from xenogeneic origin to develop a suitable matrix for auricular cartilage tissue engineering. Porcine auricular cartilage was chosen due to similar physiology to the human being. This porcine xenogeneic cartilage was successfully decellularized using a protocol set in our laboratory. This protocol consists of a mix of physical, chemical and enzymatic treatments that highly removed porcine cells resulting in a decellularized auricular scaffold that retains much of the tissue bioactivity, while removing the maximum amount of nuclear material, ready for further repopulation.

To reseed scaffolds, tissue-engineered approaches consist in several treatments, such as pulsatile perfusion, static culture injection, centrifugational force and sonication. However, seeding wasn't homogenous in all cases, and they only formed a monolayer over scaffold surface (Luo *et al.*, 2016). The use of collagen in recellularization significantly improved penetration of cells (Martinello *et al.*, 2014). Yet, resulted in non-homogeneous overall distribution. Facilitating cell-cell interconnections and preserving cell-ECM junctions are necessary to maintain cell adhesion

and proliferation, that is assured by cell sheet technology. It can also limit scaffold degradation and their toxic metabolites (Chen *et al*., 2019). Current research has introduced cell sheet as a tool for cartilage engineering. It was used to replace biodegradable scaffold. In our work, we investigated the use of these cell sheet to recellularize our decellularized auricular porcine cartilage, as well as evaluating the ability of these cell sheets to regenerate cartilaginous defect in allogenic models.

Uniform seeding of cartilage is a still a challenge due to the dense auricular elastic cartilage tissue. Many studies have incubated elastic scaffolds in elastase to deplete elastic fibers in order to better recellularize scaffold (homogenously with cells). Others, introduced channels to simplify the recellularization of full-thickness porcine cartilage discs. These channels acted as conduits that helped penetrating cells and nutrients, supporting cell viability and proliferation. However, the degree of recellularization of through cartilage tissue was limited, channels weren't enough to allow complete recellularization (Lehmann *et al*., 2019; Luo *et al*., 2015). In our case we didn't even bother to remove elastic fiber for better repopulation of cells. Instead, we were able to overcome this challenge by adopting a methodology that first included preparation of cell sheets from rabbit cells and culturing them *in vitro* for 2 weeks in chondrogenic medium.

We have used a mechanical system to synthesize cell sheets from different progenitors and different species. All cells produced successfully cell sheets, and by referring to our results regarding the best cell source for auricular regeneration, it was obviously to choose AuP that had a great and rapid tendency to form cell sheets. Rabbit AuP were chosen to recellularize porcine cartilage, due to the high availability of these cells and in order to develop a xenogeneic construct system *in vitro*. And more specifically, these rabbit origin cell sheets were intended to fill defect in an allogenic rabbit model to highly regenerate auricular cartilaginous defects *in vivo*.

Current studies have used sandwich models that were applicable on acellular cartilage tissue. Models was presented by culturing chondrocytes layer by layer to form an engineered cartilage tissue after several weeks *in vitro* and *in vivo* (Chen *et al*., 2015; Chiu *et al*., 2019; Gong *et al*., 2011). In our work, we have used the method of sandwich model, however, this time rabbit cell sheets were folded in a sandwich model without any addition of cells in order to homogenously recellularize cartilage. Cartilage was homogenously recellularized when cell sheets were wrapped

all over the cartilage for 2 weeks, cells deeply penetrated porcine cartilage that reconstructed a cartilaginous tissue *in vitro*.

In a rabbit model, auricular cartilaginous defects were produced and this time cell sheets were used as cell carriers to deliver cells to the defect area. Cell sheets were created *in vitro* in presence of chondrogenic medium. After 3 weeks of culture, cells proliferated and expressed cartilaginous markers. Their morphology and composition were compared to native auricular tissue that showed high similarity in composition compared to native auricular cartilage. At this stage, they were harvested and were ready to be implanted *in vivo*. After 2 months of implantation, defects were regenerated. This is shown by histological analysis and IHC analyses that marked the expression of ELN and COL2A1. In order to better analyze quality of regenerated cartilage we characterized cell sheet just before implantation and cell sheet after implantation. It wasn't really precise since after 2 months of implantation, cell sheets were fully integrated with tissue. However, we tried to harvest the minimum possible amount of the area where cell sheet was implanted. Implants were compared to cell sheet prepared *in vitro* and showed a great expression of ELN, ACAN, SOX9 and most of all COL2A1. Collagen II is highly expressed in cartilage tissue giving it strength and some elasticity in addition to elastin. This protein is a triple helix, consisting of 2 two identical chains of alpha-1 and one single chain of alpha-2. In all our experiment, we analyzed and marked COL2A1 gene, showing that collagen II produced in our experiments was mature and stable.

It would have been more interesting to prepare cell sheet produced by GFP-transfected cells and to implant them *in vivo* so that we can track cells after implantation and see if they accumulated in the defect site or they interacted with the surrounding tissue. Despite this, when analyzing IHC results, we could conclude that these cells circulated the defect and regenerated the defect in continuity with the surrounding tissue, in contrast to the unfilled defect that showed clear interruption of cartilage in both IHC and Safranin O results. The interest of this comparison was to assist that when we introduced cell sheets, cells were viable and proliferated and regenerated the defect. Thus, cell sheet technology acted as a tool to regenerate defects of rabbits. We have discussed before, the use of decellularized porcine cartilage as a scaffold for cartilage tissue engineering. Although this scaffold was fully regenerated using cell sheets, however, the use of such scaffold may cause many ethical problems later in human clinical trials. Since many studies have demonstrated the ability of plant tissues that have been decellularized, to leave behind a

cellulosic functional scaffold that in turn can be support for *in vitro* 3D culture as well as a biocompatible *in vivo* implantable scaffold. Then, in another goal of this work, we aimed to explore other scaffolds for cartilage engineering and turned towards recently described vegetal cellulosic tissues, namely apple's hypanthium. The cellular part was removed by using the anionic surfactant Sodium dodecyl sulfate (SDS). It is one of the widely used ionic product to eliminate cellular remnants. Many studies have indicated that traces of SDS detergent can remain attached to the tissue even after well rinsing using water, SDS can cause undesirable effects on the recellularization of the entire tissue (Cebotari *et al*., 2010; Syed *et al*., 2014). Thus, according to many researchers, it was necessary to remove remaining traces of SDS that induce a cytotoxic activity on cells, prior to recellularization of the biomaterial (Alizadeh *et al.*, 2019). Hickey *et al.*, in their studies, performed a salt treatment, to remove any SDS molecules, suggesting that SDS may form micelles within the apple tissue that can limit its recellularization potential, thus salt treatment aims to untighten these micelles, liberating them with water (Hickey *et al*., 2018). In contrast, in our study we didn't add any type of treatment. We were limited to extensive washing steps of distilled water that were changed every 2 hrs and kept over 24 hrs with agitation. Water was then changed into PBS and kept overnight. This is correlated by several studies that uses distilled water and PBS (Cebotari *et al*., 2010; Lin *et al*., 2019; Zvarova *et al*., 2016). This was sufficient to remove cytotoxicity from tissue.

Plants are characterized by higher availability compared to animal tissues. We have already proved that our four cell sources have the capacity to differentiate into cartilage when encapsulated in hydrogels, so it was interesting to evaluate viability and chondrogenic potential of the same cells in apple scaffolds. Viability assays revealed that cells proliferated in apple hypanthium tissue remained viable in scaffolds up to 3 weeks. This is correlated with other studies that showed that cells were able to proliferate and kept viable up to 12 weeks of culture (Modulevsky *et al*., 2014). Another idea to point out is that when these tissue were fixed, section of OCT were cut horizontally and vertically till reaching nearly all the block. These slides were stained and analyzed. This shows, according to our results, cells didn't accumulate of the surface of the scaffold, however, proliferated and colonized deeply this scaffold. The produced scaffold was able not only to support cell adhesion and proliferation, but also sustain and correct cellular function. For instance, white rubber like substance was observed on apple scaffolds, this was also explained by gene expression that demonstrated by ECM matrix deposition and gene expression of elastin and cartilaginous

markers, indicating that apple scaffolds possess great potential to regenerate different tissue. Our results were consistent with those described in literature where apple and other vegetal scaffolds such as carrot, onions, celery successfully generated adipose, and bone tissue (Y.-W. Cheng *et al*., 2020; J. Lee *et al*., 2019; Negrini *et al*., 2020). However, our work was the first to show that apple scaffolds promoted cartilage tissue regeneration.

Many studies have reported the great potential of alginate hydrogels in cartilage healing, regulation of cell phenotype and enhancement of the chondrogenic potential of cells. This hydrogel is extensively used in cartilage tissue engineering due to its high viscosity and printable material, low cytotoxicity and biocompatibility *in vivo*. Different studies have used alginate for cartilage 3D printing (Markstedt *et al*., 2015; Möller *et al.*, 2017; Ouyang *et al*., 2017) .

In an another study, alginate was combined with COL1 and agarose to enhance biological functionality of generated cartilage tissue (Yang *et al.*, 2018). Furthermore, when MSC were encapsulated within alginate beads, they secreted specific paracrine factors that endogenously regenerated cartilage *in vitro* (Sahu *et al*., 2021). On the other side, alginate hydrogels possess some limitation by their weak mechanical property and poor structure stability. In our hands, however, apple scaffolds showed a higher tendency and outperformed alginate potential to direct chondrogenic differentiation into cartilage tissue. This highlights the beneficial of apple scaffold potential to promote proliferation and chondrogenic differentiation and suggest its use for cartilage or other tissues engineering, regarding its ease of use and wide availability.

In a final, step, we induced a novel approach where cells are cultured to form cell sheets, then decellularized to remove cells, leaving behind potent cell-secreted matrix (CSM).

Current research has been able to prepare decellularized CSM from different cells, mainly from MSC, chondrocytes and intestine sub mucosa (Decaris *et al*., 2012; Taghavi et al., 2020; Z. Wang *et al.*, 2018). In our study, we kept the rabbit AuP cell model where rabbit AuP were cultured in chondrogenic conditions to produce CSM. Indeed, we showed that rabbit ear perichondrocytes could provide large amounts of extracellular matrix for cartilage tissue engineering. The subsequent freeze-drying allowed the plates to be preserved for a longer time (several months) and especially at room temperature.

This appears as an innovative approach since our data demonstrated that lyophilized CSM exhibited a great ability to enhance chondrogenic differentiation where a significant increase in gene expression was observed compared to cells seeded on plastic plates. As expected, after decellularization and lyophilization of the CSM, the protein amount is decreased due to the cell removal. However, ECM proteins are concerned by this decrease, since total collagens, GAG and elastin are also diminished. Although these latter may be intracellular proteins, we should consider that the detergent treatment affect also the ECM network as well. Mass spectroscopy analysis of the remaining protein by proteomics showed that apart of ECM proteins, several intracellular ones are still attached to the lyophilized substrate. Among them, a large part is involved in cytoskeleton or cell adhesion. This is not surprising since this protein network is normally linked to ECM through focal adhesions and may certainly remain attached throughout the preparation of lyophilized plates. SDS treatment for decellularization could also create bonds to stabilize some protein-protein interaction, what could explain the persistence of several other intracellular proteins, like histones for example. Despite the presence of intracellular proteins, lyophilized CSM were highly considered for their biological effects and we used them to investigate some potential applications.

Chondrocytes dedifferentiation remains an ongoing challenge in cartilage tissue reconstruction. They adapt their phenotype according to the type of collagen they produce. This is explained that upon *in vitro* expansion of chondrocytes on monolayer surfaces, COL2A1, ACAN and SOX9 genes which constitute the master genes for cartilage tissue, are downregulated, whereas COL1 is highly upregulated in these cells. Even structural differences are noticed when observing these cells microscopically, where primary chondrocytes exhibit a round shape that shifts towards a more flattered shape, spindle shaped cells.

Many efforts have been made in order to decrease this phenomenon, such as encapsulating chondrocytes in 3D hydrogels with hypoxia conditions, involving different growth factors in cartilage repair, co-culturing techniques that combined different progenitors with chondrocytes in specific ratios. However, many limitations were associated with each technique. For instance, chondrocytes damage and aging have been linked to the use of many growth factors, and co-culturing techniques have resulted in time-consuming processes and donor-site morbidity. Our method of lyophilized CSM provides a tool to support chondrocyte expansion *in vitro*, where

chondrocytes retained their profile after passage 5 and significantly increased master cartilage genes, with a significant low expression of hypertrophic gene markers COLX and dedifferentiation marker COL1. Our results surpassed those of Mao *et al.*, where they used CSM that limited dedifferentiation of these cells and decreased COL1. Although their CSM promoted dedifferentiation, however, they did not focus on the increase and upregulation of cartilage markers such as ACAN, COL2A1 that were significantly upregulated in our study (Mao *et al*., 2019). In addition, upon analyzing the gene expression of chondrocytes after the passage 5 on lyophilized CSM coated plates compared to plastic plates, we could clearly suggest that not only articular chondrocytes limited their dedifferentiation and increased cartilage markers expression, but also most importantly, these lyophilized CSM coated plates helped and induced the secretion of elastin markers in these cells. Thus, providing critical importance of using these articular chondrocytes in promoting elastin cartilage engineering.

Consequently, chondrocytes seeded on lyophilized CSM-coated plates showed better proliferation and viability when compared to those seeded on plastic plates. We have also tested cells initially seeded on lyophilized CSM coated plates for 3 passages and then switched to plastic plates, that showed a significant increase in viability, indicating that these cells have created a memory of the coated CSM and maintained its profile even when seeded after on plastic plates. This also shed light on the rapid restoration of chondrocyte's phenotype, since coated matrix accelerated and rapidly restored chondrocyte profile.

Our findings on lyophilized substrates were obtained by using auricular perichondrocytes as ECM producing cells regarding several observations throughout our study: their proliferation rate (to obtain enough cells rapidly), their chondrogenic potential and the fact that they don't need hypoxia to differentiate. It would be very interesting to investigate other cell types, as they probably secrete and leave different supramolecular complexes behind and therefore others sets of signals. For example, it would be of interest to explore different differentiation pathways using the same plate preparation (ex: lyophilized CSM produced by osteoblast or myoblast respectively for driving osteogenesis or myogenesis of progenitors). Cellular morphology on lyophilized CSM-coated plates is also a critical concept to fully investigate in the future.

All in all, we provide a new approach of using CSM coating for several cell culture assays, including differentiation, proliferation. Such prepared plates can also be advantageously used for

cell expansion with phenotype preservation and opens a route for multiple screening tests with current plastic devices.

1-Conclusion

AuP turned out to be the best cell sources to regenerate auricular elastic cartilage. Being cultured in normal oxygen levels, these cells outperformed other progenitors in expression of different cartilaginous markers. On the contrary, these cells weren't affected by the low oxygen levels, that had no effect on cartilage markers, indicating that hypoxia is ineffective and unbeneficial for AuP. As predicted, BMMSC presented the best chondrogenic profile in low hypoxic medium.

It is noteworthy to mention that we were the first to prepare cell sheets from auricular progenitor cells. These cells have presented a good potential in repopulating xenogeneic cartilage, where they proliferated and deeply penetrated the scaffold, while regenerating auricular cartilage *in vitro,* and *in vivo* by reconstructing and regenerating cartilaginous defects for the first time in allogenic rabbit models. After implantation, their analyses showed a great elastic cartilage profile that highly resembled the native tissue.

To deepen our knowledge and to explore scaffolds for auricular cartilage tissue engineering, we proceeded to investigate more decellualrized natural scaffolds and were interested more in cellulosic scaffolds that hold great promise for regenerative medicine. We successfully decellularized apple tissue and confirmed their suitability to retain different progenitors and stem cells. Most importantly, apple scaffold significantly promoted cartilage markers expression and cartilage tissue generation and surpassed chondrogenic potential of the gold standard alginate hydrogels. These results highly suggest the importance of apples as alternative biostable scaffolds for cartilage tissue engineering and regenerative medicine.

Finally, and as a research and development (R&D) approach, we have created a strategy that uses CSM lyophilized on plastic plates as a support for several cell culture assays. The use of these naturally CSM coated plates allow xenogeneic chondrogenesis of human progenitor cells. This also promotes the growth, phenotype maintenance of chondrocytes upon expansion and enhances viability when compared to cells seeded on plastic culture plates.

2-Perspectives

In order to deepen the results obtained during the thesis, different perspectives are possible.

In view of the results produced during this thesis, it would be interesting to complete this study by investigating clinical trials using autologous AuP for cartilage defects repair. Cell sheets are also very promising tools for cell therapy and tissue engineering. We have already investigated and showed the ability of cell sheets to form cartilage tissue *in vivo*. Our results need to be extended to larger tissue defect repair *in vivo* in order to envisage a further clinical trials. In parallel, some preliminary results were obtained where cell sheets highly expressed osteogenic markers when cultured in osteogenic medium. It seems critical to configure a chondrogenic cell sheet together with an osteogenic cell sheet to construct and form an osteochondral junction. Characterization of this junction would be very useful to define the requirements needed for regeneration of an osteochondral defect to be investigated also in animal models. It may also bring insights in tissue-tissue junction construction in general.

Regarding apple scaffolds, it is interesting to test their chondrogenic potential *in vivo* by creating cartilage-defects animal models. Also testing different cells to produce other tissue such as bone or muscle tissues from apple scaffolds are also appealing.

It seems also important to investigate the mechanical properties of our scaffolds (cells sheets, apple hypanthium) by measuring their stiffness and their degree of elasticity and flexibility using Young's modulus equation and to see to which level these scaffolds can withstand stress. This will make our work ready and applicable for clinical trials.

Concerning our last series of experiments with CSM-coated plates, several perspectives can be envisaged. First of all, homogenous cell population should be chosen in order to limit cellular variability and thus increase reproducibility. A critical evaluation of decellularization strategies such as the choice of agents that best remove DNA material is required to rinse well and remove traces of histone and intracellular proteins that are trapped using SDS.

Indeed, different cell sources could be investigated for preparing various tissues. Moreover, these plates could be used as supports for the manufacture of personalized cellular patches, thus

preparation of such plates should be highly automated for their use in industrial *in vitro* applications. This would also provide cell culture carriers that aid in large preparation of cells, under appropriate environment conditions, holding promising future for reconstructive surgery and cell therapy.

ECM Coated plates exists already on the market. However, all of them are made by coating a single ECM protein brought in solution. Not only, we propose plates with naturally secreted proteins but they are also organized as a cell specific ECM. This work led us to start an Intellectual property (IP) for patented process.

VI-References

Aamodt, J.M., Grainger, D.W., 2016. Extracellular matrix-based biomaterial scaffolds and the host response. Biomaterials 86, 68–82. https://doi.org/10.1016/j.biomaterials.2016.02.003

Abarca-Buis, R., Contreras-Figueroa, M.E., Garciadiego-Cázares, D., Krötzsch, E., 2020. Control of fibrosis by TGFβ signalling modulation promotes redifferentiation during limited regeneration of mouse ear. Int J Dev Biol 64, 423–432. https://doi.org/10.1387/ijdb.190237ra

Adamski, M., Fontana, G., Gershlak, J.R., Gaudette, G.R., Le, H.D., Murphy, W.L., 2018. Two Methods for Decellularization of Plant Tissues for Tissue Engineering Applications. Journal of Visualized Experiments : JoVE. https://doi.org/10.3791/57586

Ahmed, N.E.-M.B., Murakami, M., Kaneko, S., Nakashima, M., 2016. The effects of hypoxia on the stemness properties of human dental pulp stem cells (DPSCs). Sci Rep 6. https://doi.org/10.1038/srep35476

Ahn, J., Kumar, H., Cha, B.-H., Park, S., Arai, Y., Han, I., Park, S.G., Lee, S.-H., 2016. AIMP1 downregulation restores chondrogenic characteristics of dedifferentiated/degenerated chondrocytes by enhancing TGF-β signal. Cell Death Dis 7, e2099. https://doi.org/10.1038/cddis.2016.17

Akbari, P., Waldman, S.D., Cushing, S.L., Papsin, B.C., Propst, E.J., Weber, J.F., Yeger, H., Farhat, W.A., 2017. Bioengineering pediatric scaffold-free auricular cartilaginous constructs. The Laryngoscope 127. https://doi.org/10.1002/lary.26395

Aldana, A.A., Abraham, G.A., 2017. Current advances in electrospun gelatin-based scaffolds for tissue engineering applications. Int J Pharm 523, 441–453. https://doi.org/10.1016/j.ijpharm.2016.09.044

Alio del Barrio, J.L., Chiesa, M., Garagorri, N., Garcia-Urquia, N., Fernandez-Delgado, J., Bataille, L., Rodriguez, A., Arnalich-Montiel, F., Zarnowski, T., Álvarez de Toledo, J.P., Alio, J.L., De Miguel, M.P., 2015. Acellular human corneal matrix sheets seeded with human adipose-derived mesenchymal stem cells integrate functionally in an experimental animal model. Experimental Eye Research 132, 91–100. https://doi.org/10.1016/j.exer.2015.01.020

Alizadeh, M., Rezakhani, L., Soleimannejad, M., Sharifi, E., Anjomshoa, M., Alizadeh, A., 2019. Evaluation of vacuum washing in the removal of SDS from decellularized bovine pericardium: method and device description. Heliyon 5, e02253. https://doi.org/10.1016/j.heliyon.2019.e02253

Almany, L., Seliktar, D., 2005. Biosynthetic hydrogel scaffolds made from fibrinogen and polyethylene glycol for 3D cell cultures. Biomaterials 26, 2467–2477. https://doi.org/10.1016/j.biomaterials.2004.06.047

Al-Masawa, M.-E., Wan Kamarul Zaman, W.S., Chua, K.-H., 2020. Biosafety evaluation of culture-expanded human chondrocytes with growth factor cocktail: a preclinical study. Sci Rep 10, 21583. https://doi.org/10.1038/s41598-020-78395-y

Amaral, R.J.F.C. do, Pedrosa, C. da S.G., Kochem, M.C.L., Silva, K.R. da, Aniceto, M., Claudio-da-Silva, C., Borojevic, R., Baptista, L.S., 2012. Isolation of human nasoseptal chondrogenic cells: A promise for cartilage engineering. Stem Cell Research 8, 292–299. https://doi.org/10.1016/j.scr.2011.09.006

Amorim, S., Soares da Costa, D., Pashkuleva, I., Reis, C.A., Reis, R.L., Pires, R.A., 2021. 3D hydrogel mimics of the tumor microenvironment: the interplay among hyaluronic acid, stem cells and cancer cells. Biomater Sci 9, 252–260. https://doi.org/10.1039/d0bm00843e

Anderson, D.E., Markway, B.D., Bond, D., McCarthy, H.E., Johnstone, B., 2016. Responses to altered oxygen tension are distinct between human stem cells of high and low chondrogenic capacity. Stem Cell Res Ther 7. https://doi.org/10.1186/s13287-016-0419-8

Andriolo, L., Di Martino, A., Altamura, S.A., Boffa, A., Poggi, A., Busacca, M., Zaffagnini, S., Filardo, G., 2020. Matrix-assisted chondrocyte transplantation with bone grafting for knee osteochondritis dissecans: stable results at 12 years. Knee Surg Sports Traumatol Arthrosc. https://doi.org/10.1007/s00167-020-06230-y

Ansari, S., Diniz, I.M., Chen, C., Aghaloo, T., Wu, B.M., Shi, S., Moshaverinia, A., 2017. Alginate/hyaluronic acid hydrogel delivery system characteristics regulate the differentiation of periodontal ligament stem cells toward chondrogenic lineage. J Mater Sci Mater Med 28, 162. https://doi.org/10.1007/s10856-017-5974-8

Araki, K., Taira, M., Miyagawa, S., Kanaya, T., Okuda, N., Toda, K., Kuratani, T., Ueno, T., Sawa, Y., 2020. Autologous skeletal myoblast sheet implantation for pediatric dilated cardiomyopathy: A case report. Gen Thorac Cardiovasc Surg. https://doi.org/10.1007/s11748-020-01540-x

Armingol, E., Officer, A., Harismendy, O., Lewis, N.E., 2021. Deciphering cell-cell interactions and communication from gene expression. Nat Rev Genet 22, 71–88. https://doi.org/10.1038/s41576-020-00292-x

Asadi, M., Lotfi, H., Salehi, R., Mehdipour, A., Zarghami, N., Akbarzadeh, A., Alizadeh, E., 2020. Hepatic cell-sheet fabrication of differentiated mesenchymal stem cells using decellularized extracellular matrix and thermoresponsive polymer. Biomed Pharmacother 134, 111096. https://doi.org/10.1016/j.biopha.2020.111096

Asnaghi, M.A., Power, L., Barbero, A., Haug, M., Köppl, R., Wendt, D., Martin, I., 2020. Biomarker Signatures of Quality for Engineering Nasal Chondrocyte-Derived Cartilage. Front Bioeng Biotechnol 8, 283. https://doi.org/10.3389/fbioe.2020.00283

Bae, H.C., Park, H.J., Wang, S.Y., Yang, H.R., Lee, M.C., Han, H.-S., 2018. Hypoxic condition enhances chondrogenesis in synovium-derived mesenchymal stem cells. Biomater Res 22, 28. https://doi.org/10.1186/s40824-018-0134-x

Baker, B.M., Chen, C.S., 2012. Deconstructing the third dimension: how 3D culture microenvironments alter cellular cues. J Cell Sci 125, 3015–3024. https://doi.org/10.1242/jcs.079509

Bakhshandeh, B., Zarrintaj, P., Oftadeh, M.O., Keramati, F., Fouladiha, H., Sohrabi-jahromi, S., Ziraksaz, Z., 2017. Tissue engineering; strategies, tissues, and biomaterials. Biotechnology and Genetic Engineering Reviews 33, 144–172. https://doi.org/10.1080/02648725.2018.1430464

Basler, M., Pontiggia, L., Biedermann, T., Reichmann, E., Meuli, M., Mazzone, L., 2020. Bioengineering of Fetal Skin: Differentiation of Amniotic Fluid Stem Cells into Keratinocytes. Fetal Diagn Ther 47, 198–204. https://doi.org/10.1159/000502181

Beck, J.N., Singh, A., Rothenberg, A.R., Elisseeff, J.H., Ewald, A.J., 2013. The independent roles of mechanical, structural and adhesion characteristics of 3D hydrogels on the regulation of cancer invasion and dissemination. Biomaterials 34, 9486–9495. https://doi.org/10.1016/j.biomaterials.2013.08.077

Beriat, G.K., Akmansu, S.H., Dogan, C., Ezerarslan, H., Han, U., Saglam, M., Senel, O.O., Kocaturk, S., 2012. The effect of subcutaneous Insulin-like Growth Factor-1 (IGF-1) injection on rabbit auricular cartilage autograft viability. Bosn J Basic Med Sci 12, 213–218. https://doi.org/10.17305/bjbms.2012.2440

Bernstein, J.L., Cohen, B.P., Lin, A., Harper, A., Bonassar, L.J., Spector, J.A., 2018. Tissue Engineering Auricular Cartilage Using Late Passage Human Auricular Chondrocytes. Ann Plast Surg 80, S168–S173. https://doi.org/10.1097/SAP.0000000000001400

Berthiaume, F., Maguire, T.J., Yarmush, M.L., 2011. Tissue Engineering and Regenerative Medicine: History, Progress, and Challenges. Annu. Rev. Chem. Biomol. Eng. 2, 403–430. https://doi.org/10.1146/annurev-chembioeng-061010-114257

Bi, H., Jin, Y., 2013. Current progress of skin tissue engineering: Seed cells, bioscaffolds, and construction strategies. Burns Trauma 1, 63–72. https://doi.org/10.4103/2321-3868.118928

Bichara, D.A., Pomerantseva, I., Zhao, X., Zhou, L., Kulig, K.M., Tseng, A., Kimura, A.M., Johnson, M.A., Vacanti, J.P., Randolph, M.A., Sundback, C.A., 2014. Successful Creation of Tissue-Engineered Autologous Auricular Cartilage in an Immunocompetent Large Animal Model. Tissue Engineering Part A 20, 303–312. https://doi.org/10.1089/ten.tea.2013.0150

Binder, B.Y.K., Sagun, J.E., Leach, J.K., 2015. Reduced serum and hypoxic culture conditions enhance the osteogenic potential of human mesenchymal stem cells. Stem Cell Rev 11, 387–393. https://doi.org/10.1007/s12015-014-9555-7

Blasi-Romero, A., Palo-Nieto, C., Sandström, C., Lindh, J., Strømme, M., Ferraz, N., 2021. In Vitro Investigation of Thiol-Functionalized Cellulose Nanofibrils as a Chronic Wound Environment Modulator. Polymers (Basel) 13. https://doi.org/10.3390/polym13020249

Bonaventure, J., Kadhom, N., Cohen-Solal, L., Ng, K.H., Bourguignon, J., Lasselin, C., Freisinger, P., 1994. Reexpression of cartilage-specific genes by dedifferentiated human articular chondrocytes cultured in alginate beads. Exp Cell Res 212, 97–104. https://doi.org/10.1006/excr.1994.1123

Bonnans, C., Chou, J., Werb, Z., 2014. Remodelling the extracellular matrix in development and disease. Nat Rev Mol Cell Biol 15, 786–801. https://doi.org/10.1038/nrm3904

Bourgine, P.E., Pippenger, B.E., Todorov, A., Tchang, L., Martin, I., 2013. Tissue decellularization by activation of programmed cell death. Biomaterials 34, 6099–6108.

Bracaglia, L.G., Fisher, J.P., 2015. ECM-Based Biohybrid Materials for Engineering Compliant, Matrix-Dense Tissues. Adv Healthc Mater 4, 2475–2487. https://doi.org/10.1002/adhm.201500236

Brandl, A., Angele, P., Roll, C., Prantl, L., Kujat, R., Kinner, B., 2010. Influence of the growth factors PDGF-BB, TGF-beta1 and bFGF on the replicative aging of human articular chondrocytes during in vitro expansion. J Orthop Res 28, 354–360. https://doi.org/10.1002/jor.21007

Brennan, J.R., Cornett, A., Chang, B., Crotts, S.J., Nourmohammadi, Z., Lombaert, I., Hollister, S.J., Zopf, D.A., 2021. Preclinical assessment of clinically streamlined, 3D-printed, biocompatible single- and two-stage tissue scaffolds for ear reconstruction. J Biomed Mater Res B Appl Biomater 109, 394–400. https://doi.org/10.1002/jbm.b.34707

Brent, B., 1980. The correction of microtia with autogenous cartilage grafts: II. Atypical and complex deformities. Plast. Reconstr. Surg. 66, 13–21. https://doi.org/10.1097/00006534-198007000-00002

Brouki Milan, P., Pazouki, A., Joghataei, M.T., Mozafari, M., Amini, N., Kargozar, S., Amoupour, M., Latifi, N., Samadikuchaksaraei, A., 2020. Decellularization and preservation of human skin: A platform for tissue engineering and reconstructive surgery. Methods 171, 62–67. https://doi.org/10.1016/j.ymeth.2019.07.005

Browe, D.C., Coleman, C.M., Barry, F.P., Elliman, S.J., 2019. Hypoxia Activates the PTHrP – MEF2C Pathway to Attenuate Hypertrophy in Mesenchymal Stem Cell Derived Cartilage. Sci Rep 9, 1–12. https://doi.org/10.1038/s41598-019-49499-x

Burridge, K., 2017. Focal Adhesions: a personal perspective on a half century of progress. FEBS J 284, 3355–3361. https://doi.org/10.1111/febs.14195

Buzaboon, N., Alshammary, S., 2020. Clinical Applicability of Adult Human Mesenchymal Stem Cell Therapy in the Treatment of Knee Osteoarthritis. Stem Cells Cloning 13, 117–136. https://doi.org/10.2147/SCCAA.S268940

Cakici, C., Buyrukcu, B., Duruksu, G., Haliloglu, A.H., Aksoy, A., Isık, A., Uludag, O., Ustun, H., Subası, C., Karaoz, E., 2013. Recovery of fertility in azoospermia rats after injection of adipose-tissue-derived mesenchymal stem cells: the sperm generation. Biomed Res Int 2013, 529589. https://doi.org/10.1155/2013/529589

Camacho-Cardenosa, M., Quesada-Gómez, J.M., Camacho-Cardenosa, A., Leal, A., Dorado, G., Torrecillas-Baena, B., Casado-Díaz, A., 2020. Effects of normobaric cyclic hypoxia exposure on mesenchymal stem-cell differentiation-pilot study on bone parameters in elderly. World J Stem Cells 12, 1667–1690. https://doi.org/10.4252/wjsc.v12.i12.1667

Cao, Y., Vacanti, J.P., Paige, K.T., Upton, J., Vacanti, C.A., 1997. Transplantation of Chondrocytes Utilizing a Polymer-Cell Construct to Produce Tissue-Engineered Cartilage in the Shape of a Human Ear: Plastic &amp Reconstructive Surgery 100, 297–302. https://doi.org/10.1097/00006534-199708000-00001

Caron, M.M.J., Emans, P.J., Coolsen, M.M.E., Voss, L., Surtel, D. a. M., Cremers, A., van Rhijn, L.W., Welting, T.J.M., 2012. Redifferentiation of dedifferentiated human articular chondrocytes: comparison of 2D and 3D cultures. Osteoarthritis Cartilage 20, 1170–1178. https://doi.org/10.1016/j.joca.2012.06.016

Carvalho, T., Guedes, G., Sousa, F.L., Freire, C.S.R., Santos, H.A., 2019. Latest Advances on Bacterial Cellulose-Based Materials for Wound Healing, Delivery Systems, and Tissue Engineering. Biotechnol J 14, e1900059. https://doi.org/10.1002/biot.201900059

Cebotari, S., Tudorache, I., Jaekel, T., Hilfiker, A., Dorfman, S., Ternes, W., Haverich, A., Lichtenberg, A., 2010. Detergent decellularization of heart valves for tissue engineering: toxicological effects of residual detergents on human endothelial cells. Artif Organs 34, 206–210. https://doi.org/10.1111/j.1525-1594.2009.00796.x

Chang, B., Cornett, A., Nourmohammadi, Z., Law, J., Weld, B., Crotts, S.J., Hollister, S.J., Lombaert, I.M.A., Zopf, D.A., 2020. Hybrid Three-Dimensional-Printed Ear Tissue Scaffold With Autologous Cartilage Mitigates Soft Tissue Complications. Laryngoscope. https://doi.org/10.1002/lary.29114

Charlier, E., Deroyer, C., Ciregia, F., Malaise, O., Neuville, S., Plener, Z., Malaise, M., de Seny, D., 2019. Chondrocyte dedifferentiation and osteoarthritis (OA). Biochem Pharmacol 165, 49–65. https://doi.org/10.1016/j.bcp.2019.02.036

Chen, C., Huang, K., Zhu, J., Bi, Y., Wang, L., Jiang, J., Zhu, T., Yan, X., Zhao, J., 2020. A novel elastic and controlled-release poly(ether-ester-urethane)urea scaffold for cartilage regeneration. J Mater Chem B 8, 4106–4121. https://doi.org/10.1039/c9tb02754h

Chen, G., Zhang, Wangqian, Zhang, K., Wang, S., Gao, Y., Gu, J., He, L., Li, W., Zhang, C., Zhang, Wei, Li, M., Hao, Q., Zhang, Y., 2020. Hypoxia-Induced Mesenchymal Stem Cells Exhibit Stronger Tenogenic Differentiation Capacities and Promote Patellar Tendon Repair in Rabbits. Stem Cells Int 2020, 8822609. https://doi.org/10.1155/2020/8822609

Chen, S., Chen, W., Chen, Y., Mo, X., Fan, C., 2021a. Chondroitin sulfate modified 3D porous electrospun nanofiber scaffolds promote cartilage regeneration. Mater Sci Eng C Mater Biol Appl 118, 111312. https://doi.org/10.1016/j.msec.2020.111312

Chen, S., Nakamoto, T., Kawazoe, N., Chen, G., 2015. Engineering multi-layered skeletal muscle tissue by using 3D microgrooved collagen scaffolds. Biomaterials 73, 23–31. https://doi.org/10.1016/j.biomaterials.2015.09.010

Chen, S., Wang, J., Chen, Y., Mo, X., Fan, C., 2021b. Tenogenic adipose-derived stem cell sheets with nanoyarn scaffolds for tendon regeneration. Mater Sci Eng C Mater Biol Appl 119, 111506. https://doi.org/10.1016/j.msec.2020.111506

Chen, Wei, Xu, Y., Li, H., Dai, Y., Zhou, G., Zhou, Z., Xia, H., Liu, H., 2020. Tanshinone IIA Delivery Silk Fibroin Scaffolds Significantly Enhance Articular Cartilage Defect Repairing via Promoting Cartilage Regeneration. ACS Appl Mater Interfaces 12, 21470–21480. https://doi.org/10.1021/acsami.0c03822

Chen, Weiming, Xu, Y., Li, Y., Jia, L., Mo, X., Jiang, G., Zhou, G., 2020. 3D printing electrospinning fiber-reinforced decellularized extracellular matrix for cartilage regeneration. Chemical Engineering Journal 382, 122986. https://doi.org/10.1016/j.cej.2019.122986

Chen, X., Zhang, R., Zhang, Q., Xu, Z., Xu, F., Li, D., Li, Y., 2019a. Microtia patients: Auricular chondrocyte ECM is promoted by CGF through IGF-1 activation of the IGF-1R/PI3K/AKT pathway. J. Cell. Physiol. 234, 21817–21824. https://doi.org/10.1002/jcp.27316

Chen, Y.-H., Chung, Y.-C., Wang, I.-J., Young, T.-H., 2012. Control of cell attachment on pH-responsive chitosan surface by precise adjustment of medium pH. Biomaterials 33, 1336–1342. https://doi.org/10.1016/j.biomaterials.2011.10.048

Cheng, H.W., Yuan, M.T., Li, C.W., Chan, B.P., 2020. Cell-derived matrices (CDM)-Methods, challenges and applications. Methods Cell Biol 156, 235–258. https://doi.org/10.1016/bs.mcb.2020.01.001

Cheng, M.-S., Yi, X., Zhou, Q., 2020. Overexpression of HIF-1alpha in Bone Marrow Mesenchymal Stem Cells Promote the Repair of Mandibular Condylar Osteochondral Defect in a Rabbit Model. J Oral Maxillofac Surg. https://doi.org/10.1016/j.joms.2020.10.013

Cheng, N.-C., Tu, Y.-K., Lee, N.-H., Young, T.-H., 2020. Influence of Human Platelet Lysate on Extracellular Matrix Deposition and Cellular Characteristics in Adipose-Derived Stem Cell Sheets. Front Cell Dev Biol 8, 558354. https://doi.org/10.3389/fcell.2020.558354

Cheng, Y.-W., Shiwarski, D.J., Ball, R.L., Whitehead, K.A., Feinberg, A.W., 2020b. Engineering Aligned Skeletal Muscle Tissue Using Decellularized Plant-Derived Scaffolds. ACS Biomater. Sci. Eng. 6, 3046–3054. https://doi.org/10.1021/acsbiomaterials.0c00058

Chetty, A., Steynberg, T., Moolman, S., Nilen, R., Joubert, A., Richter, W., 2008. Hydroxyapatite-coated polyurethane for auricular cartilage replacement: an in vitro study. J Biomed Mater Res A 84, 475–482. https://doi.org/10.1002/jbm.a.31465

Chhapola, S., Matta, I., 2012. Cartilage-perichondrium: an ideal graft material? Indian J Otolaryngol Head Neck Surg 64, 208–213. https://doi.org/10.1007/s12070-011-0306-7

Chiu, L.L.Y., Weber, J.F., Waldman, S.D., 2019a. Engineering of scaffold-free tri-layered auricular tissues for external ear reconstruction: Engineering Tri-layered Auricular Tissues. The Laryngoscope 129, E272–E283. https://doi.org/10.1002/lary.27823

Chung, J.H.Y., Kade, J.C., Jeiranikhameneh, A., Ruberu, K., Mukherjee, P., Yue, Z., Wallace, G.G., 2020. 3D hybrid printing platform for auricular cartilage reconstruction. Biomed Phys Eng Express 6, 035003. https://doi.org/10.1088/2057-1976/ab54a7

Cohen, B.P., Hooper, R.C., Puetzer, J.L., Nordberg, R., Asanbe, O., Hernandez, K.A., Spector, J.A., Bonassar, L.J., 2016. Long-Term Morphological and Microarchitectural Stability of Tissue-Engineered, Patient-Specific Auricles In Vivo. Tissue Eng Part A 22, 461–468. https://doi.org/10.1089/ten.tea.2015.0323

Contentin, R., Demoor, M., Concari, M., Desancé, M., Audigié, F., Branly, T., Galéra, P., 2020. Comparison of the Chondrogenic Potential of Mesenchymal Stem Cells Derived from Bone Marrow and Umbilical Cord Blood Intended for Cartilage Tissue Engineering. Stem Cell Rev Rep 16, 126–143. https://doi.org/10.1007/s12015-019-09914-2

Courtenay, J.C., Deneke, C., Lanzoni, E.M., Costa, C.A., Bae, Y., Scott, J.L., Sharma, R.I., 2018. Modulating cell response on cellulose surfaces; tunable attachment and scaffold mechanics. Cellulose 25, 925–940. https://doi.org/10.1007/s10570-017-1612-3

Cruz, R.L.J., Ross, M.T., Powell, S.K., Woodruff, M.A., 2020. Advancements in Soft-Tissue Prosthetics Part A: The Art of Imitating Life. Front Bioeng Biotechnol 8. https://doi.org/10.3389/fbioe.2020.00121

Cui, H., Webber, M.J., Stupp, S.I., 2010. Self-assembly of peptide amphiphiles: from molecules to nanostructures to biomaterials. Biopolymers 94, 1–18. https://doi.org/10.1002/bip.21328

Da Sacco, S., Perin, L., Sedrakyan, S., 2018. Amniotic fluid cells: current progress and emerging challenges in renal regeneration. Pediatr Nephrol 33, 935–945. https://doi.org/10.1007/s00467-017-3711-7

Danoy, M., Tauran, Y., Poulain, S., Jellali, R., Bruce, J., Leduc, M., Le Gall, M., Gilard, F., Kido, T., Arakawa, H., Araya, K., Mori, D., Kato, Y., Kusuhara, H., Plessy, C., Miyajima, A., Sakai, Y., Leclerc, E., 2021. Multi-omics analysis of hiPSCs-derived HLCs matured on-chip revealed patterns typical of liver regeneration. Biotechnol Bioeng. https://doi.org/10.1002/bit.27667

De Paolis, A., Bikson, M., Nelson, J.T., de Ru, J.A., Packer, M., Cardoso, L., 2017. Analytical and numerical modeling of the hearing system: Advances towards the assessment of hearing damage. Hear Res 349, 111–128. https://doi.org/10.1016/j.heares.2017.01.015

Decaris, M.L., Mojadedi, A., Bhat, A., Leach, J.K., 2012. Transferable cell-secreted extracellular matrices enhance osteogenic differentiation. Acta Biomater 8, 744–752. https://doi.org/10.1016/j.actbio.2011.10.035

Delas, B., Dehesdin, D., 2008. Anatomie de l'oreille externe. EMC - Oto-rhino-laryngologie 3, 1–9. https://doi.org/10.1016/S0246-0351(08)46927-1

Deng, Z., Qian, T., Hang, F., 2020. Three-Dimensional Printed Hydrogels with High Elasticity, High Toughness, and Ionic Conductivity for Multifunctional Applications. ACS Biomater Sci Eng 6, 7061–7070. https://doi.org/10.1021/acsbiomaterials.0c01413

DeQuach, J.A., Mezzano, V., Miglani, A., Lange, S., Keller, G.M., Sheikh, F., Christman, K.L., 2010. Simple and High Yielding Method for Preparing Tissue Specific Extracellular Matrix Coatings for Cell Culture. PLoS One 5. https://doi.org/10.1371/journal.pone.0013039

Derks, M., Sturm, T., Haverich, A., Hilfiker, A., 2013. Isolation and chondrogenic differentiation of porcine perichondrial progenitor cells for the purpose of cartilage tissue engineering. Cells Tissues Organs (Print) 198, 179–189. https://doi.org/10.1159/000354897

Dikici, S., Claeyssens, F., MacNeil, S., 2019a. Decellularised baby spinach leaves and their potential use in tissue engineering applications: Studying and promoting neovascularisation. J Biomater Appl 34, 546–559. https://doi.org/10.1177/0885328219863115

Ding, H., Cheng, Y., Niu, X., Hu, Y., 2020. Application of electrospun nanofibers in bone, cartilage and osteochondral tissue engineering. J Biomater Sci Polym Ed 1–26. https://doi.org/10.1080/09205063.2020.1849922

Duan, L., Ma, B., Liang, Y., Chen, J., Zhu, W., Li, M., Wang, D., 2015. Cytokine networking of chondrocyte dedifferentiation in vitro and its implications for cell-based cartilage therapy. Am J Transl Res 7, 194–208.

Duisit, J., Amiel, H., Wüthrich, T., Taddeo, A., Dedriche, A., Destoop, V., Pardoen, T., Bouzin, C., Joris, V., Magee, D., Vögelin, E., Harriman, D., Dessy, C., Orlando, G., Behets, C., Rieben, R., Gianello, P., Lengelé, B., 2018a. Perfusion-decellularization of human ear grafts enables ECM-based scaffolds for auricular vascularized composite tissue engineering. Acta Biomaterialia 73, 339–354. https://doi.org/10.1016/j.actbio.2018.04.009

Duisit, J., Orlando, G., Debluts, D., Maistriaux, L., Xhema, D., de Bisthoven, Y.-A.J., Galli, C., Peloso, A., Behets, C., Lengelé, B., Gianello, P., 2018b. Decellularization of the Porcine Ear Generates a Biocompatible, Nonimmunogenic Extracellular Matrix Platform for Face Subunit Bioengineering. Ann Surg 267, 1191–1201. https://doi.org/10.1097/SLA.0000000000002181

Dutta, S.D., Patel, D.K., Lim, K.-T., 2019. Functional cellulose-based hydrogels as extracellular matrices for tissue engineering. J Biol Eng 13, 55. https://doi.org/10.1186/s13036-019-0177-0

Duval, E., Baugé, C., Andriamanalijaona, R., Bénateau, H., Leclercq, S., Dutoit, S., Poulain, L., Galéra, P., Boumédiene, K., 2012. Molecular mechanism of hypoxia-induced chondrogenesis and its application in in vivo cartilage tissue engineering. Biomaterials 33, 6042–6051. https://doi.org/10.1016/j.biomaterials.2012.04.061

Duval, E., Bouyoucef, M., Leclercq, S., Baugé, C., Boumédiene, K., 2016. Hypoxia inducible factor 1 alpha down-regulates type i collagen through Sp3 transcription factor in human chondrocytes. IUBMB Life 68, 756–763. https://doi.org/10.1002/iub.1539

Ebihara, G., Sato, M., Yamato, M., Mitani, G., Kutsuna, T., Nagai, T., Ito, S., Ukai, T., Kobayashi, M., Kokubo, M., Okano, T., Mochida, J., 2012. Cartilage repair in transplanted scaffold-free chondrocyte sheets using a minipig model. Biomaterials 33, 3846–3851. https://doi.org/10.1016/j.biomaterials.2012.01.056

Eea, M., Hh, B., M, E.-Z., Arh, F., N, K., I, H., K, G., Ma, A., M, M., Aka, A., 2019. Combination of Human Amniotic Fluid Derived-Mesenchymal Stem Cells and Nano-hydroxyapatite Scaffold Enhances Bone Regeneration [WWW Document]. Open access Macedonian journal of medical sciences. https://doi.org/10.3889/oamjms.2019.730

Elebring, E., Kuna, V.K., Kvarnström, N., Sumitran-Holgersson, S., 2017. Cold-perfusion decellularization of whole-organ porcine pancreas supports human fetal pancreatic cell attachment and expression of endocrine and exocrine markers. J Tissue Eng 8, 2041731417738145. https://doi.org/10.1177/2041731417738145

Enomura, M., Murata, S., Terado, Y., Tanaka, M., Kobayashi, S., Oba, T., Kagimoto, S., Yabuki, Y., Morita, K., Uemura, T., Maegawa, J., Taniguchi, H., 2020. Development of a Method for Scaffold-Free Elastic Cartilage Creation. Int J Mol Sci 21. https://doi.org/10.3390/ijms21228496

Fan, Z., Xie, X., Zhu, S., Liao, X., Yin, Z., Zhang, Y., Liu, F., 2020. Novel pre-vascularized tissue-engineered dermis based on stem cell sheet technique used for dermis-defect healing. Regen Biomater 7, 627–638. https://doi.org/10.1093/rb/rbaa039

Farag, A., Vaquette, C., Hutmacher, D.W., Bartold, P.M., Ivanovski, S., 2017. Fabrication and Characterization of Decellularized Periodontal Ligament Cell Sheet Constructs, in: Seymour, G.J., Cullinan, M.P., Heng, N.C.K. (Eds.), Oral Biology. Springer New York, New York, NY, pp. 403–412. https://doi.org/10.1007/978-1-4939-6685-1_23

Farag, A., Vaquette, C., Theodoropoulos, C., Hamlet, S.M., Hutmacher, D.W., Ivanovski, S., 2014. Decellularized Periodontal Ligament Cell Sheets with Recellularization Potential. J Dent Res 93, 1313–1319. https://doi.org/10.1177/0022034514547762

Fernandes, T.L., Cortez de SantAnna, J.P., Frisene, I., Gazarini, J.P., Gomes Pinheiro, C.C., Gomoll, A.H., Lattermann, C., Hernandez, A.J., Franco Bueno, D., 2020. Systematic Review of Human Dental Pulp Stem Cells for Cartilage Regeneration. Tissue Eng Part B Rev 26, 1–12. https://doi.org/10.1089/ten.TEB.2019.0140

Fernandes, T.L., Shimomura, K., Asperti, A., Pinheiro, C.C.G., Caetano, H.V.A., Oliveira, C.R.G.C.M., Nakamura, N., Hernandez, A.J., Bueno, D.F., 2018. Development of a Novel Large Animal Model to Evaluate Human Dental Pulp Stem Cells for Articular Cartilage Treatment. Stem Cell Rev Rep 14, 734–743. https://doi.org/10.1007/s12015-018-9820-2

Firmin, F., 1998. Ear reconstruction in cases of typical microtia. Personal experience based on 352 microtic ear corrections. Scandinavian Journal of Plastic and Reconstructive Surgery and Hand Surgery 32, 35–47. https://doi.org/10.1080/02844319850158930

Firmin, F., Marchac, A., 2016. Malformations de l'oreille. Annales de Chirurgie Plastique Esthétique 61, 420–428. https://doi.org/10.1016/j.anplas.2016.07.018

Firmin, F., Marchac, A., 2011. A novel algorithm for autologous ear reconstruction. Semin Plast Surg 25, 257–264. https://doi.org/10.1055/s-0031-1288917

Fischer, R., Kessler, B.M., 2015. Gel-aided sample preparation (GASP)—A simplified method for gel-assisted proteomic sample generation from protein extracts and intact cells. Proteomics 15, 1224–1229. https://doi.org/10.1002/pmic.201400436

Fontana, G., Gershlak, J., Adamski, M., Lee, J.-S., Matsumoto, S., Le, H.D., Binder, B., Wirth, J., Gaudette, G., Murphy, W.L., 2017a. Biofunctionalized Plants as Diverse Biomaterials for Human Cell Culture. Advanced Healthcare Materials 6, 1601225. https://doi.org/10.1002/adhm.201601225

Fouad, H., Sabry, D., Elsetohy, K., Fathy, N., 2016. Therapeutic efficacy of amniotic membrane stem cells and adipose tissue stem cells in rats with chemically induced ovarian failure. J Adv Res 7, 233–241. https://doi.org/10.1016/j.jare.2015.05.002

Fox, J.W., Edgerton, M.T., 1976. The fan flap: an adjunct to ear reconstruction. Plast. Reconstr. Surg. 58, 663–667. https://doi.org/10.1097/00006534-197612000-00001

Foyt, D.A., Taheem, D.K., Ferreira, S.A., Norman, M.D.A., Petzold, J., Jell, G., Grigoriadis, A.E., Gentleman, E., 2019. Hypoxia impacts human MSC response to substrate stiffness during chondrogenic differentiation. Acta Biomater 89, 73–83. https://doi.org/10.1016/j.actbio.2019.03.002

Fu, R.-H., Wang, Y.-C., Liu, S.-P., Shih, T.-R., Lin, H.-L., Chen, Y.-M., Sung, J.-H., Lu, C.-H., Wei, J.-R., Wang, Z.-W., Huang, S.-J., Tsai, C.-H., Shyu, W.-C., Lin, S.-Z., 2014. Decellularization and Recellularization Technologies in Tissue Engineering. Cell Transplant 23, 621–630. https://doi.org/10.3727/096368914X678382

Gaggi, G., Di Credico, A., Izzicupo, P., Sancilio, S., Di Mauro, M., Iannetti, G., Dolci, S., Amabile, G., Di Baldassarre, A., Ghinassi, B., 2020. Decellularized Extracellular Matrices and Cardiac Differentiation: Study on Human Amniotic Fluid-Stem Cells. Int J Mol Sci 21. https://doi.org/10.3390/ijms21176317

Gale, A.L., Mammone, R.M., Dodson, M.E., Linardi, R.L., Ortved, K.F., 2019. The effect of hypoxia on chondrogenesis of equine synovial membrane-derived and bone marrow-derived mesenchymal stem cells. BMC Vet. Res. 15, 201. https://doi.org/10.1186/s12917-019-1954-1

Galuzzi, M., Perteghella, S., Antonioli, B., Tosca, M.C., Bari, E., Tripodo, G., Sorrenti, M., Catenacci, L., Mastracci, L., Grillo, F., Marazzi, M., Torre, M.L., 2018. Human Engineered Cartilage and Decellularized Matrix as an Alternative to Animal Osteoarthritis Model. Polymers (Basel) 10. https://doi.org/10.3390/polym10070738

Gandia, C., Armiñan, A., García-Verdugo, J.M., Lledó, E., Ruiz, A., Miñana, M.D., Sanchez-Torrijos, J., Payá, R., Mirabet, V., Carbonell-Uberos, F., Llop, M., Montero, J.A., Sepúlveda, P., 2008. Human dental pulp stem cells improve left ventricular function, induce angiogenesis, and reduce infarct size in rats with acute myocardial infarction. Stem Cells 26, 638–645. https://doi.org/10.1634/stemcells.2007-0484

Gao, W., Zhang, L., Zhang, Y., Sun, C., Chen, X., Wang, Y., 2017. Adipose-derived mesenchymal stem cells promote liver regeneration and suppress rejection in small-for-size liver allograft. Transpl Immunol 45, 1–7. https://doi.org/10.1016/j.trim.2017.07.005

García-Gareta, E., Abduldaiem, Y., Sawadkar, P., Kyriakidis, C., Lali, F., Greco, K.V., 2020. Decellularised scaffolds: just a framework? Current knowledge and future directions. J Tissue Eng 11. https://doi.org/10.1177/2041731420942903

Gentile, P., Ghione, C., Ferreira, A.M., Crawford, A., Hatton, P.V., 2017. Alginate-based hydrogels functionalised at the nanoscale using layer-by-layer assembly for potential cartilage repair. Biomater Sci 5, 1922–1931. https://doi.org/10.1039/c7bm00525c

Gershlak, J.R., Hernandez, S., Fontana, G., Perreault, L.R., Hansen, K.J., Larson, S.A., Binder, B.Y.K., Dolivo, D.M., Yang, T., Dominko, T., Rolle, M.W., Weathers, P.J., Medina-Bolivar, F., Cramer, C.L., Murphy, W.L., Gaudette, G.R., 2017a. Crossing kingdoms: Using decellularized plants as perfusable tissue engineering scaffolds. Biomaterials 125, 13–22. https://doi.org/10.1016/j.biomaterials.2017.02.011

Ghaedi, M., Le, A.V., Hatachi, G., Beloiartsev, A., Rocco, K., Sivarapatna, A., Mendez, J.J., Baevova, P., Dyal, R.N., Leiby, K.L., White, E.S., Niklason, L.E., 2018. Bioengineered lungs generated from human iPSCs-derived epithelial cells on native extracellular matrix. J Tissue Eng Regen Med 12, e1623–e1635. https://doi.org/10.1002/term.2589

Gilpin, S.E., Guyette, J.P., Gonzalez, G., Ren, X., Asara, J.M., Mathisen, D.J., Vacanti, J.P., Ott, H.C., 2014. Perfusion decellularization of human and porcine lungs: bringing the matrix to clinical scale. J. Heart Lung Transplant. 33, 298–308. https://doi.org/10.1016/j.healun.2013.10.030

Golchin, A., Chatziparasidou, A., Ranjbarvan, P., Niknam, Z., Ardeshirylajimi, A., 2020. Embryonic Stem Cells in Clinical Trials: Current Overview of Developments and Challenges. Adv Exp Med Biol. https://doi.org/10.1007/5584_2020_592

Gonçalves, A.I., Rodrigues, M.T., Lee, S.-J., Atala, A., Yoo, J.J., Reis, R.L., Gomes, M.E., 2013. Understanding the role of growth factors in modulating stem cell tenogenesis. PLoS One 8, e83734. https://doi.org/10.1371/journal.pone.0083734

Gong, Y.Y., Xue, J.X., Zhang, W.J., Zhou, G.D., Liu, W., Cao, Y., 2011. A sandwich model for engineering cartilage with acellular cartilage sheets and chondrocytes. Biomaterials 32, 2265–2273. https://doi.org/10.1016/j.biomaterials.2010.11.078

Graziano, A., d'Aquino, R., Cusella-De Angelis, M.G., De Francesco, F., Giordano, A., Laino, G., Piattelli, A., Traini, T., De Rosa, A., Papaccio, G., 2008. Scaffold's surface geometry significantly affects human stem cell bone tissue engineering. J. Cell. Physiol. 214, 166–172. https://doi.org/10.1002/jcp.21175

Gu, L., Li, T., Song, X., Yang, X., Li, S., Chen, L., Liu, P., Gong, X., Chen, C., Sun, L., 2020. Preparation and characterization of methacrylated gelatin/bacterial cellulose composite hydrogels for cartilage tissue engineering. Regen Biomater 7, 195–202. https://doi.org/10.1093/rb/rbz050

Guillaume-Gentil, O., Akiyama, Y., Schuler, M., Tang, C., Textor, M., Yamato, M., Okano, T., Vörös, J., 2008. Polyelectrolyte Coatings with a Potential for Electronic Control and Cell Sheet Engineering. Adv. Mater. 20, 560–565. https://doi.org/10.1002/adma.200700758

Guo, S., Zhang, Yusen, Zhang, Yanmin, Meng, F., Li, M., Yu, Z., Chen, Y., Cui, G., 2020. Multiple Intravenous Injections of Valproic Acid-Induced Mesenchymal Stem Cell from Human-Induced Pluripotent Stem Cells Improved Cardiac Function in an Acute Myocardial Infarction Rat Model. Biomed Res Int 2020, 2863501. https://doi.org/10.1155/2020/2863501

Guyette, J.P., Charest, J.M., Mills, R.W., Jank, B.J., Moser, P.T., Gilpin, S.E., Gershlak, J.R., Okamoto, T., Gonzalez, G., Milan, D.J., Gaudette, G.R., Ott, H.C., 2016. Bioengineering Human Myocardium on Native Extracellular Matrix. Circ. Res. 118, 56–72. https://doi.org/10.1161/CIRCRESAHA.115.306874

Gz, J., Hw, K., 2018. Efficacy of Collagen and Alginate Hydrogels for the Prevention of Rat Chondrocyte Dedifferentiation [WWW Document]. Journal of tissue engineering. https://doi.org/10.1177/2041731418802438

Hackley, S.A., 2015. Evidence for a vestigial pinna-orienting system in humans. Psychophysiology 52, 1263–1270. https://doi.org/10.1111/psyp.12501

Han, H.S., Lee, H., You, D., Nguyen, V.Q., Song, D.-G., Oh, B.H., Shin, S., Choi, J.S., Kim, J.D., Pan, C.-H., Jo, D.-G., Cho, Y.W., Choi, K.Y., Park, J.H., 2020. Human adipose stem cell-derived extracellular nanovesicles for treatment of chronic liver fibrosis. J Control Release 320, 328–336. https://doi.org/10.1016/j.jconrel.2020.01.042

Han, S., Li, Y.Y., Chan, B.P., 2016. Extracellular Protease Inhibition Alters the Phenotype of Chondrogenically Differentiating Human Mesenchymal Stem Cells (MSCs) in 3D Collagen Microspheres. PLoS One 11, e0146928. https://doi.org/10.1371/journal.pone.0146928

Hao, Y., Zerdoum, A.B., Stuffer, A.J., Rajasekaran, A.K., Jia, X., 2016. Biomimetic Hydrogels Incorporating Polymeric Cell-Adhesive Peptide To Promote the 3D Assembly of Tumoroids. Biomacromolecules 17, 3750–3760. https://doi.org/10.1021/acs.biomac.6b01266

Hartzell, L.D., Chinnadurai, S., 2018. Microtia and Related Facial Anomalies. Clin Perinatol 45, 679–697. https://doi.org/10.1016/j.clp.2018.07.007

Harvestine, J.N., Orbay, H., Chen, J.Y., Sahar, D.E., Leach, J.K., 2018. Cell-secreted extracellular matrix, independent of cell source, promotes the osteogenic differentiation of human stromal vascular fraction. J Mater Chem B 6, 4104–4115. https://doi.org/10.1039/C7TB02787G

Hashimoto, Y., Tsuchiya, T., Doi, R., Matsumoto, K., Higami, Y., Kobayashi, E., Nagayasu, T., 2019. Alteration of the extracellular matrix and alpha-gal antigens in the rat lung scaffold reseeded using human vascular and adipogenic stromal cells. J Tissue Eng Regen Med 13, 2067–2076. https://doi.org/10.1002/term.2923

He, A., Ye, A., Song, N., Liu, N., Zhou, G., Liu, Y., Ye, X., 2020. Phenotypic redifferentiation of dedifferentiated microtia chondrocytes through a three-dimensional chondrogenic culture system. Am J Transl Res 12, 2903–2915.

Hellingman, C.A., Verwiel, E.T.P., Slagt, I., Koevoet, W., Poublon, R.M.L., Nolst-Trenité, G.J., Baatenburg de Jong, R.J., Jahr, H., van Osch, G.J.V.M., 2011. Differences in cartilage-forming capacity of expanded human chondrocytes from ear and nose and their gene expression profiles. Cell Transplant 20, 925–940. https://doi.org/10.3727/096368910X539119

Hickey, R.J., Modulevsky, D.J., Cuerrier, C.M., Pelling, A.E., 2018. Customizing the shape and microenvironment biochemistry of biocompatible macroscopic plant-derived cellulose scaffolds. ACS Biomaterials Science and Engineering 4, 3726–3736. https://doi.org/10.1021/acsbiomaterials.8b00178

Ho, S.S., Murphy, K.C., Binder, B.Y.K., Vissers, C.B., Leach, J.K., 2016. Increased Survival and Function of Mesenchymal Stem Cell Spheroids Entrapped in Instructive Alginate Hydrogels. Stem Cells Transl Med 5, 773–781. https://doi.org/10.5966/sctm.2015-0211

Hoch, A.I., Mittal, V., Mitra, D., Vollmer, N., Zikry, C.A., Leach, J.K., 2016. Cell-secreted matrices perpetuate the bone-forming phenotype of differentiated mesenchymal stem cells. Biomaterials 74, 178–187. https://doi.org/10.1016/j.biomaterials.2015.10.003

Holzwarth, J.M., Ma, P.X., 2011. Biomimetic nanofibrous scaffolds for bone tissue engineering. Biomaterials 32, 9622–9629. https://doi.org/10.1016/j.biomaterials.2011.09.009

Hong, Y., Yu, M., Weng, W., Cheng, K., Wang, H., Lin, J., 2013. Light-induced cell detachment for cell sheet technology. Biomaterials 34, 11–18. https://doi.org/10.1016/j.biomaterials.2012.09.043

Hu, D., Zhang, Deying, Liu, B., Liu, Y., Zhou, Y., Yu, Y., Shen, L., Long, C., Zhang, Dan, Liu, X., Lin, T., He, D., Xu, T., Timashev, P., Butnaru, D., Zhang, Y., Wei, G., 2020. Human ucMSCs seeded in a decellularized kidney scaffold attenuate renal fibrosis by reducing epithelial-mesenchymal transition via the TGF-β/Smad signaling pathway. Pediatr Res 88, 192–201. https://doi.org/10.1038/s41390-019-0736-6

Huang, X., Hou, Y., Zhong, L., Huang, D., Qian, H., Karperien, M., Chen, W., 2018. Promoted Chondrogenesis of Cocultured Chondrocytes and Mesenchymal Stem Cells under Hypoxia Using In-situ Forming Degradable Hydrogel Scaffolds. Biomacromolecules 19, 94–102. https://doi.org/10.1021/acs.biomac.7b01271

Huang, Y., Wang, J., Yang, F., Shao, Y., Zhang, X., Dai, K., 2017. Modification and evaluation of micro-nano structured porous bacterial cellulose scaffold for bone tissue engineering. Mater Sci Eng C Mater Biol Appl 75, 1034–1041. https://doi.org/10.1016/j.msec.2017.02.174

Huang, Z., Godkin, O., Schulze-Tanzil, G., 2017. The Challenge in Using Mesenchymal Stromal Cells for Recellularization of Decellularized Cartilage. Stem Cell Rev and Rep 13, 50–67. https://doi.org/10.1007/s12015-016-9699-8

Hughes, C.S., Postovit, L.M., Lajoie, G.A., 2010. Matrigel: a complex protein mixture required for optimal growth of cell culture. Proteomics 10, 1886–1890. https://doi.org/10.1002/pmic.200900758

Huh, M.-I., Lee, K.-P., Kim, J., Yi, S., Park, B.-U., Kim, H.K., 2018. Generation of Femtosecond Laser-Cut Decellularized Corneal Lenticule Using Hypotonic Trypsin-EDTA Solution for Corneal Tissue Engineering. J Ophthalmol 2018. https://doi.org/10.1155/2018/2590536

Hung, S.-C., Pochampally, R.R., Chen, S.-C., Hsu, S.-C., Prockop, D.J., 2007. Angiogenic effects of human multipotent stromal cell conditioned medium activate the PI3K-Akt pathway in hypoxic endothelial cells to inhibit apoptosis, increase survival, and stimulate angiogenesis. Stem Cells 25, 2363–2370. https://doi.org/10.1634/stemcells.2006-0686

Husak, Z., Dworzak, M.N., 2017. Chronic stress induces CD99, suppresses autophagy, and affects spontaneous adipogenesis in human bone marrow stromal cells. Stem Cell Res Ther 8, 83. https://doi.org/10.1186/s13287-017-0532-3

Ibsirlioglu, T., Elçin, A.E., Elçin, Y.M., 2020. Decellularized biological scaffold and stem cells from autologous human adipose tissue for cartilage tissue engineering. Methods 171, 97–107. https://doi.org/10.1016/j.ymeth.2019.04.020

Imashiro, C., Shimizu, T., 2021. Fundamental Technologies and Recent Advances of Cell-Sheet-Based Tissue Engineering. Int J Mol Sci 22. https://doi.org/10.3390/ijms22010425

Inaba, R., Khademhosseini, A., Suzuki, H., Fukuda, J., 2009. Electrochemical desorption of self-assembled monolayers for engineering cellular tissues. Biomaterials 30, 3573–3579. https://doi.org/10.1016/j.biomaterials.2009.03.045

Inui, T., Haneda, S., Sasaki, M., Furuoka, H., Ito, M., Yanagawa, M., Hiyama, M., Tabata, Y., Sasaki, N., 2019. Enhanced chondrogenic differentiation of equine bone marrow-derived mesenchymal stem cells in zirconia microwell substrata. Res Vet Sci 125, 345–350. https://doi.org/10.1016/j.rvsc.2019.07.005

Ishii, M., Shibata, R., Numaguchi, Y., Kito, T., Suzuki, H., Shimizu, K., Ito, A., Honda, H., Murohara, T., 2011. Enhanced angiogenesis by transplantation of mesenchymal stem cell sheet created by a novel magnetic tissue engineering method. Arterioscler. Thromb. Vasc. Biol. 31, 2210–2215. https://doi.org/10.1161/ATVBAHA.111.231100

Ito, K., Matsuoka, K., Matsuzaka, K., Morinaga, K., Inoue, T., 2015. Hypoxic condition promotes differentiation and mineralization of dental pulp cells *in vivo*. Int Endod J 48, 115–123. https://doi.org/10.1111/iej.12288

Ito, M., Nomura, S., Morita, H., Komuro, I., 2020. Trends and Limitations in the Assessment of the Contractile Properties of Human Induced Pluripotent Stem Cell-Derived Cardiomyocytes From Patients With Dilated Cardiomyopathy. Front Cardiovasc Med 7, 154. https://doi.org/10.3389/fcvm.2020.00154

Ito, S., Sato, M., Yamato, M., Mitani, G., Kutsuna, T., Nagai, T., Ukai, T., Kobayashi, M., Kokubo, M., Okano, T., Mochida, J., 2012. Repair of articular cartilage defect with layered chondrocyte sheets and cultured synovial cells. Biomaterials 33, 5278–5286. https://doi.org/10.1016/j.biomaterials.2012.03.073

Iyer, K., Dearman, B.L., Wagstaff, M.J.D., Greenwood, J.E., 2016a. A Novel Biodegradable Polyurethane Matrix for Auricular Cartilage Repair: An In Vitro and In Vivo Study.

Journal of Burn Care & Research 37, e353–e364. https://doi.org/10.1097/BCR.0000000000000281

Jahangirian, H., Azizi, S., Rafiee-Moghaddam, R., Baratvand, B., Webster, T.J., 2019. Status of Plant Protein-Based Green Scaffolds for Regenerative Medicine Applications. Biomolecules 9. https://doi.org/10.3390/biom9100619

Jahr, H., Gunes, S., Kuhn, A.-R., Nebelung, S., Pufe, T., 2019. Bioreactor-Controlled Physoxia Regulates TGF-β Signaling to Alter Extracellular Matrix Synthesis by Human Chondrocytes. Int J Mol Sci 20. https://doi.org/10.3390/ijms20071715

Jang, C.H., Koo, Y., Kim, G., 2020. ASC/chondrocyte-laden alginate hydrogel/PCL hybrid scaffold fabricated using 3D printing for auricle regeneration. Carbohydrate Polymers 248, 116776. https://doi.org/10.1016/j.carbpol.2020.116776

Javidpou, M., Seifati, S.-M., Farashahi-Yazd, E., Hajizadeh-Tafti, F., Golzadeh, J., Akyash, F., Aflatoonian, B., 2020. Mesenchymal Stem/Stromal-Like Cells from Diploid and Triploid Human Embryonic Stem Cells Display Different Gene Expression Profiles. Iran Biomed J 25, 99–105. https://doi.org/10.29252/ibj.25.2.99

Jessop, Z.M., Javed, M., Otto, I.A., Combellack, E.J., Morgan, S., Breugem, C.C., Archer, C.W., Khan, I.M., Lineaweaver, W.C., Kon, M., Malda, J., Whitaker, I.S., 2016. Combining regenerative medicine strategies to provide durable reconstructive options: auricular cartilage tissue engineering. Stem Cell Res Ther 7, 19. https://doi.org/10.1186/s13287-015-0273-0

Jeyakumar, V., Niculescu-Morzsa, E., Bauer, C., Lacza, Z., Nehrer, S., 2019. Redifferentiation of Articular Chondrocytes by Hyperacute Serum and Platelet Rich Plasma in Collagen Type I Hydrogels. Int J Mol Sci 20. https://doi.org/10.3390/ijms20020316

Jiang, Y., Tuan, R.S., 2015. Origin and function of cartilage stem/progenitor cells in osteoarthritis. Nat Rev Rheumatol 11, 206–212. https://doi.org/10.1038/nrrheum.2014.200

Jin, G.-Z., Kim, H.-W., 2018a. Efficacy of collagen and alginate hydrogels for the prevention of rat chondrocyte dedifferentiation. J Tissue Eng 9, 204173141880243. https://doi.org/10.1177/2041731418802438

Johns, A.L., Lucash, R.E., Im, D.D., Lewin, S.L., 2015. Pre and post-operative psychological functioning in younger and older children with microtia. J Plast Reconstr Aesthet Surg 68, 492–497. https://doi.org/10.1016/j.bjps.2014.12.019

Jones, E.S., Gibson, J.A.G., Dobbs, T.D., Whitaker, I.S., 2020. The psychological, social and educational impact of prominent ears: A systematic review. J Plast Reconstr Aesthet Surg 73, 2111–2120. https://doi.org/10.1016/j.bjps.2020.05.075

Jung, H., Lee, D.-S., Park, S.K., Choi, J.S., Jung, W.-K., Park, W.S., Choi, I.-W., 2018. Fucoxanthin Inhibits Myofibroblast Differentiation and Extracellular Matrix Production in Nasal Polyp-Derived Fibroblasts via Modulation of Smad-Dependent and Smad-Independent Signaling Pathways. Mar Drugs 16. https://doi.org/10.3390/md16090323

Junka, R., Yu, X., 2015. Novel Acellular Scaffold Made from Decellularized Schwann Cell Sheets for Peripheral Nerve Regeneration. Regen. Eng. Transl. Med. 1, 22–31. https://doi.org/10.1007/s40883-015-0003-2

Kagimoto, S., Takebe, T., Kobayashi, S., Yabuki, Y., Hori, A., Hirotomi, K., Mikami, T., Uemura, T., Maegawa, J., Taniguchi, H., 2016. Autotransplantation of Monkey Ear Perichondrium-Derived Progenitor Cells for Cartilage Reconstruction. Cell Transplant 25, 951–962. https://doi.org/10.3727/096368916X690917

Kainuma, S., Miyagawa, S., Toda, K., Yoshikawa, Y., Hata, H., Yoshioka, D., Kawamura, T., Kawamura, A., Kashiyama, N., Ito, Y., Iseoka, H., Ueno, T., Kuratani, T., Nakamoto, K., Sera, F., Ohtani, T., Yamada, T., Sakata, Y., Sawa, Y., 2021. Long-term Outcomes of Autologous Skeletal Myoblast Cell-sheet Transplantation for End-stage Ischemic Cardiomyopathy. Mol Ther. https://doi.org/10.1016/j.ymthe.2021.01.004

Kandalam, S., Sindji, L., Delcroix, G.J.-R., Violet, F., Garric, X., André, E.M., Schiller, P.C., Venier-Julienne, M.-C., des Rieux, A., Guicheux, J., Montero-Menei, C.N., 2017. Pharmacologically active microcarriers delivering BDNF within a hydrogel: Novel strategy for human bone marrow-derived stem cells neural/neuronal differentiation guidance and therapeutic secretome enhancement. Acta Biomater 49, 167–180. https://doi.org/10.1016/j.actbio.2016.11.030

Kaukonen, R., Jacquemet, G., Hamidi, H., Ivaska, J., 2017. Cell-derived matrices for studying cell proliferation and directional migration in a complex 3D microenvironment. Nat Protoc 12, 2376–2390. https://doi.org/10.1038/nprot.2017.107

Kavand, Hanie, van Lintel, H., Bakhshi Sichani, S., Bonakdar, S., Kavand, Hamed, Koohsorkhi, J., Renaud, P., 2019. Cell-Imprint Surface Modification by Contact Photolithography-Based Approaches: Direct-Cell Photolithography and Optical Soft Lithography Using PDMS Cell Imprints. ACS Appl Mater Interfaces 11, 10559–10566. https://doi.org/10.1021/acsami.9b00523

Kaw, A., Jones, D.G., Zhang, M., 2016. The use of animal tissues alongside human tissue: Cultural and ethical considerations. Clin Anat 29, 19–24. https://doi.org/10.1002/ca.22642

Kaynak Bayrak, G., Gümüşderelioğlu, M., 2019. Construction of cardiomyoblast sheets for cardiac tissue repair: comparison of three different approaches. Cytotechnology 819–833. https://doi.org/10.1007/s10616-019-00325-2

Kc, P., Shah, M., Shaik, R., Hong, Y., Zhang, G., 2020. Preseeding of Mesenchymal Stem Cells Increases Integration of an iPSC-Derived CM Sheet into a Cardiac Matrix. ACS Biomater Sci Eng 6, 6808–6818. https://doi.org/10.1021/acsbiomaterials.0c00788

Keane, T.J., Swinehart, I.T., Badylak, S.F., 2015. Methods of tissue decellularization used for preparation of biologic scaffolds and in vivo relevance. Methods 84, 25–34. https://doi.org/10.1016/j.ymeth.2015.03.005

Khaghani, S.A.B., Akbarova, G., Soon, C.F., Dilbazi, G., 2018. Effect of transforming growth factor-β2 on biological regulation of multilayer primary chondrocyte culture. Cell Tissue Bank 19, 763–775. https://doi.org/10.1007/s10561-018-9732-z

Khatab, S., Leijs, M.J., van Buul, G., Haeck, J., Kops, N., Nieboer, M., Bos, P.K., Verhaar, J.A.N., Bernsen, M., van Osch, G.J.V.M., 2020. MSC encapsulation in alginate microcapsules prolongs survival after intra-articular injection, a longitudinal in vivo cell and bead integrity tracking study. Cell Biol Toxicol 36, 553–570. https://doi.org/10.1007/s10565-020-09532-6

Kim, B.S., Choi, J.S., Kim, J.D., Choi, Y.C., Cho, Y.W., 2012. Recellularization of decellularized human adipose-tissue-derived extracellular matrix sheets with other human cell types. Cell Tissue Res 348, 559–567. https://doi.org/10.1007/s00441-012-1391-y

Kim, G., Jung, Y., Cho, K., Lee, H.J., Koh, W.-G., 2020. Thermoresponsive poly(N-isopropylacrylamide) hydrogel substrates micropatterned with poly(ethylene glycol) hydrogel for adipose mesenchymal stem cell spheroid formation and retrieval. Mater Sci Eng C Mater Biol Appl 115, 111128. https://doi.org/10.1016/j.msec.2020.111128

Kim, H., Kim, Y., Park, J., Hwang, N., Lee, Y., Hwang, Y., 2019. Recent Advances in Engineered Stem Cell-Derived Cell Sheets for Tissue Regeneration. Polymers 11, 209. https://doi.org/10.3390/polym11020209

Kim, I.G., Hwang, M.P., Du, P., Ko, J., Ha, C., Do, S.H., Park, K., 2015. Bioactive cell-derived matrices combined with polymer mesh scaffold for osteogenesis and bone healing. Biomaterials 50, 75–86. https://doi.org/10.1016/j.biomaterials.2015.01.054

Kim, J., Song, S.H., Jin, Y., Park, H.-J., Yoon, H., Jeon, S., Cho, S.-W., 2016. Multiphoton luminescent graphene quantum dots for in vivo tracking of human adipose-derived stem cells. Nanoscale 8, 8512–8519. https://doi.org/10.1039/c6nr02143c

Kim, M., Lee, J.Y., Jones, C.N., Revzin, A., Tae, G., 2010. Heparin-based hydrogel as a matrix for encapsulation and cultivation of primary hepatocytes. Biomaterials 31, 3596–3603. https://doi.org/10.1016/j.biomaterials.2010.01.068

Kim, S., Lee, S., Kim, K., 2018. Bone Tissue Engineering Strategies in Co-Delivery of Bone Morphogenetic Protein-2 and Biochemical Signaling Factors. Adv. Exp. Med. Biol. 1078, 233–244. https://doi.org/10.1007/978-981-13-0950-2_12

Kim, Y.S., Majid, M., Melchiorri, A.J., Mikos, A.G., 2019. Applications of decellularized extracellular matrix in bone and cartilage tissue engineering. Bioengineering & Translational Medicine 4, 83–95. https://doi.org/10.1002/btm2.10110

Kiyama, R., Nonoyama, T., Wada, S., Semba, S., Kitamura, N., Nakajima, T., Kurokawa, T., Yasuda, K., Tanaka, S., Gong, J.P., 2018. Micro patterning of hydroxyapatite by soft lithography on hydrogels for selective osteoconduction. Acta Biomater 81, 60–69. https://doi.org/10.1016/j.actbio.2018.10.002

Klar, A.S., Güven, S., Biedermann, T., Luginbühl, J., Böttcher-Haberzeth, S., Meuli-Simmen, C., Meuli, M., Martin, I., Scherberich, A., Reichmann, E., 2014. Tissue-engineered dermo-epidermal skin grafts prevascularized with adipose-derived cells. Biomaterials 35, 5065–5078. https://doi.org/10.1016/j.biomaterials.2014.02.049

Kobayashi, S., Takebe, T., Inui, M., Iwai, S., Kan, H., Zheng, Y.-W., Maegawa, J., Taniguchi, H., 2011. Reconstruction of human elastic cartilage by a CD44+ CD90+ stem cell in the ear perichondrium. Proceedings of the National Academy of Sciences 108, 14479–14484. https://doi.org/10.1073/pnas.1109767108

Kobayashi, Shinji, Takebe, T., Zheng, Y.-W., Mizuno, M., Yabuki, Y., Maegawa, J., Taniguchi, H., 2011. Presence of cartilage stem/progenitor cells in adult mice auricular perichondrium. PLoS ONE 6, e26393. https://doi.org/10.1371/journal.pone.0026393

Kolesnikova, T.A., Kohler, D., Skirtach, A.G., Möhwald, H., 2012. Laser-induced cell detachment, patterning, and regrowth on gold nanoparticle functionalized surfaces. ACS Nano 6, 9585–9595. https://doi.org/10.1021/nn302891u

Kuevda, E.V., Gubareva, E.A., Gumenyuk, I.S., Sotnichenko, A.S., Gilevich, I.V., Nakokhov, R.Z., Rusinova, T.V., Yudina, T.G., Red'ko, A.N., Alekseenko, S.N., 2017. Modification of Rat Lung Decellularization Protocol Based on Dynamic Conductometry of Working Solution. Bull Exp Biol Med 162, 703–706. https://doi.org/10.1007/s10517-017-3692-3

Kuna, V.K., Kvarnström, N., Elebring, E., Holgersson, S.S., 2018. Isolation and Decellularization of a Whole Porcine Pancreas. J Vis Exp. https://doi.org/10.3791/58302

Kundu, J., Michaelson, A., Talbot, K., Baranov, P., Young, M.J., Carrier, R.L., 2016. Decellularized retinal matrix: Natural platforms for human retinal progenitor cell culture. Acta Biomater 31, 61–70. https://doi.org/10.1016/j.actbio.2015.11.028

Kuramoto, G., Hammad, I.A., Einerson, B.D., Allshouse, A.A., Debbink, M., Grainger, D.W., Silver, R.M., Okano, T., 2020. Human Mesenchymal Stem Cell Sheets Improve Uterine Incision Repair in a Rodent Hysterotomy Model. Am J Perinatol. https://doi.org/10.1055/s-0040-1721718

Lakatos, K., Kalomoiris, S., Merkely, B., Nolta, J.A., Fierro, F.A., 2016. Mesenchymal Stem Cells Respond to Hypoxia by Increasing Diacylglycerols. J. Cell. Biochem. 117, 300–307. https://doi.org/10.1002/jcb.25292

Lane, S.W., Williams, D.A., Watt, F.M., 2014. Modulating the stem cell niche for tissue regeneration. Nat. Biotechnol. 32, 795–803. https://doi.org/10.1038/nbt.2978

Langer, R., Vacanti, J., 2016. Advances in Tissue Engineering. J Pediatr Surg 51, 8–12. https://doi.org/10.1016/j.jpedsurg.2015.10.022

Larochette, N., El-Hafci, H., Potier, E., Setterblad, N., Bensidhoum, M., Petite, H., Logeart-Avramoglou, D., 2020. Osteogenic-differentiated mesenchymal stem cell-secreted extracellular matrix as a bone morphogenetic protein-2 delivery system for ectopic bone formation. Acta Biomater 116, 186–200. https://doi.org/10.1016/j.actbio.2020.09.003

Lee, J., Jung, H., Park, N., Park, S.-H., Ju, J.H., 2019a. Induced Osteogenesis in Plants Decellularized Scaffolds. Sci Rep 9, 20194. https://doi.org/10.1038/s41598-019-56651-0

Lee, Jienny, Shin, M.S., Kim, M.O., Jang, S., Oh, S.W., Kang, M., Jung, K., Park, Y.S., Lee, Jongsung, 2016. Apple ethanol extract promotes proliferation of human adult stem cells, which involves the regenerative potential of stem cells. Nutr Res 36, 925–936. https://doi.org/10.1016/j.nutres.2016.06.010

Lee, Y.-C., Chan, Y.-H., Hsieh, S.-C., Lew, W.-Z., Feng, S.-W., 2019. Comparing the Osteogenic Potentials and Bone Regeneration Capacities of Bone Marrow and Dental Pulp Mesenchymal Stem Cells in a Rabbit Calvarial Bone Defect Model. Int J Mol Sci 20. https://doi.org/10.3390/ijms20205015

Lee, Y.N., Yi, H.-J., Seo, E.H., Oh, J., Lee, S., Ferber, S., Okano, T., Shim, I.K., Kim, S.C., 2021. Improvement of the therapeutic capacity of insulin-producing cells trans-differentiated from human liver cells using engineered cell sheet. Stem Cell Res Ther 12, 3. https://doi.org/10.1186/s13287-020-02080-0

Lehmann, J., Nürnberger, S., Narcisi, R., Stok, K.S., van der Eerden, B.C.J., Koevoet, W.J.L.M., Kops, N., ten Berge, D., van Osch, G.J., 2019. Recellularization of auricular cartilage via elastase-generated channels. Biofabrication 11, 035012. https://doi.org/10.1088/1758-5090/ab1436

Leslie, S.K., Cohen, D.J., Hyzy, S.L., Dosier, C.R., Nicolini, A., Sedlaczek, J., Schwartz, Z., Boyan, B.D., 2018. Microencapsulated rabbit adipose stem cells initiate tissue regeneration in a rabbit ear defect model. Journal of Tissue Engineering and Regenerative Medicine 12, 1742–1753. https://doi.org/10.1002/term.2702

Li, H., Chen, R., Jia, Z., Wang, C., Xu, Y., Li, C., Xia, H., Meng, D., 2020. Porous fish collagen for cartilage tissue engineering. Am J Transl Res 12, 6107–6121.

Li, J., He, F., Pei, M., 2011. Creation of an in vitro microenvironment to enhance human fetal synovium-derived stem cell chondrogenesis. Cell Tissue Res. 345, 357–365. https://doi.org/10.1007/s00441-011-1212-8

Li, S., Poche, J.N., Liu, Y., Scherr, T., McCann, J., Forghani, A., Smoak, M., Muir, M., Berntsen, L., Chen, C., Ravnic, D.J., Gimble, J., Hayes, D.J., 2018. Hybrid Synthetic-Biological Hydrogel System for Adipose Tissue Regeneration. Macromol Biosci 18, e1800122. https://doi.org/10.1002/mabi.201800122

Li, T., Chen, S., Pei, M., 2020. Contribution of neural crest-derived stem cells and nasal chondrocytes to articular cartilage regeneration. Cell Mol Life Sci 77, 4847–4859. https://doi.org/10.1007/s00018-020-03567-y

Li, X.S., Sun, J.J., 2019. [Regenerative medicine of tissue engineering : auricular cartilage regeneration and functional reconstruction]. Lin Chung Er Bi Yan Hou Tou Jing Wai Ke Za Zhi 33, 567–571. https://doi.org/10.13201/j.issn.1001-1781.2019.06.024

Li, Y., Wang, S., Huang, R., Huang, Z., Hu, B., Zheng, W., Yang, G., Jiang, X., 2015. Evaluation of the effect of the structure of bacterial cellulose on full thickness skin wound repair on a microfluidic chip. Biomacromolecules 16, 780–789. https://doi.org/10.1021/bm501680s

Liao, G.P., Choi, Y., Vojnits, K., Xue, H., Aroom, K., Meng, F., Pan, H.Y., Hetz, R.A., Corkins, C.J., Hughes, T.G., Triolo, F., Johnson, A., Moise, K.J., Lally, K.P., Cox, C.S., Li, Y., 2017. Tissue Engineering to Repair Diaphragmatic Defect in a Rat Model. Stem Cells Int 2017, 1764523. https://doi.org/10.1155/2017/1764523

Liaw, C.-Y., Ji, S., Guvendiren, M., 2018. Engineering 3D Hydrogels for Personalized In Vitro Human Tissue Models. Adv Healthc Mater 7. https://doi.org/10.1002/adhm.201701165

Lim, J.-Y., Ra, J.C., Shin, I.S., Jang, Y.H., An, H.-Y., Choi, J.-S., Kim, W.C., Kim, Y.-M., 2013. Systemic transplantation of human adipose tissue-derived mesenchymal stem cells for the regeneration of irradiation-induced salivary gland damage. PLoS ONE 8, e71167. https://doi.org/10.1371/journal.pone.0071167

Lim, M.H., Jeun, J.H., Kim, D.H., Park, S.H., Kim, S.-J., Lee, W.S., Hwang, S.H., Lim, J.Y., Kim, S.W., 2020. Evaluation of Collagen Gel-Associated Human Nasal Septum-Derived Chondrocytes As a Clinically Applicable Injectable Therapeutic Agent for Cartilage Repair. Tissue Eng Regen Med 17, 387–399. https://doi.org/10.1007/s13770-020-00261-9

Lin, C.-H., Hsia, K., Tsai, C.-H., Ma, H., Lu, J.-H., Tsay, R.-Y., 2019. Decellularized porcine coronary artery with adipose stem cells for vascular tissue engineering. Biomed Mater 14, 045014. https://doi.org/10.1088/1748-605X/ab2329

Lin, T., Wu, N., Wang, L., Zhang, R., Pan, R., Chen, Y.-F., 2021. Inhibition of chondrocyte apoptosis in a rat model of osteoarthritis by exosomes derived from miR-140-5p-overexpressing human dental pulp stem cells. Int J Mol Med 47. https://doi.org/10.3892/ijmm.2020.4840

Liu, Yi, Li, D., Yin, Z., Luo, X., Liu, W., Zhang, W., Zhang, Z., Cao, Y., Liu, Yu, Zhou, G., 2016. Prolonged in vitro precultivation alleviates post-implantation inflammation and promotes stable subcutaneous cartilage formation in a goat model. Biomed Mater 12, 015006. https://doi.org/10.1088/1748-605X/12/1/015006

Lo Monaco, M., Gervois, P., Beaumont, J., Clegg, P., Bronckaers, A., Vandeweerd, J.-M., Lambrichts, I., 2020. Therapeutic Potential of Dental Pulp Stem Cells and Leukocyte- and Platelet-Rich Fibrin for Osteoarthritis. Cells 9. https://doi.org/10.3390/cells9040980

Longoni, A., Utomo, L., van Hooijdonk, I.E., Bittermann, G.K., Vetter, V.C., Kruijt Spanjer, E.C., Ross, J., Rosenberg, A.J., Gawlitta, D., 2020. The chondrogenic differentiation potential of dental pulp stem cells. Eur Cell Mater 39, 121–135. https://doi.org/10.22203/eCM.v039a08

Lou, Z., 2020. Full-thickness cartilage graft myringoplasty combined with topical application of bFGF for repair of perforations with extensive epithelialization. Auris Nasus Larynx. https://doi.org/10.1016/j.anl.2020.11.013

Lu, T.-Y., Lin, B., Kim, J., Sullivan, M., Tobita, K., Salama, G., Yang, L., 2013. Repopulation of decellularized mouse heart with human induced pluripotent stem cell-derived

cardiovascular progenitor cells. Nat Commun 4, 2307. https://doi.org/10.1038/ncomms3307

Luo, L., Eswaramoorthy, R., Mulhall, K.J., Kelly, D.J., 2016a. Decellularization of porcine articular cartilage explants and their subsequent repopulation with human chondroprogenitor cells. Journal of the Mechanical Behavior of Biomedical Materials 55, 21–31. https://doi.org/10.1016/j.jmbbm.2015.10.002

Luo, L., Eswaramoorthy, R., Mulhall, K.J., Kelly, D.J., 2015. Decellularization of porcine articular cartilage explants and their subsequent repopulation with human chondroprogenitor cells. J Mech Behav Biomed Mater 55, 21–31. https://doi.org/10.1016/j.jmbbm.2015.10.002

Luquetti, D.V., Heike, C.L., Hing, A.V., Cunningham, M.L., Cox, T.C., 2012. Microtia: Epidemiology and genetics. Am. J. Med. Genet. 158A, 124–139. https://doi.org/10.1002/ajmg.a.34352

Ma, T., Grayson, W.L., Fröhlich, M., Vunjak-Novakovic, G., 2009. Hypoxia and Stem Cell-Based Engineering of Mesenchymal Tissues. Biotechnol Prog 25, 32–42. https://doi.org/10.1002/btpr.128

Maghsoudlou, P., Georgiades, F., Smith, H., Milan, A., Shangaris, P., Urbani, L., Loukogeorgakis, S.P., Lombardi, B., Mazza, G., Hagen, C., Sebire, N.J., Turmaine, M., Eaton, S., Olivo, A., Godovac-Zimmermann, J., Pinzani, M., Gissen, P., De Coppi, P., 2016. Optimization of Liver Decellularization Maintains Extracellular Matrix Micro-Architecture and Composition Predisposing to Effective Cell Seeding. PLoS ONE 11, e0155324. https://doi.org/10.1371/journal.pone.0155324

Mao, Y., Block, T., Singh-Varma, A., Sheldrake, A., Leeth, R., Griffey, S., Kohn, J., 2019. Extracellular matrix derived from chondrocytes promotes rapid expansion of human primary chondrocytes in vitro with reduced dedifferentiation. Acta Biomaterialia 85, 75–83. https://doi.org/10.1016/j.actbio.2018.12.006

Mao, Y., Hoffman, T., Wu, A., Kohn, J., 2018. An Innovative Laboratory Procedure to Expand Chondrocytes with Reduced Dedifferentiation. Cartilage 9, 202–211. https://doi.org/10.1177/1947603517746724

Marchionni, C., Bonsi, L., Alviano, F., Lanzoni, G., Di Tullio, A., Costa, R., Montanari, M., Tazzari, P.L., Ricci, F., Pasquinelli, G., Orrico, C., Grossi, A., Prati, C., Bagnara, G.P., 2009. Angiogenic potential of human dental pulp stromal (stem) cells. Int J Immunopathol Pharmacol 22, 699–706. https://doi.org/10.1177/039463200902200315

Marino, L., Castaldi, M.A., Rosamilio, R., Ragni, E., Vitolo, R., Fulgione, C., Castaldi, S.G., Serio, B., Bianco, R., Guida, M., Selleri, C., 2019. Mesenchymal Stem Cells from the Wharton's Jelly of the Human Umbilical Cord: Biological Properties and Therapeutic Potential. Int J Stem Cells 12, 218–226. https://doi.org/10.15283/ijsc18034

Markstedt, K., Mantas, A., Tournier, I., Martínez Ávila, H., Hägg, D., Gatenholm, P., 2015. 3D Bioprinting Human Chondrocytes with Nanocellulose-Alginate Bioink for Cartilage Tissue Engineering Applications. Biomacromolecules 16, 1489–1496. https://doi.org/10.1021/acs.biomac.5b00188

Martinello, T., Bronzini, I., Volpin, A., Vindigni, V., Maccatrozzo, L., Caporale, G., Bassetto, F., Patruno, M., 2014. Successful recellularization of human tendon scaffolds using adipose-derived mesenchymal stem cells and collagen gel: Recellularization of human tendon scaffolds. J Tissue Eng Regen Med 8, 612–619. https://doi.org/10.1002/term.1557

Martínez Ávila, H., Feldmann, E.-M., Pleumeekers, M.M., Nimeskern, L., Kuo, W., de Jong, W.C., Schwarz, S., Müller, R., Hendriks, J., Rotter, N., van Osch, G.J.V.M., Stok, K.S.,

Gatenholm, P., 2015. Novel bilayer bacterial nanocellulose scaffold supports neocartilage formation in vitro and in vivo. Biomaterials 44, 122–133. https://doi.org/10.1016/j.biomaterials.2014.12.025

Mata, M., Milian, L., Oliver, M., Zurriaga, J., Sancho-Tello, M., de Llano, J.J.M., Carda, C., 2017. In Vivo Articular Cartilage Regeneration Using Human Dental Pulp Stem Cells Cultured in an Alginate Scaffold: A Preliminary Study. Stem Cells Int 2017, 8309256. https://doi.org/10.1155/2017/8309256

Matsuura, K., Utoh, R., Nagase, K., Okano, T., 2014. Cell sheet approach for tissue engineering and regenerative medicine. Journal of Controlled Release 190, 228–239. https://doi.org/10.1016/j.jconrel.2014.05.024

Mayorca-Guiliani, A.E., Willacy, O., Madsen, C.D., Rafaeva, M., Elisabeth Heumüller, S., Bock, F., Sengle, G., Koch, M., Imhof, T., Zaucke, F., Wagener, R., Sasaki, T., Erler, J.T., Reuten, R., 2019. Decellularization and antibody staining of mouse tissues to map native extracellular matrix structures in 3D. Nat Protoc 14, 3395–3425. https://doi.org/10.1038/s41596-019-0225-8

Mazza, G., Rombouts, K., Rennie Hall, A., Urbani, L., Vinh Luong, T., Al-Akkad, W., Longato, L., Brown, D., Maghsoudlou, P., Dhillon, A.P., Fuller, B., Davidson, B., Moore, K., Dhar, D., De Coppi, P., Malago, M., Pinzani, M., 2015. Decellularized human liver as a natural 3D-scaffold for liver bioengineering and transplantation. Sci Rep 5, 13079. https://doi.org/10.1038/srep13079

Menaa, F., Abdelghani, A., Menaa, B., 2015. Graphene nanomaterials as biocompatible and conductive scaffolds for stem cells: impact for tissue engineering and regenerative medicine. J Tissue Eng Regen Med 9, 1321–1338. https://doi.org/10.1002/term.1910

Meretoja, V.V., Dahlin, R.L., Wright, S., Kasper, F.K., Mikos, A.G., 2013. The effect of hypoxia on the chondrogenic differentiation of co-cultured articular chondrocytes and mesenchymal stem cells in scaffolds. Biomaterials 34, 4266–4273. https://doi.org/10.1016/j.biomaterials.2013.02.064

Merrilees, M., Buunk, N., Zuo, N., Larsen, N., Karimi, S., Tucker, N., 2021. Use of Stacked Layers of Electrospun L-Lactide/Glycolide Co-Polymer Fibers for Rapid Construction of Skin Sheets. Bioengineering (Basel) 8. https://doi.org/10.3390/bioengineering8010007

Meyer, M., 2019. Processing of collagen based biomaterials and the resulting materials properties. Biomed Eng Online 18. https://doi.org/10.1186/s12938-019-0647-0

Min, S.-H., Kim, J.-H., Lee, M.-I., Kwak, H.-H., Woo, H.-M., Shim, J.-H., Choi, D.-M., Lee, J.-S., Jeong, J.-Y., Kang, B.-J., 2020. Evaluation of Auricular Cartilage Reconstruction Using a 3-Dimensional Printed Biodegradable Scaffold and Autogenous Minced Auricular Cartilage. Ann Plast Surg 85, 185–193. https://doi.org/10.1097/SAP.0000000000002313

Mirzaei, S., Karkhaneh, A., Soleimani, M., Ardeshirylajimi, A., Seyyed Zonouzi, H., Hanaee-Ahvaz, H., 2017. Enhanced chondrogenic differentiation of stem cells using an optimized electrospun nanofibrous PLLA/PEG scaffolds loaded with glucosamine: enhanced chondrogenic differentiation of stem cells. J. Biomed. Mater. Res. 105, 2461–2474. https://doi.org/10.1002/jbm.a.36104

Mitani, G., Sato, M., Lee, J.I.K., Kaneshiro, N., Ishihara, M., Ota, N., Kokubo, M., Sakai, H., Kikuchi, T., Mochida, J., 2009. The properties of bioengineered chondrocyte sheets for cartilage regeneration. BMC Biotechnol. 9, 17. https://doi.org/10.1186/1472-6750-9-17

Miyanaga, T., Ueda, Y., Miyanaga, A., Yagishita, M., Hama, N., 2018. Angiogenesis after administration of basic fibroblast growth factor induces proliferation and differentiation of

mesenchymal stem cells in elastic perichondrium in an in vivo model: mini review of three sequential republication-abridged reports. Cell. Mol. Biol. Lett. 23, 49. https://doi.org/10.1186/s11658-018-0113-1

Modulevsky, D.J., Cuerrier, C.M., Pelling, A.E., 2016a. Biocompatibility of Subcutaneously Implanted Plant-Derived Cellulose Biomaterials. PLoS ONE 11, e0157894. https://doi.org/10.1371/journal.pone.0157894

Modulevsky, D.J., Lefebvre, C., Haase, K., Al-Rekabi, Z., Pelling, A.E., 2014. Apple Derived Cellulose Scaffolds for 3D Mammalian Cell Culture. PLoS One 9. https://doi.org/10.1371/journal.pone.0097835

Möller, T., Amoroso, M., Hägg, D., Brantsing, C., Rotter, N., Apelgren, P., Lindahl, A., Kölby, L., Gatenholm, P., 2017. In Vivo Chondrogenesis in 3D Bioprinted Human Cell-laden Hydrogel Constructs: Plastic and Reconstructive Surgery - Global Open 5, e1227. https://doi.org/10.1097/GOX.0000000000001227

Moreno-Layseca, P., Icha, J., Hamidi, H., Ivaska, J., 2019. Integrin trafficking in cells and tissues. Nat Cell Biol 21, 122–132. https://doi.org/10.1038/s41556-018-0223-z

Mumme, M., Barbero, A., Miot, S., Wixmerten, A., Feliciano, S., Wolf, F., Asnaghi, A.M., Baumhoer, D., Bieri, O., Kretzschmar, M., Pagenstert, G., Haug, M., Schaefer, D.J., Martin, I., Jakob, M., 2016a. Nasal chondrocyte-based engineered autologous cartilage tissue for repair of articular cartilage defects: an observational first-in-human trial. Lancet 388, 1985–1994. https://doi.org/10.1016/S0140-6736(16)31658-0

Mumme, M., Steinitz, A., Nuss, K.M., Klein, K., Feliciano, S., Kronen, P., Jakob, M., von Rechenberg, B., Martin, I., Barbero, A., Pelttari, K., 2016b. Regenerative Potential of Tissue-Engineered Nasal Chondrocytes in Goat Articular Cartilage Defects. Tissue Eng Part A 22, 1286–1295. https://doi.org/10.1089/ten.TEA.2016.0159

Nagata, S., 1993. A new method of total reconstruction of the auricle for microtia. Plast Reconstr Surg 92, 187–201. https://doi.org/10.1097/00006534-199308000-00001

Nakajima, K., Kunimatsu, R., Ando, K., Ando, T., Hayashi, Y., Kihara, T., Hiraki, T., Tsuka, Y., Abe, T., Kaku, M., Nikawa, H., Takata, T., Tanne, K., Tanimoto, K., 2018. Comparison of the bone regeneration ability between stem cells from human exfoliated deciduous teeth, human dental pulp stem cells and human bone marrow mesenchymal stem cells. Biochem Biophys Res Commun 497, 876–882. https://doi.org/10.1016/j.bbrc.2018.02.156

Namiri, M., Kazemi Ashtiani, M., Abbasalizadeh, S., Mazidi, Z., Mahmoudi, E., Nikeghbalian, S., Aghdami, N., Baharvand, H., 2018. Improving the biological function of decellularized heart valves through integration of protein tethering and three-dimensional cell seeding in a bioreactor. J Tissue Eng Regen Med 12, e1865–e1879. https://doi.org/10.1002/term.2617

Nasonova, M.V., Glushkova, T.V., Borisov, V.V., Velikanova, E.A., Burago, A.Y., Kudryavtseva, Y.A., 2015. Biocompatibility and Structural Features of Biodegradable Polymer Scaffolds. Bull. Exp. Biol. Med. 160, 134–140. https://doi.org/10.1007/s10517-015-3114-3

Negrini, N.C., Toffoletto, N., Farè, S., Altomare, L., 2020. Plant Tissues as 3D Natural Scaffolds for Adipose, Bone and Tendon Tissue Regeneration. Frontiers in Bioengineering and Biotechnology 8. https://doi.org/10.3389/fbioe.2020.00723

Nemeth, C.L., Janebodin, K., Yuan, A.E., Dennis, J.E., Reyes, M., Kim, D.-H., 2014. Enhanced chondrogenic differentiation of dental pulp stem cells using nanopatterned PEG-GelMA-HA hydrogels. Tissue Eng Part A 20, 2817–2829. https://doi.org/10.1089/ten.TEA.2013.0614

Neybecker, P., Henrionnet, C., Pape, E., Mainard, D., Galois, L., Loeuille, D., Gillet, P., Pinzano, A., 2018. In vitro and in vivo potentialities for cartilage repair from human advanced knee osteoarthritis synovial fluid-derived mesenchymal stem cells. Stem Cell Res Ther 9, 329. https://doi.org/10.1186/s13287-018-1071-2

Nixon, A.J., Sparks, H.D., Begum, L., McDonough, S., Scimeca, M.S., Moran, N., Matthews, G.L., 2017. Matrix-Induced Autologous Chondrocyte Implantation (MACI) Using a Cell-Seeded Collagen Membrane Improves Cartilage Healing in the Equine Model. J Bone Joint Surg Am 99, 1987–1998. https://doi.org/10.2106/JBJS.16.00603

Novais, A., Lesieur, J., Sadoine, J., Slimani, L., Baroukh, B., Saubaméa, B., Schmitt, A., Vital, S., Poliard, A., Hélary, C., Rochefort, G.Y., Chaussain, C., Gorin, C., 2019. Priming Dental Pulp Stem Cells from Human Exfoliated Deciduous Teeth with Fibroblast Growth Factor-2 Enhances Mineralization Within Tissue-Engineered Constructs Implanted in Craniofacial Bone Defects. Stem Cells Transl Med 8, 844–857. https://doi.org/10.1002/sctm.18-0182

Nürnberger, S., Schneider, C., van Osch, G.V.M., Keibl, C., Rieder, B., Monforte, X., Teuschl, A.H., Mühleder, S., Holnthoner, W., Schädl, B., Gahleitner, C., Redl, H., Wolbank, S., 2019. Repopulation of an auricular cartilage scaffold, AuriScaff, perforated with an enzyme combination. Acta Biomaterialia 86, 207–222. https://doi.org/10.1016/j.actbio.2018.12.035

Oh, S.-J., Choi, K.-U., Choi, S.-W., Kim, S.-D., Kong, S.-K., Lee, S., Cho, K.-S., 2020. Comparative Analysis of Adipose-Derived Stromal Cells and Their Secretome for Auricular Cartilage Regeneration. Stem Cells Int 2020, 8595940. https://doi.org/10.1155/2020/8595940

Oh, S.-J., Park, H.-Y., Choi, K.-U., Choi, S.-W., Kim, S.-D., Kong, S.-K., Cho, K.-S., 2018. Auricular Cartilage Regeneration with Adipose-Derived Stem Cells in Rabbits. Mediators Inflamm 2018. https://doi.org/10.1155/2018/4267158

Ohara, T., Muneta, T., Nakagawa, Y., Matsukura, Y., Ichinose, S., Koga, H., Tsuji, K., Sekiya, I., 2016. <Original Article>Hypoxia enhances proliferation through increase of colony formation rate with chondrogenic potential in primary synovial mesenchymal stem cells. J. Med. Dent. Sci. 63, 61–70. https://doi.org/10.11480/jmds.630401

Ohishi, M., Schipani, E., 2010. Bone marrow mesenchymal stem cells. J. Cell. Biochem. 109, 277–282. https://doi.org/10.1002/jcb.22399

Okano, T., Yamada, N., Sakai, H., Sakurai, Y., 1993. A novel recovery system for cultured cells using plasma-treated polystyrene dishes grafted with poly(N-isopropylacrylamide). J. Biomed. Mater. Res. 27, 1243–1251. https://doi.org/10.1002/jbm.820271005

Okubo, R., Asawa, Y., Watanabe, M., Nagata, S., Nio, M., Takato, T., Hikita, A., Hoshi, K., 2019. Proliferation medium in three-dimensional culture of auricular chondrocytes promotes effective cartilage regeneration in vivo. Regen Ther 11, 306–315. https://doi.org/10.1016/j.reth.2019.10.002

Onoshima, D., Yukawa, H., Baba, Y., 2015. Multifunctional quantum dots-based cancer diagnostics and stem cell therapeutics for regenerative medicine. Adv. Drug Deliv. Rev. 95, 2–14. https://doi.org/10.1016/j.addr.2015.08.004

Ott, H.C., Matthiesen, T.S., Goh, S.-K., Black, L.D., Kren, S.M., Netoff, T.I., Taylor, D.A., 2008. Perfusion-decellularized matrix: using nature's platform to engineer a bioartificial heart. Nature Medicine 14, 213–221. https://doi.org/10.1038/nm1684

Otto, I.A., Levato, R., Webb, W.R., Khan, I.M., Breugem, C.C., Malda, J., 2018a. Progenitor cells in auricular cartilage demonstrate cartilage-forming capacity in 3D hydrogel culture. Eur Cell Mater 35, 132–150. https://doi.org/10.22203/eCM.v035a10

Ouyang, A., Cerchiari, A.E., Tang, X., Liebenberg, E., Alliston, T., Gartner, Z.J., Lotz, J.C., 2017. Effects of cell type and configuration on anabolic and catabolic activity in 3D co-culture of mesenchymal stem cells and nucleus pulposus cells. J Orthop Res 35, 61–73. https://doi.org/10.1002/jor.23452

Ozguldez, H.O., Cha, J., Hong, Y., Koh, I., Kim, P., 2018. Nanoengineered, cell-derived extracellular matrix influences ECM-related gene expression of mesenchymal stem cells. Biomater Res 22, 32. https://doi.org/10.1186/s40824-018-0141-y

Öztürk, E., Hobiger, S., Despot-Slade, E., Pichler, M., Zenobi-Wong, M., 2017. Hypoxia regulates RhoA and Wnt/β-catenin signaling in a context-dependent way to control re-differentiation of chondrocytes. Sci Rep 7, 9032. https://doi.org/10.1038/s41598-017-09505-6

Paino, F., La Noce, M., Tirino, V., Naddeo, P., Desiderio, V., Pirozzi, G., De Rosa, A., Laino, L., Altucci, L., Papaccio, G., 2014. Histone deacetylase inhibition with valproic acid downregulates osteocalcin gene expression in human dental pulp stem cells and osteoblasts: evidence for HDAC2 involvement. Stem Cells 32, 279–289. https://doi.org/10.1002/stem.1544

Palaninathan, V., Raveendran, S., Rochani, A.K., Chauhan, N., Sakamoto, Y., Ukai, T., Maekawa, T., Kumar, D.S., 2018. Bioactive bacterial cellulose sulfate electrospun nanofibers for tissue engineering applications. J Tissue Eng Regen Med 12, 1634–1645. https://doi.org/10.1002/term.2689

Pang, K., Du, L., Wu, X., 2010. A rabbit anterior cornea replacement derived from acellular porcine cornea matrix, epithelial cells and keratocytes. Biomaterials 31, 7257–7265. https://doi.org/10.1016/j.biomaterials.2010.05.066

Park, E.H., Lim, H.-S., Lee, S., Roh, K., Seo, K.-W., Kang, K.-S., Shin, K., 2018. Intravenous Infusion of Umbilical Cord Blood-Derived Mesenchymal Stem Cells in Rheumatoid Arthritis: A Phase Ia Clinical Trial. Stem Cells Transl Med 7, 636–642. https://doi.org/10.1002/sctm.18-0031

Park, J.Y., Choi, Y.-J., Shim, J.-H., Park, J.H., Cho, D.-W., 2017. Development of a 3D cell printed structure as an alternative to autologs cartilage for auricular reconstruction: 3D CELL PRINTED STRUCTURE FOR AURICULAR RECONSTRUCTION. J. Biomed. Mater. Res. 105, 1016–1028. https://doi.org/10.1002/jbm.b.33639

Park, M., Lee, D., Shin, S., Hyun, J., 2015. Effect of negatively charged cellulose nanofibers on the dispersion of hydroxyapatite nanoparticles for scaffolds in bone tissue engineering. Colloids Surf B Biointerfaces 130, 222–228. https://doi.org/10.1016/j.colsurfb.2015.04.014

Pattappa, G., Krueckel, J., Schewior, R., Franke, D., Mench, A., Koch, M., Weber, J., Lang, S., Pfeifer, C.G., Johnstone, B., Docheva, D., Alt, V., Angele, P., Zellner, J., 2020. Physioxia Expanded Bone Marrow Derived Mesenchymal Stem Cells Have Improved Cartilage Repair in an Early Osteoarthritic Focal Defect Model. Biology (Basel) 9. https://doi.org/10.3390/biology9080230

Peck, S.H., Bendigo, J.R., Tobias, J.W., Dodge, G.R., Malhotra, N.R., Mauck, R.L., Smith, L.J., 2019. Hypoxic Preconditioning Enhances Bone Marrow-Derived Mesenchymal Stem Cell Survival in a Low Oxygen and Nutrient-Limited 3D Microenvironment. Cartilage 1947603519841675. https://doi.org/10.1177/1947603519841675

Pedroni, A.C.F., Diniz, I.M.A., Abe, G.L., Moreira, M.S., Sipert, C.R., Marques, M.M., 2018. Photobiomodulation therapy and vitamin C on longevity of cell sheets of human dental pulp stem cells. J. Cell. Physiol. 233, 7026–7035. https://doi.org/10.1002/jcp.26626

Perez, R.A., El-Fiqi, A., Park, J.-H., Kim, T.-H., Kim, J.-H., Kim, H.-W., 2014. Therapeutic bioactive microcarriers: Co-delivery of growth factors and stem cells for bone tissue engineering. Acta Biomaterialia 10, 520–530. https://doi.org/10.1016/j.actbio.2013.09.042

Perez-Puyana, V., Jiménez-Rosado, M., Romero, A., Guerrero, A., 2020. Polymer-Based Scaffolds for Soft-Tissue Engineering. Polymers (Basel) 12. https://doi.org/10.3390/polym12071566

Pettinato, G., Lehoux, S., Ramanathan, R., Salem, M.M., He, L.-X., Muse, O., Flaumenhaft, R., Thompson, M.T., Rouse, E.A., Cummings, R.D., Wen, X., Fisher, R.A., 2019. Generation of fully functional hepatocyte-like organoids from human induced pluripotent stem cells mixed with Endothelial Cells. Sci Rep 9, 8920. https://doi.org/10.1038/s41598-019-45514-3

Pham, D.T., Tiyaboonchai, W., 2020. Fibroin nanoparticles: a promising drug delivery system. Drug Deliv 27, 431–448. https://doi.org/10.1080/10717544.2020.1736208

Phan, N.V., Wright, T., Rahman, M.M., Xu, J., Coburn, J.M., 2020. In Vitro Biocompatibility of Decellularized Cultured Plant Cell-Derived Matrices. ACS Biomater Sci Eng 6, 822–832. https://doi.org/10.1021/acsbiomaterials.9b00870

Pleumeekers, M.M., Nimeskern, L., Koevoet, W.L.M., Karperien, M., Stok, K.S., van Osch, G.J.V.M., 2015. Cartilage Regeneration in the Head and Neck Area: Combination of Ear or Nasal Chondrocytes and Mesenchymal Stem Cells Improves Cartilage Production. Plastic and Reconstructive Surgery 136, 762e–774e. https://doi.org/10.1097/PRS.0000000000001812

Pomerantseva, I., Bichara, D.A., Tseng, A., Cronce, M.J., Cervantes, T.M., Kimura, A.M., Neville, C.M., Roscioli, N., Vacanti, J.P., Randolph, M.A., Sundback, C.A., 2016a. Ear-Shaped Stable Auricular Cartilage Engineered from Extensively Expanded Chondrocytes in an Immunocompetent Experimental Animal Model. Tissue Eng Part A 22, 197–207. https://doi.org/10.1089/ten.TEA.2015.0173

Powell, S.K., Cruz, R.L.J., Ross, M.T., Woodruff, M.A., 2020. Past, Present, and Future of Soft-Tissue Prosthetics: Advanced Polymers and Advanced Manufacturing. Adv Mater 32, e2001122. https://doi.org/10.1002/adma.202001122

Powles-Glover, N., Maconochie, M., 2018. Prenatal and postnatal development of the mammalian ear. Birth Defects Res 110, 228–245. https://doi.org/10.1002/bdr2.1167

Pradhan, S., Clary, J.M., Seliktar, D., Lipke, E.A., 2017. A three-dimensional spheroidal cancer model based on PEG-fibrinogen hydrogel microspheres. Biomaterials 115, 141–154. https://doi.org/10.1016/j.biomaterials.2016.10.052

Puschmann, T.B., Zandén, C., De Pablo, Y., Kirchhoff, F., Pekna, M., Liu, J., Pekny, M., 2013. Bioactive 3D cell culture system minimizes cellular stress and maintains the in vivo-like morphological complexity of astroglial cells. Glia 61, 432–440. https://doi.org/10.1002/glia.22446

Qiao, K., Guo, S., Zheng, Y., Xu, X., Meng, H., Peng, J., Fang, Z., Xie, Y., 2018. Effects of graphene on the structure, properties, electro-response behaviors of GO/PAA composite hydrogels and influence of electro-mechanical coupling on BMSC differentiation. Mater Sci Eng C Mater Biol Appl 93, 853–863. https://doi.org/10.1016/j.msec.2018.08.047

Qiu, Y., Xu, X., Guo, W., Zhao, Y., Su, J., Chen, J., 2020. Mesoporous Hydroxyapatite Nanoparticles Mediate the Release and Bioactivity of BMP-2 for Enhanced Bone Regeneration. ACS Biomater Sci Eng 6, 2323–2335. https://doi.org/10.1021/acsbiomaterials.9b01954

Rahman, S., Griffin, M., Naik, A., Szarko, M., Butler, P.E.M., 2018. Optimising the decellularization of human elastic cartilage with trypsin for future use in ear reconstruction. Sci Rep 8. https://doi.org/10.1038/s41598-018-20592-x

Rajalekshmi, R., Kaladevi Shaji, A., Joseph, R., Bhatt, A., 2021. Scaffold for liver tissue engineering: Exploring the potential of fibrin incorporated alginate dialdehyde-gelatin hydrogel. Int J Biol Macromol 166, 999–1008. https://doi.org/10.1016/j.ijbiomac.2020.10.256

Ramm, R., Goecke, T., Theodoridis, K., Hoeffler, K., Sarikouch, S., Findeisen, K., Ciubotaru, A., Cebotari, S., Tudorache, I., Haverich, A., Hilfiker, A., 2020. Decellularization combined with enzymatic removal of N-linked glycans and residual DNA reduces inflammatory response and improves performance of porcine xenogeneic pulmonary heart valves in an ovine in vivo model. Xenotransplantation 27, e12571. https://doi.org/10.1111/xen.12571

Rana, D., Zreiqat, H., Benkirane-Jessel, N., Ramakrishna, S., Ramalingam, M., 2017. Development of decellularized scaffolds for stem cell-driven tissue engineering. J Tissue Eng Regen Med 11, 942–965. https://doi.org/10.1002/term.2061

Reboredo, J.W., Weigel, T., Steinert, A., Rackwitz, L., Rudert, M., Walles, H., 2016. Investigation of Migration and Differentiation of Human Mesenchymal Stem Cells on Five-Layered Collagenous Electrospun Scaffold Mimicking Native Cartilage Structure. Adv Healthc Mater 5, 2191–2198. https://doi.org/10.1002/adhm.201600134

Rees, A., Powell, L.C., Chinga-Carrasco, G., Gethin, D.T., Syverud, K., Hill, K.E., Thomas, D.W., 2015. 3D Bioprinting of Carboxymethylated-Periodate Oxidized Nanocellulose Constructs for Wound Dressing Applications. Biomed Res Int 2015, 925757. https://doi.org/10.1155/2015/925757

Ren, Z., Ma, S., Jin, L., Liu, Z., Liu, D., Zhang, X., Cai, Q., Yang, X., 2017. Repairing a bone defect with a three-dimensional cellular construct composed of a multi-layered cell sheet on electrospun mesh. Biofabrication 9, 025036. https://doi.org/10.1088/1758-5090/aa747f

Robertson, M.J., Dries-Devlin, J.L., Kren, S.M., Burchfield, J.S., Taylor, D.A., 2014. Optimizing recellularization of whole decellularized heart extracellular matrix. PLoS ONE 9, e90406. https://doi.org/10.1371/journal.pone.0090406

Robins, J.C., Akeno, N., Mukherjee, A., Dalal, R.R., Aronow, B.J., Koopman, P., Clemens, T.L., 2005. Hypoxia induces chondrocyte-specific gene expression in mesenchymal cells in association with transcriptional activation of Sox9. Bone 37, 313–322. https://doi.org/10.1016/j.bone.2005.04.040

Rodas-Junco, B.A., Canul-Chan, M., Rojas-Herrera, R.A., De-la-Peña, C., Nic-Can, G.I., 2017. Stem Cells from Dental Pulp: What Epigenetics Can Do with Your Tooth. Front Physiol 8, 999. https://doi.org/10.3389/fphys.2017.00999

Rodríguez-Vázquez, M., Vega-Ruiz, B., Ramos-Zúñiga, R., Saldaña-Koppel, D.A., Quiñones-Olvera, L.F., 2015. Chitosan and Its Potential Use as a Scaffold for Tissue Engineering in Regenerative Medicine. Biomed Res Int 2015. https://doi.org/10.1155/2015/821279

Rorick, C.B., Mitchell, J.A., Bledsoe, R.H., Floren, M.L., Wilkins, R.M., 2020. Cryopreserved, Thin, Laser-Etched Osteochondral Allograft maintains the functional components of

articular cartilage after 2 years of storage. J Orthop Surg Res 15, 521. https://doi.org/10.1186/s13018-020-02049-y

Rosa, R.G., Joazeiro, P.P., Bianco, J., Kunz, M., Weber, J.F., Waldman, S.D., 2014. Growth factor stimulation improves the structure and properties of scaffold-free engineered auricular cartilage constructs. PLoS ONE 9, e105170. https://doi.org/10.1371/journal.pone.0105170

Safi, I.N., Mohammed Ali Hussein, B., Al-Shammari, A.M., 2019. In vitro periodontal ligament cell expansion by co-culture method and formation of multi-layered periodontal ligament-derived cell sheets. Regen Ther 11, 225–239. https://doi.org/10.1016/j.reth.2019.08.002

Sahai, N., Gogoi, M., Tewari, R.P., 2020. 3D printed Chitosan Composite Scaffold for Chondrocytes differentiation. Curr Med Imaging. https://doi.org/10.2174/1573405616666201217112939

Sahu, N., Agarwal, P., Grandi, F., Bruschi, M., Goodman, S., Amanatullah, D., Bhutani, N., 2021. Encapsulated Mesenchymal Stromal Cell Microbeads Promote Endogenous Regeneration of Osteoarthritic Cartilage Ex Vivo. Adv Healthc Mater e2002118. https://doi.org/10.1002/adhm.202002118

Saka, N., Watanabe, Y., Abe, S., Yajima, A., Kawano, H., 2019. Implant-type tissue-engineered cartilage derived from human auricular chondrocyte may maintain cartilaginous property even under osteoinductive condition. Regen Med Res 7, 1. https://doi.org/10.1051/rmr/190001

Sakai, Y., Koike, M., Hasegawa, H., Yamanouchi, K., Soyama, A., Takatsuki, M., Kuroki, T., Ohashi, K., Okano, T., Eguchi, S., 2013. Rapid fabricating technique for multi-layered human hepatic cell sheets by forceful contraction of the fibroblast monolayer. PLoS One 8, e70970. https://doi.org/10.1371/journal.pone.0070970

Sakai, Y., Koike, M., Kawahara, D., Hasegawa, H., Murai, T., Yamanouchi, K., Soyama, A., Hidaka, M., Takatsuki, M., Fujita, F., Kuroki, T., Eguchi, S., 2018. Controlled cell morphology and liver-specific function of engineered primary hepatocytes by fibroblast layer cell densities. J. Biosci. Bioeng. 126, 249–257. https://doi.org/10.1016/j.jbiosc.2018.02.006

Samadi, P., Saki, S., Khoshinani, H.M., Sheykhhasan, M., 2020. Therapeutic applications of mesenchymal stem cells: A comprehensive review. Curr Stem Cell Res Ther. https://doi.org/10.2174/1574888X15666200914142709

Sawyer, J.D., Wilson, M.L., Neumeister, M.W., 2018. A Systematic Review of Surgical Management of Melanoma of the External Ear. Plast Reconstr Surg Glob Open 6, e1755. https://doi.org/10.1097/GOX.0000000000001755

Saygili, E., Kaya, E., Ilhan-Ayisigi, E., Saglam-Metiner, P., Alarcin, E., Kazan, A., Girgic, E., Kim, Y.-W., Gunes, K., Eren-Ozcan, G.G., Akakin, D., Sun, J.-Y., Yesil-Celiktas, O., 2021. An alginate-poly(acrylamide) hydrogel with TGF-β3 loaded nanoparticles for cartilage repair: Biodegradability, biocompatibility and protein adsorption. Int J Biol Macromol. https://doi.org/10.1016/j.ijbiomac.2021.01.069

Schenke-Layland, K., Vasilevski, O., Opitz, F., König, K., Riemann, I., Halbhuber, K.J., Wahlers, T., Stock, U.A., 2003. Impact of decellularization of xenogeneic tissue on extracellular matrix integrity for tissue engineering of heart valves. J. Struct. Biol. 143, 201–208. https://doi.org/10.1016/j.jsb.2003.08.002

Schmidt, S., Abinzano, F., Mensinga, A., Teßmar, J., Groll, J., Malda, J., Levato, R., Blunk, T., 2020. Differential Production of Cartilage ECM in 3D Agarose Constructs by Equine

Articular Cartilage Progenitor Cells and Mesenchymal Stromal Cells. Int J Mol Sci 21. https://doi.org/10.3390/ijms21197071

Schwarz, S., Koerber, L., Elsaesser, A.F., Goldberg-Bockhorn, E., Seitz, A.M., Dürselen, L., Ignatius, A., Walther, P., Breiter, R., Rotter, N., 2012. Decellularized Cartilage Matrix as a Novel Biomatrix for Cartilage Tissue-Engineering Applications. Tissue Engineering Part A 18, 2195–2209. https://doi.org/10.1089/ten.tea.2011.0705

Serban, M.A., Liu, Y., Prestwich, G.D., 2008. Effects of extracellular matrix analogues on primary human fibroblast behavior. Acta Biomaterialia 4, 67–75. https://doi.org/10.1016/j.actbio.2007.09.006

Shafiee, A., Kabiri, M., Langroudi, L., Soleimani, M., Ai, J., 2016. Evaluation and comparison of the *in vitro* characteristics and chondrogenic capacity of four adult stem/progenitor cells for cartilage cell-based repair: comparative chondrogenesis of adult stem/progenitor cells. J. Biomed. Mater. Res. 104, 600–610. https://doi.org/10.1002/jbm.a.35603

Shafiee, A., Seyedjafari, E., Sadat Taherzadeh, E., Dinarvand, P., Soleimani, M., Ai, J., 2014. Enhanced chondrogenesis of human nasal septum derived progenitors on nanofibrous scaffolds. Materials Science and Engineering: C 40, 445–454. https://doi.org/10.1016/j.msec.2014.04.027

Sharma, K., Mujawar, M.A., Kaushik, A., 2019. State-of-Art Functional Biomaterials for Tissue Engineering. Front. Mater. 6. https://doi.org/10.3389/fmats.2019.00172

Shi, W., Sun, M., Hu, X., Ren, B., Cheng, J., Li, C., Duan, X., Fu, X., Zhang, J., Chen, H., Ao, Y., 2017. Structurally and Functionally Optimized Silk-Fibroin-Gelatin Scaffold Using 3D Printing to Repair Cartilage Injury In Vitro and In Vivo. Adv Mater 29. https://doi.org/10.1002/adma.201701089

Shi, Y., Ma, J., Zhang, X., Li, H., Jiang, L., Qin, J., 2015. Hypoxia combined with spheroid culture improves cartilage specific function in chondrocytes. Integr Biol (Camb) 7, 289–297. https://doi.org/10.1039/c4ib00273c

Shimizu, R., Kamei, N., Adachi, N., Hamanishi, M., Kamei, G., Mahmoud, E.E., Nakano, T., Iwata, T., Yamato, M., Okano, T., Ochi, M., 2015. Repair mechanism of osteochondral defect promoted by bioengineered chondrocyte sheet. Tissue Eng Part A 21, 1131–1141. https://doi.org/10.1089/ten.TEA.2014.0310

Shotorbani, B.B., André, H., Barzegar, A., Zarghami, N., Salehi, R., Alizadeh, E., 2018. Cell sheet biofabrication by co-administration of mesenchymal stem cells secretome and vitamin C on thermoresponsive polymer. J Mater Sci Mater Med 29, 170. https://doi.org/10.1007/s10856-018-6180-z

Silva, A.S., Santos, L.F., Mendes, M.C., Mano, J.F., 2020. Multi-layer pre-vascularized magnetic cell sheets for bone regeneration. Biomaterials 231, 119664. https://doi.org/10.1016/j.biomaterials.2019.119664

Smith, C.A., Board, T.N., Rooney, P., Eagle, M.J., Richardson, S.M., Hoyland, J.A., 2017. Human decellularized bone scaffolds from aged donors show improved osteoinductive capacity compared to young donor bone. PLoS One 12, e0177416. https://doi.org/10.1371/journal.pone.0177416

Speichert, S., Molotkov, N., El Bagdadi, K., Meurer, A., Zaucke, F., Jenei-Lanzl, Z., 2019. Role of Norepinephrine in IL-1β-Induced Chondrocyte Dedifferentiation under Physioxia. Int J Mol Sci 20. https://doi.org/10.3390/ijms20051212

Stephan, S., Reinisch, J., 2018. Auricular Reconstruction Using Porous Polyethylene Implant Technique. Facial Plast Surg Clin North Am 26, 69–85. https://doi.org/10.1016/j.fsc.2017.09.009

Sterodimas, A., de Faria, J., 2013. Human Auricular Tissue Engineering in an Immunocompetent Animal Model. Aesthetic Surgery Journal 33, 283–289. https://doi.org/10.1177/1090820X12472902

Sullivan, D.C., Mirmalek-Sani, S.-H., Deegan, D.B., Baptista, P.M., Aboushwareb, T., Atala, A., Yoo, J.J., 2012. Decellularization methods of porcine kidneys for whole organ engineering using a high-throughput system. Biomaterials 33, 7756–7764. https://doi.org/10.1016/j.biomaterials.2012.07.023

Sundberg, J., Götherström, C., Gatenholm, P., 2015. Biosynthesis and in vitro evaluation of macroporous mineralized bacterial nanocellulose scaffolds for bone tissue engineering. Biomed Mater Eng 25, 39–52. https://doi.org/10.3233/BME-141245

Syed, O., Walters, N.J., Day, R.M., Kim, H.-W., Knowles, J.C., 2014. Evaluation of decellularization protocols for production of tubular small intestine submucosa scaffolds for use in oesophageal tissue engineering. Acta Biomater 10, 5043–5054. https://doi.org/10.1016/j.actbio.2014.08.024

Taghavi, H., Soleimani Rad, J., Mehdipour, A., Ferdosi Khosroshahi, A., Kheirjou, R., Hasanpour, M., Roshangar, L., 2020. Effect of Mineral Pitch on the Proliferation of Human Adipose Derived Stem Cells on Acellular Scaffold. Adv Pharm Bull 10, 623–629. https://doi.org/10.34172/apb.2020.075

Tajima, K., Kuroda, K., Otaka, Y., Kinoshita, R., Kita, M., Oyamada, T., Kanai, K., 2020. Decellularization of canine kidney for three-dimensional organ regeneration. Vet World 13, 452–457. https://doi.org/10.14202/vetworld.2020.452-457

Takaku, Y., Murai, K., Ukai, T., Ito, S., Kokubo, M., Satoh, M., Kobayashi, E., Yamato, M., Okano, T., Takeuchi, M., Mochida, J., Sato, M., 2014. In vivo cell tracking by bioluminescence imaging after transplantation of bioengineered cell sheets to the knee joint. Biomaterials 35, 2199–2206. https://doi.org/10.1016/j.biomaterials.2013.11.071

Takebe, T., Sekine, K., Kimura, M., Yoshizawa, E., Ayano, S., Koido, M., Funayama, S., Nakanishi, N., Hisai, T., Kobayashi, T., Kasai, T., Kitada, R., Mori, A., Ayabe, H., Ejiri, Y., Amimoto, N., Yamazaki, Y., Ogawa, S., Ishikawa, M., Kiyota, Y., Sato, Y., Nozawa, K., Okamoto, S., Ueno, Y., Taniguchi, H., 2017. Massive and Reproducible Production of Liver Buds Entirely from Human Pluripotent Stem Cells. Cell Rep 21, 2661–2670. https://doi.org/10.1016/j.celrep.2017.11.005

Takeuchi, R., Kuruma, Y., Sekine, H., Dobashi, I., Yamato, M., Umezu, M., Shimizu, T., Okano, T., 2016. In vivo vascularization of cell sheets provided better long-term tissue survival than injection of cell suspension. J Tissue Eng Regen Med 10, 700–710. https://doi.org/10.1002/term.1854

Takizawa, D., Sato, M., Okada, E., Takahashi, T., Maehara, M., Tominaga, A., Sogo, Y., Toyoda, E., Watanabe, M., 2020. Regenerative effects of human chondrocyte sheets in a xenogeneic transplantation model using immune-deficient rats. J Tissue Eng Regen Med 14, 1296–1306. https://doi.org/10.1002/term.3101

Talaat, W., Aryal Ac, S., Al Kawas, S., Samsudin, A.B.R., Kandile, N.G., Harding, D.R.K., Ghoneim, M.M., Zeiada, W., Jagal, J., Aboelnaga, A., Haider, M., 2020. Nanoscale Thermosensitive Hydrogel Scaffolds Promote the Chondrogenic Differentiation of Dental

Pulp Stem and Progenitor Cells: A Minimally Invasive Approach for Cartilage Regeneration. Int J Nanomedicine 15, 7775–7789. https://doi.org/10.2147/IJN.S274418

Tan Timur, U., Caron, M., van den Akker, G., van der Windt, A., Visser, J., van Rhijn, L., Weinans, H., Welting, T., Emans, P., Jahr, H., 2019. Increased TGF-β and BMP Levels and Improved Chondrocyte-Specific Marker Expression In Vitro under Cartilage-Specific Physiological Osmolarity. Int J Mol Sci 20. https://doi.org/10.3390/ijms20040795

Tani, G., Usui, N., Kamiyama, M., Oue, T., Fukuzawa, M., 2010. In vitro construction of scaffold-free cylindrical cartilage using cell sheet-based tissue engineering. Pediatr. Surg. Int. 26, 179–185. https://doi.org/10.1007/s00383-009-2543-3

Tanzer, R.C., 1959. Total reconstruction of the external ear. Plast Reconstr Surg Transplant Bull 23, 1–15. https://doi.org/10.1097/00006534-195901000-00001

Thorp, H., Kim, K., Kondo, M., Grainger, D.W., Okano, T., 2020. Fabrication of hyaline-like cartilage constructs using mesenchymal stem cell sheets. Sci Rep 10, 20869. https://doi.org/10.1038/s41598-020-77842-0

Togo, T., Utani, A., Naitoh, M., Ohta, M., Tsuji, Y., Morikawa, N., Nakamura, M., Suzuki, S., 2006. Identification of cartilage progenitor cells in the adult ear perichondrium: utilization for cartilage reconstruction. Lab. Invest. 86, 445–457. https://doi.org/10.1038/labinvest.3700409

Toyoda, E., Sato, M., Takahashi, T., Maehara, M., Okada, E., Wasai, S., Iijima, H., Nonaka, K., Kawaguchi, Y., Watanabe, M., 2019. Transcriptomic and Proteomic Analyses Reveal the Potential Mode of Action of Chondrocyte Sheets in Hyaline Cartilage Regeneration. IJMS 21, 149. https://doi.org/10.3390/ijms21010149

Tracy, L.E., Minasian, R.A., Caterson, E.J., 2016. Extracellular Matrix and Dermal Fibroblast Function in the Healing Wound. Adv Wound Care (New Rochelle) 5, 119–136. https://doi.org/10.1089/wound.2014.0561

Unkovskiy, A., Spintzyk, S., Brom, J., Huettig, F., Keutel, C., 2018. Direct 3D printing of silicone facial prostheses: A preliminary experience in digital workflow. J Prosthet Dent 120, 303–308. https://doi.org/10.1016/j.prosdent.2017.11.007

Urbano, J.J., da Palma, R.K., de Lima, F.M., Fratini, P., Guimaraes, L.L., Uriarte, J.J., Alvarenga, L.H., Miglino, M.A., Vieira, R. de P., Prates, R.A., Navajas, D., Farrè, R., Oliveira, L.V.F., 2017. Effects of two different decellularization routes on the mechanical properties of decellularized lungs. PLoS One 12, e0178696. https://doi.org/10.1371/journal.pone.0178696

Utomo, L., Pleumeekers, M.M., Nimeskern, L., Nürnberger, S., Stok, K.S., Hildner, F., van Osch, G.J.V.M., 2015. Preparation and characterization of a decellularized cartilage scaffold for ear cartilage reconstruction. Biomed. Mater. 10, 015010. https://doi.org/10.1088/1748-6041/10/1/015010

Vas, W.J., Shah, M., Blacker, T.S., Duchen, M.R., Sibbons, P., Roberts, S.J., 2018. Decellularized Cartilage Directs Chondrogenic Differentiation: Creation of a Fracture Callus Mimetic. Tissue Eng Part A 24, 1364–1376. https://doi.org/10.1089/ten.TEA.2017.0450

Vasanthan, J., Gurusamy, N., Rajasingh, S., Sigamani, V., Kirankumar, S., Thomas, E.L., Rajasingh, J., 2020. Role of Human Mesenchymal Stem Cells in Regenerative Therapy. Cells 10. https://doi.org/10.3390/cells10010054

Vayas, R., Reyes, R., Rodríguez-Évora, M., Del Rosario, C., Delgado, A., Évora, C., 2017. Evaluation of the effectiveness of a bMSC and BMP-2 polymeric trilayer system in cartilage repair. Biomed Mater 12, 045001. https://doi.org/10.1088/1748-605X/aa6f1c

Vieira, S., Vial, S., Reis, R.L., Oliveira, J.M., 2017. Nanoparticles for bone tissue engineering. Biotechnol. Prog. 33, 590–611. https://doi.org/10.1002/btpr.2469

Visscher, D.O., Gleadall, A., Buskermolen, J.K., Burla, F., Segal, J., Koenderink, G.H., Helder, M.N., van Zuijlen, P.P.M., 2019a. Design and fabrication of a hybrid alginate hydrogel/poly(ε-caprolactone) mold for auricular cartilage reconstruction. Journal of Biomedical Materials Research Part B: Applied Biomaterials 107, 1711–1721. https://doi.org/10.1002/jbm.b.34264

Visscher, D.O., Gleadall, A., Buskermolen, J.K., Burla, F., Segal, J., Koenderink, G.H., Helder, M.N., van Zuijlen, P.P.M., 2019b. Design and fabrication of a hybrid alginate hydrogel/poly(ε-caprolactone) mold for auricular cartilage reconstruction. J. Biomed. Mater. Res. Part B Appl. Biomater. 107, 1711–1721. https://doi.org/10.1002/jbm.b.34264

von Bomhard, A., Elsaesser, A., Riepl, R., Pippich, K., Faust, J., Schwarz, S., Koerber, L., Breiter, R., Rotter, N., 2019. Cartilage regeneration using decellularized cartilage matrix: Long-term comparison of subcutaneous and intranasal placement in a rabbit model. Journal of Cranio-Maxillofacial Surgery 47, 682–694. https://doi.org/10.1016/j.jcms.2019.01.010

von Bomhard, A., Veit, J., Bermueller, C., Rotter, N., Staudenmaier, R., Storck, K., The, H.N., 2013. Prefabrication of 3D cartilage contructs: towards a tissue engineered auricle--a model tested in rabbits. PLoS ONE 8, e71667. https://doi.org/10.1371/journal.pone.0071667

Walawalkar, S., Almelkar, S., 2020. Fabricating a pre-vascularized large-sized metabolically-supportive scaffold using Brassica oleracea leaf. J Biomater Appl 885328220968388. https://doi.org/10.1177/0885328220968388

Wang, F., Hu, Y., He, D., Zhou, G., Yang, X., Ellis, E., 2017. Regeneration of subcutaneous tissue-engineered mandibular condyle in nude mice. J Craniomaxillofac Surg 45, 855–861. https://doi.org/10.1016/j.jcms.2017.03.017

Wang, H., Li, Y., Chen, J., Wang, X., Zhao, F., Cao, S., 2014. [Chondrogenesis of bone marrow mesenchymal stem cells induced by transforming growth factor beta3 gene in Diannan small-ear pigs]. Zhongguo Xiu Fu Chong Jian Wai Ke Za Zhi 28, 149–154.

Wang, L.-R., Lin, Y.-Q., Wang, J.-T., Pan, L.-L., Huang, K.-T., Wan, L., Zhu, G.-Q., Liu, W.-Y., Braddock, M., Zheng, M.-H., 2015. Recent advances in re-engineered liver: de-cellularization and re-cellularization techniques. Cytotherapy 17, 1015–1024. https://doi.org/10.1016/j.jcyt.2015.04.003

Wang, P., Sun, Y., Shi, X., Shen, H., Ning, H., Liu, H., 2021. 3D printing of tissue engineering scaffolds: a focus on vascular regeneration. Biodes Manuf 1–35. https://doi.org/10.1007/s42242-020-00109-0

Wang, T., Dong, N., Yan, H., Wong, S.Y., Zhao, W., Xu, K., Wang, D., Li, S., Qiu, X., 2019. Regeneration of a neoartery through a completely autologous acellular conduit in a minipig model: a pilot study. J Transl Med 17, 24. https://doi.org/10.1186/s12967-018-1763-5

Wang, X., Li, B., Zhang, C., 2019. Preparation of BMP-2/chitosan/hydroxyapatite antibacterial bio-composite coatings on titanium surfaces for bone tissue engineering. Biomed Microdevices 21, 89. https://doi.org/10.1007/s10544-019-0437-2

Wang, X., Wu, T.T., Jiang, L., Rong, D., Zhu, Y.Q., 2017. Deferoxamine-Induced Migration and Odontoblast Differentiation via ROS-Dependent Autophagy in Dental Pulp Stem Cells. Cell Physiol Biochem 43, 2535–2547. https://doi.org/10.1159/000484506

Wang, X., Xue, Y., Ye, W., Pang, J., Liu, Z., Cao, Y., Zheng, Y., Ding, D., 2018. The MEK-ERK1/2 signaling pathway regulates hyaline cartilage formation and the redifferentiation of dedifferentiated chondrocytes in vitro. Am J Transl Res 10, 3068–3085.

Wang, X.-Y., Pei, Y., Xie, M., Jin, Z.-H., Xiao, Y.-S., Wang, Y., Zhang, L.-N., Li, Y., Huang, W.-H., 2015. An artificial blood vessel implanted three-dimensional microsystem for modeling transvascular migration of tumor cells. Lab Chip 15, 1178–1187. https://doi.org/10.1039/c4lc00973h

Wang, Y., Xu, Y., Zhou, G., Liu, Y., Cao, Y., 2020. Biological Evaluation of Acellular Cartilaginous and Dermal Matrixes as Tissue Engineering Scaffolds for Cartilage Regeneration. Front Cell Dev Biol 8, 624337. https://doi.org/10.3389/fcell.2020.624337

Wang, Y., Yuan, X., Yu, K., Meng, H., Zheng, Y., Peng, J., Lu, S., Liu, X., Xie, Y., Qiao, K., 2018. Fabrication of nanofibrous microcarriers mimicking extracellular matrix for functional microtissue formation and cartilage regeneration. Biomaterials 171, 118–132. https://doi.org/10.1016/j.biomaterials.2018.04.033

Wang, Z., Han, L., Sun, T., Ma, J., Sun, S., Ma, L., Wu, B., 2020. Extracellular matrix derived from allogenic decellularized bone marrow mesenchymal stem cell sheets for the reconstruction of osteochondral defects in rabbits. Acta Biomater 118, 54–68. https://doi.org/10.1016/j.actbio.2020.10.022

Wang, Z., Li, Zhiye, Li, Zhijin, Wu, B., Liu, Y., Wu, W., 2018. Cartilaginous extracellular matrix derived from decellularized chondrocyte sheets for the reconstruction of osteochondral defects in rabbits. Acta Biomaterialia 81, 129–145. https://doi.org/10.1016/j.actbio.2018.10.005

Wasyłeczko, M., Sikorska, W., Chwojnowski, A., 2020. Review of Synthetic and Hybrid Scaffolds in Cartilage Tissue Engineering. Membranes (Basel) 10. https://doi.org/10.3390/membranes10110348

Wei, F., Qu, C., Song, T., Ding, G., Fan, Z., Liu, D., Liu, Y., Zhang, C., Shi, S., Wang, S., 2012. Vitamin C treatment promotes mesenchymal stem cell sheet formation and tissue regeneration by elevating telomerase activity. J. Cell. Physiol. 227, 3216–3224. https://doi.org/10.1002/jcp.24012

Weizel, A., Distler, T., Schneidereit, D., Friedrich, O., Bräuer, L., Paulsen, F., Detsch, R., Boccaccini, A.R., Budday, S., Seitz, H., 2020. Complex mechanical behavior of human articular cartilage and hydrogels for cartilage repair. Acta Biomater 118, 113–128. https://doi.org/10.1016/j.actbio.2020.10.025

Wernheden, E., Krogerus, C., Andersen, P.S., Hesselfeldt-Nielsen, J., 2019. [Congenital anomalies of the external ear]. Ugeskr Laeger 181.

Westin, C.B., Trinca, R.B., Zuliani, C., Coimbra, I.B., Moraes, Â.M., 2017. Differentiation of dental pulp stem cells into chondrocytes upon culture on porous chitosan-xanthan scaffolds in the presence of kartogenin. Mater Sci Eng C Mater Biol Appl 80, 594–602. https://doi.org/10.1016/j.msec.2017.07.005

Whitney, G.A., Mera, H., Weidenbecher, M., Awadallah, A., Mansour, J.M., Dennis, J.E., 2012. Methods for producing scaffold-free engineered cartilage sheets from auricular and articular chondrocyte cell sources and attachment to porous tantalum. Biores Open Access 1, 157–165. https://doi.org/10.1089/biores.2012.0231

Wise, S.G., Yeo, G.C., Hiob, M.A., Rnjak-Kovacina, J., Kaplan, D.L., Ng, M.K.C., Weiss, A.S., 2014. Tropoelastin: a versatile, bioactive assembly module. Acta Biomater 10, 1532–1541. https://doi.org/10.1016/j.actbio.2013.08.003

Wongin, S., Narkbunnam, R., Waikakul, S., Chotiyarnwong, P., Aresanasuwan, T., Roytrakul, S., Viravaidya-Pasuwat, K., 2020. Construction and Evaluation of Osteochondral-Like Tissue Using Chondrocyte Sheet and Cancellous Bone. Tissue Eng Part A. https://doi.org/10.1089/ten.TEA.2020.0107

Wrenn, S.M., Griswold, E.D., Uhl, F.E., Uriarte, J.J., Park, H.E., Coffey, A.L., Dearborn, J.S., Ahlers, B.A., Deng, B., Lam, Y.-W., Huston, D.R., Lee, P.C., Wagner, D.E., Weiss, D.J., 2018. Avian lungs: A novel scaffold for lung bioengineering. PLoS One 13, e0198956. https://doi.org/10.1371/journal.pone.0198956

Wu, J., Yin, N., Chen, S., Weibel, D., Wang, H., 2019. Simultaneous 3D cell distribution and bioactivity enhancement of bacterial cellulose (BC) scaffold for articular cartilage tissue engineering. Cellulose 26. https://doi.org/10.1007/s10570-018-02240-9

Wu, Y.-K., Tu, Y.-K., Yu, J., Cheng, N.-C., 2020. The Influence of Cell Culture Density on the Cytotoxicity of Adipose-Derived Stem Cells Induced by L-Ascorbic Acid-2-Phosphate. Sci Rep 10, 104. https://doi.org/10.1038/s41598-019-56875-0

Xia, H., Zhao, D., Zhu, H., Hua, Y., Xiao, K., Xu, Y., Liu, Yanqun, Chen, W., Liu, Yu, Zhang, W., Liu, W., Tang, S., Cao, Y., Wang, X., Chen, H.H., Zhou, G., 2018. Lyophilized Scaffolds Fabricated from 3D-Printed Photocurable Natural Hydrogel for Cartilage Regeneration. ACS Appl. Mater. Interfaces 10, 31704–31715. https://doi.org/10.1021/acsami.8b10926

Xie, L., Chan, K.-Y., Quirke, N., 2017. Poly(ethylene glycol) (PEG) in a Polyethylene (PE) Framework: A Simple Model for Simulation Studies of a Soluble Polymer in an Open Framework. Langmuir 33, 11746–11753. https://doi.org/10.1021/acs.langmuir.7b02253

Xing, Q., Yates, K., Tahtinen, M., Shearier, E., Qian, Z., Zhao, F., 2015. Decellularization of fibroblast cell sheets for natural extracellular matrix scaffold preparation. Tissue Eng Part C Methods 21, 77–87. https://doi.org/10.1089/ten.tec.2013.0666

Xu, S., Lu, F., Cheng, L., Li, C., Zhou, X., Wu, Y., Chen, H., Zhang, K., Wang, L., Xia, J., Yan, G., Qi, Z., 2017. Preparation and characterization of small-diameter decellularized scaffolds for vascular tissue engineering in an animal model. Biomed Eng Online 16, 55. https://doi.org/10.1186/s12938-017-0344-9

Xu, Y., Duan, L., Li, Y., She, Y., Zhu, J., Zhou, G., Jiang, G., Yang, Y., 2020. Nanofibrillar Decellularized Wharton's Jelly Matrix for Segmental Tracheal Repair. Advanced Functional Materials 30, 1910067. https://doi.org/10.1002/adfm.201910067

Xue, J., He, A., Zhu, Y., Liu, Y., Li, D., Yin, Z., Zhang, W., Liu, W., Cao, Y., Zhou, G., 2018. Repair of articular cartilage defects with acellular cartilage sheets in a swine model. Biomed. Mater. 13, 025016. https://doi.org/10.1088/1748-605X/aa99a4

Xue, K., Zhang, X., Qi, L., Zhou, J., Liu, K., 2016. Isolation, identification, and comparison of cartilage stem progenitor/cells from auricular cartilage and perichondrium. Am J Transl Res 8, 732–741.

Xue, M., Jackson, C.J., 2015. Extracellular Matrix Reorganization During Wound Healing and Its Impact on Abnormal Scarring. Adv Wound Care (New Rochelle) 4, 119–136. https://doi.org/10.1089/wound.2013.0485

Yan, J., Chen, X., Pu, C., Zhao, Y., Liu, X., Liu, T., Pan, G., Lin, J., Pei, M., Yang, H., He, F., 2020. Synovium stem cell-derived matrix enhances anti-inflammatory properties of rabbit articular chondrocytes via the SIRT1 pathway. Mater Sci Eng C Mater Biol Appl 106, 110286. https://doi.org/10.1016/j.msec.2019.110286

Yang, R., Wang, X., Liu, S., Zhang, W., Wang, P., Liu, X., Ren, Y., Tan, X., Chi, B., 2020. Bioinspired poly (γ-glutamic acid) hydrogels for enhanced chondrogenesis of bone marrow-derived mesenchymal stem cells. International Journal of Biological Macromolecules 142, 332–344. https://doi.org/10.1016/j.ijbiomac.2019.09.104

Yang, S., Zhu, B., Yin, P., Zhao, L., Wang, Y., Fu, Z., Dang, R., Xu, J., Zhang, J., Wen, N., 2020. Integration of Human Umbilical Cord Mesenchymal Stem Cells-Derived Exosomes with Hydroxyapatite-Embedded Hyaluronic Acid-Alginate Hydrogel for Bone Regeneration. ACS Biomater Sci Eng 6, 1590–1602. https://doi.org/10.1021/acsbiomaterials.9b01363

Yang, W., Chen, Q., Xia, R., Zhang, Y., Shuai, L., Lai, J., You, X., Jiang, Y., Bie, P., Zhang, L., Zhang, H., Bai, L., 2018. A novel bioscaffold with naturally-occurring extracellular matrix promotes hepatocyte survival and vessel patency in mouse models of heterologous transplantation. Biomaterials 177, 52–66. https://doi.org/10.1016/j.biomaterials.2018.05.026

Yang, X., Han, G., Pang, X., Fan, M., 2012. Chitosan/collagen scaffold containing bone morphogenetic protein-7 DNA supports dental pulp stem cell differentiation in vitro and in vivo. J Biomed Mater Res A. https://doi.org/10.1002/jbm.a.34064

Yang, X., Lu, Z., Wu, H., Li, W., Zheng, L., Zhao, J., 2018a. Collagen-alginate as bioink for three-dimensional (3D) cell printing based cartilage tissue engineering. Materials Science and Engineering: C 83, 195–201. https://doi.org/10.1016/j.msec.2017.09.002

Yao, Q., Cosme, J.G.L., Xu, T., Miszuk, J.M., Picciani, P.H.S., Fong, H., Sun, H., 2017. Three dimensional electrospun PCL/PLA blend nanofibrous scaffolds with significantly improved stem cells osteogenic differentiation and cranial bone formation. Biomaterials 115, 115–127. https://doi.org/10.1016/j.biomaterials.2016.11.018

Yao, Y., Zhang, T., Chen, H., Zheng, S., Chen, Y., Zhang, S., 2020. Enhanced chondrogenesis in a coculture system with genetically manipulated dedifferentiated chondrocytes and ATDC5 cells. Biotechnol Bioeng 117, 3173–3181. https://doi.org/10.1002/bit.27482

Yin, J., Qiu, S., Shi, B., Xu, X., Zhao, Y., Gao, J., Zhao, S., Min, S., 2018. Controlled release of FGF-2 and BMP-2 in tissue engineered periosteum promotes bone repair in rats. Biomed Mater 13, 025001. https://doi.org/10.1088/1748-605X/aa93c0

Yoshida, A., Kitajiri, S.-I., Nakagawa, T., Hashido, K., Inaoka, T., Ito, J., 2011. Adipose tissue-derived stromal cells protect hair cells from aminoglycoside. Laryngoscope 121, 1281–1286. https://doi.org/10.1002/lary.21551

Yu, J., Wang, M.-Y., Tai, H.-C., Cheng, N.-C., 2018. Cell sheet composed of adipose-derived stem cells demonstrates enhanced skin wound healing with reduced scar formation. Acta Biomater 77, 191–200. https://doi.org/10.1016/j.actbio.2018.07.022

Yue, H., Pathak, J.L., Zou, R., Qin, L., Liao, T., Hu, Y., Kuang, W., Zhou, L., 2021. Fabrication of chondrocytes/chondrocyte-microtissues laden fibrin gel auricular scaffold for microtia reconstruction. J Biomater Appl 35, 838–848. https://doi.org/10.1177/0885328220954415

Zhang, C., Salick, M.R., Cordie, T.M., Ellingham, T., Dan, Y., Turng, L.-S., 2015. Incorporation of poly(ethylene glycol) grafted cellulose nanocrystals in poly(lactic acid) electrospun nanocomposite fibers as potential scaffolds for bone tissue engineering. Mater Sci Eng C Mater Biol Appl 49, 463–471. https://doi.org/10.1016/j.msec.2015.01.024

Zhang, L., He, A., Yin, Z., Yu, Z., Luo, X., Liu, W., Zhang, W., Cao, Y., Liu, Y., Zhou, G., 2014. Regeneration of human-ear-shaped cartilage by co-culturing human microtia chondrocytes with BMSCs. Biomaterials 35, 4878–4887. https://doi.org/10.1016/j.biomaterials.2014.02.043

Zhang, Q.-Y., Bai, J.-D., Wu, X.-A., Liu, X.-N., Zhang, M., Chen, W.-Y., 2020. Microniche geometry modulates the mechanical properties and calcium signaling of chondrocytes. J Biomech 104, 109729. https://doi.org/10.1016/j.jbiomech.2020.109729

Zhang, W., Yang, G., Wang, X., Jiang, L., Jiang, F., Li, G., Zhang, Z., Jiang, X., 2017. Magnetically Controlled Growth-Factor-Immobilized Multilayer Cell Sheets for Complex Tissue Regeneration. Adv. Mater. Weinheim 29. https://doi.org/10.1002/adma.201703795

Zhang, W., Zhu, Y., Li, J., Guo, Q., Peng, J., Liu, S., Yang, J., Wang, Y., 2016. Cell-Derived Extracellular Matrix: Basic Characteristics and Current Applications in Orthopedic Tissue Engineering. Tissue Eng Part B Rev 22, 193–207. https://doi.org/10.1089/ten.TEB.2015.0290

Zhang, X., Qi, L., Chen, Y., Xiong, Z., Li, J., Xu, P., Pan, Z., Zhang, H., Chen, Z., Xue, K., Liu, K., 2019a. The in vivo chondrogenesis of cartilage stem/progenitor cells from auricular cartilage and the perichondrium. Am J Transl Res 11, 2855–2865.

Zhang, Y., Feng, G., Xu, G., Qi, Y., 2019. Microporous acellular extracellular matrix combined with adipose-derived stem cell sheets as a promising tissue patch promoting articular cartilage regeneration and interface integration. Cytotherapy 21, 856–869. https://doi.org/10.1016/j.jcyt.2019.02.005

Zhang, Y., Hao, C., Guo, W., Peng, X., Wang, M., Yang, Z., Li, X., Zhang, X., Chen, M., Sui, X., Peng, J., Lu, S., Liu, S., Guo, Q., Jiang, Q., 2020. Co-culture of hWJMSCs and pACs in double biomimetic ACECM oriented scaffold enhances mechanical properties and accelerates articular cartilage regeneration in a caprine model. Stem Cell Res Ther 11. https://doi.org/10.1186/s13287-020-01670-2

Zhao, C., Li, Y., Peng, G., Lei, X., Zhang, G., Gao, Y., 2020. Decellularized liver matrix-modified chitosan fibrous scaffold as a substrate for C3A hepatocyte culture. J Biomater Sci Polym Ed 31, 1041–1056. https://doi.org/10.1080/09205063.2020.1738690

Zhao, Q., Hai, B., Kelly, J., Wu, S., Liu, F., 2021. Extracellular vesicle mimics made from iPS cell-derived mesenchymal stem cells improve the treatment of metastatic prostate cancer. Stem Cell Res Ther 12, 29. https://doi.org/10.1186/s13287-020-02097-5

Zheng, X.-F., Lu, S.-B., Zhang, W.-G., Liu, S.-Y., Huang, J.-X., Guo, Q.-Y., 2011. Mesenchymal stem cells on a decellularized cartilage matrix for cartilage tissue engineering. Biotechnology and Bioprocess Engineering 16, 593–602. https://doi.org/10.1007/s12257-010-0348-9

Zhou, G., Jiang, H., Yin, Z., Liu, Y., Zhang, Q., Zhang, C., Pan, B., Zhou, J., Zhou, X., Sun, H., Li, D., He, A., Zhang, Z., Zhang, W., Liu, W., Cao, Y., 2018. In Vitro Regeneration of Patient-specific Ear-shaped Cartilage and Its First Clinical Application for Auricular Reconstruction. EBioMedicine 28, 287–302. https://doi.org/10.1016/j.ebiom.2018.01.011

Zhou, J., Fritze, O., Schleicher, M., Wendel, H.-P., Schenke-Layland, K., Harasztosi, C., Hu, S., Stock, U.A., 2010. Impact of heart valve decellularization on 3-D ultrastructure, immunogenicity and thrombogenicity. Biomaterials 31, 2549–2554. https://doi.org/10.1016/j.biomaterials.2009.11.088

Zhou, Q., Li, B., Zhao, J., Pan, W., Xu, J., Chen, S., 2016. IGF-I induces adipose derived mesenchymal cell chondrogenic differentiation in vitro and enhances chondrogenesis in vivo. In Vitro Cell. Dev. Biol. Anim. 52, 356–364. https://doi.org/10.1007/s11626-015-9969-9

Zhou, S., Wang, Y., Zhang, K., Cao, N., Yang, R., Huang, J., Zhao, W., Rahman, M., Liao, H., Fu, Q., 2020. The Fabrication and Evaluation of a Potential Biomaterial Produced with

Stem Cell Sheet Technology for Future Regenerative Medicine. Stem Cells Int 2020, 9567362. https://doi.org/10.1155/2020/9567362

Zhou, Y., Xie, S., Tang, Y., Li, X., Cao, Y., Hu, J., Lu, H., 2021. Effect of book-shaped acellular tendon scaffold with bone marrow mesenchymal stem cells sheets on bone-tendon interface healing. J Orthop Translat 26, 162–170. https://doi.org/10.1016/j.jot.2020.02.013

Zhou, Y., Yue, Z., Chen, Z., Wallace, G., 2020. 3D Coaxial Printing Tough and Elastic Hydrogels for Tissue Engineering Using a Catechol Functionalized Ink System. Adv Healthc Mater 9, e2001342. https://doi.org/10.1002/adhm.202001342

Ziegler, M.E., Sorensen, A.M., Banyard, D.A., Evans, G.R.D., Widgerow, A.D., 2021. Improving In Vitro Cartilage Generation by Co-Culturing Adipose-Derived Stem Cells and Chondrocytes on an Allograft Adipose Matrix Framework. Plast Reconstr Surg 147, 87–99. https://doi.org/10.1097/PRS.0000000000007511

Zvarova, B., Uhl, F.E., Uriarte, J.J., Borg, Z.D., Coffey, A.L., Bonenfant, N.R., Weiss, D.J., Wagner, D.E., 2016. Residual Detergent Detection Method for Nondestructive Cytocompatibility Evaluation of Decellularized Whole Lung Scaffolds. Tissue Eng Part C Methods 22, 418–428. https://doi.org/10.1089/ten.TEC.2015.0439

Résumé en français

I-Introduction

1-Anomalies de l'oreille externe

L'oreille externe est sujete à de nombreuses pathologies, principalement dues à des malformations congénitales ou à des causes acquises, telles que les traumatismes, les accidents et parfois le cancer.

1.1 Les anoties et microties congénitales

Les microties et anoties correspondent à des pertes de substance auriculaire congénitales plus ou moins totales. La microtie est une croissance anormale ou un sous-développement de l'oreille externe. Elle peut aller d'une anomalie mineure jusqu'à l'anotie, qui se caractérise par une absence totale de l'oreille externe et elle constitue la forme la plus grave de microtie. Anomalies auriculaires congénitales se présentent sous la forme de malformations isolées ou peuvent être associées à d'autres syndromes, notamment ceux liés à la région cranio-faciale. La microtie allant de 0,8 à 8,3 pour 10000 naissances vivantes peut affecter un côté (unilatéral) ou les deux côtés (bilatéral), où les hommes courent un risque plus élevé que les femmes. Elle peut également être associée à plusieurs syndromes tels que le syndrome d'Alport, la dysplasie spondyloïde, entraînant une perte auditive et l'absence de structure cartilagineuse externe (Hartzell et Chinnadurai, 2018). Qu'il s'agisse d'une difformité majeure ou mineure, les deux cas peuvent avoir un impact important sur l'estime et la perception de soi d'un enfant en grandissant, ce qui affecte sa santé psychologique (Johns *et al*., 2015).

1.2 Traumatismes de l'oreille externe et amputations

Le pavillon de l'oreille étant une structure saillante, il est plus susceptible d'être endommagé accidentellement par des traumatismes, des amputations, des brûlures et des lésions cancéreuses. En raison de leur localisation latéro-faciale et de leur hélice, les oreilles sont largement exposées au soleil. C'est donc logiquement qu'elles sont plus sensibles à différents carcinomes tels que le carcinome basocellulaire, le carcinome épidermoïde ou le mélanome. De plus, les morsures d'animaux et les accidents sont une cause fréquente de traumatisme.

2-Options actuelles de traitement

2.1-Reconstruction avec du cartilage autologue

La correction d'une oreille normale a toujours été un défi pour les chirurgiens. Tanzer a été le premier à décrire une reconstruction de l'oreille à partir de cartilage costal autologue qui a été plus tard considérée comme la méthode de référence. Sa technique était révolutionnaire puisqu'elle était la seule solution pour les patients souffrant de microtie. Cependant, cette dernière était une technique lourde qui nécessitait une procédure chirurgicale en 6 étapes. La première étape consistait à transposer le lobule dans sa position anatomique normale. Il a ensuite créé le cadre en prélevant sur les côtes pour reconstruire la base, l'hélice et l'antihélix. Ensuite, il a combiné la charpente et, au bout de 4 mois, a projeté la charpente un peu loin de la tête et a recouvert le sillon rétro-auriculaire d'une greffe de peau épaisse. Après 4 mois supplémentaires, le tunnel auditif a été fermé et 6 semaines plus tard, la conque et le tragus ont été reconstruits à l'aide de greffes de cartilage (Tanzer, 1959). D'autres scientifiques se sont appuyés sur la technique de Tanzer et l'ont optimisée.

Les deux chirurgiens qui ont grandement contribué à la reconstruction de l'oreille ont été Brent et Nagata. Brent établit une technique en quatre étapes, étape par étape, pour corriger la microtie (Brent, 1980). Il commence par insérer une armature cartilagineuse autologue dans une poche de peau, puis transpose le lobule, construit le tragus et enfin, construit le sillon rétro-auriculaire. Bien que des résultats satisfaisants aient été obtenus avec cette technique, elle a été critiquée par Firmin, qui a souligné que les contours étaient encore imparfaits et que le tragus était parfois décevant, ainsi que lorsque le lambeau rétro-auriculaire se détériorait avec le temps (Firmin, 1998). Nagata, en revanche, a présenté une technique en deux étapes pour reconstruire des oreilles microtiques. Il a commencé par construire un cadre complet de cartilage de côtes et par le découper en une forme semi-lunaire. Ensuite, il a fixé le cadre fermement derrière l'anthélix pour reconstruire la paroi postérieure de la conque. Cela a permis d'éviter une rétraction secondaire de la peau. Pour terminer l'étape de la transplantation, un rabat articulé recouvrant le greffon de cartilage a été ajouté (Nagata,1993). En France, Françoise Firmin avait également réalisé la plupart de ses reconstructions d'oreilles en deux étapes séparées par un délai de six mois (Firmin et Marchac,

2011). Le principal avantage des techniques en deux temps est qu'elles sont moins longues, mais plus difficiles et qu'elles nécessitent des chirurgiens expérimentés.

D'autre part, la morbidité du site donneur était fortement associée à la reconstruction autologue, ainsi qu'à l'infection qui la suit et qui entraîne une nécrose de la peau et l'extrusion de l'armature.

2.2- Reconstruction à l'aide d'un cadre synthétique

Pour limiter les complications associées au cartilage costal autologue et pour éliminer la morbidité du site donneur, l'utilisation de cadres synthétiques a été abordée par plusieurs scientifiques. Des matériaux tels que le caoutchouc, le tantale, le polyéthylène, le verre acrylique de silicone et les polyamides ont été utilisés pour la production d'armatures alloplastiques. Plusieurs groupes de scientifiques ont mis au point les armatures.

Ces armatures ont éliminé la résorption liée aux armatures cartilagineuses, ainsi que la variabilité. D'autre part, cette technique augmentait le risque de complications graves lorsqu'elle endommageait les tissus sus-jacents et adjacents et provoquait parfois une infection et l'extrusion de l'implant, et n'était pas recommandée chez les patients âgés.

2.3- Prothèses d'oreilles

Les prothèses d'oreilles sont d'autres alternatives pour la reconstruction auriculaire. Une prothèse d'oreille est une oreille artificielle généralement fabriquée à partir de matériaux synthétiques qui imitent la caractérisation des tissus natifs, comme le silicone, et fixée à la tête à l'aide de clips magnétiques, d'adhésif ou de vis en titane ancrées dans l'os. Le poly(méthylméthacrylate), était l'un des polymères les plus utilisés dans les prothèses depuis le 20e siècle.

Plus récemment, les rénovations dans le domaine des prothèses ont conduit au développement de nouveaux matériaux spécialisés et de méthodes de réticulation, afin d'optimiser leur aptitude à l'impression 3D et de permettre ainsi un large éventail de propriétés mécaniques et visuelles.

Non seulement les prothèses d'oreille améliorent la reconstruction esthétique, mais elles dirigent également les ondes sonores dans le conduit auditif, fournissant ainsi un bon environnement pour les membranes de l'oreille interne.

Un autre avantage de cette technique est qu'elle élimine également l'utilisation du cartilage costal et qu'elle peut être placée directement sur les restes de tissus sains sans qu'aucune intervention

chirurgicale ne soit nécessaire. En outre, elle apporte une grande valeur ajoutée à la vie sociale et psychologique du patient. Au contraire, de nombreuses limitations ont limité le succès de cette prothèse. La couleur, par exemple, était très difficile à assortir à la couleur de la peau native. L'utilisation de vis en titane provoquait une irritation locale et induisait une inflammation et des dommages aux tissus mous environnants.

3-Ingénieire tissulaire

Les dommages et la dégénérescence des tissus et des organes, dus à des maladies ou à des accidents, touchent tous les organismes. La correction et le traitement de ces problèmes est une question majeure à prendre en compte, surtout après la pénurie de donneurs et la faible disponibilité des greffons nécessaires au remplacement. Pour cela, une nouvelle approche de fabrication de remplacement vivant en laboratoire a été appelée "ingénierie tissulaire". Langer et Vacanti ont été les premiers à définir les principes de l'ingénierie tissulaire. Ils ont défini cette approche comme une technologie qui utilise les principes de base de l'ingénierie et des sciences de la vie pour maintenir, améliorer ou restaurer les fonctions des tissus (Langer et Vacanti, 1993). Le principe de l'ingénierie tissulaire consiste à isoler et à prélever des cellules de différentes sources telles que des cellules autologues, allogéniques ou même xénogéniques. Ces cellules seront ensuite développées et ensemencées avec des biomatériaux qui favorisent la croissance et la maturation cellulaire en présence de signaux et de molécules spécifiques permettant aux cellules de migrer et de remplacer des tissus plus anciens (Bakhshandeh *et al*., 2017). Ensemble, ces trois composantes de base forment la triade du génie tissulaire.

3.1-Sources de cellules pour l'ingénierie tissulaire

Que les cellules soient directement ensemencées sur l'échafaudage transplanté ou amplifiées *in vitro*, le choix de ces cellules est une étape très critique. Les cellules sont les composants biologiques de base des tissus, et donc les sources de cellules peuvent affecter le type et la façon dont les échafaudages se régénèrent. En outre, le choix des cellules doit garantir un environnement exempt de pathogènes. Les cellules souches embryonnaires sont pluripotentes et capables de se renouveler et de se différencier dans différentes niches cellulaires. Elles peuvent également inclure des cellules souches adultes à leurs différents stades de maturation. Après la récolte des cellules, elles sont cultivées et mises en culture *in vitro* pour augmenter leur nombre, maintenir leur profil de différenciation ou d'indifférenciation pour être ensuite ensemencées sur des échafaudages afin

de reconstruire et de concevoir des constructions (Golchin *et al*., 2020). Non seulement le profil est important, mais le maintien des propriétés mécaniques est également une exigence. Pour commencer, les cellules doivent adhérer au site d'adhésion cellulaire de l'échafaudage pour le coloniser et commencer leur prolifération. Ensuite, en fonction des signaux ou des facteurs de croissance présents, les cellules commencent à se différencier dans leurs lignées spécifiques et remodèlent le tissu remplacé. Les cellules reçoivent leurs signaux et leurs molécules par l'intermédiaire de protéines appelées intégrines, ancrées à la matrice extracellulaire.

Les cellules souches mésenchymateuses dérivées de la moelle osseuse (BMMSC) sont la source la plus courante de cellules souches. Ces cellules sont simples à récolter et se caractérisent par une bonne accessibilité et un faible risque de tumorigénicité. Une source supplémentaire de cellules souches provient du sang de cordon, où il est constitué d'abondantes cellules souches hématopoïétiques. En raison de leur grande disponibilité, de nombreuses études ont utilisé le sang de cordon ombilical (CB-MSC) et les cellules souches dérivées du liquide amniotique (AFSC), dans des applications de médecine régénérative. Également, et en raison de leur faible antigénicité, de leur grande capacité de prolifération et de différenciation, les cellules souches dérivées du tissu adipeux (ADSC) sont des sources très pratiques dans de nombreuses approches de médecine régénérative. Les ADSC ont été utilisées pour mettre au point des substituts dermo-épithéliaux de la peau où ils ont été encapsulés dans des échafaudages tridimensionnels (3D) et implantés chez des rats immunodéficients. Récemment, de nombreux progéniteurs ont été identifiés et ils ont montré un potentiel prometteur pour la transplantation de cellules auto et allogéniques. Parmi ces progéniteurs, le tissu de la cloison nasale humaine a été évalué. La cloison nasale est principalement constituée de cartilage hyalin et les progéniteurs qui en sont dérivés possèdent des caractéristiques uniques, ce qui en fait des sources intéressantes pour la thérapie cellulaire et les applications cliniques. Les progéniteurs dérivés de la tissu nasale (NsP) sont des progéniteurs cellulaires stables et expansibles qui peuvent être étendus à plus de 30 passages sans aucune sénescence ou perte de phénotype. Ils possèdent une capacité de multi-lignage et d'auto-renouvellement (Elsaesser *et al*., 2016). Shafiee et al., se sont concentrés sur les NsP en tant que sources potentielles pour l'ingénierie tissulaire (Shafiee *et al*., 2014). Pleumeekers et al., ont convenu que la combinaison de progéniteurs nasaux avec la BMMSC réduisait le nombre de chondrocytes requis et améliorait la chondrogenèse en réduisant l'hypertrophie du cartilage (Pleumeekers *et al*., 2015). Leurs caractéristiques multi-lignes ont été prouvées par des études qui

ont montré une différenciation en lignées ostéogéniques et chondrogéniques où elles possédaient des marqueurs de surface stables et chondrogéniques d'une part et un potentiel chondrogénique supérieur et une production de matrice extracellulaire d'autre part (Shafiee *et al*., 2016).

On outre, les cellules souches de la pulpe dentaire (DPSC) sont des cellules souches mésenchymateuses hautement accessibles et indifférenciées, présentes dans le tissu de la pulpe dentaire et caractérisées par leur auto-renouvellement illimité ainsi que par leur potentiel de différenciation multipotent. Les cellules souches dentaires ont été utilisées dans de nombreuses applications d'ingénierie tissulaire.

3.2- Biomatériaux pour l'ingénierie tissulaire

L'échafaudage est l'élément central utilisé pour soutenir, abriter et diriger la croissance des cellules soit ensemencées dans l'échafaudage, soit migrées du milieu environnant. Un échafaudage idéal doit répondre à ces spécifications. Tout d'abord, il doit être biocompatible, donc capable de remplir sa fonction sans induire de réaction inflammatoire. Ce biomatériau devrait également être biodégradable, pour être facilement éliminé de l'organisme et devrait s'intégrer sans nuire au tissu natif. La porosité est une condition importante pour une interaction et une pénétration optimales des cellules dans les échafaudages. Elle devrait fournir un réseau de pores ouvert et interconnectés qui facilite l'échange de métabolites et de nutriments et favorise leur transport. En outre, la structure choisie doit être facile à traiter et souple à manipuler, en fonction des besoins des tissus. En outre, elle devrait conserver sa fonction biomécanique après son implantation in vivo, afin de reconstruire un tissu pleinement intégré à son environnement (Nasonova *et al*., 2015).

Comprendre et définir le tissu natif à reconstruire est une étape essentielle de l'ingénierie tissulaire. Avant de choisir les sources cellulaires et la structure appropriée pour héberger les cellules, il faut comprendre les fonctions biologiques et biomécaniques du tissu en question. Les caractéristiques mécaniques devraient être étudiées davantage et la comparaison entre la structure et la construction devrait être mieux évaluée. Par conséquent, on a récemment mis l'accent sur l'augmentation de la biocomplexité des matrices pour mieux imiter la dynamique naturelle de la matrice extracellulaire. Différentes sources cellulaires ont été impliquées dans diverses applications d'ingénierie tissulaire.

3.2.1 Biomatériaux naturels et synthétiques

L'ingénierie tissulaire a utilisé une variété de biomatériaux naturels (collagène, fibroïne de soie, chitosane, acide hyaluronique, alginate, agarose) et synthétiques (céramiques, nanomatériaux, poly

acide glycolique) etc. pour réparer et remplacer les tissus perdus ou malades. Ces biomatériaux servent d'échafaudage 3D, fournissant l'environnement approprié et satisfaisant aux propriétés de volume et de surface pour éviter l'échec des constructions après l'implantation.

Les structures 3D ont fait l'objet d'une attention remarquable dans la culture cellulaire in vitro. En effet, ces structures 3D imitent l'environnement naturel trouvé *in vivo*. De sorte que la morphologie de la cellule ressemble beaucoup à sa forme normale dans le corps. Dans l'ingénierie des tissus cartilagineux, il a été démontré que les chondrocytes encapsulés dans des hydrogels 3D, maintiennent et conservent leur stabilité phénotypique, ce qui limite leur dédifférenciation (Gz et Hw, 2018). De nombreux échafaudages 3D naturels et synthétiques ont été évalués pour leurs propriétés chondrogéniques, mais il existe une demande croissante pour d'autres échafaudages de substitution qui pourraient améliorer l'ingénierie tissulaire du cartilage.

3.2.2 Échafaudages décellularisés

3.2.2.1 Les tissus animaux

En raison des défis liés à la préparation de matrices synthétiques pouvant imiter le microenvironnement cellulaire, il y a eu une demande croissante pour l'utilisation de la matrice extracellulaire d'origine naturelle obtenue à l'aide de processus de décellularisation. La décellularisation est l'élimination des cellules et du matériel génétique d'un tissu natif tout en conservant ses propriétés structurelles, biochimiques et mécaniques (Keane *et al*., 2015). Ces échafaudages bio-dérivés pourraient alors être utilisés soit comme tissu personnalisé lorsqu'ils sont repeuplés par les propres cellules du patient, soit comme support biologique allogène ou xénogénique pour développer des tissus ou des organes artificiels.

Les critères de production d'un bon échafaudage efficace sont que la matrice extracellulaire décellularisée doit avoir moins de 50ng d'ADN double brin (ADNdb) par mg de poids sec de matrice extracellulaire, moins de 200bp de longueur de fragment d'ADN et aucun matériel nucléaire visible lors de la coloration avec le 4'6-diamidino-2-phénylindole (DAPI). Les protéines de la matrice extracellulaire telles que la fibronectine, le collagène, les protéoglycanes doivent être conservées pendant les processus de décellularisation ainsi que la structure et l'intégrité. Enfin, l'échafaudage décellularisé devrait pouvoir atteindre ses propriétés biomécaniques afin de restaurer sa fonction après la transplantation (García-Gareta *et al*., 2020).

La réduction de l'immunogénicité de l'échafaudage est un facteur critique pour l'utilisation d'un échafaudage décellularisé dans les applications cliniques. Les facteurs capables d'induire l'immunogénicité sont les matériaux génétiques tels que l'ADN, l'ARN et les antigènes. Des épitopes spécifiques doivent être mesurés, tels que les épitopes alpha-gal qui peuvent induire la réponse immunitaire en cascade du complément et les complexes majeurs d'histocompatibilité situés sur la membrane cellulaire. Ensuite, la restauration des propriétés mécaniques est une caractéristique essentielle pour assurer un échafaudage optimal.

En raison de la forte densité du cartilage, le tissu natif doit être perturbé afin de permettre aux produits chimiques et aux réactifs d'augmenter leur efficacité de décellularisation. Cela pourrait être réalisé en exposant d'abord le tissu à des traitements physiques et mécaniques tels que des cycles de gel-dégel, la pression osmotique, ce qui augmenterait la lyse cellulaire et donc exposerait moins le tissu aux réactifs chimiques, ce qui est très important pour la rétention de la microstructure et la préservation des protéines ECM. La décellularisation a été réalisée en utilisant différentes stratégies et méthodes.

3.2.2.2 Tissus végétaux

L'une des principales limites du génie tissulaire est l'absence d'un système vasculaire organisé et fonctionnel permettant le transfert et la diffusion de l'oxygène et des nutriments. La difficulté de créer un tel réseau de vaisseaux et de conduits de perfusion a poussé les chercheurs à se concentrer davantage sur les plantes et les tissus végétaux (Jahangirian et al., 2019). Les plantes et les animaux exploitent des approches différentes des produits chimiques et du transport des fluides, mais ils partagent de grandes similitudes dans leur réseau vasculaire. La structure des plantes possède des propriétés mécaniques similaires, semblables à celles des tissus humains, et présente un tissu multifonctionnel. Sachant que la cellulose est la plus abondante dans les parois cellulaires des plantes, elle a également été étudiée en tant que composé biocompatible naturel et il a été démontré qu'elle favorise la cicatrisation des blessures et a été utilisée dans un large éventail d'applications d'ingénierie tissulaire.

Récemment, des extraits de pommes décellularisées se sont avérées biocompatibles une fois implantées *in vivo* dans des modèles animaux. Ces similitudes se sont accumulées et ont incité les chercheurs à s'intéresser davantage aux plantes et à leur système vasculaire après les techniques de perfusion visant à décelluláriser ces tissus. La décellularisation, comme mentionné

précédemment, permet d'éliminer le matériel cellulaire, tout en préservant le réseau vasculaire intact. Ces techniques ont été appliquées à diverses espèces de plantes pour donner naissance à des échafaudages acellulaires d'ingénierie tissulaire. De nombreuses plantes de différents groupes botaniques ont subi une décellularisation. Parmi celles-ci, les épinards, les tiges de persil, les racines poilues d'arachides. Les épinards ont été choisis en raison de leur grande disponibilité et de leur vascularité dense. Des analyses tant quantitatives que qualitatives ont montré la perte de matière nucléaire avec une bonne conservation de la structure et de la composition native du tissu végétal. Une fois perfusées avec des cellules endothéliales, elles ont pu reconstituer un réseau de vascularisation en utilisant les nervations du tissu natif.

3.2.3 Feuillets de cellules

Récemment, la technologie de feuillets cellulaires ou « cell sheets » a émergé. Ces derniers sont obtenus en cultivant des cellules à hyperconfluence en favorisant le dépôt de matrice extracellulaire. Le tapis obtenu est alors très cellularisé et constitué d'une matrice extracellulaire élaborée et structurée. Ces feuillets cellulaires conservent leurs jonctions cellule-cellule, et peuvent être recueillis tels quels pour plusieurs applications. Ils peuvent être ainsi transplantés sous forme de feuillet unique ou de piles de feuillets cellulaires superposéets pour régénérer des tissus et organes endommagés. Divers systèmes ont été utilisés pour construire et préparer ces feuillets de cellules. Il s'agit notamment de boîtes sensibles à la température, de systèmes électro-réactifs, sensibles au pH, photo-réactifs, magnétiques et enfin mécaniques.

Avec le développement rapide de la technologie des feuillets cellulaires, cette technologie a été impliquée dans un large éventail de tissus et d'organes, en particulier la régénération du cartilage. Cette approche permet de surmonter différents problèmes liés à l'ingénierie tissulaire conventionnelle. Par exemple, les constructions de l'ingénierie tissulaire manquent de complexité spatiale dans l'organisation des tissus, et les sources de chondrocytes sont toujours des facteurs clés qui limitent l'ingénierie du cartilage à grande échelle et limitent leur succès. Pour cela, il est impératif de définir les caractéristiques et le phénotype des feuillets cellulaires par rapport à la structure native du cartilage. Par rapport aux monocouches, les feuilles de chondrocytes multicouches ont montré un niveau d'expression accru des marqueurs et des protéines chondrogéniques et adhésives, montrant que les feuillets de chondrocytes multicouches régénèrent les défauts du cartilage en imitant étroitement la structure native et en sécrétant des facteurs de

croissance tels que le TGF-β et la prostaglandine (Takizawa et al., 2020). Par rapport à un échafaudage de cellules isolées, les feuillets de chondrocytes ont régénéré des lésions partielles et complètes, avec une bonne intégration entre le cartilage articulaire natif et le cartilage articulaire artificiel.

3.3 Facteurs de croissance et environnements hypoxiques

Une large gamme de facteurs de croissance et de molécules de signalisation joue un rôle essentiel dans la croissance, la prolifération et la différenciation des cellules. Les facteurs de croissance les plus utilisés comprennent les facteurs de croissance apparenté à l'insuline 1 et 2 (IGF-1 et IGF-2), les facteurs de croissance des fibroblastes (bFGF, bGFG-2), les facteurs de croissance endothélilal vasculaire (VGEF), les protéines osseuses morphogénétique (BMP) et le facteur de croissance transformant bêta (TGF-β). Ces facteurs de croissance sont délivrés par différents moyens, notamment par des transporteurs où les plasmides d'ADN codent le gène des facteurs de croissance souhaités.

L'hypoxie est l'un des facteurs les plus remarquables qui affectent les cellules de multiples façons. Elle joue un rôle important dans différentes caractéristiques cellulaires, où elle affecte la migration, la prolifération et le métabolisme des cellules. L'hypoxie intervient dans ces modifications cellulaires par la voie HIF, en induisant des facteurs inductibles par l'hypoxie (HIF1α, HIF2α), pour stimuler la chondrogenèse par l'augmentation du facteur de transcription SOX-9, ainsi que COL2A1 et ACAN.

Afin de réussir la construction du cartilage, les sources de cellules, les échafaudages et le milieu environnant doivent être bien choisis pour imiter le tissu natif.

II-Objectifs

La reconstruction du cartilage auriculaire reste l'une des techniques les plus difficiles pour la chirurgie de la tête et du cou. L'ingénierie tissulaire est une approche alternative et prometteuse, qui utilise des cellules, des échafaudages et des facteurs de croissance pour assembler des constructions fonctionnelles qui peuvent améliorer, restaurer ou remplacer des tissus et des organes endommagés. Malgré des progrès significatifs dans ce domaine, de nombreux problèmes restent sans solution.

Plusieurs échafaudages ont été utilisés, mais aucun matériau imitant parfaitement la nature du cartilage élastique n'a encore été proposé. Malgré les progrès significatifs des approches d'ingénierie tissulaire, une optimisation est encore nécessaire pour améliorer la croissance, la différenciation et l'intégration cellulaires lors de l'implantation *in vivo*.

Divers échafaudages ont été conçus et utilisés pour remplacer les reconstructions chirurgicales, mais ces échafaudages se sont dégradés au fil des semaines ou des mois, et l'espace a ensuite été remplacé par des cellules prolifératives, ce qui a entraîné une fibrose. Les injections de cellules en suspension sont également une option mais ne conviennent pas vraiment à la reconstruction de larges défauts tissulaires, car peu de cellules injectées sont intégrées dans les tissus de l'hôte.

Mon projet de thèse vise à étudier de nouvelles approches de la réparation du cartilage auriculaire par l'utilisation d'échafaudages décellularisés et à les évaluer *in vitro* et *in vivo*. Des échafaudages animaux (cartilage natif) ou végétaux (pomme) ont été testés après caractérisation de différentes sources cellulaires pour leur capacité à régénérer le cartilage. Par ailleurs, nous avons mis en évidence et étudié l'utilisation de nouvelles matrices, à savoir les feuillets cellulaires, comme support potentiel pour l'ingénierie du cartilage.

Afin de contribuer à un meilleur potentiel de recellularisation et de reconstruction, l'objectif principal a été divisé en plusieurs tâches :

- Caractérisation des meilleures sources cellulaires capables d'exprimer des marqueurs chondrogéniques et élastiques, et d'améliorer la formation du cartilage pour être utilisées dans la reconstruction des défauts du cartilage auriculaire.

- Développement d'un modèle animal de défaut et de reconstruction du cartilage

- Étude de la technologie des feuillets cellulaires à partir de périchondrocytes auriculaires pour la production de cartilage *in vitro* ainsi que d'un échafaudage cellularisé à introduire sur le site de la lésion pour régénérer le défaut cartilagineux *in vivo* chez le lapin.

- Développement de plusieurs utilisations *in vitro* des feuillets cellulaires décellularisés puis lyophilisés, comme support de culture cellulaire apportant un environnement particulier.

- Conception et ingénierie de nouvelles matrices cellulosiques à partir de tissu de pomme pour l'ingénierie du cartilage auriculaire.

III-Résultats

1-Effets de l'hypoxie sur la différenciation chondrogénique des cellules progénitrices de différentes origines

Les approches d'ingénierie des tissus cartilagineux dépendent essentiellement des sources cellulaires utilisées, qu'elles soient directement ensemencées sur des échafaudages transplantés ou développées *in vitro*. Dans la première partie de ma thèse, nous nous sommes intéressés à la production et à la régénération du tissu de cartilage auriculaire. Le travail consistait à choisir la source cellulaire qui produisait le mieux le tissu de cartilage auriculaire. Il était nécessaire d'étudier les progéniteurs de la région de la tête qui proviennent de différentes origines embryologiques. Pour cette raison, nous avons choisi des périchodrocytes auriculaires (AuP), des périchondrocytes nasaux (NsP) et des cellules souches de pulpe dentaire (DPSC). Ces cellules ont été comparées à celles de la BMMSC (les cellules souches mésenchymateuses dérivées de la moelle osseuse). Ces quatre types de cellules ont été encapsulées dans des billes d'alginate 3D qui ont servi de modèles pour la chondrogenèse. De plus, dans cette étude, nous avons également cherché à étudier l'effet de l'hypoxie sur le potentiel des cellules à former du tissu cartilagineux auriculaire. Pour ce faire, nous avons encapsulé les quatre sources cellulaires dans des billes d'alginate et les avons cultivées dans des conditions normales (21 % O2) et à faible teneur en oxygène (3 % O2).

Nos résultats ont suggéré qu'après deux semaines de culture, tous les types de cellules étaient capables de produire des matrices extracellulaires cartilagineuses, comme le montre la coloration histologique. Plus clairement, les périchodrocytes auriculaires présentaient la plus forte expression de gènes cartilagineux en milieu chondrogènique normoxique. Il est intéressant de noter qu'en dehors de cette augmentation, l'expression relativement faible du COLX indique la préservation du phénotype dans ce type cellulaire par rapport aux autres progéniteurs. D'autre part, si l'environnement hypoxique a fortement stimulé la chondrogenèse chez les hBMMSC, elle est sans effet sur celle des progéniteurs du périchondre auriculaire.

Dans l'ensemble, ces résultats indiquent que parmi nos cellules testées, les AuP produisent fortement une matrice extracellulaire élastique cartilagineuse et que l'hypoxie n'est pas nécessaire et n'a pas affecté leur chondrogenèse, contrairement aux progéniteurs issus de la moëlle osseuse, BMMSC. Cela pourrait s'expliquer par des mécanismes d'action différents induits par l'hypoxie. Il serait intéressant d'évaluer le rôle respectif des facteurs HIF-1 et HIF-2 dans cette réponse. Par

ailleurs, il n'est pas exclu que cette différence provienne aussi du stade de différenciation entre les différents progéniteurs. En effet, les périchondrocytes seraient plus engagés vers la voie chondrogénique que les cellules souches mésenchymateuses de la moëlle osseuse. Ce qui relève l'intérêt de connaître le type cellulaire approprié pour chaque tissu.

Pour conclure, les périchondrocytes auriculaires sont les meilleurs candidats pour l'ingénierie du tissu cartilagineux élastique. L'hypoxie, s'avère inefficace et peu bénéfique pour ces cellules. Nos résultats mettent en évidence le rôle de l'oxygène dans la promotion et l'amélioration de la qualité du cartilage élastique. De plus, l'introduction de ces cellules permet de s'affranchir d'utiliser des équipements pour l'hypoxie. Pour approfondir nos résultats, des études in vivo sur des modèles animaux devraient être conçues pour tenter de régénérer et de réparer le cartilage auriculaire.

2-Les feuillets cellulaires comme outils pour la reconstruction du cartilage de l'oreille *in vivo*

De nombreux chercheurs utilisent encore les approches 2D, car elles apportent efficacité et simplicité aux applications de culture cellulaire. Cependant, les recherches récentes se concentrent davantage sur l'auto-assemblage et la culture en 3D pour reproduire les interactions cellule-cellule in vitro et pour imiter l'environnement *in vivo*. La technologie des feuillets cellulaires est basée sur le recueil de tapis cellulaire sans enzymes protéolytiques ni agents chélateurs, ce qui permet de préserver les jonctions cellule-cellule et la matrice extracellulaire sécrétée par les cellules. La récupération du tapis de cellules sous la forme d'un feuillet intact permet de l'utiliser dans des diverses applications.

Nous avons déjà montré dans la première partie de notre thèse que les périchondrocytes auriculaires présentaient le meilleur potentiel chondrogénique par rapport aux différentes sources cellulaires testées. À partir de là, nous avons testé différentes sources cellulaires pour leur potentiel à former des feuillets cellulaires et nous nous sommes principalement concentrés sur les périchondrocytes auriculaires et leur tendance à régénérer le cartilage *in vitro*. Malgré la grande capacité des cellules souches et des progéniteurs à produire des feuillets cellulaires, les périchondrocytes auriculaires de lapin ont été les meilleurs pour former un feuillet cellulaire intact, souple et flexible après un mois de culture. Ces dernières ont ensuite été caractérisées et ont révélé une composition de matrice extracellulaire similaire au cartilage auriculaire natif.

Les feuillets cellulaires ont été étudiés dans différentes applications *in vitro* et *in vivo*. Tout d'abord, ils ont été utilisés comme supports, afin de re-coloniser du cartilage décellularisé du porc. Deux méthodes d'application différentes ont été utilisées et les résultats ont montré que le fait d'envelopper complétement le cartilage décellularisé avec des feuillets cellulaires favorisait une meilleure recellularisation. Ceci est démontré par une pénétration profonde des cellules et une distribution homogène dans tout le tissu cartilagineux après deux semaines de culture.

Pour mieux appréhender la biocompatibilité des feuillets cellulaires et la réparation du cartilage, nous avons créé un modèle animal de défaut cartilagineux dans l'oreille de lapin, par chirurgie. Ces derniers ont ensuite été comblés par des feuillets cellulaires, préalablement cultivés en milieu chondrogénique i*n vitro* pendant plusieurs semaines. Après 2 mois d'implantation *in vivo*, ces feuillets cellulaires présentaient une bonne intégration dans le tissu hôte et un bon comblement des défauts par un tissu de nature cartilagineuse.

En bref, notre étude montre que les feuillets cellulaires peuvent être considérées comme un outil de choix pour des approches d'ingénierie, favorisant et améliorant la régénération du cartilage *in vitro* ainsi que la réparation du tissu *in vivo*.

3-Ingénierie des tissus cartilagineux à l'aide d'échafaudages cellulosiques de pommes

Afin d'investiguer de nouveaux biomatériaux et en raison des progrès récents dans l'utilisation de tissus d'origine végétale, nous nous sommes intéressés à l'hypanthium de pomme comme biomatériau pour l'ingénierie du cartilage.

Dans cette étude, nous montrons que les pommes décellularisées fournissent des échafaudages cellulosiques pour la culture 3D de différents progéniteurs humains.

Les matrices de pommes permettent prolifération et une viabilité élevées après 21 jours de culture lorsqu'elles ont été ensemencées avec des périchondrocytes humains. Par la suite, nous avons montré que plusieurs types cellulaires ensemencés sur de telles matrices décellularisées, sont capable de croître et de produire un tissu riche en matrice extracellulaire. Des différences existent entre les types cellulaires, notamment en ce qui concerne la réponse à l'hypoxie.

L'analyse histologique et par RT-PCR montre que le tissu formé est de nature cartilagineuse avec une forte expression des gènes cartilagineux tels que COL2A1, ACAN, COMP, SOX9 et ELN.

C’est notamment le cas des périchondrocytes auriculaires et nasaux ainsi que les BMMSC. Par contre, l’utilisation des progéniteurs issus de pulpe dentaire montrent plutôt un profil ostéogénique.

De plus, le potentiel d’induction chondrogénique est supérieur à celui de l’alginate, utilisé comme modèle de référence. Cela souligne l'intérêt du potentiel de matrices de pomme pour favoriser la prolifération et la différenciation chondrogénique et encourage son utilisation pour le cartilage ou d'autres approches d'ingénierie tissulaire, compte tenu de sa facilité de mise en oeuvre et de sa grande disponibilité.

En conclusion, nous démontrons ici les effets avantageux des matrices de pomme sur la prolifération et la différenciation de différents progéniteurs. Elles constituent un échafaudage naturel et poreux qui guide la différenciation chondrogénique des différentes cellules progénitrices i*n vitro*. L'évaluation *in vivo* du potentiel chondrogénique de ces échafaudages serait intéressante pour de futures expériences.

4-Matrices sécrétées par les cellules : Nouvelles approches pour les applications de culture cellulaire

Dans la dernière partie de ma thèse, nous avons décrit une nouvelle approche pour différentes applications de culture cellulaire.

Nous avons voulu étudier le potentiel d'une matrice extracellulaire, naturellement sécrétée et organisée par les cellules, à influencer la croissance et le comportement des cellules, notamment les processus de différenciation et de dédifférenciation. Des périchondrocytes auriculaires de lapin (AuP) ont été cultivés en conditions chondrogéniques jusqu’à hyperconfluence, pour favoriser la production et le dépôt de matrice extracellulaire. Les tapis cellulaires ont ensuite été décellularisés, lyophilisés et stockés pour leur utilisation future. La matrice restante a, tout d’abord, été caractérisée en mesurant la quantité de protéines totales et particulières (collagènes, élastine, GAG), ainsi que par analyse protéomique avant d’être utilisée comme substrat pour de multiples applications de culture cellulaire. Ainsi, les CSM (matrices sécrétées par les cellules) lyophilisées présentent de bonnes quantités de protéines matricielles ainsi que des protéines importantes pour le métabolisme du cartilage. Néanmoins, l’analyse protéomique montre la persistance de nombreuses protéines cellulaires, et en particulier, certaines liées au cytosquelette. Pour la suite, nous avons considéré comme telle, la composition des substrats ainsi lyophilisée et procédé à plusieurs expériences, en montrant tout d’abord que le support pouvait accueillir des cellules

allogèniques et xénogéniques. Ensuite, nous avons montré qu'une CSM issue de cellules chondrogéniques, favorisait la chondrogenèse de progéniteurs humains avec une forte augmentation des marqueurs cartilagineux (COL2A1, ELN, COMP et SOX 9) et une diminution de COL1 et COLX.

L'ingénierie tissulaire nécessite de grandes quantités de cellules et beaucoup de types cellulaires sont sujets à une dédifférenciation phénotypique lors de leur multiplication par passages successifs. Pour évaluer la possibilité de limiter ce phénomène, nous avons cultivé des chondrocytes articulaires humains pendant plusieurs passages, parallèlement sur plastique et des CSM lyophilisées. Nos résultats ont révélé que non seulement la CSM lyophilisée favorisait une forte prolifération, mais aussi la formation d'un cartilagineux avec une meilleure expression des marqueurs cartilagineux (SOX9, ACAN, COL2A1 et ELN) et une diminution de COLX et du marqueur de dédifférenciation COL1, par rapport aux chondrocytes ensemencés sur des plaques de plastique.

En résumé, nous avons mis au point un outil de culture cellulaire simple et abordable, qui améliore la prolifération, la différenciation et préserve le phénotype des chondrocytes lors de l'expansion *in vitro*. Son utilisation pourrait très facilement s'étendre à d'autres tissus et applications.

IV-Discussion

En raison de la faible vascularité du tissu cartilagineux, les défauts du cartilage guérissent mal et entraînent de nombreuses maladies dégénératives du cartilage. De nombreuses stratégies cliniques ont été utilisées pour réparer ces défauts afin d'obtenir un tissu fonctionnel similaire au tissu natif. Cependant, ces procédés chirurgicaux sont restés difficiles. En raison de la disponibilité limitée des tissus autologues de donneurs de cartilage et de leur principale association avec la morbidité du site du donneur, et afin de mieux régénérer les défauts cartilagineux, une grande importance a été accordée ces dernières années à la construction de cartilage par ingénierie tissulaire.

Une caractéristique importante est l'utilisation d'un échafaudage inerte, avec des pores interconnectés pour permettre le transport des nutriments et des déchets. Il doit également être biodégradable et surtout façonnable et adaptable au défaut. En outre, le biomatériau choisi devrait

accélérer l'infiltration et l'attachement des cellules pour permettre la migration et la prolifération (Wasyłeczko *et al*.,2020).

En plus du biomatériau, les sources cellulaires jouent un rôle essentiel dans la qualité des constructions de tissus. L'objectif est de sélectionner une source cellulaire qui pourrait être facilement isolée, étendue et capable d'exprimer des marqueurs cartilagineux. Ces sources vont des chondrocytes, aux cellules souches, en passant par différents progéniteurs.

Les chondrocytes sont les seules cellules présentes dans le tissu cartilagineux. Ces cellules devraient être principalement utilisées dans les processus de reconstruction du cartilage, où les chondrocytes autologues sont les meilleurs pour régénérer les propres tissus du patient. Cependant, lors de l'amplification de ces cellules, leur tendance à exprimer le collagène II diminue et l'expression du collagène I augmente en parallèle, ce qui rend ces cellules inefficaces pour produire du tissu cartilagineux stable (Yang *et al*., 2018).

Les cellules souches mésenchymlateuses ont un taux de prolifération stable plus élevé que les chondrocytes, et plusieurs études ont signalé le potentiel de ces cellules à réparer les défauts cartilagineux (Buzaboon et Alshammary, 2020 ; Rorick *et al*., 2020). La sélection des cellules pour la génération de tissus cartilagineux reste l'un des défis remarquables des stratégies d'ingénierie tissulaire.

Dans une première étape de nos travaux, nous avons cherché à choisir le meilleur type cellulaire capable d’exprimer les gènes du cartilage lorsqu'il est encapsulé dans des billes d'alginate 3D. On sait surtout que les cellules souches mésenchymateuses dérivées de la moelle osseuse (BMMSC) encapsulées dans des billes d'alginate 3D et en conditions de faible hypoxie expriment des marqueurs cartilagineux élevés (Duval *et al*., 2012, 2016 ; Peck *et al*., 2019 ; Schmidt *et al*., 2020). Les hydrogels d'alginate ont été choisis en raison de leur fort potentiel de soutien de la prolifération cellulaire, de leur capacité à retenir une plus grande quantité de fluides et d'eau. Ils sont également caractérisés par une biocompatibilité et une biodégradabilité élevées (Ansari *et al*., 2017 ; Gentile *et al*., 2017). En tant qu'hydrogel puissant, l'alginate s'est avéré induire la formation de tissu cartilagineux *in vitro* dans de nombreux rapports (Jin *et* Kim, 2018 ; Khatab *et al*., 2020). Pour préparer de tels hydrogels, il suffit de les réticuler avec du calcium pendant 10 minutes et ils sont prêts à l'emploi.

En faisant référence à la région de tête, nous avons été très intéressés de voir si des progéniteurs d'origine embryologique différente, possèdent un potentiel chondrogénique similaire lorsqu'ils sont encapsulés dans des hydrogels sous différents niveaux d'oxygène en culture.

Les cellules progénitrices auriculaires (AuP), les cellules progénitrices nasales (NsP) et les cellules souches de la pulpe dentaire (DPSC) ont été comparées à modèle de référence, les cellules BMMSC. Dans un premier temps, les cellules ont été testées pour leur capacité à se différencier en 3 lignages (chondro-, adipo- et ostéogénique). Le potentiel chondrogénique des cellules a été comparé en atmosphère normale ou en faible teneur d'oxygène. Il est important de mentionner qu'aucune étude n'a encore étudié l'effet de l'hypoxie sur les AuP. Nous avons ainsi montré que l'hypoxie n'était pas nécessaire et n'avait pas d'effet sur le potentiel chondrogénique de l'AuP. La condition normoxique, en revanche, semble être suffisante pour obtenir une bonne production de marqueurs du cartilage.

Nos résultats sont complémentaires de ceux d'Otto et al., qui ont comparé la capacité chondrogénique des AuP équins aux BMMSC encapsulés dans des hydrogels 3D à base de gélatine (Otto *et al*., 2018). De façon similaire, les AuP en normoxie ont surpassé les BMMSC (augmentation des marqueurs de cartilage et diminution de ceux de l'hypertrophie. Dans notre étude, nous montrons que l'effet de l'hypoxie (3%) n'est pas nécessaire à l'expression des gènes du cartilage chez les AuP, alors qu'elle a un effet synergique pour le BMMSC. Ainsi, les AuP ont été choisis comme la meilleure source de cellules pour notre deuxième série d'expériences. La deuxième étape a consisté à choisir le meilleur support pour l'ingénierie des tissus cartilagineux, en étudiant de multiples biomatériaux.

Il a été démontré que divers échafaudages synthétiques produisaient des formes et des tailles variées qui offraient de bonnes propriétés mécaniques et chimiques de l'échafaudage pour améliorer la qualité du cartilage technique. Cependant, la plupart de ces polymères se dégradent lors de l'implantation et peuvent être métabolisés dans l'organisme, ce qui entraîne des effets secondaires toxiques. En outre, ces échafaudages synthétiques manquent de propriétés biologiques et peuvent provoquer des réponses immunitaires (Liu *et al*., 2016).

Malgré leur reproductibilité limitée, les échafaudages naturels présentent une réponse biologique supérieure et une meilleure biocompatibilité par rapport aux échafaudages synthétiques. En dépit

de ces avantages, les échafaudages naturels et synthétiques manquent de caractérisation et de traitement détaillé de la microorganisation et de la structure des tissus (Perez-Puyana *et al*., 2020).

En raison de leur microenvironnement naturel et de leur préservation des structures et des protéines tissulaires, les échafaudages naturels dérivés de tissus natifs sont devenus populaires ces dernières années. Après décellularisation, ils offrent de nombreux avantages par rapport aux échafaudages artificiels. Cela comprend une biocompatibilité améliorée, une capacité accrue de repeuplement cellulaire et des propriétés biomécaniques accrues. L'objectif de tout protocole de décellularisation est d'éliminer efficacement, suffisamment de matières cellulaires et nucléaires, afin de limiter le caractère immunogénique. Beaucoup de méthodes existent notamment l'utilisation de SDS, comme dèjà décrit (Utomo *et al*., 2015) pour le cartilage natif. Dans cette étude, nous avons utilisé du cartilage auriculaire d'origine porcine afin de développer une matrice appropriée pour l'ingénierie tissulaire. Il a été choisi en raison de sa physiologie similaire à celle de l'homme. Ce cartilage xénogénique porcin a été décellularisé avec succès grâce à un protocole établi dans notre laboratoire. Ce protocole consiste en un mélange de traitements physiques, chimiques et enzymatiques qui ont permis d'éliminer fortement les cellules porcines et d'obtenir un cartilage auriculaire décellularisé qui conserve une grande partie de la bioactivité du tissu, tout en éliminant le maximum de matière nucléaire. Il serait d'ailleurs très intéressant d'évaluer d'autres protocoles de décellularisation et de caractériser les protéines résiduelles. Ainsi décellularisés, plusieurs approches peuvent être envisagées pour la recolonisation des tissus par des cellules d'intérêt.

Pour réensemencer les échafaudages, les approches d'ingénierie tissulaire consistent en plusieurs traitements, tels que la perfusion pulsatile, l'injection de culture statique, la force centrifuge et la sonication. Cependant, l'ensemencement n'était pas homogène dans tous les cas, et il ne se formait qu'une monocouche à la surface de l'échafaudage (Luo *et al*., 2016). L'utilisation du collagène dans la recellularisation a considérablement amélioré la pénétration des cellules (Martinello *et al*., 2014). Cependant, il en résulte une distribution globale non homogène. La facilitation des interconnexions entre cellules et la préservation des jonctions cellule-matrice extracellulaires sont nécessaires pour maintenir l'adhésion et la prolifération des cellules. Les recherches actuelles ont introduit les feuillets cellulaires comme outil d'ingénierie du cartilage car ils permettent de limiter la dispersion des cellules. Dans notre travail, nous les avons utilisés pour la recolonisation de

cartilage auriculaire de porc décellularisé et démontré leur intérêt. Par ailleurs, leur utilisation tels quels, a permis de corriger un défaut cartilagineux *in vivo*, chez un modèle allogénique le lapin.

L'ensemencement uniforme du cartilage est encore un défi en raison de la densité du tissu élastique du cartilage auriculaire. De nombreuses études ont fait incuber des échafaudages élastiques dans de l'élastase pour épuiser les fibres élastiques afin de mieux les recoloniser (de manière homogène avec les cellules). D'autres, ont introduit des canaux pour simplifier la recellularisation des disques de cartilage de porc. Ces canaux ont agi comme des conduits qui ont aidé les cellules et les nutriments à pénétrer, favorisant la viabilité et la prolifération des cellules. Cependant, le degré de réticulation du tissu cartilagineux était limité, les canaux n'étant pas suffisants pour permettre une réticulation complète (Luo *et al*., 2015 ; Lehmann *et al*., 2019). Dans notre cas, nous n'avons même pas pris la peine de retirer les fibres élastiques pour une meilleure repopulation des cellules. Au lieu de cela, nous avons pu surmonter ce défi en adoptant une méthodologie qui comprenait d'abord la préparation de feuillets de cellules chondrogénique qui ont servi de vecteur cellulaire.

Nous avons utilisé un système mécanique pour synthétiser des feuilles cellulaires provenant de différents progéniteurs et de différentes espèces. Toutes les cellules testées ont produit avec succès des feuillets cellulaires, et en se référant à nos résultats concernant la meilleure source de cellules pour la régénération auriculaire, il était évident de choisir les AuP qui avait une grande et rapide tendance à former des feuillets cellulaires. De plus, ces cellules prolifèrent relativement vite, ce qui n’est pas négligeable pour obtenir une quantité suffisante de cellules. Nous avons également choisi des cellules de lapin pour coloniser un cartilage porcin afin d’évaluer un système de reconstruction xénogénique *in vitro*. Et plus spécifiquement, ces feuillets cellulaires d'origine lapine étaient destinés à combler un défaut dans un modèle de défauts cartilagineux auriculaires chez le lapin allogènique.

Des études ont utilisé des modèles de sandwich qui étaient applicables sur le tissu cartilagineux acellulaire. D’autres consistent à cultiver des chondrocytes couche par couche pour former un tissu cartilagineux artificiel après plusieurs semaines *in vitro* et *in vivo* (Gong *et al*., 2011 ; Chen *et al*., 2015 ; Chiu, Weber *et* Waldman, 2019). Dans notre travail, nous avons utilisé la méthode du modèle sandwich, mais cette fois-ci, nous avons enroulé étroitement le feuillet autour du tissu décellularisé. Le cartilage a été rellularisé de manière homogène lorsque les feuillets cellulaires

ont entouré tout le cartilage pendant 2 semaines, les cellules ont pénétré profondément dans le cartilage porcin, qui a reconstruit un tissu cartilagineux *in vitro*.

Dans un modèle de lapin, des défauts cartilagineux auriculaires ont été produits et, cette fois, des feuillets de cellules ont été utilisés comme vecteurs de cellules pour les acheminer et les maintenir dans la zone du défaut. Les feuillets cellulaires ont été créés *in vitro* en présence d'un milieu chondrogénique. Après 3 semaines de culture, les cellules ont proliféré et ont exprimé des marqueurs cartilagineux. Leur morphologie et leur composition ont été comparées à celles du tissu auriculaire natif qui a montré une grande similitude de composition par rapport au cartilage auriculaire natif. À ce stade, elles ont été récoltées et étaient prêtes à être implantées *in vivo*. Après deux mois d'implantation, analyses histologiques et les analyses IHC montrent clairement un tissu néoformé de type cartilagineux élastique. Afin de mieux analyser la qualité du cartilage régénéré, nous avons caractérisé le feuillet cellulaire avant l'implantation et une biopsie de la zone du défaut 2 mois après l'implantation. Ce n'était pas vraiment précis car après 2 mois d'implantation, les feuillets cellulaires étaient complètement intégrés aux tissus. Cependant, nous avons essayé de prélever le plus possible dans la zone où le feuillet a été implanté. On observe une grande expression d'ELN, d'ACAN, de SOX9 et surtout de COL2A1, caractéristique du cartilage.

Il aurait été intéressant de préparer des feuillets produits par des cellules exprimant la GFP et de les implanter *in vivo* afin de pouvoir les suivre et voir si elles se sont accumulées dans le site du défaut ou si elles ont interagi avec le tissu environnant. De plus, on ne peut pas exclure que des cellules de l'hôte migrent dans la zone du défaut et participent à la réparation. Toutefois, en analysant les résultats histologiques, nous avons pu conclure que l'apport de cellules par le feuillet a nettement contribué à la réparation car les témoins, où le défaut n'a pas été comblé, ne présentent pas une organisation tissulaire et une réparation adéquate. L'intérêt de cette comparaison était de montrer que lorsque nous avons introduit les feuillets, les cellules étaient viables et prolifèraient et participent à la régénération du défaut. Ainsi, la technologie des feuillets cellulaires se pose comme un outil pour régénérer les défauts tissulaires et particulièrement de cartilage.

Nous avons évoqué l'utilisation de cartilage de porc décellularisé comme matrice pour l'ingénierie des tissus cartilagineux. Bien que cet échafaudage ait été entièrement régénéré à l'aide de feuillets cellulaires, son utilisation peut toutefois poser de nombreux problèmes éthiques lors d'essais cliniques ultérieurs sur l'homme. Dans ce cadre, de nombreuses études ont démontré la capacité

des tissus végétaux décellularisés, à constituer un échafaudage cellulosique fonctionnel qui peut à son tour servir de support à une culture 3D *in vitro* ainsi qu'un échafaudage biocompatible implantable *in vivo*. Ainsi, dans un autre but de ce travail, nous avons cherché à explorer d'autres échafaudages pour l'ingénierie du cartilage et nous nous sommes tournés vers les tissus cellulosiques végétaux récemment décrits, à savoir l'hypanthium de la pomme. La partie cellulaire a été enlevée à l'aide du tensioactif anionique, dodécylsulfate de sodium (SDS). C'est l'un des produits ioniques les plus utilisés pour éliminer les restes cellulaires. De nombreuses études ont indiqué que des traces de détergent SDS peuvent rester attachées au tissu même après un bon rinçage à l'eau, le SDS peut provoquer des effets indésirables sur la réticulation du tissu entier (Cebotari *et al*., 2010 ; Syed *et al*., 2014). Ainsi, selon de nombreux chercheurs, il est nécessaire d'éliminer les traces restantes de SDS qui induisent une activité cytotoxique sur les cellules, avant de procéder à la recellularisation du biomatériau (Alizadeh *et al*., 2019). Dans leurs études, Hickey *et al*., ont effectué un traitement au sel, pour éliminer toutes les molécules de SDS, suggérant que le SDS peut former des micelles dans le tissu de la pomme qui peuvent limiter son potentiel de réticulation, ainsi le traitement au sel vise à desserrer ces micelles, en les libérant avec de l'eau (Hickey *et al*., 2018). En revanche, dans notre étude, nous n'avons ajouté aucun type de traitement. Nous nous sommes limités à de longues étapes de lavage à l'eau distillée avec des changements toutes les 2 heures pendant 24 heures sous agitation. L'eau était ensuite changée en PBS pendant la nuit. Ceci est corrélé par plusieurs études qui utilisent de l'eau distillée et du PBS (Cebotari *et al*., 2010 ; Zvarova *et al*., 2016 ; Lin *et al*., 2019). Cela était suffisant pour éliminer la cytotoxicité des tissus.

Les plantes sont caractérisées par une plus grande disponibilité que les tissus animaux. Nous avons déjà prouvé que nos quatre sources cellulaires ont la capacité de se différencier en cartilage lorsqu'elles sont encapsulées dans des hydrogels, il était donc intéressant d'évaluer la viabilité et le potentiel chondrogénique des mêmes cellules dans des matrices de pommes. Les tests de viabilité ont révélé que les cellules prolifèrent et restent viables au moins plusieurs semaines. Ceci est corrélé avec d'autres études qui ont montré que les cellules étaient capables de proliférer et restaient viables jusqu'à 12 semaines de culture (Modulevsky *et al*., 2014). Une autre idée à souligner est que lorsque ces tissus ont été fixés, des sections d'OCT ont été coupées horizontalement et verticalement jusqu'à atteindre presque tout le bloc. Ces lames ont été colorées et analysées. Cela montre, d'après nos résultats, que les cellules ne se sont pas accumulées à la

surface de l'échafaudage, mais ont proliféré et colonisé profondément le tissu. L'échafaudage ainsi produit était non seulement capable de soutenir l'adhésion et la prolifération des cellules, mais aussi de maintenir et d'orienter leur fonction. Par exemple, une formation tissulaire blanchâtre est observée, ce qui s'explique par l'expression et le dépôt importants de matrice extracellulaire. Nos résultats étaient conformes à ceux décrits dans la littérature où les échafaudages de pommes et d'autres végétaux tels que la carotte, l'oignon, le céleri ont permis de générer des tissus adipeux et osseux (Lee *et al*., 2019 ; Cheng *et al*., 2020 ; Negrini *et al.*, 2020). Cependant, nos travaux sont les premiers à montrer que les échafaudages issus de pommes favorisaient la régénération de tissu cartilagineux.

Plusieurs biomatériaux ont été décrits comme supportant ou favorisant la chondrogenèse. Les hydrogels d'alginate représentent l'un des modèles les plus décrits et les plus aboutis. Cet hydrogel est largement utilisé dans l'ingénierie des tissus cartilagineux en raison de sa haute viscosité et de sa matière imprimable, de sa faible cytotoxicité et de sa biocompatibilité *in vivo*. Différentes études ont utilisé l'alginate pour l'impression 3D du cartilage (Markstedt *et al*., 2015 ; Möller *et al*., 2017; Ouyang *et al*., 2017).

Dans une autre étude, l'alginate a été combiné avec le COL1 et l'agarose pour améliorer la fonctionnalité biologique du tissu cartilagineux généré (Yang *et al*., 2018). En outre, lorsque des BMMSC ont été encapsulées dans des billes d'alginate, elles ont sécrété des facteurs paracrines spécifiques qui ont régénéré le cartilage de manière endogène *in vitro* (Sahu *et al*., 2021). Ainsi, nos présents résultats, démontrent également pour la première fois que, les matrices de pommes sont un meilleur substrat pour la chondrogenèse, ce qui conforte l'intérêt de son utilisation pour l'ingénierie du cartilage ou d'autres tissus, en raison de sa malléabilité et de sa grande disponibilité.

Dans une dernière partie de notre travail, nous avons développé une nouvelle approche permettant d'optimiser le microenvironnement cellulaire lors de culture 2D. Des cellules sont ainsi cultivées pour former des feuillets cellulaires qui sont ensuite décellularisés. La matrice extracellulaire restante appelée (CSM : cell secreted matrices) est ensuite lyophilisée directement sur les plaques de culture qui seront utilisées pour diverses applications.

La notion de CSM a été utilisée dans différentes études avec des BMMSC, des chondrocytes et des cellules de la sous-muqueuse intestinale (Decaris *et al*., 2012 ; Wang *et al*., 2018 ; Taghavi *et al*., 2020). Dans notre étude, nous avons gardé le modèle cellulaire des AuP de lapin mis en

conditions chondrogénique, pour produire les CSM. En effet, nous avons montré que les périchondrocytes auriculaires de lapin pouvaient fournir de grandes quantités de matrice extracellulaire pour l'ingénierie des tissus cartilagineux. La lyophilisation qui s'ensuit a permis de conserver les plaques pendant un temps plus long (plusieurs mois) et surtout à température ambiante.

Cette approche semble innovante puisque nos données ont démontré que la CSM lyophilisée présentait une grande capacité à améliorer la différenciation chondrogénique où une augmentation significative de l'expression des gènes particuliers a été observée par rapport aux cellules ensemencées sur des plaques de plastique. Comme prévu, après la décellularisation et la lyophilisation, la quantité totale de protéines est réduite en raison de l'élimination des cellules. Cependant, les protéines extracellulaires sont également concernées par cette baisse, puisque les collagènes totaux, les GAG et l'élastine sont également diminués. Bien que ces dernières puissent être des protéines intracellulaires, nous devons considérer que le traitement au détergent affecte également le réseau matriciel lors de la décellularisation. L'analyse par spectrométrie de masse desprotéines restantes a montré de plus, que plusieurs protéines intracellulaires sont encore attachées au substrat lyophilisé. Parmi elles, une grande partie est impliquée dans l'adhésion cellulaire ou le cytosquelette. Cela n'est pas surprenant puisque ce réseau de protéines est normalement lié à la matrice extracellulaire par des adhésions focales et peut certainement rester attaché tout au long de la préparation des plaques lyophilisées. Le traitement du SDS pour la décellularisation pourrait également créer des liens pour stabiliser certaines interactions protéine-protéine, ce qui pourrait expliquer la persistance, a priori étonante, de plusieurs autres protéines intracellulaires voire nucléaires, comme les histones par exemple. Néanmoins, nous avons considérés les substrats lyophilisés tels quels et procédé à des tests d'applications potentielles.

La dédifférenciation des chondrocytes reste un défi permanent dans la reconstruction des tissus cartilagineux. En effet, lors de l'amplification *in vitro* des chondrocytes sur les surfaces 2D plastique, on observe une diminution de l'expression des gènes COL2A1, ACAN et SOX9, au détriment de COL1, expliquant ainsi la perte de phénotype cartilagineux. Les différences structurelles sont remarquables même lors de l'observation de ces cellules au microscope, où les chondrocytes primaires présentent une forme plutôt arrondie qui devient plus aplatie et fusiforme au fur et à mesure de la dédifférenciation.

De nombreux efforts ont été faits pour diminuer ce phénomène, comme l'encapsulation des chondrocytes dans des hydrogels 3D avec des conditions d'hypoxie, l'implication de différents facteurs de croissance, des techniques de co-culture qui combinent différents progéniteurs avec des chondrocytes dans des ratios spécifiques. Toutefois, de nombreuses limitations ont été associées à chaque technique.

Notre méthode de CSM lyophilisée fournit un outil innovant et intéressant pour plusieurs applications comme décrit dans les résultats. Une approche similaire a été décrite récemment, par Mao et al., qui ont comparé des CSM issues de BMMSC et des chondrocytes articulaires. Ils ont également montré que leur méthode limite la dédifférenciation mais ne montre qu'une diminution de COL1 sans aucune modification de COL2, ou ACAN, qui sont très nettement augmentés dans notre étude (Mao *et al*., 2019).

Nous avons également testé des cellules initialement ensemencées sur des plaques lyophilisées revêtues de CSM pendant 3 passages puis passées sur des plaques en plastique, et inversement. Comme attendu, une augmentation significative de la croissance est observée quand les chondrocytes sont sur des CSM, et de façon intéressante, ces cellules continuent de se diviser plus rapidement, même quand elles sont repassées sur plastique, indiquant qu'une forme de mémoire cellulaire est maintenue du fait de la période au contact de la CSM.

Par ailleurs, nous montrons aussi que la mise en culture sur CSM permettait de recouvrer le phénotype cartilagineux à des chondrocytes dédifférenciés. Comme précisé par ailleurs, il a déjà été montré que la mise en culture 3D pendnat une période minimale de 3 semaines (alginate) permettait d'inverser le processus de dédifférenciation et faire ré exprimer les gènes spécifiques du cartilage. Il est intéressant de noter que notre modèle permet de réaliser cela en un temps plus court et surtout sur des systèmes de culture (2D) beaucoup plus facile à mettre en œuvre.

Nos résultats sur les substrats lyophilisés ont été obtenus en utilisant des périchondrocytes auriculaires comme cellules productrices de matrice extracellulaire. Plusieurs observations ont été faites tout au long de notre étude : leur taux de prolifération (pour obtenir rapidement un nombre suffisant de cellules), leur potentiel chondrogénique et le maintien et recouvrement du phénotype. Il serait très intéressant d'étudier d'autres types de cellules, car elles sécrètent et laissent probablement derrière elles différents complexes supramoléculaires et donc d'autres ensembles de signaux. Par exemple, il serait intéressant d'explorer différentes voies de différenciation en utilisant

la même préparation de plaque (ex : CSM lyophilisée produite par ostéoblastes ou myoblastes respectivement pour conduire l'ostéogenèse ou la myogénèse de progéniteurs).

Au total, nous proposons une nouvelle approche consistant à utiliser un revêtement de CSM lyophilisée pour plusieurs applications de culture cellulaire, notamment la différenciation et la prolifération. Ces plaques préparées peuvent également être utilisées avantageusement pour l'amplification cellulaire avec préservation du phénotype et peuvent également être une voie pour de multiples tests de screening car adaptables à tous les dispositifs de culture 2D sur plastique actuels.

V-Conclusion et perspectives

1-Conclusions

Les AuP se sont révélées être les meilleures sources de cellules pour régénérer le cartilage élastique auriculaire. Cultivées à des niveaux d'oxygène normaux, ces cellules ont surpassé les autres progéniteurs en ce qui concerne l'expression de différents marqueurs cartilagineux. Au contraire, l'hypoxie est inefficace et peu bénéfique pour l'AuP. Comme prévu, les BMMSC montrent le meilleur profil chondrogénique mais nécessitent un environnement hypoxique.

Nous avons ensuite utilisé ces cellules pour préparer des feuillets, ce qui n'avait pas été décrit pour des cellules progénitrices auriculaires. Ces feuillets ont permis de recoloniser un cartilage xénogénique décellularisé et de réparer un défaut de cartilage auriculaire *in vivo,* pour la première fois dans des modèles de lapins allogèniques.

Pour approfondir nos connaissances et explorer les matrices pour l'ingénierie du cartilage auriculaire, nous avons procédé à l'étude d'échafaudages naturels décellularisés qui sont très prometteurs pour la médecine régénérative. Nous avons réussi à décelluloriser des tissus de pomme et confirmé leur biocompatibilité vis-à-vis de différents progéniteurs et cellules souches. Plus important encore, la structure de la pomme a favorisé de manière significative l'expression des marqueurs du cartilage et la génération de tissu cartilagineux et a dépassé le potentiel chondrogénique des hydrogels d'alginate utilisés comme référence. Ces résultats suggèrent fortement l'importance de ce genre de tissu en tant que support alternatif pour l'ingénierie des tissus cartilagineux et pour la médecine régénérative en général.

Enfin, et comme approche de recherche et développement (R&D), nous avons créé une stratégie qui utilise des CSM lyophilisées sur des plaques de plastique comme support pour plusieurs essais de culture cellulaire. L'utilisation de ces plaques naturellement revêtues de CSM permet une chondrogenèse de cellules progénitrices humaines. Cela favorise également la croissance, le maintien du phénotype des chondrocytes lors de leur multiplication et améliore leur viabilité par rapport aux cellules ensemencées sur des plaques de culture en plastique.

2-Perspectives

Afin d'approfondir les résultats obtenus au cours de la thèse, différentes perspectives sont possibles.

Au vu des résultats obtenus au cours de cette thèse, il serait intéressant de compléter cette étude par des essais cliniques utilisant des AuP autologues pour la réparation des défauts du cartilage. Les feuillets cellulaires sont également des outils très prometteurs pour la thérapie cellulaire et l'ingénierie tissulaire. Nous avons montré leur capacité à former du tissu cartilagineux *in vivo*. Nos résultats doivent être étendus à la réparation de défauts tissulaires plus importants *in vivo* afin d'envisager par la suite, des essais cliniques. En parallèle, des résultats préliminaires ont été obtenus lorsque des feuillets cellulaires obtenus de cellules ostéogénique. Il pourrait être intéressant de les combiner avec des feuillets chondrogéniques afin de construire une jonction ostéochondrale. La caractérisation de cette jonction serait très utile pour définir les conditions nécessaires à la régénération d'un défaut ostéochondral et pourrait être utile pour améliorer la prise de greffe. Elle peut également apporter des informations sur la construction de diverses jonctions tissu-tissu en général.

En ce qui concerne les échafaudages de pommes, il est primordial de tester leur potentiel chondrogénique in vivo en créant des modèles animaux de défauts cartilagineux. Il est également intéressant de tester différentes cellules pour produire d'autres tissus tels que des tissus osseux ou musculaires.

Il est important d'étudier les propriétés mécaniques des tissus reconstruits à l'aide de nos échafaudages (feuillets de cellules, hypanthium de pomme) en mesurant leur rigidité et leur degré d'élasticité et de flexibilité à l'aide de l'équation du module de Young et de voir jusqu'à quel niveau

ces échafaudages peuvent résister aux contraintes. En effet, il est primordial que le tissu reconstruit soit fonctionnel et réponde aux exigences et contraintes liiées à son rôle (maintien, élasticité, rétention d'eau, etc). Nos travaux seront ainsi prêts et applicables pour les essais cliniques.

En ce qui concerne notre dernière série d'expériences avec des plaques revêtues de CSM, plusieurs perspectives peuvent être envisagées. Tout d'abord, une population cellulaire homogène devrait être choisie afin de limiter la variabilité cellulaire et donc d'augmenter la reproductibilité. Une évaluation critique des stratégies de décellularisation telles que le choix des agents qui éliminent le mieux le matériel d'ADN est nécessaire pour bien rincer et éliminer les traces d'histone et de protéines intracellulaires qui sont piégées, probablement en raison du SDS.

En effet, différentes sources cellulaires pourraient être étudiées pour la préparation de divers tissus. La préparation de ces plaques pourrait être réalisée à façon ou à haute échelle, de manière automatisée pour leur utilisation dans des applications industrielles in vitro. Cela permettrait également de disposer de supports de culture cellulaire qui facilitent la préparation de grandes quantités de cellules, dans des conditions d'environnement appropriées, ce qui ouvre des perspectives prometteuses pour la recherche *in vitro*, chirurgie reconstructive et la thérapie cellulaire. En outre, ces plaques pourraient être utilisées comme supports pour la fabrication de patchs cellulaires personnalisés.

Des plaques revêtues de matrice extracellulaire existent déjà sur le marché. Cependant, elles sont toutes fabriquées en adsorbant sur le plastique, une seule protéine de la matrice mise en solution. Non seulement, nous proposons des plaques avec des protéines naturellement sécrétées par les cellules, mais elles sont également déposées et organisées comme une matrice extracellulaire spécifique à un tissu particulier, qui contient les signaux nécessaires à induire les effets que nous avons décrits dans cette dernière partie. Ce travail nous a conduit à lancer une procédure de PI (propriété intellectuelle) pour l'évaluation et dépôt d'un brevet.